

# Characterisation of Lentiviral Vpr Function and Mechanism

Christoffer van Tulleken

University College London

Department of Infection and Immunity

A thesis submitted for the degree of

Doctor of Philosophy

July 2017

## **Declaration**

I confirm that the work presented in this thesis is my own other than where I have indicated that information, images or data come from other sources.

## Acknowledgements

As a clinician starting comparatively late in life in a molecular lab I have been given immense support and assistance by everyone in the Towers Laboratory and from colleagues and collaborators in our division at UCL.

I would particularly like to thank Greg who has been an invaluable source of inspiration and advice about both the technical and metaphysical aspects of this PhD (and science in general). He has been a true mentor.

(Choon Ping) Tan rescued me from a failing project and help establish the techniques and procedures that have seen me through to the end of this PhD. Becky Sumner took over from Tan as a post-doctoral mentor with a seemingly limitless supply of positivity and help. Stephane Hue helped me to understand phylogenetics, use the required programs and showed me how to align un-alignable sequences. Hataf Khan helped make the HIV-1 M mutants and has been a great friend and sounding board. Layal Liverpool was my student and friend for almost a year and helped with the CypA over expression and knock down experiments. David Stirling was endlessly generous with his time and help using the Hermes and the multiple failed attempts to visualise stained plasmids. Claire and Yasu were on my thesis committee and provided ongoing advice particularly at upgrade. Elizabetta Gropelli sequenced the initial NF $\kappa$ B promoter and was a great source of inspiration and advice. Petra Mlcochova, Isobel Honeyborne, Jane Turner, Doug Fink, Doug King and Tafima Haider have all helped variously and continuously with advice, friendship and protocols. Matt Tranter helped read the manuscript and gave advice on statistics. Christine my mother-in-law provided work space, company and lots of advice while my mother Kit edited the final manuscript in more detail than I could have ever asked for. My daughter Lyra arrived just in time to force a viva reschedule. I am grateful to my examiners Richard and Leo for allowing me to enjoy my first week with her without pressure.

My brothers and both my parents support me endlessly throughout everything I do and this PhD has been no exception – I am fortunate beyond words to have had their love and support.

The same is true of my wife, Dinah. She has also put up with late nights and failed experiments as much as if it was her own project. If there was any justice in the world this thesis would have her name on the cover.

## Abstract

Genetic conflict between viruses and their hosts has driven an 'arms race', forcing the evolution of both immune defenses and multiple viral strategies to counteract and evade them. In the case of HIV many of these processes are well characterised – the virus carries with it a set of accessory proteins which target specific host restriction factors. Of these accessory proteins Vpr is the least well understood, with no described role that adequately explains its conservation across all known primate lentiviruses.

Unpublished data from our lab indicate that Vpr is able to rescue infection in macrophages from addition of cGAMP, a second messenger protein produced by the cytosolic DNA sensor cGAS which activates antiviral immune signalling pathways.

This study first sought to test the hypothesis that Vpr has evolved to counteract cGAS/STING mediated cytosolic DNA sensing using a co-transfection assay to test Vpr proteins from all groups of primate lentiviruses. Initial observations appeared to demonstrate specific degradation of innate immune signalling proteins. It was subsequently shown that HIV-1 M Vpr antagonises expression from all tested co-transfected plasmids. This phenotype was demonstrated to be species specific, and to correlate with both the history of zoonotic transmission and localisation of Vpr to the nuclear rim. Additionally, it was shown that Vpr antagonises NF $\kappa$ B signalling activated by TNF $\alpha$ , independent of an effect on expression from transfected plasmids, but with the same dependence on nuclear localisation, putatively by the same mechanism.

Next, this study characterised an observation that the Vpr from the lentivirus infecting a mona monkey (SIVmon) stimulates NF $\kappa$ B signalling. It was hypothesised that the SIVmon Vpr might have molecular binding partners in common with the HIV-1 M Vpr and conditions were optimised for proteomics studies to determine these binding partners.

This study provides insights into the role of Vpr in antagonising innate immune sensing. Additionally, overexpression assays have been used widely in the literature describing Vpr. The data presented here indicate that observations using these assays, apparently demonstrating specific degradation of host cellular proteins, should be interpreted cautiously.

<b>Declaration</b> .....	<b>2</b>
<b>Acknowledgements</b> .....	<b>3</b>
<b>Abstract</b> .....	<b>4</b>
<b>List of Tables</b> .....	<b>14</b>
<b>Abbreviations</b> .....	<b>15</b>
<b>1 Chapter 1: Introduction</b> .....	<b>20</b>
1.1 HIV history and Origins .....	20
1.1.1 The history of retroviruses .....	20
1.1.2 Classification of retroviruses .....	20
1.1.3 Discovery of HIV-1 .....	21
1.1.4 The Origins of HIV .....	21
1.2 Clinical HIV and HIV Epidemiology .....	29
1.2.1 Clinical HIV infection .....	29
1.2.2 Treatment and prevention of HIV infection .....	31
1.3 Overview: HIV-1 structure .....	33
1.3.1 The HIV genome .....	33
1.3.2 Overview of Transcription, Translation and gene products .....	34
1.3.3 HIV-1 mature virion structure .....	35

1.4	The Viral Life Cycle .....	38
1.4.1	Receptor Binding .....	38
1.4.2	Co-receptor engagement.....	39
1.4.3	Membrane fusion .....	40
1.4.4	Post-entry events .....	42
1.4.5	Reverse Transcription.....	47
1.4.6	The mechanism of Reverse Transcription (figure 1.8).....	47
1.4.7	Integration .....	51
1.4.8	Latency .....	54
1.4.9	Transcription of HIV .....	56
1.4.10	Assembly, maturation and budding. ....	59
1.5	HIV and the Innate Immune System .....	65
1.5.1	The adaptive and innate immune systems – history and overview .....	65
1.5.2	Cytosolic RNA sensing - RLRs .....	67
1.5.3	Cytosolic DNA sensing .....	68
1.5.4	PRRs and HIV-1 .....	73
1.5.5	Evasion of DNA sensing by microbial pathogens and HIV .....	73
1.6	HIV accessory proteins, restriction factors and co-factors .....	77

1.6.1	Tetherin and Vpu .....	77
1.6.2	TRIM5 $\alpha$ .....	78
1.6.3	APOBEC3G and Vif.....	79
1.6.4	SAMHD1 and Vpx.....	79
1.6.5	SERINC and Nef.....	81
1.6.6	MX2 and Capsid .....	81
1.6.7	Schlafen11 .....	81
1.6.8	IFITM1–3.....	81
1.7	Viral Protein R - overview .....	83
1.7.1	Structure .....	84
1.7.2	Functions .....	86
<b>2</b>	<b>Chapter 2: Materials and Methods.....</b>	<b>97</b>
2.1	DNA preparation and manipulation .....	97
2.1.1	Preparation of plasmid DNA - Small scale.....	97
2.1.2	Preparation of plasmid DNA - Large Scale .....	97
2.1.3	Agarose gel electrophoresis and purification of DNA .....	97
2.1.4	Restriction enzyme digestion.....	97
2.1.5	DNA ligation.....	98

2.1.6	Production of competent <i>E. coli</i> bacteria .....	98
2.1.7	Transformation of <i>E. coli</i> .....	98
2.1.8	Bacterial colony screening .....	99
2.1.9	Vpr Plasmid construction .....	99
2.1.10	Site directed mutagenesis (SDM) .....	99
2.2	Cell culture .....	101
2.2.1	Maintenance of cells .....	101
2.2.2	Fugene-6 transfection .....	101
2.2.3	Generation of cell line with integrated NF $\kappa$ B sensitive reporter .....	101
2.3	Reporter gene assays .....	101
2.4	RNA extraction and cDNA synthesis .....	102
2.5	qRT-PCR .....	103
2.6	Preparing short hairpin RNA (shRNA)-expressing MLV vectors .....	103
2.7	Protein analysis .....	104
2.7.1	SDS-PAGE .....	104
2.7.2	Nu-PAGE .....	104
2.8	Immunoblotting .....	105
2.9	Silver staining of proteins .....	105

2.10	Immunofluorescence and Confocal Microscopy .....	105
2.11	Immunoprecipitation assays .....	106
2.12	Transcriptional Profiling .....	106
2.13	Phylogenetic analysis .....	108
2.14	Structural alignments .....	108
<b>3</b>	<b>Chapter 3 Antagonism of reconstituted innate immune sensing in 293 cells with lentiviral Vprs .....</b>	<b>109</b>
3.1	HIV-1 M Vpr is able to rescue a spreading infection in monocyte derived macrophages from addition of cGAMP .....	109
3.2	Co-expression of cGAS/STING activates an NFκB-sensitive promoter....	109
3.3	Co-expression of cGAS/STING induces expression of endogenous NFκB genes	112
3.4	Co-expression of HIV-1 YU2 Vpr selectively antagonises NF-κB induced expression of luciferase .....	114
3.5	Expression of HIV-1 M Vpr does not cause an increase in LIVE/DEAD cell staining .....	116
3.6	Primate Vprs exhibit differential antagonism of cGAS/STING induced NF-κB promoter driven expression of luciferase .....	118
3.7	Codon optimised HIV-1 M Vpr shows greater antagonism of cGAS/STING mediated NFκB promoter activation than HIV-2 .....	120

3.8	NF $\kappa$ B signal inhibition by Vpr is unaffected by FLAG epitope tags at the Vpr N-terminal .....	122
3.9	Inhibition of NF $\kappa$ B induced signalling is not conserved across all Vprs from different primate lineages. ....	125
3.10	Correlation of NF $\kappa$ B signal inhibition with Vpr phylogeny .....	127
3.11	SIVcpz Vpr from the eastern chimpanzee does not antagonise cGAS/STING stimulated NF $\kappa$ B signalling. ....	129
3.12	Inhibition of differentially activated NF $\kappa$ B signalling by Vpr .....	133
3.13	The pattern of species specific antagonism by primate lentiviral Vprs is preserved across different NF $\kappa$ B activating stimuli.....	135
3.14	HIV-1 M Vpr causes loss of TRAF2 & TRAF6 on immunoblot.....	137
<b>4</b>	<b>Chapter 4 - HIV Vpr non-specifically suppresses expression from co-transfected plasmids .....</b>	<b>139</b>
4.1	HIV-1 M Vpr antagonism of NF $\kappa$ B signalling requires transfection of the activating stimulus .....	139
4.2	HIV-1 M Vpr inhibits expression from a co-transfected GFP encoding plasmid	141
4.3	HIV-1 M Vpr inhibits mRNA expression from co-transfected cGAS and STING encoding plasmids. ....	142

4.4	HIV-1 M Vpr inhibits luciferase expression from different promoter constructs 144	144
4.5	HIV-1 M Vpr inhibits expression from a panel of viral promoters.....	146
4.6	HIV-1 M Vpr inhibits expression from two human promoters.....	148
4.7	HIV-1 M Vpr inhibits expression from a transfected NF $\kappa$ B promoter but not from the same promoter when it is integrated into the cell genome using a retrovirus 149	149
4.8	Nuclear localisation and inhibition of expression .....	150
4.9	Visualisation of co-transfected stained expression vector .....	155
4.10	Transfected HIV-1 M Vpr antagonises NF $\kappa$ B luciferase expression stimulated by added TNF $\alpha$ at an integrated reporter. ....	157
<b>5</b>	<b>Chapter 5: Characterisation of SIVmon (mona monkey) Vpr to identify determinants of block to sensing .....</b>	<b>159</b>
5.1	SIVmon Vpr activates NF $\kappa$ B signalling .....	159
5.2	SIVmon Vpr expression activates a co-transfected NF $\kappa$ B reporter and SIVmon Vpr expression is suppressed by co-transfection of HIV-1M Vpr.....	161
5.3	SIVmon Vpr activates NF $\kappa$ B signalling from an integrated reporter .....	163
5.4	Mutagenesis of SIVmon Vpr .....	164
5.5	SIVmon Vpr specifically activates NF $\kappa$ B signalling.....	165

5.6	Depletion of Nup358 reduces SIVmon Vpr NF $\kappa$ B signalling.....	167
5.7	Depletion of cyclophilin A reduces SIVmon Vpr NF $\kappa$ B signalling .....	169
5.8	Overexpression of CypA or Nup358cyp leaves SIVmon Vpr activated NF $\kappa$ B signalling unaffected. ....	171
5.9	SIVmon Vpr does not co-immunoprecipitate with co-transfected members of the pathway .....	172
5.10	SIVmon localises to the nucleus .....	173
5.11	Optimization of SIVmon Vpr expression for determination of binding partner by SILAC.....	176
5.12	Transcriptional signature of SIVmon Vpr .....	178
<b>6</b>	<b>Chapter 6: Discussion .....</b>	<b>180</b>
6.1	Function and Mechanism of HIV-1 M Vpr .....	181
6.1.1	Antagonism of expression from co-transfected plasmids .....	181
6.1.2	Antagonism of NF $\kappa$ B activation by TNF $\alpha$ at an integrated reporter... ..	182
6.1.3	Reconciling the effects on co-transfected plasmids and TNF $\alpha$ signalling 183	
6.2	Future work on HIV-1 M Vpr .....	184
6.2.1	Transfection Assays .....	184
6.2.2	Vpr expressing lentiviral vectors .....	184

6.2.3	Microscopy.....	185
6.2.4	Reporter plasmid circularisation assay .....	186
6.2.5	Effects on NFκB subunit localisation .....	186
6.2.6	Future species specificity characterisation .....	186
6.3	SIVmon Vpr.....	188
6.4	Conclusion .....	191
<b>7</b>	<b>Appendix of tables .....</b>	<b>192</b>
	<b>Bibliography.....</b>	<b>198</b>

## List of Tables

Table 2.1 Bacterial colony screening .....	99
Table 2.2 SDM PCR components .....	100
Table 2.3 Cycling parameters .....	100
Table 4.1 Correlation between rim localisation and inhibition of expression .....	150
Table 4.2 Vpr mutant phenotypes .....	151
Table 7.1 Plasmids used in this study .....	192
Table 7.2 Primers for qRT-PCR .....	196
Table 7.3 SDM primer sequences .....	197
Table 7.4 Antibodies used in this study .....	197

## Abbreviations

6HB	6-helix bundle
Ab	antibody
AIDS	acquired immune deficiency syndrome
APC	antigen presenting cell
APOBEC3	Apolipoprotein B mRNA-editing enzyme catalytic polypeptide-like 3
APS	ammonium persulfate
ART	Antiretroviral therapy
AZT	azidothymidine
BLAST	Basic Local Alignment Search Tool
BSA	bovine serum albumin
CA	capsid
cART	combined ART
CCL	chemokine ligand
CCR5	C-C chemokine receptor 5
CD4	cluster of differentiation 4
CD8	cluster of differentiation 8
CDK	cyclin-dependent kinase
cDNA	Complementary DNA
cGAMP	cyclic GMP-AMP or cyclic [G(2'-5')pA(3'-5')p]
cGAS	cyclic GMP-AMP synthase
CHR	C-terminal helical region
CLR	C-type lectin receptors
CMV	Cytomegalovirus
cPPT	central PPT
CPSF6	cleavage and polyadenylation specificity factor 6
CsA	cyclosporine A
Ct	cycle threshold
CTD	C-terminal domain
CTL	cytotoxic T lymphocyte
CXCR4	C-X-C chemokine receptor 4
CypA	cyclophilin A
DBP	DNA binding protein
DC	dendritic cell
DC-SIGN	dendritic cell-specific intercellular adhesion molecule-3-grabbing
DMEM	Dulbecco's Modified Eagle Medium
DMSO	dimethyl sulphoxide

EDTA	ethylenediaminetetraacetic acid
EIAV	Equine Infectious Anaemia Virus
ELISA	enzyme-linked immunosorbent assay
EM	electron microscopy
Env	envelope
ER	endoplasmic reticulum
ESCRT	endosomal sorting complexes required for transport
FBS	foetal bovine serum
FISH	fluorescent <i>in situ</i> hybridisation
FIV	Feline Immunodeficiency Virus
FoC	fate of capsid
FRAP	fluorescence recovery after photobleaching
FSC-H	forward scatter height
Gag	Group specific antigen
GALT	gut associated lymphoid tissue
GFP	green fluorescent protein
gp120	glycoprotein 120kDa
gp160	glycoprotein 160kDa
gp41	glycoprotein 41kDa
GPI	glycophosphatidylinositol
GWAS	Genome-wide association study
HA	hemagglutinin
HAART	highly active ART
HIV	Human Immunodeficiency Virus
HLA	human leukocyte antigen
HTLV	Human T-Lymphotropic Virus
ICAM-1	intracellular adhesion molecule 1
IF	immunofluorescence
IFN	interferon
IFNAR2	IFN $\alpha/\beta$ receptor 2
IL-2	interleukin 2
IN	integrase
ISG	IFN-stimulated gene
IU	infectious unit
Jun	Jun proto-oncogene
kb	Kilobase
kDa	Kilodalton
LB	lysogeny broth

LEDGF/p75	lens epithelium-derived growth factor
LTNP	Long-term non-progressor
LTR	long terminal repeat
MA	matrix
MDM	Monocyte-derived macrophage
MFI	mean fluorescence intensity
MHC	major histocompatibility complex
MLV	Murine Leukaemia Virus
MOI	multiplicity of infection
MxB	Myxovirus resistance protein B
NC	nucleocapsid
Nef	negative regulatory factor
NES	nuclear export signal
NFAT	nuclear factor of activated Tcells
NFκB	nuclear factor κB
NHEJ	Non-homologous end joining
NHR	N-terminal helical region
NLS	nuclear localisation signal
NMR	nuclear magnetic resonance
NPC	nuclear pore complex
NTD	N-terminal domain
Nup	nucleoporin
ORF	Open reading frame
OWM	Old world monkey
p-TEFb	positive transcription elongation factor b
PAGE	polyacrylamide gel electrophoresis
PAMP	Pathogen-associated molecular pattern
PBMC	peripheral blood mononucleocytes
PBS	phosphate buffered saline
PBS	primer binding site
PCP	Pneumocystis carinii pneumonia
PEG	polyethylene glycol
PFA	paraformaldehyde
PHA	phytohemagglutinin
PI	PR inhibitor
PIC	pre-integration complex
POD	peroxidase
PPIase	peptidyl-prolyl isomerase

PPT	polypurine tract
PR	protease
PRR	pattern recognition receptor
PVDF	polyvinylidene difluoride
qPCR	quantitative/real time PCR
RANBP2	Ran binding protein 2, a.k.a. Nup358
Rev	regulator of expression of virion proteins
RING	Really Interesting New Gene
RLU	relative light units
RNAPII	RNA polymerase II
RPMI	Roswell Park Memorial Institute Medium
RRE	Rev responsive element
RRM	RNA recognition motif
RS	arginine/serine-rich
RT	reverse transcriptase
RTC	reverse transcription complex
SAMHD1	sterile $\alpha$ motif and HD domain-containing protein 1
SDM	site directed mutagenesis
SDS	sodium dodecyl sulphate
SGA	single genome analysis
SIV	Simian Immunodeficiency Virus
SP	spacer peptide
SR	serine/arginine-rich
SSC-H	side scatter height
STING	stimulator of IFN genes
SV40	Simian Virus 40
TAE	Tris acetate EDTA
TAK-1	tumour growth factor- $\beta$ activated kinase 1
TAR	transactivation responsive region
Tat	trans-activator of transcription
TCR	T cell receptor
TE	Tris EDTA
TEMED	tetramethylethylenediamine
T <sub>m</sub>	melting temperature
TNF $\alpha$	tumour necrosis factor $\alpha$
TNPO3	transportin 3, a.k.a. TRN-SR2
TRIM	tripartite motif
UTR	untranslated region

V3	variable loop 3
Vif	viral infectivity factor
VLP	Virus-like particle
Vpr	viral protein r
Vpu	Viral protein u
Vpx	Viral protein x
VS	Virological synapse
VSV	Vesicular stomatitis virus
VSV-G	VSV G envelope protein
WHO	World Health Organisation
WT	Wild type
Ψ	HIV-1 packaging signal

# **1 Chapter 1: Introduction**

## **1.1 HIV history and Origins**

### **1.1.1 The history of retroviruses**

Agents of disease that we now know to be retroviruses were discovered at the beginning of the 20th century. Equine infectious anaemia virus (EIAV) and avian leukaemia virus (ALV) were partially described in 1904 and 1908, respectively, using extracts from infected animals, filtered so that they were free from cells or bacteria (1,2). The pathology caused by these viruses was poorly understood at the time, so neither of these discoveries had the same impact as another series of experiments performed by a young pathologist at the Rockefeller Institute called Peyton Rous. A farmer's wife asked him to investigate a Plymouth Barred Rock hen which had a large tumour and, after transplanting the tumour to other hens, he successfully demonstrated that further tumours could be induced with a cell free filtrate (3). Rous's discovery showed clearly for the first time that a tumour could be caused by infection, although it would be 53 years until the discovery of the first human oncovirus: Epstein-Barr (EBV). The isolation of these first retroviruses set in motion a series of immense scientific paradigm shifts, but these did not happen quickly; it would be 55 years before the significance of Rous's discovery was recognised with the award of the Nobel Prize.

Our modern understanding of the life cycle of retroviruses, requiring the conversion of an RNA genome into a DNA provirus, was proposed by Howard Temin in 1964 with a seemingly heretical challenge to the "Central Dogma" of molecular biology: that genetic information is transferred in a hierarchy from DNA to RNA to protein. By the mid 1970's the discovery of reverse transcriptase confirmed this hypothesis (4,5) and this paved the way for the huge advances in the understanding of cellular biology, cancer biology and human retroviruses that continue to this day.

### **1.1.2 Classification of retroviruses**

The family Retroviridae of enveloped viruses is divided into two families: Spumavirinae (a poorly characterised group which cause foaming of cultured cells); and Orthoretrovirinae, which includes the genus Lentivirus from "lente" in Latin, so called because of the prolonged incubation period between infection and disease (Freed and Martin, 2001). The lentiviral genome is carried as two non-identical, single strands of positive sense RNA and its replication has two defining hallmarks – the genomic RNA must be reverse transcribed into a linear

double stranded DNA copy and this DNA must be subsequently integrated into the host cell genome.

Lentiviruses cause chronic persistent infection in bovines, equines, ovines, felines and primates (6). Most are exogenous, transmitting horizontally between hosts, whilst some have infected germ line cells and are transmitted vertically as genomic loci. Examples include prosimian endogenous lentiviruses, which infected germ-line cells of lemurs approximately four million years ago (8,9). These “viral fossils” allow direct inferences about the timescales of lentiviral evolution (10).

### **1.1.3 Discovery of HIV-1**

In June 1981, the CDC published a case series of five young men who were treated for a rare *Pneumocystis carinii* (now *jiroveci*) pneumonia in Los Angeles, California (11). They were the first cases of HIV-1 infection to be recorded. The causative agent was unknown but immunodeficiency and subsequent infection with opportunistic pathogens lead to individuals being classified as having acquired immune deficiency syndrome or AIDS. The discovery of the first human retrovirus human T-cell lymphotropic virus type I (HTLV-I) by Robert Gallo had required the development of techniques both for culturing T lymphocytes and for the sensitive detection of reverse transcriptase that would prove essential in the isolation of HIV-1. In 1983, in the laboratory of Luc Montagnier at the Pasteur Institute in Paris, Barré-Sinoussi et al described their isolation of a new human retrovirus from a lymph node of a patient with lymphadenopathy (12). In early 1984 Robert Gallo’s group published four papers describing in more detail the new human retrovirus as the probable cause of AIDS and several more labs isolated what we now know as HIV in quick succession, each giving it a different name but by 1986 the International Committee on Taxonomy of Viruses recommended the current name of Human Immunodeficiency Virus or HIV. A second similar virus, also a simian zoonosis, was discovered in 1986; HIV was renamed HIV-1 and the new virus named HIV-2.

Over three decades later HIV has become, by almost any metric, the most studied virus on earth and basic science research has transformed the clinical picture. What was previously an almost universally fatal disease can now be treated so that in the developed world, life expectancy is approaching that of non-infected people in some patient cohorts (13,14).

### **1.1.4 The Origins of HIV**

The majority of emerging infectious diseases have a zoonotic origin and HIV is no exception. But among primate lentiviruses the Human Immunodeficiency Virus type 1 (HIV-1) is unique in terms of pathogenicity and pandemic spread. Lentiviruses are known to infect over 40 different

species of primate (figure 1.1A) but, despite the wide distribution across species and geography, there are only 12 known zoonotic transmission events to human beings (figure 1.1 B). HIV-1 has four groups (M, N, O and P), each from a separate transmission event. M and N originated in chimpanzees (*Pan troglodytes troglodytes*) whilst O and P were likely transmitted from Gorillas (*Gorilla gorilla gorilla*) (15–18).

#### **1.1.4.1 HIV-2 origins**

HIV-2 is known to have had at least eight independent host transfers from sooty mangabeys (*Cercocebus atys*), each one creating a distinct lineage, although in most cases only a single sequence has been isolated (18,19). HIV-2 remains largely confined to west Africa and whilst it causes an illness similar to HIV-1, disease progression is slower with a larger number of patients failing to progress to end stage infection. It also appears to be less transmissible (20).

#### **1.1.4.2 HIV-1 origins**

Like HIV-2, HIV-1 groups N, O and P are found almost exclusively in west Africa. Only the HIV-1 M (for Main group) has spread to any appreciable degree. The pandemic has infected 60 million people and killed over half of them originated from a single transmission event from a chimpanzee most probably during the early part of the 20th century (21–23). There are nine subtypes of HIV-1 M: A-D, F-H, J and K. Subtype C is predominant in Africa and the Indian sub-continent accounting for almost half of cases world-wide, whilst subtype B is the dominant subtype in the Americas, Australia, and western Europe recombinant subtypes are being detected with increasing frequency (24).

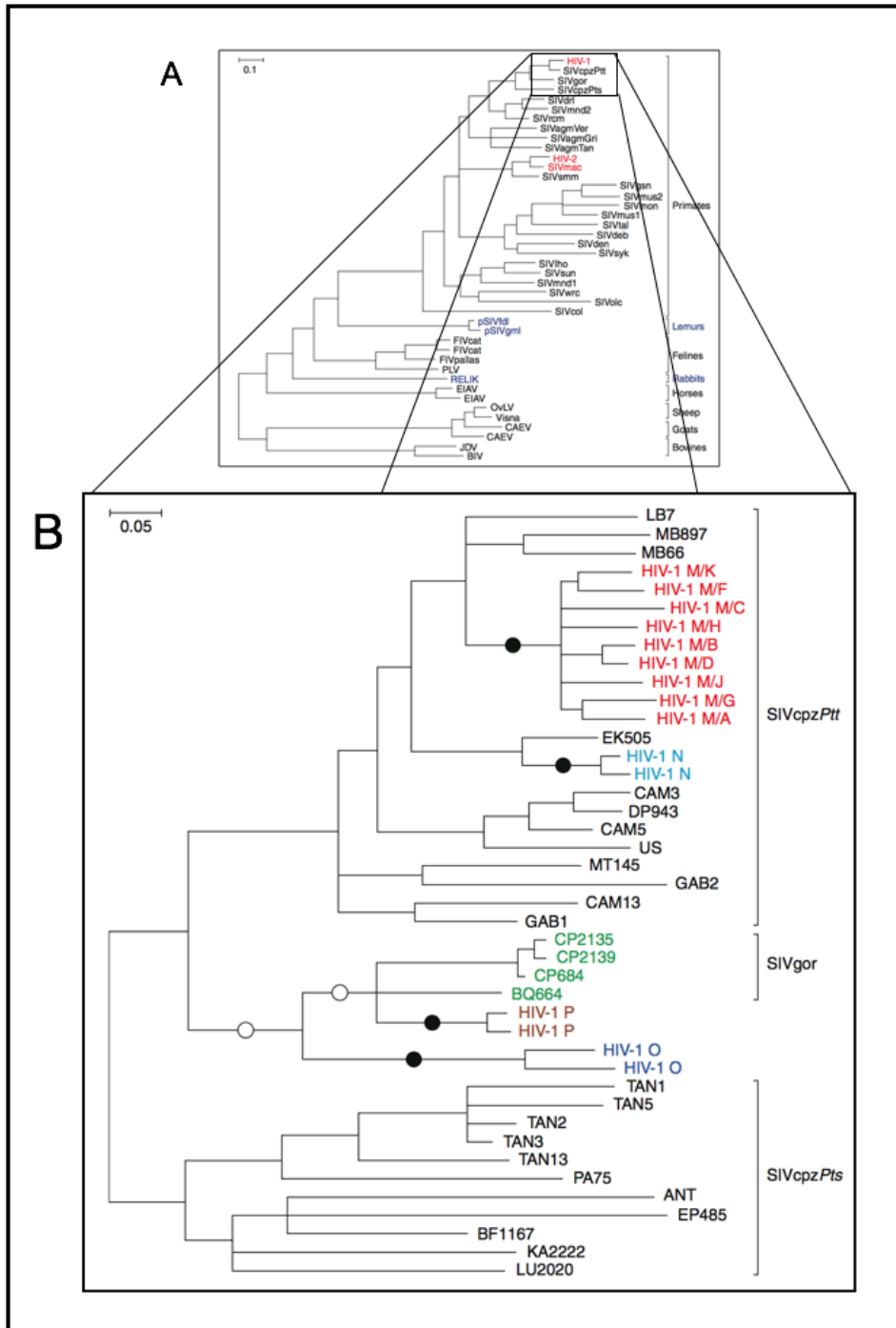


**Figure 1.1 Phylogeny of lentiviruses (A) and SIVcpz/HIV-1 (B).** (A) Mammalian lentiviruses phylogenetic relationships of *Pol*; host species are shown at the right. HIV-1, HIV-2, and SIVmac are in red; endogenous viruses in purple, exogenous viruses are in black. Horizontal branch lengths are shown to scale. Scale bar represents 0.10 aa replacements per site. (B) Phylogenetic relationships of representative SIVcpz, HIV-1, and SIVgor strains shown for a region of *Pol*. SIVcpz in black, SIVgor in green. The four clades of HIV-1 are shown in different colours. Black circles show zoonotic transmission to humans. White circles show branch possibilities for chimpanzee-to-gorilla transmission. Scale bar represents 0.05 nt substitutions per site. Both trees estimated using maximum likelihood methods (25). Adapted from Sharp, P.M., and Hahn, B.H. (2011). *Origins of HIV and the AIDS pandemic*. Cold Spring Harb. Perspect.

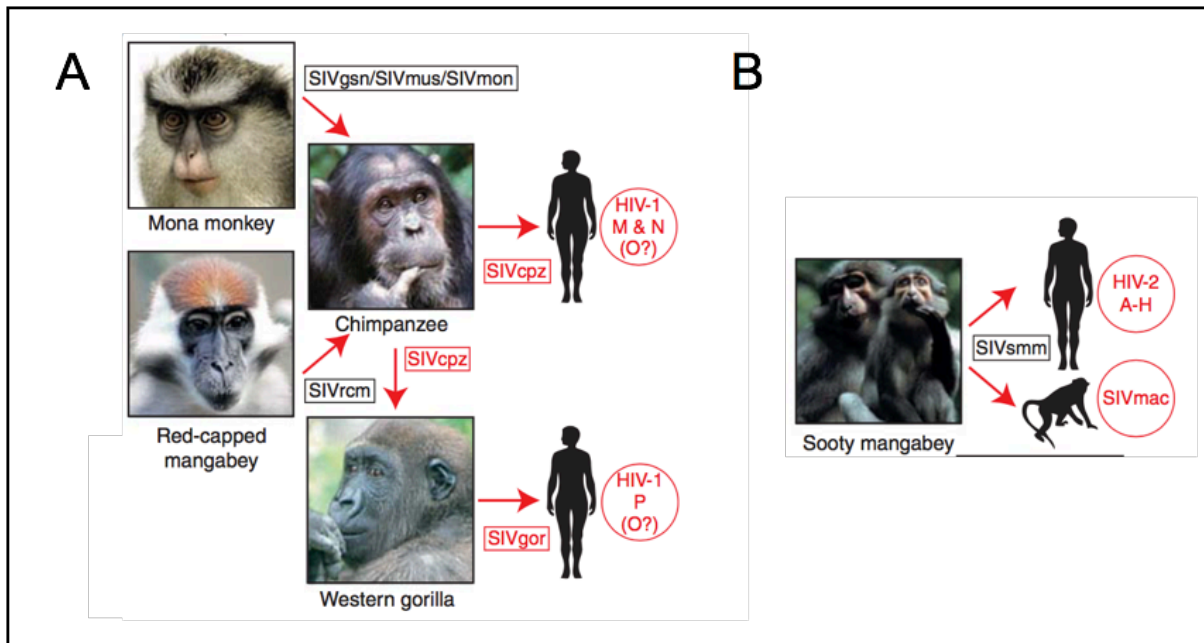


**Figure 1.2 Origins of HIV.** 40 different lentiviruses infect old world monkeys and African apes. Known examples of cross species transmission are highlighted in red with transmissions of HIV-1 from Gorillas and Chimpanzees (A) and HIV-2 from Sooty mangabeys (B). Adapted from Sharp, P.M., and Hahn, B.H. (2011). Origins of HIV and the AIDS pandemic. Cold Spring Harb. Perspect (18).

### 1.1.4.3 Simian Immunodeficiency Viruses

SIVs are each named with a three letter designation derived from the common name of the corresponding non-human primate species; e.g. SIVrcm for SIVs from red-capped mangabey, SIVgsn for greater spot nosed monkeys, etc. Most primate species harbour a single lineage of SIV which clusters in a phylogenetic group with viral sequences from the same species indicating that the vast majority of spread is within not between species. There have been recombination events between each of the different major lineages which complicate the SIV phylogeny. The position a virus takes in an evolutionary tree varies depends on the genomic region which is analysed. SIVrcm, SIVmnd2 and SIVgsn all show discordant phylogenies depending on the region analysed indicating that both cross species transmission and subsequent co-infection with divergent strains have occurred (26–29). There have been some significant cross species transmissions however with substantial secondary spread including SIVgor and most notably HIV-1 and 2 (figure 1.2A and B). There are also SIVs that have emerged as a result of recombination including SIVcpz (26,30,31). Chimpanzees hunt other monkeys and through this predation may have acquired SIV. Phylogenetic analysis has shown that SIVcpz is a complex mosaic generated from recombination (see figure 1.3 A and B). The 3' LTR, the 5' half and the *nef* gene align most closely with SIVrcm (red capped mangabey - *Cercocebus torquatus*) while the *vpu*, *tat*, *rev* and *env* genes align most closely with a clade of SIV's from Cercopithecus species (the greater spot nosed, moustached and mona

monkeys) (17,32). The current range of the central *P.t.trogodytes* overlaps with these two species and this recombination most likely occurred in a single chimp and became the ancestor of today's SIVcpzPtt (figure 2 A). No other SIV has been observed in a chimpanzee despite frequent exposure from hunting other small primates (33).

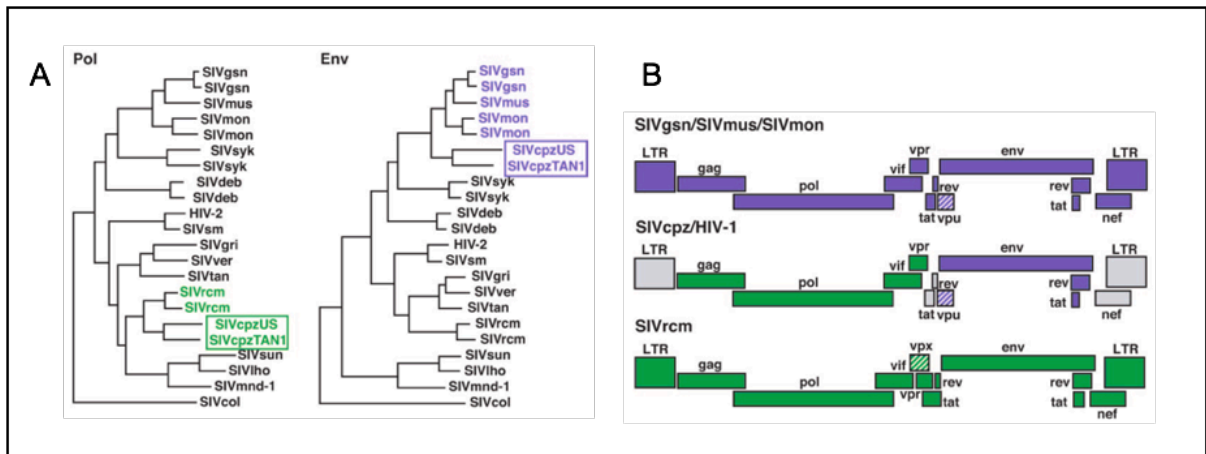


**Figure 1.3 Recombination of SIVcpz.** (A) Maximum-likelihood phylogenies of primate lentivirus Pol and Env sequences. The close alignment of SIVcpz to SIVrcm in Pol, and of SIVcpz to SIVgsn, SIVmus, and SIVmon in Env, are highlighted in green and purple, respectively. (B) Schematic of the genome of SIVcpz. Genomic regions are colored as in (A) according to their alignment with SIVrcm (green) or the SIVgsn/SIVmus/SIVmon lineage (purple). Grey areas are of unknown origin. Vpu and vpx genes are highlighted. Adapted from Sharp, P.M., Shaw, G.M., and Hahn, B.H. (2005). Simian immunodeficiency virus infection of chimpanzees. *J. Virol.* 79, 3891–3902

Mitochondrial DNA sequencing has been used to classify chimpanzees into four subspecies: *Pan troglodytes troglodytes*, *Pan troglodytes schweinfurtheii*, *Pan troglodytes verus* and *Pan troglodytes ellioti*. These subspecies are geographically separated from each other across western and central equatorial Africa. Of these four subspecies only two are known to harbour SIV: *Pan troglodytes troglodytes* in west/central Africa and *Pan troglodytes schweinfurtheii* in central/east Africa. SIV has not been detected in either *P.t. verus* or *P.t. ellioti* suggesting that chimpanzees acquired SIVcpz after the geographical isolation of West African and Nigerian subspecies (34).

Sequence analysis of SIVcpz strains reveals two separate lineages SIVcpzPtt and SIVcpzPts (17), which show only 50-70% homology in their Gag, Pol and Env protein sequences. Initial studies of SIV prevalence were undertaken on animals captured as infants and so under represented the rates of infection in the wild (35). Subsequent development of non-invasive methods for the detection and characterisation of SIVcpz in faecal and urine samples has meant that many thousands of samples from almost 100 field sites are available for analysis. Wild seroprevalence appears highly variable. Some chimpanzee troops in both east and west

Africa have up to 50% prevalence whilst in other areas cases are rare or absent (21,36). It was initially believed that SIVs were non-pathogenic in their natural hosts but sequential faecal sampling in habituated populations of eastern chimpanzees showed that SIV infection is associated with a 10-16 fold increase in risk of death at a given age as well as reduced fertility (37). Additionally, AIDS like illness and pathology following infection has been described in wild *P.t.schweinfurthii* chimps at post mortem and in a captive *P.t.troglodytes* with low CD4+ counts and infection with unusual and diverse pathogens (38).

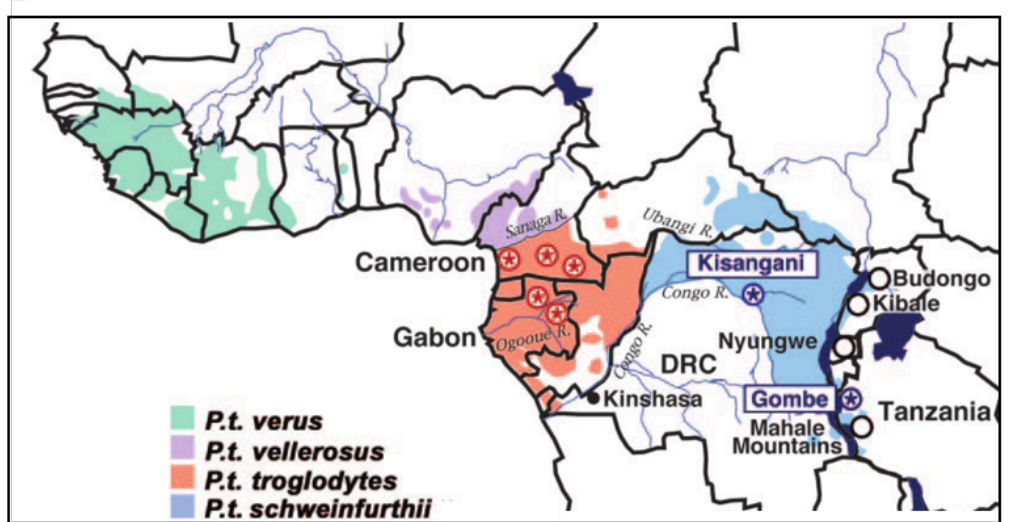


**Figure 1.4 Chimpanzee Reservoirs of Pandemic and Non-pandemic HIV-1.** Study sites in Uganda, Rwanda, Tanzania and Democratic Republic of Congo are indicated. Asterisks indicate the presence of natural SIVcpz infection. Adapted from Sharp, P.M., Shaw, G.M., and Hahn, B.H. (2005). Simian immunodeficiency virus infection of chimpanzees. *J. Virol.* 79, 3891–3902 (39).

#### 1.1.4.4 Zoonotic transmission of SIV

The same faecal sampling studies also traced the ancestor of HIV-1M and N to particular *P. t. troglodytes* communities in south eastern and central Cameroon (40). HIV-1 group N is most closely related to SIVcpzPtt from groups in the Dja forest of South Central Cameroon and group M aligns best with chimpanzee viruses from the confluence of the Sangha and Ngoko rivers on the border of Cameroon and Central African Republic (figure 1.4). The details of the transmission are unknown, and possibly unknowable, but must have involved blood or mucous membrane exposure to blood or bodily fluids from an infected ape: hunting and butchering bushmeat offers the most likely explanation. The secondary forests of west-central Africa where HIV-1 M crossed the species barrier have dense thorny foliage meaning hunters acquire multiple skin breaches and so butchery of bushmeat offers ample opportunity for blood to blood contact (figure 1.5). Although the first case reports of HIV were only published in 1981 the earliest record of HIV-1 infection is from 1959. The virus was found a serum sample from

a Bantu male living in Leopoldville, Belgian Congo (now Kinshasa in the DRC) and molecular clock analyses date the start of the group M epidemic to the beginning of the 20<sup>th</sup> century (23,36,41).



**Figure 1.5 Bayaka hunter butchering a mona monkey.** Photo C. van Tulleken.

Whilst SIV cpzPtt is known to have transmitted to humans at least twice there is no known counterpart of SIVcpzPtt in humans (41). Since SIVcpzPtt strains have transmitted to humans and gorillas a minimum of five times the lack of evidence of similar transmission from Pts chimpanzees from the east is striking and infections rates determined by field sampling are estimated to match those found in *P. t. troglodytes*. Differences in interactions between humans and apes in central and east Africa may explain the lack of observed transmissions or it may be that transmissions have gone unrecognised because of a lack of human testing using lineage specific serological tests. But it may also be that there is a molecular species barrier. SIVcpzPtt has been found to replicate in CD4 cells *in vitro* but these assays are unlikely to recapitulate the necessary conditions for *in vivo* transmission and replication (27).

This study identifies SIV and HIV Vpr proteins which, when ectopically expressed, differentially antagonise innate immune signalling pathways and expression from transfected DNA. This

may be a determinant of cross species spread since all the viral lineages that have spread to humans do antagonise sensing and many of those that have not spread are much less able to antagonise sensing including SIVcpzPts *Vpr*. A sequence alignment of all available HIV-1, SIVcpz and SIVgor *Vprs* was constructed which shows an 11-18 residue deletion at the C-terminal end of the protein. Additionally, an SIV *Vpr* from a mona monkey has been identified as stimulating NFκB signalling in the absence of co-transfected immune protein and may prove to be a useful tool for dissection of NFκB signalling pathways.

#### **1.1.4.5 Origins of *Vpr* and *Vpx***

Two of the six major lineages of primate lentiviruses encode *Vpx*: HIV-2/SIVsm (sooty mangabey) related viruses and a lineage represented by SIVrcm (from red capped mangabeys). However all extant lineages of SIV and HIV encode a paralog of *Vpx*: *Vpr* (42,43) (figure 1.3A and B). *Vpr* and *vpx* share sequence similarity and thus a common ancestry. It was previously believed that the additional *Vpx* gene in SIVsm resulted from a gene duplication event after the divergence of this lineage but this would require that the *vpx* and *vpr* from SIVsm are more closely related to each other than to *vpr* from any other lineage and, as can be seen from the phylogenetic trees generated for this thesis as well as those published previously (43,44), this is not the case. *Vpr* from SIVsm is more closely related to *vpr* from HIV-1/SIVcpz but *vpx* is more closely related to the *vpr* of SIVagm. This is inconsistent with a duplication event after divergence. A duplication before divergence of the different lineages seems unlikely as it would mean that *vpx* had been deleted from multiple separate lineages. Thus, the most parsimonious explanation seems to be that SIVsm acquired *vpx* by recombination rather than duplication, presumably in a monkey co-infected with both viruses. There is other evidence of recombination between these lineages (SIVagm has had its own 3' gag and 5' pol genes replaced with those of SIVsm) and these African green monkeys and sooty mangabeys share habitats in West Africa.

## 1.2 Clinical HIV and HIV Epidemiology

Over 70% of the estimated 35 million people living with HIV are in sub-Saharan Africa (45). Prevalence is increasing due to improved access to antiretroviral therapy increasing the life expectancy of infected individuals: in 2015 over 17 million people were estimated to be on antiretroviral therapy compared with just 7.5 million in 2010. In summer 2016 United Nations member states committed to ending the AIDS epidemic by 2030 setting out a Political Declaration calling for access to comprehensive sexuality education, harm reduction services and focused outreach to at risk groups (young women, men who have sex with men, commercial sex workers, injecting drug users, transgender, incarcerated and displaced people) (46). Whilst efforts globally have reduced heterosexual transmission, regressive attitudes toward harm reduction policies in many countries, especially in the former Soviet bloc and eastern Europe, have limited the implementation of demonstrably effective opioid substitution and needle exchange programs (47).

In western Europe, Australasia and the Americas the primary route of transmission is between men who have sex with men and incidence has remained constant (48) owing to a complex and poorly understood combination of “therapeutic optimism” (an increase in risk taking behaviour following the availability of effective treatment), the increased risk of transmission associated with receptive anal intercourse and limited access to care determined by societal factors like stigma (49,50).

Globally HIV is the fifth leading cause of loss of life calculated by disability adjusted life years (51) but deaths have decreased from 2.3 million in 2005 to just over 1 million in 2015 (52).

### 1.2.1 Clinical HIV infection

HIV targets cells expressing CD4 and chemokine receptors CCR5 and/or CXCR4 including T cells, monocytes, macrophages and dendritic cells. It has been reported that cells lacking these receptors, including renal epithelial cells and astrocytes, may also be infected (53,54) but these studies have not been replicated. Transmission appears to be of a single or small number of founder viruses and is followed by a period of rapid viral replication accompanied by a large systemic inflammatory response (55,56). Viral load then stabilises at a set point level that may have orders-of-magnitude variation ranging from <20 virions/ul of plasma up to over 1 million for reasons involving both host genetics, adaptive and innate immune responses and virus genotype (57,58). Estimates vary but some studies report that over 30% of the variation in set point viral load (SPVL) is heritable (58). Understanding this variation is

important since SPVL appears to be the most robust surrogate marker of virulence or disease progression as well as being the major risk factor for transmission (57).

The initial infection may be asymptomatic or in around 70% of people followed by a brief “flu-like” seroconversion illness or acute retroviral syndrome characterised by a rapid increase in markers of acute inflammation, the production of non-neutralising antibodies and HIV specific CD4 and CD8 T cells (59). HIV RNA in the blood falls from an initial peak at around 6 weeks post infection and the SPVL is established between weeks 9 and 12. This is typically followed by a prolonged period of clinical latency. CD4 T cells are lost progressively in the blood but gastrointestinal CD4 cells are lost early on. For example, individuals with the *HLA-B27* allele infected with clade B can mount an effective T cell mediated immune response but the eventual progression to immunodeficiency with loss of CD4 T cells is almost universal. There is both death of cells and loss of effector function but surprisingly the mechanisms underlying these processes remain unclear (60). It is not known, for example, if it is the infected cells themselves that die (61) or if it is an effect on uninfected bystander cells that is the predominant cause of cell loss (62).

The WHO classifies adult HIV patients in four clinical stages, from asymptomatic (stage 1) to AIDS (stage 4). At approximately three months following infection patients develop neutralising antibodies and this in turn selects for viral escape mutants (63). Even in the roughly 20% of patients that produce broadly neutralising antibodies, escape mutants mean that they confer little benefit to the patient (64,65).

Progressive, catastrophic immune dysfunction due to CD4 T cell depletion is the clinical hallmark of HIV-1 infection with the largest observed depletion happening early in the gastrointestinal tract. Unlike the early loss of CD4 cells in the blood, gastrointestinal T cells recover only minimally even with treatment (66). As well as loss of T cells there are effects on T cell subsets with loss of Th17 cells and the mucosal associated cells required for bacterial defense. In both humans and rhesus macaques, a combination of loss of gastrointestinal lymphocytes, endothelial apoptosis and increased gut permeability raises plasma levels of bacterial components like lipopolysaccharide which activates TLR4 leading to the production of IL-6 and TNF $\alpha$  (67). Other factors increasing inflammation include production of IFN $\alpha$  secondary to TLR7 and TLR8 activation (68), co infection with CMV (69) and dysregulation of T cell homeostasis with altered ratios of T helper 17 and regulatory T cells (70). Inflammatory markers remain increased even when CD4+ T cell counts are restored with antiretroviral therapy whilst the fact that intensification of treatment with integrase inhibitors has been observed as reducing T cell activation may indicate that ongoing viral replication on treatment may contribute to persistent elevated inflammatory markers (71).

Following the latent or asymptomatic phase often lasting up to a decade, without treatment the progression to stage 2, the symptomatic stage of infection, begins. It is characterised by unexplained weight loss (<10% of total body weight), persistent generalised lymphadenopathy, oral lesions such as thrush and oral hairy leukoplakia, hypoproliferative anaemia and thrombocytopenia and reactivation of varicella-zoster (shingles).

Stage 3, the moderately symptomatic stage, has additional clinical manifestations including greater weight loss, unexplained diarrhoea, bacterial infections including pulmonary tuberculosis, pyelonephritis, pneumonia, empyema meningitis and osteomyelitis. Mucocutaneous conditions worsen.

Stage 4 is the severely symptomatic stage. There is a move away from use of the term AIDS (Acquired Immune Deficiency Syndrome) although it is still widespread(72). Clinical conditions that allow a diagnosis of AIDS in the absence of other biological information include Penumocystis pneumonia, extrapulmonary TB, HIV encephalopathy, CNS toxoplasmosis, chronic orolabial herpes simplex, oesophageal candidiasis and Kaposi's sarcoma (73).

### **1.2.2 Treatment and prevention of HIV infection**

The advent of highly effective and relatively side effect free treatment in the developed world has meant that for people with HIV the major causes of death in high income countries are very similar to people without the virus – cancer and cardiovascular disease (14).

Since the development of combination antiretroviral therapy in the mid 1990s there are now more than 25 drugs licenced for treatment and effective single dose regimens with minimal side effects profiles are now widely available in the developed world. Life expectancy is now estimated to be approaching normal for patients with restored CD4 counts and suppressed viral loads on treatment (74). Typically, treatment will combine two nucleoside reverse transcriptase inhibitors (NRTIs) with a non-nucleoside reverse transcriptase inhibitor (NNRTIs), protease inhibitor (PI) or integrase inhibitor. Whilst these regimens reduce the plasma viral load to below the limit of detection in most people, CD4 T cell number increases are more variable and individuals with limited CD4 T cell recovery have elevated chances of poor outcomes (75). Debate continues over the CD4 threshold for starting treatment and most international guidelines have raised the required CD4 level to 500/ul. This may have a benefit of reducing transmission but may increase exposure to toxic effects of drugs and increase the chance of resistance (76). In the UK current guidelines recommend all people infected with HIV start antiretroviral treatment (77). Poor adherence increases the risk that viral replication will take place in the presence of therapy resulting in the selection of resistant viruses and it

has been shown that these viruses can transmit; there is >10% prevalence of drug resistant virus in antiretroviral naïve patients in high income countries (78).

There is robust evidence to support treatment as a prevention strategy since viral load levels, which are dramatically reduced by effective treatment, are the main factor influencing transmissibility. A 2011 study demonstrated that early initiation of treatment reduced HIV transmission in discordant couples by 96% (79) and this has been confirmed with several subsequent studies (80,81) but the implementation of “Test and Treat” strategies that use treatment as prevention has proved challenging in underdeveloped and rural settings (82). Treatment as prevention has been used for more than two decades to prevent mother to child transmission and studies conducted in developed setting indicate that only 14 days of treatment is required to reduce risk of transmission to less than 1% (83,84). Pre-exposure prophylaxis has also been shown to be extremely effective (85–87) but despite the population wide benefits as well as the economic and moral arguments (85) it is still not widely available in developed settings where state funded health care is available, a surprising deficiency in settings where more progressive policies might be expected (88).

## 1.3 Overview: HIV-1 structure

### 1.3.1 The HIV genome

All retroviruses share three common genes: *gag* (for “group specific antigen”) which codes for the proteins which form the matrix, capsid and the nucleocapsid; *pol* (for DNA polymerase) which encodes the reverse transcriptase, integrase and protease enzymes (PRO, RT and IN); and *env* (for envelope proteins) which encodes the surface and transmembrane proteins of the viral envelope (figure 1.6). Of the nine genera of retroviruses, five have a “simple genome” characterised by having not more than one coding region in addition to *gag*, *pro*, *pol* and *env*. Complex retroviruses, including all simian and human immunodeficiency viruses, have multiple splice donors in the genome giving rise to additional regulatory proteins derived from multiply spliced mRNAs. HIV is a complex retrovirus with six additional reading frames: *vif*, *vpr*, *vpu*, *tat*, *rev* and *nef*, all of which are conserved in almost all clinical isolates (figure 1.6).

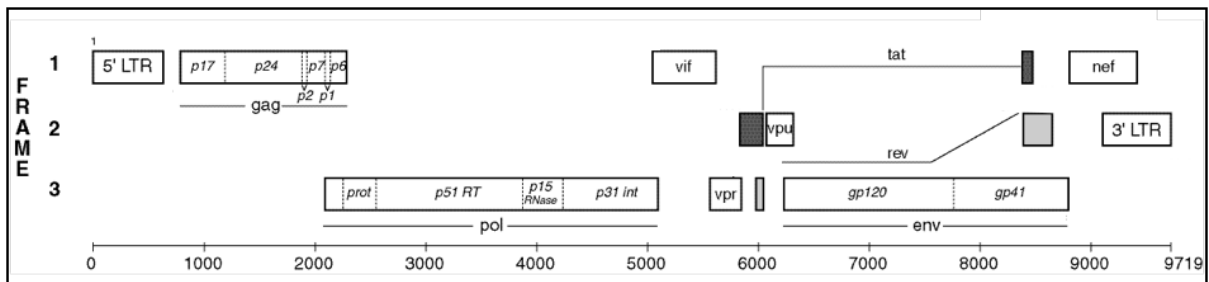


**Figure 1.6 Landmarks of the HIV-1 genome, HXB2 (K03455).** The layout of the HIV-1 genome. Boxes show the open reading frames and the non-coding, regulatory 5' and 3' LTRs. Reading frames are labelled 1,2,3 on the left and box position indicates the reading frame of each gene. Dashed lines indicate maturation cleavage sites for *gag*, *pol* and *env* polyproteins. The *tat* and *rev* spliced exons are shown as shaded rectangles. Adapted from Los Alamos National Laboratory HIV-1 Gene Map 2014.

The integrated genome of HIV-1, or provirus, is 9.7kb in length (89). Repeated sequences called Long Terminal Repeats (LTRs) flank each end of the provirus. The LTRs contain important regulatory regions for initiation of transcription and polyadenylation (90). Adjacent to these are unique untranslated regions U5 and U3. The U5 region contains the “kissing loop” required for genome dimerization and packaging. Between the LTRs are three classes of genes: i) structural proteins (Gag, Pol and Env) ii) regulatory proteins (Tat and Rev) and iii) accessory proteins (Vpu, Vpr, Vif and Nef) (91).

#### 1.3.1.1 Structure of the mRNA genome

There are a number of important structural elements of the transcribed mRNA. TAR is the target sequence for viral transactivation comprising first 45 nucleotides of the mRNA which

form a hairpin stem loop. This sequence provides the binding site for the viral Tat protein which activates transcription elongation. The RRE is the Rev responsive element and consists of 200nt between gp120 and gp41 which provide a binding site for Rev (92). The Psi elements are stem loop structures overlapping the Gag start codon which allow binding of unspliced genomic transcripts by Gag p7 (NC) protein and packaging of genomes (93,94). Finally SLIP is a TTTTTT slippery site which regulates the ribosomal frameshift out of Gag and into Pol allowing production of up to 20 times more Gag than Gag-Pol (as discussed below in 1.7.2.2 and 1.8.9.4) (95).

## **1.3.2 Overview of Transcription, Translation and gene products**

### **1.3.2.1 mRNA splicing**

The HIV-1 primary transcript contains multiple 5' splice donors and 3' splice site acceptors and generates more than 25 mRNAs (96). While many of these mRNAs are polycistronic, they generally only express a single gene product. Initiation codon efficiency and proximity to the 5' end of the mRNA determines the reading frame used.

### **1.3.2.2 Viral mRNA products**

There are three size classes of mRNA produced. First the 9.7-kb full length, unspliced RNA produces the Gag and the Gag-Pol precursor proteins or is incorporated into the virion as the RNA genome. It produces two proteins from one initiation codon due to translational frameshifting discussed above in 1.7.1.1 and below in 1.8.9.4). Second, the incompletely spliced 4kb class of RNAs use the splice donor site closest to the 5' end of the genome together with any of the central region splice acceptors. These RNAs encode Vif, Vpr, Vpu and Env and the single exon form of Tat. Finally, the doubly spliced 2kb class of mRNAs from which both introns of HIV have been spliced out. They express the two exon form of Tat, along with Rev and Nef. In each class of spliced RNA there are multiple species generated by the presence of several different 3' and 5' splice sites.

### **1.3.2.3 Gag and Gag-Pol fusion protein**

The *gag* gene produces an unspliced mRNA which encodes the 55kDa Gag myristoylated precursor protein (p55). After budding during viral maturation this polypeptide is cleaved by the virally encoded protease (PR) into the structural proteins matrix (MA, p17), capsid (CA, p24) and nucleocapsid (NC, p7), as well as p6 and the spacer peptides 1 and 2 (SP1/2) (reviewed in Freed, 2015). During translation a ribosomal frameshift event, triggered by a specific cis-acting RNA motif, occurs around 5% of the time. This means that the ribosomes shift to the pol reading frame without translation being interrupted, producing a Gag-Pol fusion

protein (98). This Gag-Pol fusion protein (p160) is the precursor for the viral enzymes. Pol encodes the enzymes protease (PR, p10), reverse transcriptase (RT, p51/66) and integrase (IN, p31). Finally, during maturation the Pol polypeptide is cleaved away from Gag by the viral protease which then digests it to produce further protease (PR, p10), RT (p66) and the integrase (detailed in section 1.8.11).

#### **1.3.2.4 Env**

The *env* gene encodes the envelope glycoprotein of 160kDa (gp160) which is produced as a precursor and then cleaved by the host protease furin into two glycoproteins of 120 and 41kDa: the external gp120 and the internal gp41. These form the stable Env heterodimers which are secreted to the cell surface forming trimers. Both binding sites for the CD4 receptor and the chemokine receptors, which act as co-receptors for HIV-1, are found on gp120 (97,99).

### **1.3.3 HIV-1 mature virion structure**

Viral particles are assemblies of both viral and host cellular macromolecules. All exogenous viruses form particles which have a common function – the protection and transmission of the viral genome, particularly from environmental challenges (like temperature, desiccation, chemicals, enzymes and pH). Whilst HIV *in vitro* has been shown to be quite hardy outside the body persisting for up to a week on a wet surface (100) in real terms, transmission requires sexual or blood contact. It may be that much of viral structure in the case of HIV has evolved to avoid the challenges of the intra and extracellular immunity; thermal and chemical challenges to transmission and replication may be less significant *in vivo*.

#### **1.3.3.1 The viral envelope**

The mature virion is roughly spherical with a lipid bilayer membrane derived from the host cell and embedded with viral Env spikes consisting of gp120/gp41 trimers as well as host cell surface proteins such as intracellular adhesion molecule 1 (ICAM-1) (99,101).

Gp41 comprises a cytoplasmic C terminal tail, a transmembrane domain and an ectodomain with two large helical regions (the C- and N- terminal helical regions or CHR and NHR). Gp120 is a globular protein that lies on the cell surface and consists of five conserved loops and five highly variable loops (C1-5 and V1-5). Env trimers are incorporated onto the surface of new HIV-1 virions during budding so that each virion has 10-15 Env spikes on the surface (Kwong et al., 1998; Wilen et al., 2012a). Env is the only viral protein exposed on the surface of the virions and is thus the major target for antibodies. It is thought that only one or two Env spikes are needed for viral fusion and maintaining a low number of surface viral proteins may contribute to antibody evasion (104).

### 1.3.3.2 The capsid core

Under the lipid bilayer of the mature virion is a shell of MA (105). Beneath MA is the conical viral core of CA protein. This mature capsid assumes the geometric configuration of a 'fullerene cone', named after the architect and systems theorist, Buckminster Fuller, who popularised the architectural use of geodesic domes where combinations of hexamers and pentamers are used to create 3 dimensional curvature in surfaces. In capsid cores hexamers of the capsid protein form a lattice which incorporates capsid-protein pentamers so that it closes. A structure consisting of only hexamers forms only tubes whilst the introduction of pentamers allows for curvature in an additional dimension allowing a closed structure to form. Estimates of the total number of subunits varies with the most recent atomic level model suggesting a lattice of 216 hexamers and 5-7 pentamers at each end of the capsid. Capsid-protein structure has been determined by X-ray crystallography (106) and cryo-electron microscopy (107).

The amino-terminal domain (NTD) of HIV-1 capsid protein comprises seven  $\alpha$ -helices and a  $\beta$ -hairpin. The carboxy-terminal domain (CTD) comprises four  $\alpha$ -helices and a flexible linker with a  $3_{10}$ -helix connecting the two structural domains (108–110). A  $3_{10}$ -helix is a protein secondary structure with three amino acid residues per turn and 10 atoms in the ring formed by making the hydrogen bond. Interactions between the N-terminal domains form the hexamers and pentamers but it is interactions between the CTDs that form the final shape of the viral core. Zhao et al showed with cryo-electron microscopy and mutagenesis studies that the structure of a tubular assembly of hexamers has a three helix bundle at the interface between three hexamers with critical hydrophobic interactions required for capsid assembly, stability and to produce infectious virus (111).

### 1.3.3.3 The viral genome

Inside the capsid core is the dimeric single stranded RNA genome. Genome RNAs are packed as a non-covalent dimer or duplex held together by the interaction of sequences in their 5' UTR which form a "kissing loop" structure. Unspliced viral RNA is selectively packaged owing to a requirement for elements located downstream of the first splice donor (112,113). It may be that in fact the genome is more than simply "packaged". Unpublished data from our lab show that changes in packaged genome length alter viral titre and recent work in RNA phages shows that an RNA genome may play a significant role in capsid assembly (114).

The viral mRNA genomes are capped at their 5' ends and poly-adenylated at the 3' ends like eukaryotic mRNAs. They are associated with the nucleocapsid and Vif as well as the integrase

and reverse transcriptase enzymes required for the early stages of infection. RNA dimerization is required for it to be packaged and for virions to be infectious (115,116).

HIV-1 particles also package a specific host transfer RNA (tRNA). RT needs both a primer and a template: the plus stranded genomic RNA forms the template and the primer is the host tRNA Lys3 which has a 3' end is complementary to a sequence at the 5' end of the viral genome called the primer binding sequence (PBS) just downstream of U5 and 18 nucleotides at the 3' end of the tRNA (117).

## 1.4 The Viral Life Cycle

The retrovirus lifecycle is, by convention, divided into two phases. The first or early phase involves entry to the cell after binding and fusion, followed by reverse transcription of the RNA genome to DNA and the subsequent integration of the viral DNA into the host genome. The late phase consists of viral gene expression and particle formation through transcription, nuclear export, assembly, budding and maturation. Transmission follows maturation and precedes progression to the early phase of the next life cycle.

### 1.4.1 Receptor Binding

The first phase of the viral replication cycle is viral entry and is a highly-orchestrated process involving a series of protein-protein interactions and the hijacking of various components of the cellular machinery (figure 1.7). CD4 and a co-receptor engagement by Env are necessary events but there are other processes (viral membrane surfing, endocytic entry, synaptic transmission, and intracellular signalling pathways activated through receptors) which may have roles in overcoming host restrictions and enhancing infection efficiency. Viral entry starts following virus host cell adhesion and ends following fusion of the cell and viral membranes and arrival of the viral capsid in the cytoplasm.

Both viral Env protein and/or host cell membrane proteins incorporated into the virion enable host cell to virus binding. Env mediated attachment can be non-specific (Env is able to interact with cell surface heparan sulfate proteoglycans (118)) or results from specific interactions between Env and  $\alpha 4\beta 7$  integrin (119), or pattern recognition receptors such as DC-SIGN (Arrighi et al., 2004). Binding to these attachment factors allows Env to come into close proximity with the viral receptor, CD4, and co-receptors and has been shown to augment infection *in vitro* and *in vivo*.

Binding of Env to the cell surface receptor CD4, its primary receptor, is the first step of entry which is known to be required for infection (121). Env comprises a glycosylated trimer of gp120 and gp41 heterodimers. There are five conserved domains (C1–C5) in the gp120 subunit along with and five variable loops (V1–V5), which show wide genetic heterogeneity between them. The variable loops are located on the surface of gp120 and their position and variability, especially the V3 loop, have important roles in immune evasion and co-receptor binding (122). The gp120 subunit binds CD4, a member of the immunoglobulin superfamily that enhances T cell receptor signalling (121,123). Direct interaction between the highly conserved CD4 binding site of gp120 and CD4 is the first irreversible step in HIV-1 entry (103,124).

Env binding to CD4 leads to conformational changes in V1 and V2 which cause the exposure of the third variable loop and formation of a 4 stranded  $\beta$ -sheet called the bridging sheet. These are both co-receptor binding sites and this initiates the third step in viral entry: co-receptor engagement (125,126).

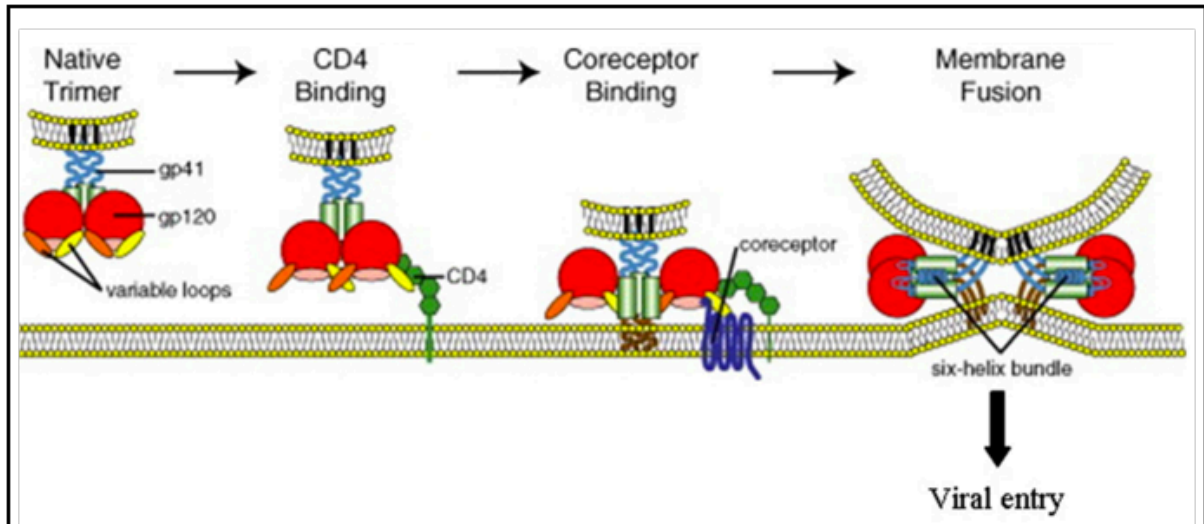


**Figure 1.7 HIV-1 entry.** The gp120 trimer (red) undergoes structural changes following binding to CD4 (green). These open variable loops V1/V2 and V3 (orange and yellow), exposing the CD4 “bridging sheet” that will be recognised by the co-receptor (CCR5 and/or CXCR4) and trigger the insertion of the gp41 fusion peptide into the cell membrane. Adapted from Connell, B.J., and Lortat-Jacob, H. (2013). Human Immunodeficiency Virus and Heparan Sulfate: From Attachment to Entry Inhibition. *Front. Immunol.* 4, 385

## 1.4.2 Co-receptor engagement

HIV-1 can use two different co-receptors, CXCR4 and CCR5 (127–132). Both CXCR4 and CCR5 are seven transmembrane domain G coupled chemokine receptors. Early studies found that CD4 was insufficient for infection by HIV and this led to the search for additional receptors (121,133). In 1995, CXCR4 was identified as a major HIV co-receptor (134). CXCR4 was found to function as a co-receptor for what was previously called T-cell line tropic strains of HIV but not for macrophage tropic viral strains unable to enter T-cell lines. The natural ligands for the CCR5 receptor (MIP-1a, MIP-1B and RANTES) were found to block entry into CD4+ T-cells and this led to the discovery of CCR5 as a co-receptor for macrophage tropic virus strains (130,135). The importance of CCR5 was demonstrated when a 32 base-pair deletion in *ccr5*, termed *ccr5* $\Delta$ 32 was discovered to cause retention of CCR5 in the endoplasmic reticulum. Homozygosity confers a high level of resistance to HIV-1 while heterozygosity confers partial resistance to infection and disease progression (136).

Chemokine receptor CCR5 using viruses are termed R5 HIV. Viruses that use CXCR4 are termed X4 HIV. Viruses that can use both co-receptors are called dual or R5X4 (137). With

few exceptions only R5 and R5X4 viruses are transmitted between infected individuals(138). This is poorly understood but likely relates to available, infectable cells at the anatomical sites of infection i.e. predominantly mucous membranes. Viral chemokine use or tropism is generally related to immune status. In early stage HIV infection, almost all HIV is CCR5-tropic, sometimes referred to as R5 virus. In patients with more advanced HIV infection, about half will have X4 virus (HIV that uses the CXCR4 co-receptor) or dual-/mixed-tropic virus (139,140). Co-receptor switching is poorly understood. X4 viruses may be more recognisable to the immune system and so do not arise until dysregulation has already occurred or it may be that the virus is forced to switch tropism after the body becomes depleted of CCR5 expressing cells (141).

Whilst the structure of CD4 alone and in complex with HIV has been solved less is known about the structure of Env with the HIV co-receptors (103,124) and the precise interactions of Env and co-receptor have yet to be elucidated.

HIV may hijack host cell machinery to gain access to sites with greater membrane fusion efficiency. If the site of attachment is distal, on filopodia or microvilli for instance, HIV has been shown on cell lines to use a “surfing” process to move to a more proximal part of the cell. This may facilitate endocytic uptake, allowing the virus to reach regions with high co-receptor expression levels enabling fusion to take place close to the nucleus, the ultimate target of the virus. It is not known if this is an important process *in vivo* (142).

### **1.4.3 Membrane fusion**

The final stage of viral entry requires further conformational change in gp120/gp41 induced by Env binding. Gp41 has a hydrophobic fusion peptide which is inserted into the host cell membrane and then folds at a hinge region bringing together the amino-terminal and carboxy-terminal helical regions of each gp41 subunit, forming a bundle of six-helices (6HB)(102). The fusion peptide brings the amino-terminal region domain close to the host cell membrane, while the gp41 transmembrane domain holds the carboxy-terminal helical region domain close to the viral membrane, so the 6HB brings the two membranes into apposition, forming a fusion pore (135).

#### **1.4.3.1 Cell to cell transfer**

The efficiency of viral infection in cell culture systems is limited by attachment of the virus to a target cell and can be improved by simple methods such as spinning the virus down in culture medium to increase the number of cellular contacts virions (spinoculation). But, in an infected person most virus is in CD4<sup>+</sup> T cells in lymphoid tissue where uninfected potential

target cells mix closely with infected potential donor cells so cell-to-cell transmission between CD4<sup>+</sup> T cells in contact with each other may represent the most frequent mechanism of HIV-1 spread (126,143,144). This cell to cell spread is estimated to be 10-100 fold more efficient than cell free spread *in vitro* and may play a role in antibody evasion *in vivo* (145,146).

Understanding of immunological synapses enabled the identification of retroviral transmission between T cells via polarized virological synapses (VS) between T cells (147). Transmission across a synapse describes virus exiting the donor cell into a synaptic cleft between the donor and the target cells. This process is separate from virus transmission facilitated by contacts between cell cytoplasm (145,148). The cellular events underpinning T cell-T cell HIV-1 virological synapses are poorly characterised but transmission depends on extensive cytoskeletal modification in donor and target cells(146,149).

The CD4-gp120 interaction is essential for the formation of a VS but it is thought to be stabilised by integrin-ICAM-1 interactions (143) and also to require lipid raft integrity, cell surface adhesion molecules, tetraspanins and tyrosine kinase signalling (143). It has also been demonstrated that HIV-1 hijacks CD4<sup>+</sup> T cell regulated secretory pathways to enable cell-to-cell transmission (119,150,151).

Dendritic cells (DCs) can cause HIV infection of co-cultured CD4<sup>+</sup> T cells without becoming infected (152). DCs are professional antigen-presenting cells (APCs) which roam peripheral tissues, sampling antigens as they do so. They are frequently located in the mucosa where exposure to foreign antigens may be more likely and may thus be among the first cells that an HIV virion encounters on transmission to a new individual. DCs migrate to the lymph nodes following binding of antigen, where they present the antigen to T cells. This initiates an adaptive immune response. Low CD4 and co-receptor expression, constitutive expression of restriction factors and blocks to transcription mean that DCs are relatively resistant to productive infection (153). Nonetheless, DC can bind HIV virions, most likely via a C-type lectin. Structural studies of the infectious synapse show that DCs produce membranous protrusions which form surface-accessible invaginations that trap virions. On contact with DCs, CD4<sup>+</sup> T cells extend filopodia, which have dense clusters of CD4 and coreceptor, into these invaginated compartments where the virus is transferred (154,155) thus enabling evasion of intracellular detection or restriction in DC.

#### **1.4.3.2 Location of Membrane Fusion**

Other mechanistic details of viral entry are less clear, especially with respect to viral particle endocytosis by target cells involved in virological synapses. It is not fully resolved whether HIV entry occurs at the cell surface or is endosomal or both. Unlike many viruses HIV does not

require entry into a low pH, intracellular compartment in order to trigger membrane fusion. It was believed that HIV fused at the surface of the cell since 1) Env expression at the surface allows cell - cell fusion 2) increasing endosomal pH does not inhibit HIV fusion and 3) preventing endocytosis of CD4 does not affect HIV infection. But a series of studies have provided inconsistent results about whether endocytosis may be necessary *in vivo* (reviewed in Uchil and Mothes, 2009). Experiments using single virion fluorescent imaging combined with lipid and content mixing assays in HeLa cells indicate that entry takes place in perinuclear compartments and therefore that fusion requires endocytosis (157). Green fluorescent protein (GFP)-fused HIV-1 Gag traffics from the surface to endosomal structures in the target cell following transmission from the donor using live microscopy (158). The generalizability of these experiments is difficult to determine since HIV is diverse both in terms of genetics and cell types infected. Allowing the fusion event to take place closer to the nucleus may improve efficiency and could help to avoid innate immune detection (reviewed in Sloan et al., 2013; Wilen et al., 2012b) and it could be the case that while HIV entry is pH independent it may still occur in endocytic vesicles in certain circumstances.

#### **1.4.4 Post-entry events**

The virus loses its envelope during entry and the remaining viral components must traffic to the nucleus, and convert the viral RNA to double stranded DNA ready for integration. While the biochemistry of reverse transcription is well understood the timing, location and cofactors for uncoating, genome replication, and nuclear trafficking have proved more challenging to investigate. It may be the case that these processes differ in different cell types especially in the cell lines that are often used to study HIV. It may also be the case that what happens to the majority of individual virions, and is easily detectable with biochemical assays is not the same as the comparatively rarer events that actually lead to infection.

##### **1.4.4.1 The constituents of the RTC or PIC**

Incoming cytoplasmic viral complexes have been referred to as either reverse transcription complexes (RTCs) or pre-integration complexes (PICs) betraying the uncertainty about the configuration of their components. Indeed, there is now evidence that the RTC comprises an intact core for much of the journey to the nucleus. Attempts to define the components of these have produced varying results probably because the composition changes, accumulating cofactors and then uncoating. As the RTC traffics and the host proteins and structure alter with location. The trigger of initiation of RT is not known and the site of RT has also been the focus of some controversy. It may be that the entire contents of an intact capsid are present including NC, a nucleic acid chaperone that coats HIV-1 genomic RNA which has been implicated in

genome dimerization and packaging, tRNA unfolding and annealing, facilitating strand transfers and destabilising secondary structures in RNA such that RT can progress. (159). IN is also present in the RTC and curiously many IN mutations inhibit RT but not those which alter its enzymatic activity. Thus IN is thought to play a structural role in the RTC. (160). Vpr, Vif and Tat may also be constituents of the RTC but their roles have not yet been elucidated. Vpr localises to the nuclear rim or nucleus and there are various models in the literature where the function of Vpr is to act as a nuclear localisation signal. This PhD proposes that Vpr is largely contained within an intact capsid core and functions to interrupt innate immune signalling through interactions at the nuclear rim only once the core is partially, or completely, disassembled.

#### **1.4.4.2 Site of uncoating**

Evidence suggests that the core traffics to the nucleus using a large number of cytoskeletal components including microtubules and actin as well as perinuclear actin filaments called microfilaments (161) but examining the relationships between HIV-1 and the cytoskeleton has proved difficult due to redundancy and toxicity of inhibiting or depleting the proteins involved. Various models have been proposed for genome uncoating and the loss of the viral capsid including i) break down after membrane fusion followed by reverse transcription within a nucleoprotein complex; (ii) gradual break down during RT regulated by host factors; (iii) RT takes place in an intact core which breaks down at the nuclear pore complex (162–167).

#### **1.4.4.3 The early uncoating hypothesis**

Experiments with transmission electron microscopy and fractionation of infected cell lysates provided some evidence that the viral core spontaneously uncoats soon after entry into the cytoplasm. However viral cores are hard to detect using visual techniques because in cross-section they are indistinguishable from cellular structures and the fractionation of infected cell lysates uses strong detergents which disrupt important interactions. These experiments therefore produced quite variable results (reviewed in Arhel, 2010). It has also been proposed that uncoating could happen gradually and *in vitro* uncoating assays suggest it is a biphasic process. When virions are stripped of their membrane and MA with detergent the resulting cores can be centrifuged through sucrose to separate the dense cores from monomeric CA and the relative proportions can then be assessed by immunoblot. (168). But there are clear differences between this assay and the uncoating processes in the cellular environment and, since a number of cellular factors are now implicated in core uncoating, the physiological relevance of these *in vitro* biochemical studies may be limited.

#### 1.4.4.4 The late uncoating hypothesis

The variation in the location and composition of cytoplasmic viral complexes may be due to attrition at each stage of viral entry - it has been calculated that only 1 in 8 virions which reverse transcribes will successfully integrate (169) but these experiments were done in various cell lines and may not closely relate to what happens during the course of infection. In primary T cells for example, it is possible that only the virions which reach the nuclear pore complex with the core intact can integrate. There is now increasingly compelling evidence that for infection to be successful the HIV-1 capsid remains intact until contact with the nuclear pore and RT takes place within an intact capsid (165,170). This hypothesis is consistent with observations of other viruses: Herpesviruses, Adenoviruses, Hepadnaviruses and Parvoviruses are all known to dock at the NPC prior to delivering their genomes to the nucleus (171).

There are multiple pieces of evidence for RT taking place within an intact capsid core. Capsid has been detected in RTCs using incorporation of fluorescent dNTPs and furthermore these intact cores could be detected in perinuclear regions as early as 30 minutes post infection (161). Intact capsids have been observed at the nuclear envelope. Cryo scanning em studies by Arhel, et al. using immunogold p24 labelling and DNA fluorescent in situ hybridization (FISH) showed that intact cores containing DNA can dock at NPCs. They also showed that the disappearance of perinuclear p24 correlates with the appearance of nuclear DNA implying that core disassembly and nuclear entry of genome are simultaneous (172). Additionally, studies using 6aa tetra-cysteine tags, which fluoresce when in complex with fluorescein arsenical binder (FIAsH) and EM has allowed comparison of the shapes of IN containing complexes both in extracellular virions and inside cells. Many cytoplasmic IN containing complexes appear as identical 100nm long conical structures and importantly were often seen in perinuclear regions. Together with the mutational and function studies these imply that intact conical cores can be found and likely have evolved to dock at the nuclear pore prior to disassembly (173).

More compelling evidence comes from observations that assembled capsid proteins interact with several nucleoporins and that these interactions are required for HIV-1 nuclear entry indicating that at least some CA must remain associated with the virus until it reaches the NPC (174–177). Nuclear pore protein Nup153 has been shown to bind hexameric CA by isothermal titration calorimetry (ITC) but not monomeric capsid strongly arguing for the presence of intact capsid at the nuclear pore (178)

It is now hypothesised that prematurely uncoated viruses may trigger innate immune sensing and cellular cofactors which bind CA are required to prevent HIV-1 DNA from being detected by cytoplasmic innate immune sensors so maintaining the integrity of the capsid until arrival at the nuclear pore may be a strategy to prevent innate immune detection, concealing viral DNA from these sensors (165,170).

#### **1.4.4.5 The relationship between Reverse Transcription and uncoating**

Despite increasing evidence that RT takes place within an intact core until recently it had been unclear how HIV imported dNTPs into the capsid. By comparing all known CA NTD crystal structures Jacques et al. showed that there is a dynamic electrostatic channel in the center of each capsid hexamer enabling the electrostatic transport of dNTPs. Previous structures suggested that the amino-terminal  $\beta$ -hairpins of each capsid monomer blocked the opening of such a potential pore, but it was demonstrated by comparing X-ray structures that this  $\beta$ -hairpin is flexible and can tilt up to 15 Å away from the axis of symmetry depending on the conditions of the crystal in the X-ray. When the constituent monomers adopt this 'open'  $\beta$ -hairpin conformation, a central channel is formed. Structures that were obtained at a high crystallization pH adopted a closed conformation, whereas structures that were obtained at a low pH adopted an open conformation suggesting that conformational change is possibly dependent on the protonation status of a histidine residue at the base of the  $\beta$ -hairpin. At physiological pH, the  $\beta$ -hairpin assumes an intermediate position, potentially indicating high flexibility. Thus, the  $\beta$ -hairpin may function as a 'molecular iris' opening and closing a central pore in the capsid hexamer. The authors also observed efficient strong-stop reverse transcription (the first DNA synthesis step) when cores were incubated with dNTPs but addition of DNase I, RNase A or benzonase did not prevent reverse transcription, supporting the idea of a size-selective pore which allows dNTPs into the interior of the capsid but not larger nucleases (178).

As well as protecting viral nucleic acid species from innate cellular immune receptors, undertaking RT in an intact capsid may help to maintain the high local concentration of RT and dNTP needed around the template for completion of RT. There is also evidence that RT may itself drive uncoating (Arhel, 2010). If RT is inhibited with NNRTIs (nevirapine) the core is stabilised and uncoating is delayed. This has been assessed using the Fate of Capsid (FoC) biochemical assay involving ultracentrifugation of virus infected cell extracts through a sucrose gradient pelleting intact cores but not monomeric capsid. The RT inhibitor, NVP, increases the proportion of intact capsid (166,179).

#### **1.4.4.6 Host proteins that influence uncoating**

Lentiviruses are unusual among the retroviridae as they can infect non-dividing cells. This requires the crossing of an intact nuclear envelope via the Nuclear Pore Complex (NPC). The NPC is fundamental to a vast array of cellular processes from cell division to gene expression. It comprises a 112MDa protein complex of over 500 molecules and 30 different proteins which forms a 39nm diameter channel. The constituent proteins are called Nups followed by number denoting nuclear mass. Nups can be classified into 6 categories depending on position and role: pore membrane proteins (POMs), coat nucleoporins, adaptor nucleoporins, channel nucleoporins, cytoplasmic filaments and nuclear basket nucleoporins. 40kDa molecules can diffuse through the pore but larger molecules require translocation using transportins or karyopherins (180) although it is likely more complex than this simply size related view. Extensive FG repeats line the channel acting as the pore's permeability barrier (181) and all transportins/karyopherins are mildly hydrophobic which may be an essential quality to pass through this channel (182). Karyopherins interact with their cargo via nuclear localisation/export signals (NLS/NESs) and direction of travel is determined by a gradient of RanGTP across the nuclear envelope. While classical NLSs have been reported in MA, IN, Vpr and in the cPPT mutations in these regions do not appear to affect nuclear entry in HeLa cells (183) and it is CA that is likely to orchestrate events prior to nuclear entry. MLV is a gamma retrovirus which is unable to infect non dividing cells and chimeric HIV-1 with MLV CA retains the MLV phenotype and certain mutations in CA (A92E and G94D) make HIV-1 cell cycle dependent (184). CA is known to interact with several host cell cofactors include CypA, TNP03, Nups358 and Nup153 and CPSF6 (discussed in section 1.10.1).

## 1.4.5 Reverse Transcription

### 1.4.5.1 Reverse Transcriptase

Whilst the exact triggers of RT are not known it is possible that exposure to dNTPs inside the target cell provide a sufficient trigger (163). Reverse Transcriptase comprises a heterodimer of p66 and p50. P66 comprises an RNA/DNA dependent DNA polymerase domain and an RNase H domain. It initially forms homodimers but the RNase H domain is cleaved from one monomer creating the functional p66/51 heterodimers often referred to simply as RT (185). The p66 monomer contains both active sites (the polymerase and the RNase) whilst p51 has a structural role. The polymerase domain assumes a hand shaped configuration. Without a ligand the thumb is opposed but moves back to reveal the nucleic acid binding cleft and the fingers move forward to form a dNTP binding pocket. (162).

### 1.4.6 The mechanism of Reverse Transcription (figure 1.8)

**Minus strand DNA priming and synthesis 1:** The viral reverse transcriptase exists as a dimer and has an RNA/DNA dependent DNA polymerase activity (enabling the production of a dsDNA product from a +ssRNA viral genome) and a ribonuclease H activity (which selectively hydrolyses the RNA part of an RNA DNA hybrid but does not degrade unhybridised RNA). Like many other DNA polymerases, RT needs both a template (in this case the plus stranded RNA genome) and a primer.

All retroviruses use tRNAs as primers for their RT enzymes. HIV-1 uses tRNA (Lys,3) which is packaged into HIV-1 virions via interactions with Gag and Pol (186). The 3' sequence of tRNA is complementary to an 18nt sequence within the HIV-1 genome called the PBS (primer binding site) which lies immediately 3' to the 5' LTR. Priming from this site reverse transcription synthesises the U5 and repeat minus strand DNA from the plus strand RNA template.

**Minus Strand transfer:** The DNA copy of the R sequence at the 5' end of the viral genome hybridises with the R sequence at the 3' end. This is called first strand transfer since the strong stop DNA minus strand is transferred from the 5' end to the 3' end of the genome RNA. The exact mechanism by which this takes place is not clear. Conventionally the complex is drawn linearly but the molecules may remain circular. In the case of in-core RT the CA and NC proteins and their organization of nucleic acid likely organise the RT process (114).

**Minus strand DNA synthesis 2:** The strong stop DNA is extended by reverse transcriptase to copy the entire remaining part of the genome RNA up through the primer binding site making a full length minus strand copy of the genome. Because of the strand transfer this DNA

molecule contains a copy of the R sequence between the U3 sequence of the viral RNA and the transferred U5 sequence. This U3 R U5 sequence is the long terminal repeat.

**Plus strand DNA priming and synthesis 1:** The distance between the polymerase and the RNase H domain of RT can accommodate 17-18 nucleotides and thus RNase H mediated degradation begins 17-18 nts behind DNA synthesis. (186). As it is copied into DNA most of the RNA genome is digested by RNase H apart from a resistant polypurine tract (ppt) at the 5' end of the u3 sequence. This residual RNA serves as a primer of the subsequent synthesis of plus strand strong stop DNA by reverse transcriptase. After initiation at the ppt this is extended through the U3 R U5 LTR and then the 18 nucleotides of the tRNA that were initially hybridised to the PBS on the genome RNA. This creates the short DNA intermediate "plus strand strong stop DNA".

**DNA plus strand transfer and synthesis 2:** RNase digestion of the 3' end of the tRNA removes it from the minus strand DNA copy and exposes the primer binding site on the plus strand strong stop DNA which can then hybridise with its complimentary PBS sequence at the other end of the newly synthesised minus strand. This is the second strand transfer and again while it is drawn in a linear fashion the plus strand strong stop may act as a bridge enabling the two ends of the minus strand to circularise. Finally, the minus and plus strands are extended by reverse transcriptase to the ends of their respective template strands creating the proviral DNA.

#### **1.4.6.1 Generation of diversity through reverse transcription**

Cellular DNA polymerases proofread using a 3' to 5' exonuclease activity which enables them to remove regions containing mis-paired bases and allowing their repair but RT lacks this ability so between 1-10 nucleotide errors are introduced during synthesis of each provirus. Reverse transcription further contributes to viral diversity by allowing recombination between the two viral genomes to occur. Each HIV-1 virion contains two +ssRNA genomes and RT readily moves between them particularly during long pauses, the strand transfers or when it encounters nicks between the genomic RNA (reviewed in Acheson, 2011; Fields et al., 2013; Hu and Hughes, 2012). This is important for generation of viral diversity through proviral recombination. The high frequency of recombination events perhaps also supports the hypothesis of in core RT as it is unclear how the RT molecule could swap between strands of the strands were floating free in the cytoplasm after uncoating.

#### **1.4.6.2 Drugs which inhibit RT**

There are two classes of ARVs which inhibit RT: nucleoside and non-nucleoside reverse transcriptase inhibitors (NRTIs and NNRTIs). There are 11 licenced NRTIs which mimic dNTPs and are incorporated into viral DNA by RT. Since they lack the 3' OH group required for incorporation of the next dNTP they act as chain terminators. The 5 licenced NNRTIs are allosteric inhibitors that cause significant conformational changes to both the polymerase active site and the primer binding site of RT (104,189).

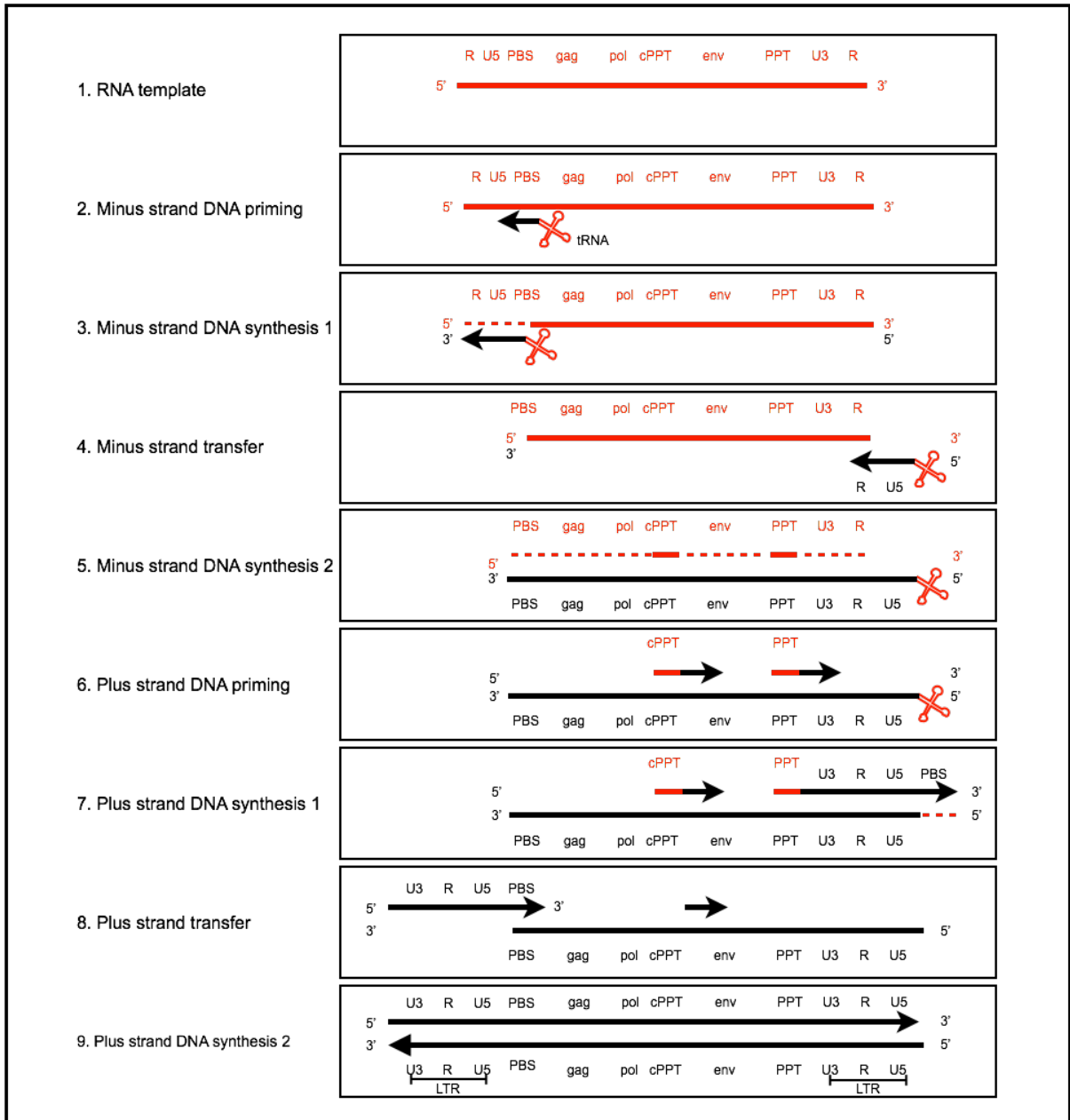


**Figure 1.8 The stages of HIV reverse transcription.** RNA is coloured red and dotted following degradation by RNase H activity. DNA is coloured black. U3 is the 3' UTR, U5' UTR, R is the repeat region - all are regions of the ITR. PBS is the primer binding site. PPT is the polypurine tract. cPPT is the central polypurine tract. Arrows show direction of polymerisation.

## 1.4.7 Integration

Once inside the nucleus the HIV-1 DNA integrates into the host genome becoming a permanent part of the target cells genome, copied to any daughter cells during replication (187).

### 1.4.7.1 Integrase

The viral integrase enzyme (IN) mediates integration. It is a polynucleotidyl transferase with three domains. The structure of the complex of DNA and integrase has not been solved. The blunt ends of the viral dsDNA are bound by a homotetramer of viral IN forming a complex called the intasome. The bound DNA is distorted in the intasome so that each of the two active sites binds a single end of the viral genome. One catalytic site enables 3' processing and the strand transfer reaction for the end of DNA it binds. The distance between these two active sites dictates the 5nt distance between the two phosphodiester bonds attacked during integration. In the first step (3' end processing), IN catalyses the removal of the two 3' nucleotides from each 3' end of the viral DNA creating a 2nt 5' overhang at each end. It then catalyses the next stage, called DNA strand transfer, where the free 3' ends target two phosphodiester bonds on each side of the target DNA backbone five nucleotides apart. The 3' ends of the viral DNA are joined to the target DNA covalently. Cellular enzymes repair the two nucleotide overhang on the viral DNA at the 5' end completing integration (190).

Raltegravir is the only IN inhibitor currently licenced. It binds to the intasome interacting with the DNA and with the Mg<sup>2+</sup> ions within the active site (104).

### 1.4.7.2 Circle formation

Viral DNA that enters the nucleus but does not successfully integrate is circularised by the host cell DNA repair enzymes forming one of several dead end viral products. An alternative way of thinking about this may be that whatever DNA is not circularized defensively by the cell, is then integrated. Linear DNA ends may be joined by non-homologous end joining (NHEJ) making a 2-LTR circle. Non-homologous end joining describes nuclear DNA repair events which act as a protective host response to double stranded DNA. The result is the ligation of viral LTRs (191). This only occurs in the nucleus so measurement of 2 LTR circles is often used as a measure of nuclear entry. Circles with a single LTR may form from homologous recombination between the LTRs in a 2-LTR circle, or from stalled RT products. Additionally viral DNA ends may autointegrate into pre-existing HIV DNA circles resulting a series of complex circular DNA structures depending on the site of integration and subsequent recombinations (162).

### **1.4.7.3 Integration site selection - genomic features associated with integration sites**

Early analysis of the DNA sequences at integration sites showed a lack of dependence on sequence specificity for the integration reaction: different proviruses have been shown to integrate at different site sequences. But after the sequence map of the human genome was completed in 2001 (192,193) it became possible to map integration sites on this and to measure the genomic features surrounding them in more detail. Schroder et al reported that in SupT1 cells HIV-1 preferentially integrates inside genes and into transcriptionally active regions of the genome (194) and all subsequent measurements of gene density in all cell lines and primary cells have shown strong preference for integration into gene rich regions, with the largest study by Wang examining over 40,000 integration sites of two different HIV1 strains (195–197).

The correlation of many genomic features with each other complicates differentiating causality from mere association with respect to the identification of those features that determine integration targeting. Active transcription units are characterised by high G/C content, gene density, CpG island density and frequencies of Alu repeats, as well as short introns, low frequencies of LINE repeats, and particular epigenetic modifications. These same features correlate with integration sites and many groups have reported correlation with transcriptionally active chromatin (H3K4 trimethylation, H3K9 and H3K14 acetylation and H4 acetylation) and negative correlation with markers of transcriptional repression like H3K27 trimethylation (194,197,198).

This favouring of active transcription units by HIV contrasts with the targeting preferences of other genomic parasites which have perhaps evolved to optimise persistence. When cells with a short half life are infected, integration within transcription units is likely to be more favourable for efficient transcription in a short time period. Integration site selection seems to be independent of route of entry; this has been demonstrated by comparing VSV-G pseudotyped virus with HIV R5 env (195).

### **1.4.7.4 Integration site selection - host factors involved in integration**

Host cell factors are important for efficient integration and target site selection. Lens Epithelium-derived growth factor p75 (LEDGF/p75) is a transcriptional co-activator which has a chromatin binding domain and is also able to form a complex with IN and is hypothesised to tether IN to genomic DNA directing integration to LEDGF binding sites. So LEDGF targets the viral genome into genes but not specific genes. Knock out or dominant negative expression causes post entry block to HIV-1 infection (199,200). LEDGF also dictates the location of

integration and fusion of the IN binding domain to other DNA binding domains retargets the viral DNA (201).

LEDGF on its own is not sufficient for integration in gene rich areas; Genome structure can also determine integration site selection; DNA distortion for example can promote integration. Very densely packaged DNA is not accessible so regions of heterochromatin such as centromeres and telomeres are cold spots for HIV-1 integration (202). In euchromatin integration is favoured within nucleosomes (203) putatively because reaction cycle completion requires distortion of DNA so DNA kinked on the nucleosome may have lower activation energy. This may also explain preference for AT rich DNA which has increased flexibility.

#### **1.4.7.5 The role of capsid in integration**

CA mutations or depletion of co-factors can also lead to reduction in gene density surrounding integrated proviruses (174,204) and HIV-1/MLV capsid chimeras have been used to show the influence of CA on integration sites (205). It has been reported that CA protein mutant N74D abrogates sensitivity to TNPO3 (a nuclear import receptor) but becomes sensitive to knockdown of other nuclear pore proteins (206,207). Although these studies need further confirmation it was this data that first suggested that specific nuclear pore protein interactions were required for PIC nuclear transit and that multiple redundant pathways may be used for nuclear entry. We now know that capsid dictates interaction with HIV1 cofactor such as CypA, TNPO3 and Nup358 whose depletion also changes the average gene density surrounding HIV-1 integration sites (204). Currently the most accurate model for predicting integration sites still shows regions of unexpectedly high and low density so there may be as yet undiscovered co factors (197).

Whilst integration into a transcriptionally active region would seem to be obviously beneficial for the virus it may come with some penalties. If a provirus is located near a highly transcribed gene in the same orientation then transcriptional read through may occur (208) and if it's in an opposite direction then convergent transcription may occur.

And while microarrays of infected and uninfected cells show that the median level of transcription for viral genes is 1.5-3x higher than host genes (194) the protein Tat enhances viral transcription up to 75 x suggesting that while a local environment can alter proviral transcription tat will enhance activity of all proviruses (209).

## 1.4.8 Latency

HIV-1 can persist as a transcriptionally inactive provirus following integration in a resting memory CD4<sup>+</sup> T cell. This is the basis for the latent reservoir (LR) with a long half-life (210). The reservoir seems to be created in the early stages of infection and has been shown to be both quantitatively and qualitatively stable. Siliciano et al. showed the half-life for latently infected cells which could produce virus in a quantitative virus outgrowth assay was 44-months (211). They estimated that eradication of the latent reservoir would therefore require over 70 years of treatment. These studies imply that the latent reservoir in resting memory CD4<sup>+</sup> T cells ensures persistence of the virus for the lifetime of the patient. For patients on long-term suppressive anti-retroviral therapy both HIV-1 DNA levels and genetic compositions seem to be stable with little evolution of the virus (212,213).

Since HIV-1 in the periphery has not been observed to establish productive infection efficiently in resting CD4<sup>+</sup> T cells (214,215) the LR may be established when activated CD4<sup>+</sup> T cells become infected and revert back to a resting memory state. HIV-1 efficiently infects activated CD4<sup>+</sup> T cells many of which are hypothesised to die quickly as a result of the cytopathic effects of the virus or host immune responses (Ho et al. 1995). However it may be that a small number of these activated infected cells survive and are able to revert back to a resting state creating the latent reservoir. What determines which T cells die and which survive remains contentious (61,62) and the anatomical location of the reservoir is also unclear. Measurements to date have focused on peripheral blood but it may well be cells in lymphnodes that play a more important role.

HIV latency was not considered important until after the advent of Highly Active Antiretroviral Therapy (HAART) in the 1990s. Prior to this RT-PCR assays for viremia (216) showed active replication through all stages of infection. The primary strategy evolved for immune response evasion is not latency but rapid generation of escape mutations which prevent recognition by neutralizing antibodies and cytotoxic T lymphocytes (217). Latency became an issue when it was clear that populations of infected cells could survive prolonged treatment courses and by as early as 1997 persistence of latently infected cells in patients, despite responses to HAART, had been demonstrated (210).

### 1.4.8.1 Maintenance of latency

Even in latently infected cells proviruses are frequently integrated in highly expressed genes suggesting that transcriptional interference plays a larger role in latency than integration into non-active heterochromatin (205). Because HIV-1 gene expression depends on host transcription factors which are induced after antigen exposure, it is possible for the

transcriptionally silent provirus to persist in cells whose very purpose is to survive for prolonged periods in a resting state.

While heterochromatin may not play a major role, other aspects of chromatin biology and structure may be important. Nucleosomes consist of 147bp of DNA wrapped around an octet of histone proteins. Post-translational modification of the histone tails regulates the nucleosomes and governs gene expression. There are two nucleosomes which consistently form in the 5' LTR of HIV even when it is integrated in transcriptionally active euchromatin. Because they overlap with transcription factor binding sites for tat these nucleosomes regulate 5'LTR transcriptional activity and therefore promote HIV gene expression (218).

In resting CD4+ T cells, therefore, the absence of the necessary activated cellular transcription factors, together with the absence of Tat and its cellular cofactors limit viral transcriptional initiation and elongation. DNA methylation and repressive histone modifications may further repress proviral transcription.

#### **1.4.8.2 Ongoing replication**

Persistent virus replication and rapid evolution in lymphoid tissue reservoirs has been demonstrated by some studies and may contribute to reservoir maintenance (71,219,220). Most studies however indicate that it is the expansion and contraction of individual CD4 cell clones that contributes to reservoir maintenance(212,221). A recent study compared HIV-1 DNA from patients after many years of suppressive ART with the viral sequences from before ART in the same patients and found that the viral populations remained genetically stable for almost 2 decades (222). The disagreement between studies may be because in the shorter duration studies, death of short lived cells in the first few months of treatment results in sequence changes which look like backwards evolution or it may be that there is ongoing viral replication but all the studies to date have measured total HIV-1 DNA and replication is occurring below the detection limit.

#### **1.4.8.3 Latency and cure**

The long half life of resting T cells has been postulated to prevent cure by ART alone and one of the main challenges in the search of an HIV cure is to develop strategies that can eliminate the persistent viral reservoir. In the latent state, the virus is unaffected by antiretroviral drugs or immune responses but if the host cell encounters antigen, or other activating stimuli, then latency may be reversed, with the subsequent initiation of virus production. This idea provides a major approach to curing HIV: infected cells in which latency is reversed may die from either direct viral cytopathic effects or be killed by specific cytotoxic T lymphocytes. Novel cellular

infections caused by virus released in this process would in theory be prevented by HAART. This approach, called shock-and-kill(223,224), comes from the early discovery that histone deacetylase (HDAC) inhibitors can reactivate HIV-1 from latency(225). Putting this approach into practice has proved challenging: while a single dose of the HDAC inhibitor vorinostat, has been shown to induce HIV Gag RNA associated with cells in some patients, it proved to be due to read through transcription of host genes, not functional *de novo* proviral transcription (226).

Compounds which are unable to activate T cells, such as HDAC inhibitors, have been the focus of drug discovery and clinical trials. Use of novel viral outgrowth assay to test drugs that do in fact activate T cells (PMA + ionomycin) showed that these agents may be necessary for viral transcription (227). This presents the likelihood of significant off target effects. Our current understanding of the mechanism of HIV latency is rudimentary and identifying small molecules capable of reactivating all HIV-1, with a tolerable side effect profile, will be a significant challenge.

### **1.4.9 Transcription of HIV**

A single promoter in the 5' LTR mediates transcription. The viral proteins come from a single primary transcript. This happens three ways: (i) alternative splicing (where ambiguous splicing signals generate unspliced, singly spliced or double spliced mRNA), (ii) leaky scanning of the initiation codon (which happens in the case of the mRNAs encoding vpu/env and rev/nef where the first initiation codon is occasionally missed allowing the second protein to be made), and (iii) ribosomal frameshifting (the mechanism by which gag and gag-pol are produced from the full length unspliced mRNA – see below).

#### **1.4.9.1 Initiation of transcription**

Initiation of transcription requires inducible host transcription factors (TFs) including NFκB, NFAT and AP-1 all of which are activated by extracellular stimuli including T-cell receptor ligation and a range of cytokines (228). Binding sites for NFκB and NFAT are present in the U3 of the LTR which also contains binding sites for other transcription factors such as Sp1, LEF and ets-1. In resting cells, both NF-κB and NFAT are cytoplasmic and inactive, and thus are not available to promote transcription. Sp1 also binds three sites in the core promoter and may act, through association with TATA-box-binding protein (TBP), TBP-associated factor (TAF) 250, and TAF55 (229). Sp1 and κB site proximity has been shown to be crucial for full LTR activation (230).

The NF- $\kappa$ B/Rel family of transcription factors both activate and inhibit the HIV-1 LTR. Once bound the p50 homodimer recruits HDAC1 and leads to chromatin condensation and transcriptional inhibition (231). p50/RelA heterodimers (the prototypical NF- $\kappa$ B complex) are able to displace p50 homodimers and induce strong transcriptional activation by recruiting p300/CREB-binding protein (CBP). CBP causes acetylation of histone tails and increased RNA Pol II and TFIIH/CDK7 complex binding. This complex mediates promoter clearance and activation of the RNA Pol II (232).

RelA has shown to enable recruitment of P-TEFb complex to the HIV LTR. This complex, comprises cyclin T1 and CDK9 and also phosphorylates the CTD of RNA Pol II. This promotes effective Pol II elongation. The complex is released from an inactive 7SK snRNP complex by HIV Tat causing increased Pol II elongation (see below) (233). HIV-1 proviral transcription is initiated when transcription factors bind the promoter in the 5' long terminal repeat (LTR). These include NF- $\kappa$ B, Sp1, the TATA box binding protein, and RNA polymerase II. The host RNAPolymerase II (RNAPII) starts transcription and enables production of a small number of viral transcripts, which can then be spliced and translated.

#### **1.4.9.2 The role of Tat**

Trans-activator of transcription (or Tat) is an early, basic 85 AA protein produced by doubly spliced HIV-1 mRNA and localised to the nucleus. Tat is not required for the initiation of transcription by RNAPII but it increases the efficiency of elongation which allows the production of more Tat in a positive feedback loop. Tat activity requires a regulatory element found downstream of the transcription start site: the transactivation – responsive region (TAR). TAR forms a stem loop structure in viral RNA with two functional regions. The first is a conserved 3-nucleotide (nt) pyrimidine bulge that binds the Tat protein. The second is a 6-nt loop which shows Tat-dependent binding to pTEFb. pTEFb has a kinase component, which, after TAR binding, causes phosphorylation of the C-terminal domain of RNA polymerase II, thus enhancing its processivity (233–236).

#### **1.4.9.3 Nuclear export of mRNA**

More than 40 different species of mRNA are produced from provirus due to splicing between 4 donor 5' splice sites and 8 acceptor 3' splice sites. These fall into three groups: 1) unspliced (9Kbp encoding Gag and Gag-Pol and are also the viral genome. 2) incompletely spliced (~4Kbp species encoding Vif, Vpr or ENv and Vpu) and 3) completely spliced ~1.8Kbp species that encode Tat, Rev or Nef (6). Only cellular messenger mRNAs which are completely spliced are transported to the cytoplasm (237). Other mRNAs produce non-functional proteins

so initially only the fully spliced viral mRNAs encoding Tat, Rev or Nef can be exported and translated.

But for viral replication retroviruses require transport of unspliced mRNA to the cytoplasm because they produce the required mRNAs from full-length transcript which has been alternatively spliced, and because their viral genomic RNAs (gRNAs) are unspliced. Accordingly they have evolved the ability to transport their intron-containing RNAs from nucleus to cytoplasm. The viral mRNAs exit the nucleus using a viral protein Rev via a pathway that normally exports small RNA species. Rev is needed to export of 9- and 4-kb unspliced and incompletely spliced mRNAs encoding viral proteins from the nucleus, but not the 2kb RNAs(238). So when Rev expression is low the 2kb class (including those encoding Rev, Tat and Nef) are expressed. As levels of Rev rise the remaining mRNAs are expressed.

Rev is an RNA binding protein which binds to the Rev responsive element, a ~250nt sequence that lies within an intron in env and is present in all incompletely spliced or unspliced viral mRNAs. Like TAR the RRE forms a stable multiple loop stem structure in the viral RNA and one of the loops has a binding site for the arginine rich RNA binding region of Rev. Like Tat, Rev binding to the RRE causes conformational changes in the RNA structure (98) and also dimerization of Rev itself. Two Rev monomers form a V shape interacting with adjacent sites in the RRE RNA and creating an interface for more Rev dimers to bind cooperatively. On the surface of the complex of Rev oligomers on the RNA there is a leucine rich nuclear export signal. Exportin-1 (Crm-1) binds to the nuclear export signal and to the GTP bound form of Ran and acts as the receptor for Rev dependent export of the RNAs bound to it. Rev itself functions as an adapter directing the viral mRNAs to a pre-existing cellular export receptor. Translocation of the mRNA, REV and exporting complex requires specific nucleoporins. Once in the cytoplasm hydrolysis of GTP bound to Ran by a protein only present in the cytoplasm induces dissociation of the export complex. Rev then shuttles back to the nucleus to pick up another RNA cargo.

#### **1.4.9.4 HIV-1 translation and frameshifting**

All other retroviruses including HIV-1 have evolved frameshifting mechanisms where sequence and structural signals in the mRNA specify a translational mRNA reading frame shift(239). All viral mRNAs are translated on cytosolic polysomes with Env and Vpu as the exceptions. They are translated on the rough ER (240). The longest viral mRNA encodes Gag and Gag-Pol. 1 in 20 times this is translated there is a + 1 frameshift at the end of Gag causing read through into Pol and synthesis of the Gag Pol Polyprotein. This frameshift is due to a hexanucleotide “slippery” sequence (UUUUUA) and a stem-loop pseudoknot structure

located just 3' to the slippery sequence. This increases the time the ribosome is associated with the slippery sequence and allows a the resultant frameshift to occur (98).

#### **1.4.10 Assembly, maturation and budding.**

Virion morphogenesis can be subdivided into assembly, budding and maturation (figure 1.9). During assembly, the virion components are packaged together. This is followed by budding, where the virion acquires a lipid envelope. Maturation is the process by which the virion develops its final infectious structure. The Gag polyprotein coordinates these stages a in a process that requires the coordinated synthesis of all viral proteins as domains of the Gag and Gag-Pro-Pol polyproteins. This ensures that components are made in correct proportions (95).

##### **1.4.10.1 Contents of a mature virion**

An assembled virion must contain 2 copies of the +ve sense viral RNA, cellular tRNA (Lys,3) which act to prime synthesis of cDNA, Env, the Gag polyproteins as well as the viral enzymes. Assembly of all components takes place on the plasma membrane (95).

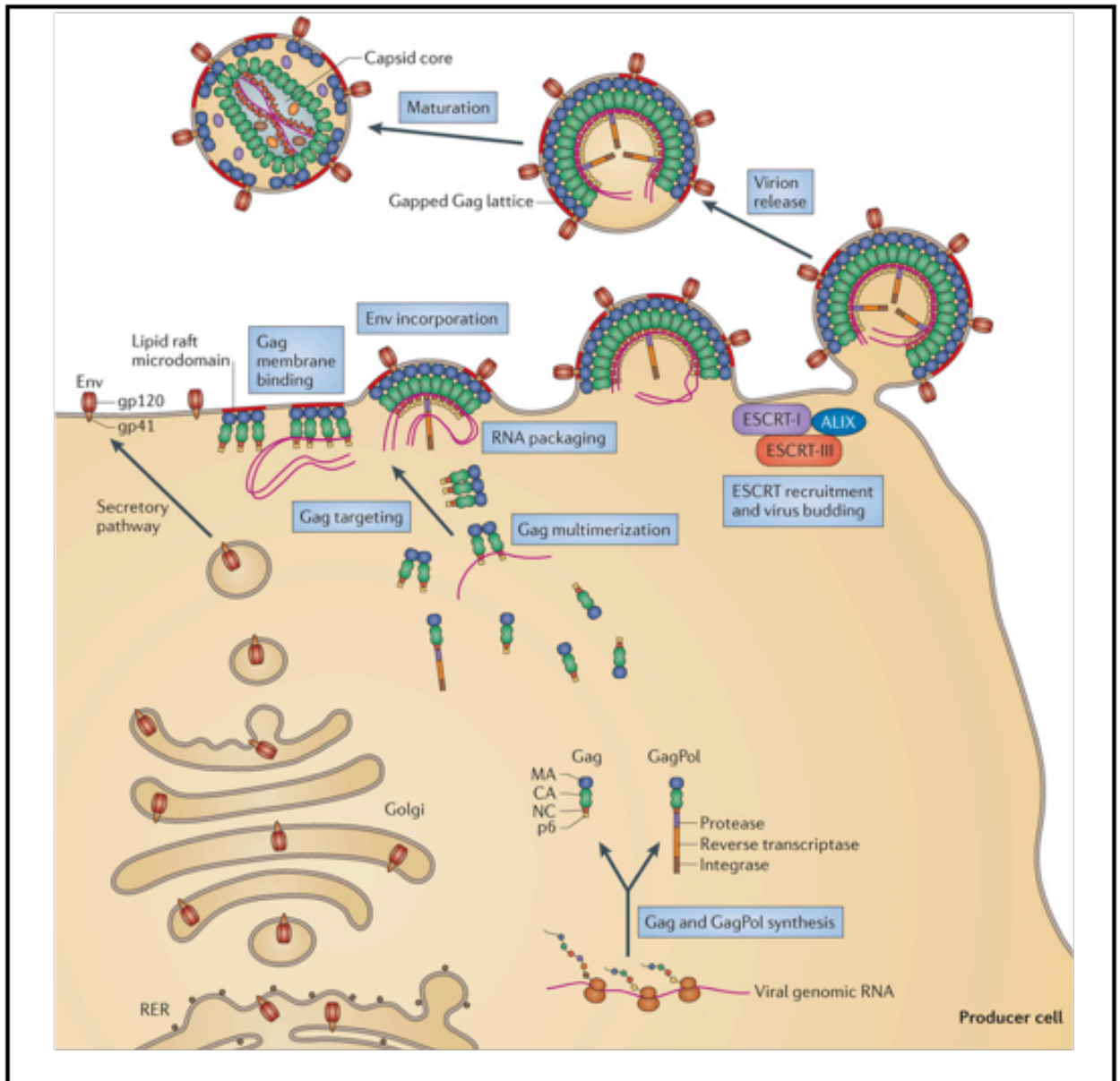


**Figure 1.9 The late stages of the HIV-1 life cycle** Assembly, budding and maturation stages are coordinated by the Gag polyprotein. Left side: Env glycoproteins are synthesised and glycosylated on the RER, and move to the membrane via the secretory pathway. Right side: Gag is synthesized in the cytosol from full-length viral RNA. 5% of the time a Gag-Pol fusion protein is produced. Gag recruits viral genomic RNA, and forms multimers. At the membrane Gag induces the recruitment and coalescence of lipid rafts which serve as platforms for virus assembly. Following Env incorporation the virion recruits ESCRT-I and the ESCRT-associated factor ALIX. ESCRT-III and VPS4 complexes are then recruited to enable virion release. During maturation the viral protease cleaves Gag and GagPol polyprotein precursors. Adapted from Freed, E.O. (2015). HIV-1 assembly, release and maturation. *Nat. Rev. Microbiol.* 13, 484–496 (97)

#### **1.4.10.2 The role of Gag and Gag-Pro-Pol**

The Gag precursor comprises matrix (MA), capsid (CA), nucleocapsid (NC) and p6 domains, and the spacer peptides, SP1 and SP2. It was previously believed that Gag acted merely as a scaffold, forming the core of the virus. Gag has now been shown to recruit genomic RNA together with viral and host proteins on route to the plasma membrane. It binds other virion components directly and acting as a single targeting signal for assembly of all components (241,242). Gag and Gag-Pro-Pol traffic to the plasma membrane without extensive polymerisation and localize to microdomains (243) (113). This may enable the incorporation of Env glycoproteins into virions (243) and may enhance cell–cell viral transfer at virological synapses (244).

Gag polyprotein coordinates virion assembly, binding the plasma membrane, making the interactions necessary for the creation of spherical particles as well as packaging the viral genomic RNA through interactions with its packaging sequence  $\Psi$ . Cytoplasmic Gag is soluble and either monomeric or in low order multimers. Folded domains within Gag are joined by flexible linking regions. These contain the protease cleavage sites. Once at the membrane, Gag extends into a rod and polymerizes at nucleation sites composed of Gag–RNA complexes (113,245).

At the amino terminal of Gag is Matrix (MA) which binds the cell membrane recruiting Env. The amino terminus is also modified during translation by the covalent attachment of a 14-carbon fatty acid. Binding of MA to the plasma membrane specific lipid phosphatidyl inositol (4,5) bisphosphate (PI(4,5)P<sub>2</sub>) exposes the myristoyl group and anchors it to the cell membrane (246). The mechanism of action of Gag targeting to the cell membrane remains unclear (247).

The central Gag domain is Capsid (CA) which enables immature virion assembly and then forms the conical core of the virus. Genome recognition and recruiting of viral RNA to the Gag complex is mediated by nucleocapsid (NC) which contains two zinc-finger-like domains. The C-terminal p6 domain is unstructured, and recruits the host ESCRT machinery that causes budding. CA also contains the binding sites for Vpr. The spacer peptides control the conformational changes needed for the maturation phase (97,187,248) .

#### **1.4.10.3 Env incorporation**

Env is inserted into ER membranes during translation and is an integral membrane protein. It becomes glycosylated during trafficking and assembles into trimers. A cellular protease (furin) processes these trimers into transmembrane (TM) gp41 and surface (SU) gp120 subunits and

which are taken to the plasma membrane by vesicular transport. It is not understood if Env is incorporated passively into new virions, or through co targeting of Gag and Env to the same specific PM site or if the MA of Gag and Env interact directly (97). Genetic and biochemical studies have shown that the long intracellular tail of gp41 helps coordinate the arrangement of Env into “raft”-like domains (249).

#### **1.4.10.4 RNA encapsidation**

RNAs traffic to the cytoplasm, following nuclear synthesis, where they are translated or packaged into new virions. Like all retroviruses, HIV-1 packages two copies of its RNA genome into the virion (115,250). The two RNA genomes in each particle enables recombination and provides some degree of redundancy if one RNA copy is damaged (162). The two RNA strands are dimerized through formation of a “kissing-loop” structure and this acts as the signal for the genome to be incorporated into virions (251).

The zinc finger like domains of the NC domain of Gag bind to a packaging signal in the 5' region and enable the genomic RNA to be incorporated. This signal spans the major splice donor and the Gag initiation codon (112). Only unspliced viral RNA is packaged precisely because packaging requires signals downstream from the first splice donor. Two copies of tRNA<sup>Lys3</sup> are packaged along with the viral genome through annealing to the mRNA at an 18 base-pair sequence termed the primer binding sites (PBS), found in the 5'LTR (117).

#### **1.4.10.5 Budding**

The Gag protein and the full-length genomic RNA assemble into a curved lattice at the cell membrane. This, with the GagPol precursor, begins the formation of the virion. The Gag-RNA contacts initiate assembly and multimerization of Gag is largely determined by CA. The Gag molecules in the immature virion assume a radial orientation around the growing partial spheroid of the nascent particle – like spokes in a three-dimensional wheel. The immature lattice of Gag is stabilized through protein interactions involving the CA-SP1 region (252) and is a continuous sheet with gaps creating the curvature that will form the viral particle (253,254). Cryoelectron microscopy (cryo-EM) and cryoelectron tomography (cryo-ET) techniques indicate the arrangement of Gag into hexamers with 8 nm spacing. Gag assembly and budding may be competitive, such that virions bud prior to the final multimerisation of Gag into shells. A virion of roughly 130 nm diameter is estimated to comprise roughly 2500 Gag molecules (241).

Membrane fission releases the particle from the cell membrane. Gag levels increase at the assembly site until budding. Gag coordinates virion assembly, but the virus additionally co-

opts the host ESCRT pathway which ends Gag polymerization and starts membrane fission (255). HIV-1, in common with other enveloped viruses, has evolved to use the same pathways that cause the membrane fission events involved in vesicle release into endosomes or that separate cells during the final stages of cytokinesis. These events are all catalysed by ESCRT factors which tighten cytoplasm-filled membrane tubules closing them off at the neck (256).

There are three short peptide motifs, or late domains, that drive release through interactions with cellular machinery. The HIV-1 p6Gag PTAP late domain mimics a cellular ESCRT-I recruiting motif, and interacts with tumour susceptibility gene 101 protein (TSG101), a part of ESCRT-I. The second p6Gag late domain, also bears a YPXL-type binding site (Tyr-Pro-X-Leu, where "X" can vary in sequence and length) for the ESCRT factor ALG2-interacting protein X (ALIX) (257).

The interactions with HIV-1 that lead to virus budding are not entirely elucidated but current evidence suggests the following sequence of events. Late domain binding to ALIX and TSG101 recruit ESCRT proteins CHMP1, CHMP2 and CHMP4 which polymerise into filaments forming a dome which starts to constrict the membrane neck of the nascent virion.. The CHMP filaments then recruit VPS4 ATPases which may allow formation of the ESCRT-III dome or removal of ESCRT-III subunits from the dome, reducing its stability and enabling the completion of fission (97,256,258).

Using fluorescently tagged Gag and TIRF microscopy, fluorescence resonance energy transfer (FRET) and fluorescence recovery after photobleaching (FRAP), the assembly time for individual particles has been estimated at 5–9 minutes. Assembling Gag molecules seem to be derived from the rapidly diffusing cytoplasmic pool rather than diffusing laterally in the membrane or entering from vesicular transport (245,259).

Innate immune processes have been selected to restrict these mechanisms. Tetherin is an antiviral protein which tethers nascent viral particles to the plasma membrane thus preventing budding. It in turn is antagonised by the Vpu accessory protein(260).

#### **1.4.10.6 Virion maturation**

Maturation is initiated simultaneous with (or immediately following) budding. This process creates the capsid core and is mediated by cleavage of the Gag and Gag-Pro-Pol polyproteins at ten different sites by viral protease (PR). This produces fully processed MA, CA, NC, p6, PR, RT, and IN proteins (6,261). The viral protease efficiency for cleavage of the target sites is variable, leading to a stepwise processing cascade. There are three categories of cleavage site: rapid, intermediate and slow . MA/CA cleavage disassembles the immature lattice leaving

a membrane bound MA layer. CA/SP1 cleavage produces free CA that can form the mature conical core and NC Sp2 cleavage is required for release of NC and formation of the NC/RNA ribonucleoprotein complex (97).

The HIV-1 protease works as a dimer. A “fireman’s grip” of two side chains activate a water molecule to break the peptide bond. During Gag assembly and budding PR becomes active through an undefined mechanism. For PR to be active it must form a dimer, so within the Gag-Pro-Pol polyprotein it is inactive. Before processing PR constructs dimerize only very weakly but transient dimeric “encounter” complexes may have enough enzymatic activity to allow the amino-terminal cleavage site to be inserted into the substrate-binding cleft. This auto-processing will cause exponential growth of levels of stable PR dimers with full catalytic activity (262). Trafficking of Gag may have evolved to prevent premature PR dimerization prior to virion budding and release.

Maturation can be inhibited using 2 classes of ARVs PIs and Maturation inhibitors. All of the 10 licenced PIs interact with the active site of the PR dimer and directly occlude substrate binding. The unlicensed maturation inhibitor Berivimat was discovered to inhibit HIV-1 by binding to the CA-SP1 site, rather than to PR, preventing cleavage.

## **1.5 HIV and the Innate Immune System**

### **1.5.1 The adaptive and innate immune systems – history and overview**

The human body provides a desirable ecological niche for microbial life providing a stable environment in terms of warmth, moisture, pH and nutrition. An elaborate system of defences has therefore evolved to protect against the microbial threats to the body including retroviruses. In vertebrates, the immune system has two branches, an ancient innate system and a more recent adaptive system. Innate immunity comprises physical barriers (skin and chemical defences like acid and mucus), cell intrinsic responses and a set of proteins and cells (including professional phagocytic cells like neutrophils, macrophages and natural killer cells). These innate immune defences do not depend on previous exposure to a pathogen and help to induce and direct the pathogen specific adaptive immune responses.

Charles Janeway was the first to describe the idea of these two interrelated systems (263). He was convinced that antigen could not be the sole determinant of whether a lymphocyte would proliferate and attack – how could a receptor with a randomly generated ligand binding site determine a suitable substrate for the initiation of an immune response? The requirement for adjuvants to elicit T and B cell adaptive responses offered experimental evidence that the adaptive immune response must rely on receptors that have been selected over evolutionary time but which are not randomly generated.

We now know that there is indeed a set of germline encoded receptors which are not randomly generated but which detect conserved molecular patterns in microbes and vaccine adjuvants called pattern recognition receptors or PRRs. They are the molecular trip wires of the cell-autonomous innate immune system and sense pathogen-associated molecular patterns (PAMPs), conserved molecular structures most of which are unique to pathogens and distinct from self. They initiate signalling cascades resulting in the production of type I interferons, pro-inflammatory cytokines and interleukin-1 $\beta$ . Type I IFNs then induce a second round of gene transcription including a large array of antipathogen genes. The IFNs signal through the Janus kinase (JAK)-signal transducer and activator of transcription (STAT) pathway (264). These processes trigger early mechanisms of host defence as well as priming and orchestrating the antigen-specific adaptive immune responses (265,266).

#### **1.5.1.1 The role of effector cells**

PRR detection of HIV activates both bystander cells and infected cells as well as activating innate immune cells such as Natural Killer (NK) cells and monocytic cells. NK cells comprise

a set antiviral effector cells. Individuals have heterogeneous activation and inhibitory receptor expression on their NK cell populations which determine the effectiveness of the NK response to infection (267). Various receptors are expressed: the polymorphic activating and inhibitory killer immunoglobulin-like receptors (KIRs) interact with MHC I families (268) which act as ligands for inhibitory KIRs. Virally mediated down-regulation of MHC I thus removes the inhibition of killing. NK cells can also recognize and kill HIV-1 infected cells through direct NK receptor recognition of viral proteins or virus-induced stress ligands. In HIV-1–infected individuals viruses are frequently selected with KIR-escape mutations, but the mechanisms remain to be resolved (269,270).

#### **1.5.1.2 The modulation of adaptive immunity**

NK cells modulate DC and T cell function, and so inform an adaptive immune response and while the cross talk between these two arms of the immune system is poorly understood in the context of HIV it is plausible that the NK response may influence subsequent antiviral T cell function. Several studies provide evidence that the clinical course of HIV infection may depend on early immune events in the first stages of infection: the severity and duration of the initial seroconversion illness are associated with the rate of CD4+ T cell depletion, AIDS related mortality (271) and certain MHC class I alleles (HLA-B27) offer protection against rapid disease progression (272) while early induction of cytokines is associated with delayed disease progression (273).

#### **1.5.1.3 Pattern Recognition Receptors**

PRRs can be divided into two groups by localisation. The extrinsic Toll-like receptors (TLRs), (located on the plasma membrane or the endosomal compartment) and the internal intracellular cytosolic nucleic acid sensors. Several families of PRRs have been characterized by structure including TLRs, nucleotide-binding oligomerization domain (Nod)-, leucine-rich repeat-containing receptors (NLRs), RIG-I-like receptors (RLRs), C-type lectin receptors (CLRs) and AIM-2 like receptors. There are also enzymes which sense intracellular nucleic acid. These include the family of OAS proteins and cGAS (274–276).

#### **1.5.1.4 External PRRs**

The first extrinsic receptors were discovered in the mid-1990s and include members of the TLR family (277). Cell extrinsic receptors are found in cells specialised in pathogen detection including epithelial and myeloid cells and are able to detect extracellular pathogens. Their ligand-binding domains project extracellularly or into the lumen of the endosome, and they have a cytosolic signalling domain (278). TLR1, TLR2, TLR4, TLR5 and TLR6, and CLRs, dectin-1, dectin-2 and mincle, are specialized in the recognition of common components of

bacterial and fungal cell walls while viral recognition outside the cell is mediated by TLR3, TLR7, TLR8, TLR9 and TLR13 (279). These are able to sense nucleic acid on the endosomal membrane of immune cells. They signal using two pathways: TLR3 activates TRIF whereas TLRs 7, 8, 9 and 13 activate MyD88. Both these adaptors activate NF $\kappa$ B but IRF3 is activated by TRIF alone and IRF7 by the MyD88 pathway. The TLRs show varying ligand specificity for ssRNA, dsRNA or other RNA motifs. (274).

#### **1.5.1.5 Internal PRRs**

Cell intrinsic receptors require intracellular localisation of the pathogen and detect viral RNA (RLRs), viral DNA (cytosolic DNA sensors) and bacterial cyclic di-guanylate monophosphate (STING). Nucleic acid species in the cytosol are powerful PAMPs indicating viral infection or DNA damage to the cell and unlike most PAMPs they are not unique to pathogens and so use of nucleic acids as a PAMP is a two edged sword. On the one hand, because all microbes must use nucleic acid, it enables detection of a wider range of pathogens, but on the other it creates the risk of recognising host nucleic acids which is the basis for several autoimmune diseases.

#### **1.5.2 Cytosolic RNA sensing - RLRs**

All three RLR receptors (RIG-I, MDA5 and LGP2) share conserved domains including: two N-terminal caspase activation and recruitment domains (CARDs) that mediate signalling to downstream adaptor proteins (275,280). They have preferences for varying RNA ligands, though the ligand for MDA-5 is least well understood. Signalling downstream of RIG-I is best understood. It depends on MAVS (mitochondrial antiviral signalling; or IPS-1, CARDIF, VISA), an adaptor protein. Binding of viral dsRNA releases the CARD and induces MAVS aggregation on the mitochondrial membrane (281). (275). CARD domains that have been released bind to the CARD domain of MAVS, creating prion like aggregations of MAVS molecules. These function as “seeds” binding more MAVS molecules into ever larger aggregates which rapidly amplify RIG-I signalling, such that small amounts of viral RNA can trigger massive IRF3 activation. MAVS aggregates recruit multiple TRAF proteins which in turn induce ubiquitination. These recruit NEMO to the MAVS signalling complex (282,283). NEMO is a subunit of IKK and TBK1 with regulatory functions and contains two ubiquitin binding domains, functioning as a ubiquitin sensor. It is crucial in viral infection for IKK and TBK1 activation and subsequent activation of NF- $\kappa$ B and IRF3(282).

### **1.5.2.1 Cytosolic RNA sensing - OAS**

The IFN-inducible protein 2'5'-oligoadenylate synthetase (OAS) and dsRNA-dependent protein kinase R (PKR) are also able to recognize cytoplasmic dsRNA. Following dsRNA binding OAS catalyzes the activation of the latent ribonuclease RNase L which then degrades viral and cellular ssRNAs - the cleaved products induce more type I IFN production via the RIG-I pathway (275,284,285). PKR is activated by binding to dsRNA and once active it inhibits translation initiation thus inhibiting viral replication and inducing type I IFN (275).

### **1.5.3 Cytosolic DNA sensing**

DNA was known to be a potent Immune stimulant long before it was discovered to be genetic material. In his Nobel Prize acceptance speech in 1908, Mechnikov, the founding father of innate immunity, stated that nucleic acids could recruit protective phagocytes.

*“There are already surgeons in France and in Germany, who introduce into the abdominal cavity nucleic acid or other substance, with the object of bringing to the scene a protective army of phagocytes to ward the microbes off. The results achieved are so encouraging that it is possible to predict new progress in the approach to the dressing of wounds.”*

Despite the intervening 100 years, it has taken until the second decade of the 21<sup>st</sup> century to understand how DNA trigger innate immune signalling. DNA is typically confined to eukaryotic nuclei and mitochondria, so cytosolic DNA indicates either infections, cellular damage or inappropriate cell division, and triggers robust immune responses including inflammasome activation and type I IFN induction.

#### **1.5.3.1 The cGAS–STING pathway of cytosolic DNA sensing**

Various receptors have been identified as putative DNA sensors for detecting viral DNA (including DDX41, DNA-PK, DAI, RNA Polymerase III, IFI-16 and several other DNA helicases) but none has been as universally accepted as Cyclic GMP-AMP (cGAMP) synthase (cGAS) (figure 1.10) (286). The role of these other proteins in cytosolic DNA sensing is uncertain as genetic studies have failed to confirm their involvement. Mouse strains and human cells knocked out or depleted of these proteins using CRISPR show no apparent defect in the induction of interferons in response to cytosolic DNA or DNA viruses. By contrast depletion or deletion of cGAS completely abolishes IFN induction by cytosolic DNA or DNA viruses. (287,288).

PQBP1 has been reported to facilitate the sensing of HIV-1 DNA by cGAS and KD has been shown in to inhibit the induction of interferon by HIV but not induction achieved by infection with DNA viruses but the relationship between HIV, PQBP1 and cGAS remains unclear (289).

cGAS activates innate immune responses mediated by the second messenger cGAMP. This activates the endoplasmic reticulum protein STING (Stimulator of Interferon inducible Genes) (290). Genetic approaches using cGAS deficient mice have shown that cGAS is a sensor for a variety of pathogens. Mice deficient in cGAS or STING do not produce interferons in response to infection by DNA viruses (e.g. HSV-1 or vaccinia virus) have high viral titres and mortality (291). Interestingly these mice are also more sensitive to infection with RNA viruses, despite the fact that they have normal interferon production in response to RNA viruses. It may be that the cGAS pathway produces basal amounts of interferons important for arresting early viral infection *in vivo*. It is also possible that infection with RNA viruses induces cellular damage with 'leakage' of cellular DNA, and that this stimulates the cGAS pathway to help the immune defense against infection with RNA viruses (292).

### **1.5.3.2 cGAS Structure and regulation by DNA binding**

cGAS is a nucleotidyltransferase (NTase) and shows structural and sequence homology to the catalytic domain of OAS. It contains a nucleotidyltransferase domain and two major DNA-binding domains (293). cGAS exists in an autoinhibited state (294) but is activated by all dsDNA independent of structure and length. This DNA-sequence-independent activation is due to cGAS binding to the sugar-phosphate backbone of dsDNA but not to any of the bases as shown by crystal structures. Single-stranded DNA with internal duplex structures can also activate cGAS and short dsDNA (~15 base pairs in length) is sufficient to bind and activate cGAS *in vitro*. Longer DNA is needed to activate the cGAS pathway in cells, putatively because of cytosolic nucleases which degrade short strands (294).

### **1.5.3.3 cGAMP functions as a second messenger**

DNA binding induces a conformational change which initiates the synthesis of cyclic GMP-AMP (cGAMP) from ATP and GTP. This cGAMP contains two phosphodiester bonds and functions as a second messenger by activating STING. (293). cGAMP can also spread from cell to cell through gap junctions enabling rapid responses by surrounding cells. This is important as some viruses have mechanisms to antagonise the production of type I IFNs in host cells which are infected (295). It may also have evolved to be incorporated into virions and some viruses incorporate cGAMP enabling a rapid response to viral infection (296).

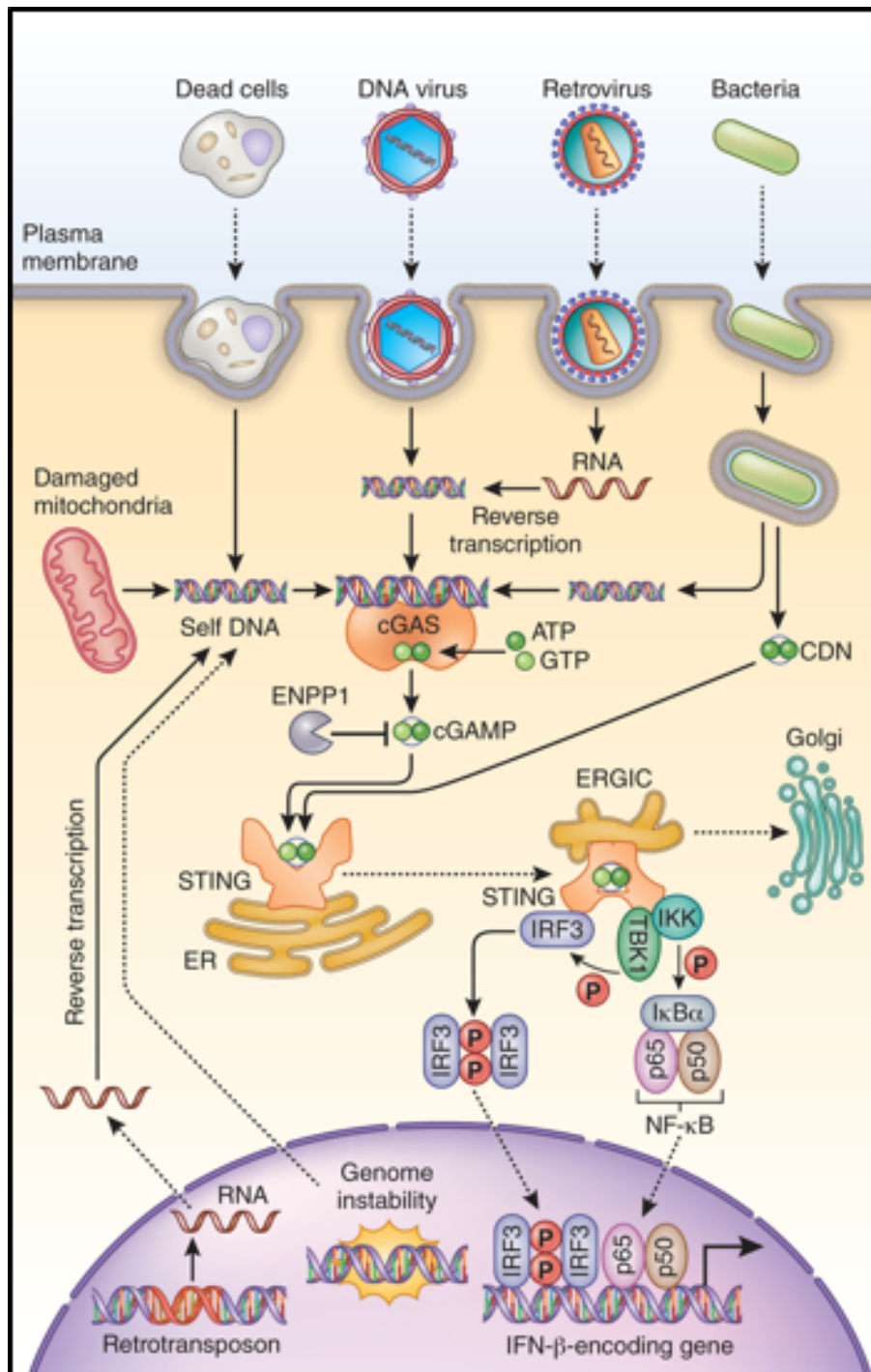


**Figure 1.10 The cGAS–STING cytosolic DNA sensing pathway.** Cytosolic DNA binds to and activates cGAS, stimulating the production of 2'3'-cGAMP. This binds to STING which once activated moves to the ER-Golgi intermediate compartment and the Golgi apparatus where it activates IKK and TBK1. TBK1 phosphorylates STING, enabling it to recruit IRF3 for phosphorylation. IRF3 then forms dimers and enters the nucleus, where, together with NF-κB it activates expression of type I IFNs and other immunomodulatory molecules. From Chen Q, et al Regulation and function of the cGAS–STING pathway of cytosolic DNA sensing from *Nature Immunology*. 13, 484–496 (2012)

#### **1.5.3.4 Activation of STING by cGAMP and bacterial cyclic dinucleotides**

Stimulator of interferon genes (STING /MITA, MYS, ERIS and TMEM173) was identified as an adaptor of type I IFN production using cDNA expression screens for genes that can activate the IFN $\beta$  promoter. STING has a wide tissue distribution (297). It contains four trans-membrane domains at the amino terminus that anchor the protein to the ER membrane, with the large carboxy-terminal domain projecting into the cytoplasm. (298) STING forms a butterfly shaped dimer on the ER membrane with or without a ligand (299–301).

cGAMP is the most potent activator of STING and it can also be activated by cyclic-dinucleotides (CDNs) secreted directly from bacteria; the CDN gene expression profile is indistinguishable cell stimulated by DNA (275). cGAMP binds to STING more tightly than other cGAMP isomers or bacterial CDNs, including cyclic di-GMP and cyclic di-AMP (294), and induces a more potent IFN- $\beta$  response (302,303).

cGAMP binds to a central crevice of the butterfly shaped STING dimer (294) and induces conformational change moving the “wings of the butterfly” closer together by about 20Å releasing the carboxy-terminal tail (CTT) which recruits and activates TANK-binding kinase 1 (TBK1) (304). This CTT, which has just 39 amino acid residues, is all that is required to activate TBK1 and recruit IRF3 to TBK1, but is not, as yet, visible in crystal structures of STING. (206,294).

#### **1.5.3.5 STING trafficking and signalling**

On activation by cGAMP, STING rapidly traffics from the ER to an ER-Golgi intermediate compartment and the Golgi apparatus and forms large punctate structures (305). Inhibition of this trafficking blocks activation of the downstream pathway suggesting that the trafficking is important for activation (306). During this process the CTT recruits and activates TBK1 which in turn phosphorylates STING at several serine and threonine residues. This phosphorylation of STING enables the subsequent phosphorylation of IRF3 by TBK1. Phosphorylated STING binds to a positively charged region of IRF3 and thereby recruits IRF3 for phosphorylation by TBK1. The phosphorylated IRF3 dimerizes and then enters the nucleus. This elaborate process of “back phosphorylation” of STING by TBK1 allows a fine degree of control of downstream signalling. While three adaptors of innate immunity, MAVS, TRIF and STING, can activate TBK1 via their respective RIG-I–MAVS, cGAS-STING, and TLR3/4-TRIF pathways, there are other pathways that also activate TBK1. However IRF3 phosphorylation

and subsequent IFN production by TBK1 is only seen in the same pathways that use MAVS, STING, or TRIF as adaptors (275).

These all share a highly conserved motif that is phosphorylated in response to stimulation with their cognate ligands and this provides a 'licensing' mechanism for the phosphorylation of IRF3 by TBK1 ensuring only a few agents that can activate TBK (e.g. viral infection) lead to IRF3 activation and IFN induction. This specification of TBK1-mediated IRF3 activation allows careful regulation of IFN production, avoiding autoimmune disease.

STING also activates the kinase IKK, which phosphorylates the I $\kappa$ B family of inhibitors of the transcription factor NF- $\kappa$ B. (305). These phosphorylated I $\kappa$ B proteins are subsequently degraded by the ubiquitin-proteasome pathway releasing NF- $\kappa$ B. This translocates to the nucleus, where it functions together with IRF3 and other transcription factors to induce the expression of interferons and inflammatory cytokines such as TNF, IL-1 $\beta$  and IL-6 as well as numerous innate immune genes, including IFN and members of the IFIT family (Abe and Barber, 2014).

Classically TBK-1 is linked to IRF-3 release and IKK phosphorylates the NF $\kappa$ B inhibitor I $\kappa$ B causing release of NF $\kappa$ B subunits but there is evidence that TBK-1 can act directly to stimulate NF $\kappa$ B signalling (307)

STING has also been reported to recruit and phosphorylate STAT6 using TBK1 which causes chemokine induction (308).

#### **1.5.3.6 Reconstitution of cGAS and STING signalling in HEK293T cells**

cGAS is induced by interferon providing positive feedback and amplification of the pathway (309). Many tumor cell lines, including the cells used in the majority of the assays in this thesis, HEK293T cells, have silenced expression of cGAS and STING and do not activate an innate immune signalling response following stimulation by DNA or DNA viruses (310). That the cGAS–STING pathway is disabled in cancer cells implies that a functional pathway might prevent transformation putatively by assisting the identification of cancer cells by the immune system.

Human Embryonic Kidney 293 cells (HEK293) and their derivatives are among the most commonly used cells in laboratories. HEK293 cells were derived in 1973 from an aborted embryo. Primary embryonic kidney cells were exposed to the sheared DNA of adenovirus type 5 (AD5) and transformed (311). Despite their widespread use in cell biology, details of their phenotype, karyotype instability, and tumorigenicity are still unclear. The chromosome number

and aberrations vary even between cells from the same culture and from different cell banks and labs. The fact that 293 or other cell lines are easily transfected is poorly understood but the utility of 293 cells in transfection experiments would imply that they lack intact DNA sensing pathways. It has been shown that transfection of DNA into cells with intact DNA sensing pathways leads to innate immune responses (312). HEK293T cells have no endogenous detectable STING, but overexpression activates IRF3 and NF $\kappa$ B and stimulates IFN- $\beta$  production (313).

cGAS regulation is poorly understood, but there are likely to be mechanisms to ensure a sensitive and specific response to foreign DNA while remaining unresponsive to self DNA. Studies have suggested that post-translational modifications of cGAS regulate its enzymatic activity their influence on overall cGAS activity is not clear (314).

Understanding of regulation of STING is also in its infancy: after STING has signalled, it is rapidly degraded, possibly by the autophagy kinase ULK1-ATG1 but the mechanism remains to be elucidated. (292,315).

#### **1.5.4 PRRs and HIV-1**

Protein and nucleic acid components of HIV are detected by a range of PRRs. The Env glycoprotein gp120 is recognised by surface TLR2 and TLR4 on epithelial cells (316). The HIV-1 genome is recognized by endosomal TLR7 and TLR8 in plasmacytoid DCs and other myeloid cells. (317). RNA helicase RIG-I/31 is a cytosolic PRR which may recognise HIV genomic RNA and induce signalling in HIV target cells (318,319). The ISG product Tetherin is expressed on the surface of cells, and 'tethers' virions to the plasma membrane to antagonise their release (320,321). It is also a PRR, inducing an signalling cascade which activates NF $\kappa$ B (322).

Interferon inducible protein 16 (IFI16) and cyclic GMP-AMP synthase (cGAS) sense infection early, by detecting viral reverse transcriptase products. Various other receptors have been identified as putative DNA sensors for detecting viral DNA: DNA-PK, DAI, RNA Polymerase III, and several other DNA helicases have been suggested but none have been as universally accepted as cGAS and IFI16 (Keating et al., 2011).

#### **1.5.5 Evasion of DNA sensing by microbial pathogens and HIV**

Viruses and bacteria have numerous strategies to antagonise or avoid the cGAS STING pathway which may include 'hiding' their DNA from the cytoplasm and using cellular co-factors.

### 1.5.5.1 The role of Capsid, CypA and CPSF6

Retroviruses and many DNA viruses may have evolved to conceal DNA in the viral core while they traverse the cytoplasm and then deliver their viral DNA into the nucleus. HIV-1 viral capsid in the cytoplasm recruits the host factors CPSF6 and CypA. CypA is a prolyl isomerase enzyme that binds to the HIV-1 capsid and isomerizes the peptide bond between residues G89 and P90 between cis and trans conformation. CPSF6 predominantly localizes to the nucleus, and enables in 3'-end mRNA processing. This may help to target HIV-1 to an advantageous nuclear entry pathway (165). Together, these host factors help coordinate reverse transcription, capsid uncoating and entry of the viral pre-integration complex into the nucleus, such that viral DNA is not exposed to the cytoplasm. HIV-1 replication in primary human monocyte-derived macrophages (MDM) is dependent on these co-factors (323). Depletion of these factors, or genetic disruption of their interaction with CA, triggers DNA sensors and activates a type 1 IFN response in macrophages infected with wild-type HIV-, suppressing replication. Blockade of IFN signalling using an IFN receptor antibody largely rescues this replication defect (165,177,323,324). Importantly, CypA and CPSF6 have been shown to be unnecessary for replication in cell lines with defective DNA sensing pathways (323,325) however experiments in our lab have shown that co-factors are required for replication in T cells, which appear to lack DNA sensing pathways. Additionally, co-factors are not required in THPs which appear to have intact pathways. Production of cGAMP is diminished after treatment with RT inhibitors but not with inhibitors of later stages in the replication cycle, indicating that reverse transcription products act as PAMPs for cGAS. The exact ligands have yet to be identified (326).

HIV-2, but not by HIV-1, can infect and activate dendritic cells (327) because HIV-2 encodes Vpx, which degrades SAMHD1. Subsequent recognition of HIV-2 PAMPs by PRRs leads to activation of dendritic cells (328,329). The HIV-1 and 2 capsids have different CypA affinity. They both form a complex with CypA but in HIV-1 CypA –capsid binding masks viral nucleic acid from the PRRs. By contrast, some studies have shown that HIV-2 capsid-CypA binding allows the viral nucleic acid in the cytosol to be sensed by cGAS. So disruption of capsid HIV-1 CypA binding in the presence of vpx leads to PRR activation in DCs. KD of cGAS prevents this activation. KD of IFI16 does not. Some studies have shown that HIV-1 with vpx alone doesn't activate sensing, i.e. in DCs SAMHD1 antagonises replication of HIV-1, but if you add vpx then the capsid interaction with CypA allows evasion of sensing by cGAS. These studies offer the possibility of a vaccine through 'recovery' of the DC innate immune response against HIV-1 through activation of cGAS using PAMPs (327,330).

It may also be that the proteins involved in nuclear import act as co-factors. Various studies describe functional interactions between capsid and components of the nuclear pore including Nup358, Nup153 and the karyopherin TNPO3 (164,167,204,331–334). Nup 153 has been shown to bind capsid at the same interface as CPSF6 and this makes it plausible that Nup153 displaces CPSF6 at the nucleus to enable uncoating, allowing DNA to enter the nucleus without exposure to cytoplasmic PRRs. These processes may enable HIV-1 to evade innate immune activation through hiding viral DNA, and viral DNA ends, from cytoplasmic PRRs (164,175,204,334).

#### **1.5.5.2 The role of TREX1**

One of the first cellular co-factors identified as being used by HIV-1 is the DNase TREX1 (335). It is perhaps an unexpected co-factor since it is an ER associated nuclease which causes HIV-1 DNA to be degraded. It may work by degrading, not genomic DNA ready for integration, but cytoplasmic DNA products of mistimed RT or DNA exposed by premature uncoating. Neither of these would be able to establish infection in any case, but both of which could provide a substrate for DNA sensors and a subsequent immune response. Depletion of the DNase TREX1 causes HIV-1 DNA to accumulate in the cytoplasm, which triggers the induction of interferon via cGAS. This suggests that HIV-1 co-opts host proteins to minimize the exposure and accumulation of viral DNA in the cytoplasm, which would otherwise trigger the cGAS–STING pathway (336–338). It is not clear why in the event of premature uncoating, or DNA synthesis, TREX1 does not degrade viral DNA universally protecting HIV-1 from activating an immune response.

#### **1.5.5.3 Specific antagonism of DNA sensing by accessory proteins**

Specific viral antagonists of cGAS/STING signalling have been noted in other viruses but not discovered in HIV. The  $\gamma$ -herpesvirus KSHV encodes ORF52, a tegument protein that inhibits cGAS activity through direct binding to cGAS as well as through binding to DNA. Herpes simplex virus type 1 encodes the regulatory protein ICP27, which interacts with STING and TBK1 and thereby prevents the phosphorylation of IRF3 by TBK1. The E1A protein of adenovirus and E7 protein of human papilloma virus inhibit STING signalling by binding to STING through a LXCXE motif (Leu-X-Cys-X-Glu, where 'X' is any amino acid) of these viral proteins (292).

#### **1.5.5.4 IFI16 and HIV**

IFI16 is an ISG and is expressed both in the nucleus and the cytosol. It has a PYHIN domain mediating protein-protein interactions and can recognise and physically bind to DNA products of RT through a HIN domain which recognises specific PAMPs (including a segment of the

LTR). Much of the literature on IFI16 is conflicting and unconvincing. It has been shown in transfected cells to co-localise with HIV-1 DNA. It signals via the adaptor STING (339). Knockdown of IFI16 has been shown to increase permissiveness to HIV-1 and improve replication although these experiments have not been replicated (340). In CD4+ T cell 'bystander cells' (i.e. non-permissive to infection), IFI16 activates the inflammasome and causes inflammatory cell death or pyroptosis to infection but these data appear, at present, unconvincing (341). It is unclear what determines interaction with STING vs activation of the inflammasome. It is hypothesised to be one of the proximate causes of CD4 helper cell loss in clinical HIV infection. HIV has been shown to induce the inflammasome in different cell types. The inflammasome is a protein complex which activates caspase-1 and stimulates the processing of pro-interleukin 1 $\beta$  into mature IL-1 $\beta$ , an inflammatory cytokine. Non-activated CD4+ T cells are not permissive to HIV infection. HIV-1 can bind and enter the cells because of SAMHD1 depletion of nucleoside pools reverse transcription is limited. These abortively infected cells are known as bystander cells. These cells die by pyroptosis, characterized by the activation of caspase-1. IFI16 is proposed to initiate this inflammasome signalling and T cell pyroptosis by detecting reverse transcriptase products in the cytoplasm. So IFI16 may drive two differential responses controlled by PAMP signalling and interactions with signalling proteins. In activated CD4+ T cells it induces an antiviral state, compared to resting T cells where infection induces inflammasome activation and pyroptosis response (342,343).

In summary, it is not clear why there would be two DNA sensors, both of which signal via STING in HIV infection. They may increase sensitivity to host DNA ligands in the cytosol. TREX1 is an exonuclease which removes DNA from the cell cytoplasm: inactivating mutations in TREX1 lead to severe pathology (Aicardi-Goutieres syndrome, a neuroinflammatory condition). Depletion of TREX1 increases detection of HIV-1 dsDNA in CD4 cells and stimulates an interferon response that abrogates infection (336). So while the primary function of TREX1 is to avoid an inflammatory response to self dsDNA it also acts as a co-factor for HIV infection by limiting recognition of cytosolic DNA PAMPs. Differential regulation of TREX1, by both host and virus, may determine innate immune responses to viral dsDNA.

## 1.6 HIV accessory proteins, restriction factors and co-factors

With only nine open reading frames HIV-1 carries with it a relatively small set of tools for evasion of innate immune detection. As well as specifically antagonising restriction factors, the IFN-stimulated factors that restrict HIV, with accessory genes (Vif, Vpu, Nef and Vpr), HIV uses cellular co-factors which may provide “cloaking” functions that enable evasion of innate immune pattern recognition receptors (PRRs).

PRR ligand binding initiates signalling cascades which activate transcription factors including IRF3, IRF7 and NFκB which in turn induce antiviral and inflammatory genes including those encoding interferon. This then causes a second wave of transcriptional changes and the induction of hundreds of ISGs. The antiviral genes that are activated include restriction factors APOBEC3, TRIM5a, SAMHD1, tetherin, Schlafen11, IFITM and MX2 all of which can limit HIV infection *in vitro*. In resting cells these proteins may be found at low levels or not at all (344–347).

The accessory proteins were so called because they were not necessary for replication in various cell types *in vitro*. As their roles became clear, it became apparent that they counteract host antiviral defense mechanisms and that there were common themes to their mechanisms for doing so. HIV-1 Vif and Vpu and Vpr lack enzymatic activity, instead serving as substrate adaptors for cellular ubiquitin ligases to antagonise immune responses. Ubiquitination consists of post-translational protein modification which enables regulation of protein degradation and trafficking. E3 ubiquitin ligases transfer ubiquitin from E2 ubiquitin-conjugating enzymes to target proteins. They are multi-protein complexes consisting of a scaffold, a specific adaptor, and a substrate that is the target protein. Each accessory protein thus targets different cellular factors using related mechanisms.

### 1.6.1 Tetherin and Vpu

The transmembrane protein tetherin acts at the plasma membrane of infected cells, physically tethering budding HIV-1 virions (321). HIV-1 has evolved the accessory protein Vpu to antagonise this restriction. Vpu is also a transmembrane protein which localises to the ER. Interestingly the parental SIVcptPtt uses Nef to antagonise tetherin. Species specificity studies have provided evidence that its antagonism was required for the pandemicity of HIV-1M. Zoonotic transmission of SIVcpz required the virus to evolve another way to antagonise tetherin. A small number of amino acid changes enable SIVcpz/HIV-1 M Vpu to target human

tetherin (348). HIV-2 antagonises tetherin with its envelope glycoprotein protein illustrating immense adaptability in viral strategies to avoid and antagonise host cell restriction.

*Δvpu* HIV-1 virions cluster on the plasma membrane without budding (349,350). Additionally, they have been shown to have fewer glycoprotein spikes. Vpu relieves the block to virus release by sequestering tetherin near the nucleus and leading to its endocytosis and degradation in the proteasome.

Tetherin also acts as a PRR. As it tethers budding virions it detaches from the actin cytoskeleton at the cortex of the cell. It is subsequently phosphorylated and recruits the signalling adaptors TRAF2, TRAF6 and the mitogen-activated protein kinase TAK-1 and induces NFκB mediated interferon production (351,352).

### **1.6.2 TRIM5 $\alpha$**

The existence of a restriction factor for the capsids of HIV-1, SIV, and other retroviruses was predicted when restricted infection was observed in a various mammalian cell lines (353). TRIM5 $\alpha$  was identified in a screen of rhesus macaque genes and was demonstrated to restrict HIV-1 infection when expressed in human cells. TRIM5 $\alpha$  is a ~500 amino acid cytoplasmic protein and it restricts early in the life cycle. TRIM5 $\alpha$  restriction is characterised by inhibition of viral cDNA synthesis (179). TRIM5 $\alpha$  is part of the large tripartite motif family. In humans there are around 100 genes in this family and all, including TRIM5 $\alpha$ , comprise a RING E3 ubiquitin ligase domain, one or two B box domains, and an alpha-helical domain. The carboxy-terminal domain is not highly conserved - in the case of TRIM5 $\alpha$  it is a PRYSPRY domain determines capsid recognition species specificity.

Different species TRIM5 $\alpha$  inhibit different retroviruses. The human TRIM5 $\alpha$  protein restricts N-MLV, as well as equine infectious anaemia virus (EIAV) but is has no effect against HIV-1. Conversely, TRIM5 $\alpha$  proteins from Old World monkey species generally inhibit HIV-1. Since TRIM5 $\alpha$  proteins often only weakly inhibit retroviruses in their host species, but are active against retroviruses found in other species they pose a barrier to cross-species transmission infection (179). The mechanisms by which TRIM5 proteins act to block retroviral infection are not completely understood. Retrotransposition events in owl monkeys and rhesus macaques resulted in chimeric TRIM5-CypA fusion proteins (TRIMCyp) with a CypA protein domain replacing the PRYSPRY domain (179,354). These proteins are potent inhibitors of lentiviruses like HIV-1 whose capsids bind CypA. TRIM5 $\alpha$  and TRIMCyp bind directly to HIV-1 capsids. Recent studies have shown that, as well as being a retroviral restriction factor, TRIM5 $\alpha$  acts as a PRR specific for capsid, and initiates innate immune AP-1 and NFκB signalling (355).

### **1.6.3 APOBEC3G and Vif**

All primate lentiviruses have the accessory gene, virion infectivity factor (Vif). It antagonises the APOBEC3 family of cytidine deaminase restriction factors which restrict HIV by causing hypermutation, cytidine to uracil deamination of the viral DNA minus strand, and suppressing DNA synthesis (356). It is expressed in many cell types, including CD4<sup>+</sup> T cells and MDMs. Incorporation into assembling virions is needed for infectivity (357). Packaged APOBEC3 may also prevent primer-binding site binding of tRNA and thus terminate synthesis of minus-strand DNA (358).

Vif induces ubiquitin mediated degradation of APOBEC prior to its incorporation into the virion. It binds to APOBEC3 molecules and recruits a cullin 5–based E3 ubiquitin ligase complex. The bound APOBEC3 proteins are ubiquitinated and degraded at the proteasome (359,360). Paradoxically, by generating sequence diversity and accelerating evolution through non-lethal mutagenesis, the packaging of small quantities of APOBEC3 proteins may provide a selective advantage to the virus, and there is experimental evidence that APOBEC3 may increase the rate of drug resistant virus and escape from cytotoxic T lymphocytes (361,362).

### **1.6.4 SAMHD1 and Vpx**

SAM domain–and HD domain–containing protein 1 (SAMHD1) is a deoxynucleoside triphosphate triphosphohydrolase expressed in myeloid cells and resting T cells (363,364). It consists of an N-terminal SAM (sterile alpha motif) domain and a C-terminal HD domain characteristic of enzymes with phosphodiesterase, phosphatase and nuclease activities. It contains an NLS and localises to the nucleus. It restricts HIV-1 infection by reducing the concentration of dNTPs to a level below the threshold required for reverse transcription. Addition of exogenous deoxynucleosides (dN) removes restriction in DCs (365). It may also have an RNA and single strand exonuclease activity which helps in restricting virus replication (366).

SAMHD1 is antagonised by virion packaged Vpx an accessory protein found only in HIV-2 and some SIVs (from both red-capped mangabeys, SIVrcm, and sooty mangabeys, SIVsm). Infection of MDMs with Vpx-containing virus-like particles (VLPs) increases their susceptibility to HIV-1 (which lacks Vpx) by two orders of magnitude. HIV-1 with packaged Vpx shows a similarly increased infection titre in DCs and MDMs (Sunseri et al., 2011). The differential binding of the HIV-1 and 2 capsids to MDM co-factors may provide an explanation as to why HIV-1 does not need to encode Vpx and similarly why HIV-2 is less pathogenic (see below).

Similar to Vif, Vpx complexes with a culin 4A–based E3 ubiquitin ligase, which includes DCAF1 and DDB1 among its constituents. This E3 ligase is involved in the regulation and degradation of various cellular DNA repair proteins, replication enzymes and transcription factors. It was shown, using mass spectrometry–pull-down, that it is hijacked by Vpx to degrade a restriction factor identified as SAMHD1 (364,370). SAMHD1 is rapidly degraded following infection levels remain depleted for 2-3 days. SAMHD1 NLS deletion localises it to the cytoplasm and renders it refractory to degradation by Vpx suggesting that Vpx specifically degrades nuclear or perinuclear SAMHD1, consistent with the idea that uncoating and RT happen very close to, or at, the nuclear pore (371,372). It may also be that, in the case of HIV-1, SAMHD1 acts as a TREX1 like co-factor degrading RT products in the cytoplasm and serving to protect the virus from innate immune recognition.

Whilst SAMHD1 degradation is mediated by Vpx it may have been Vpr that initially evolved for this purpose. The Vpr encoded by the SIV of African green monkeys (SIVagm) degrades SAMHD1. Sequence analysis of primate SAMHD1 indicates that amino acids bound by Vpx are under strong selection pressure. Theories can only be developed from extant viral sequences but there is evidence that during primate evolution, *SAMHD1* gene mutations that enabled escape from Vpx were selected. Lentiviral accessory genes often have multiple functions. During SIV evolution the Vpr open reading frame was duplicated which enable functional specialization of the two gene products. Vpx could then rapidly adapt to SAMHD1 sequence changes. Modern SIVcpz lacks Vpx, which was likely deleted during the transmission from Old World monkeys (373,374). Vif, which has an overlapping reading frame, was subsequently free to evolve to counteract APOBEC3 in chimpanzees.

It is not entirely clear how HIV-1 replicates without Vpx. It may be that the RT of HIV-1 has a higher dNTP affinity so it can synthesize DNA at lower concentrations or it may be that replication in myeloid cells is unnecessary due to T cell to T cell transmission. HIV-2 and SIV by contrast may require myeloid to T cell transmission which may be important if there are fewer activated T cells.

HIV-2, unlike HIV-1, can activate and infect dendritic cells *in vitro*. (327) This is likely because HIV-2 encodes Vpx, which degrades SAMHD1, allowing innate immune sensing of PAMPs the subsequent activation of dendritic cells (328,329). Paradoxically this degradation of a restriction factor may explain the reduced pathogenicity of HIV-2: it stimulates an earlier protective immune response by activating dendritic cells. It may be that the restriction in DCs prevents proper activation.

### **1.6.5 SERINC and Nef**

Like all accessory proteins, Nef performs multiple functions, including enhancing the infectivity of virions. It has been recently demonstrated that Nef targets serine incorporator 3 (SERINC3) and SERINC5, causing them to be redirected to endosomes from the cell membrane. Usami et al. identified SERINC3 using proteomic analysis of virions from producer cells infected with wild-type versus Nef-defective HIV-1. SERINC3 was found in Nef-defective virus but not in wild-type HIV-1 (375). Rosa et al. used a global transcriptome analysis following infection of cell lines with either wild-type or Nef-defective HIV-1 and were able to correlate SERINC5 expression with Nef-dependent changes in viral infectivity (376). It was subsequently demonstrated, using tagged SERINC3 and SERINC5, that without Nef, both proteins remain in the membrane and are virion incorporated. Nef, disrupts this incorporation. The SERINC proteins may stop the fusion pore enlarging following binding, thus preventing cytoplasmic entry of the capsid core and reducing infectivity but the antiviral mechanism is generally unclear (375,376).

### **1.6.6 MX2 and Capsid**

The GTPase MX2 or MXB was recently revealed as being able to restrict HIV-1 infection in IFN-treated cells (345,347). It localises to the nuclear membrane and suppresses infectivity following reverse transcription prior to nuclear entry. CypA capsid binding mutants are not sensitive to Mx2 restriction suggesting the possibility of direct interaction between capsid, CypA and Mx2. These mutants remain sensitive to IFN treatment, which blocks reverse transcription not nuclear entry, despite their escaping Mx2 (377). This may be evidence of further host restriction factors for HIV-1 that restrict infection before MxB gets to restrict viral nuclear entry.

### **1.6.7 Schlafen11**

SLFN11 has structural similarity to the family of RNA helicases. It acts late in the replication cycle suppressing viral protein production by binding to tRNA and thus antagonising viral-directed changes which aim to increase the amount of tRNAs available for viral protein synthesis. Increased expression levels of SLF11 in CD4+ T cells blocks protein synthesis so effectively it confers elite controller status of chronic HIV-1 infection (344,378).

### **1.6.8 IFITM1–3**

IFITM1–3 restrict early in the HIV replication cycle by inhibiting entry of a range of viruses likely by antagonising viral fusion (379). If overexpressed in cells where HIV-1 is actively

replicating they colocalise with the HIV-1 proteins Env and Gag. They have been shown to be incorporated into new virions, and restrict viral entry into new target cells (380,381).

## 1.7 Viral Protein R - overview

The literature on Vpr catalogues a series of often unrelated or inconsistent findings rather than a coherent narrative of discovery that explains its universal conservation among lentiviruses. The protein is variously described as enigmatic, multitasking, multifaceted and multifunctional. Vpr has been proposed have evolved to cause G2 cell cycle arrest, mediate nuclear import of the pre-integration complex, enable macrophage infection, activate the HIV-1 LTR as well as having wide ranging clinical effects causing dementia, nephropathy, immune dysfunction and metabolic dysregulation but despite the many functions and interactions attributed to the protein, some of which have been characterised in detail, there is no single phenotype that convincingly illuminates its conservation. Critically, while it is absolutely required for replication *in vivo*, Vpr has proven to be dispensable in most cell culture systems and this is possibly why its function has remained elusive.

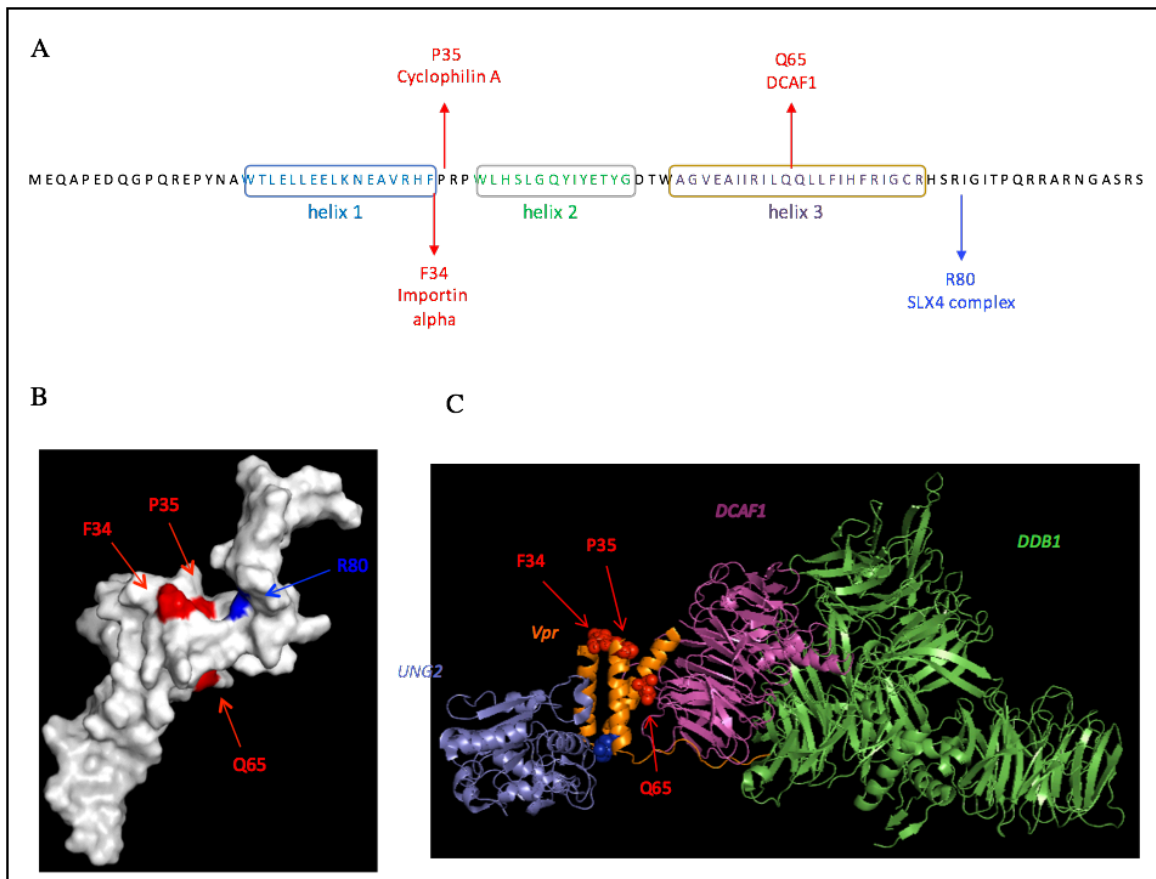


**Figure 1.11 Vpr structure and functional mutations** (A) HIV-1 M Vpr SUMA FJ496150 amino acid sequence with helices and significant mutants annotated. (B) Space filling three-dimensional cartoon structures of Vpr. (C) A representation of the DDB1-DCAF1-Vpr-UNG2 complex in ribbon representation showing how Vpr may function as an adaptor molecule. Individual proteins are colored: green, DDB1; purple, DCAF1; orange, Vpr; blue, UNG2. Images were generated using Pymol (382) Adapted with help from Hataf Khan from (383,384).

Much of the published research of Vpr derives from the findings that the other HIV-1 and 2 accessory proteins, Vpu, Vif and Vpx, have evolved to commandeer ubiquitin ligase complexes, targeting cellular restriction factors for degradation at the proteasome. HIV-1 and 2 counteract tetherin, APOBEC3G and SAMHD1 by this mechanism (385). Vpr has also been shown to have a role in ubiquitin ligase recruitment, and several putative cellular targets have been identified; UNG2 (386,387), MCM10 (388) and MUS81 (389) are downregulated in a Vpr and DCAF dependent manner. The structural basis of SAMHD1 recruitment to the DCAF–Vpx complex has recently been solved (390) but there are no similar data to explain the interaction between DDB1 and DCAF1, or DCAF1 and Vpr. Little is known about how Vpr and Vpx proteins confer substrate specificity to the same CRL4–DCAF1 E3 ligase and the precise advantages gained from degradation of these molecules remains unclear: the degradation of these molecules does not explain all the observed *in vivo* Vpr phenotypes.

Unpublished data from our lab has shown that Vpr can rescue HIV-1 infection in macrophages following stimulation with the DNA sensing pathway second messenger molecule cGAMP (see chapter 3) indicating that it may have a role in protecting HIV from innate immunity but this has not been discussed in the published literature. This observation may also explain the inconsistent finding that Vpr defective viruses are unable to replicate in macrophages. Stimulation of macrophages may be dependent on several factors (the infecting supernatant, the immunological condition of the person they were taken from etc) and Vpr may rescue only when innate sensing pathways are activated.

Additionally, although various functions of HIV-1 Vpr have been shown *in vitro*, many of the putative roles for Vpr have been studied using over expression assays but have failed to recognize the main discovery of this PhD: that Vpr antagonises expression from all tested co-transfected plasmids. The finding that Vpr suppresses expression is consistent but is often interpreted as degradation of a specific protein product (391–393). Additionally, the co-immunoprecipitation assays in many studies are performed in a single direction with tagged protein, meaning that Vpr may be precipitating non-specifically.

### **1.7.1 Structure**

Vpr is a small, basic protein (14KDa) of 96 amino acids. Among primate lentiviruses it is believed to be universally conserved (394). It was first described over 2 decades ago (395,396) and was originally described as an accessory protein because it was dispensable *in vitro* for HIV-1 replication and cytopathogenicity in lymphoid cells *in vitro*.

Vpr is virion packaged so may have a role early in infection. It is incorporated via a direct interaction with a leucine-rich (LR) motif (397,398) in the C-terminal p6 region of the Gag

precursor (399,400). Structurally Vpr comprises a flexible N-terminal region, three alpha-helical domains and C-terminal region which is believed to be unstructured (figure 1.11). Recruitment of Vpr oligomers to the plasma membrane is mediated by the HIV-1 Pr55Gag precursor. It is recruited into the virus core following assembly and cleavage of the Pr55Gag precursor. It is tightly associated with viral RNA in the mature virion (401).

Vpr binding to Pr55Gag is crucial for Vpr oligomerization and localisation at the cell membrane during Pr55Gag assembly. Oligomer function is unclear (402). Vpr incorporation has also been used to target molecules (cellular or viral proteins or drugs) into viral particles. HIV particles can be labelled with Vpr fused to GFP in order to localise intracellular virus during early infection (402).

Efficient packaging requires the integrity of the  $\alpha$ -helices and the p6 region of the Gag precursor which has a leucine-rich motif (403–405). It is not clear how many particles of Vpr are incorporated. Experiments with cysteine labelled MT-4 cells determined that Vpr is present in a molar ratio of approx. 1:7 (406) but monomeric or oligomeric Vpr may interact with multimeric Gag. Interactions with other cellular proteins may reduce the amount of Vpr available for Gag interactions so the true value may differ significantly from this estimate (407).

NMR, fluorescence spectroscopy and circular dichroism spectroscopy have all been used to investigate Vpr structures (the latter technique uses the differential absorption of left or right handed circularly polarised light that occurs when a molecule contains one or more chiral chromophores; it allows the analysis of the secondary structure and conformation of macromolecules and can be used to study how secondary structure changes with environment) (383,408–410). Structural studies of the full-length molecule have proved technically challenging due to difficulties in crystallization. Use of NMR techniques is complicated by the self-association properties of Vpr and the fact that the structure of Vpr depends critically on the solution conditions.

Morellet and colleagues determined the tertiary structure of full length Vpr using nuclear magnetic resonance analysis. The polypeptide was dissolved in acidic aqueous-organic solvents (383). There are three amphipathic  $\alpha$ -helical domains  $\alpha$ -H1 (17–33),  $\alpha$ -H2 (38–50) and  $\alpha$ -H3 (55–77). These are linked and surround a hydrophobic core. Conserved prolines in positions 5, 10, 14 and 35 in the N-terminal domain show cis/trans isomerization and a CypA interaction between 14 and 35 may determine correct folding (411,412).

Between residues 73 and 96 of the C-terminal domain there are six arginines, resembling an arginine-rich protein transduction domain. This may explain why Vpr can be used for transduction and how it crosses lipid bilayer membranes (413–415).

Effects on the cell cycle (apoptosis, cell-cycle arrest, defects in mitosis) have been observed to be C-terminal domain dependent (416). The three  $\alpha$ -helices may have a role in nuclear localisation mediated by Vpr (417). The leucine rich third helix of Vpr presents a stretch of hydrophobic side chains on one side which forms a leucine-zipper like motif (418). This region may enable oligomer formation. (419,420).

Vpr forms dimers, trimers, tetramers and higher order multimers (420) but the relationship between multimerization and function remains unclear. Flow cytometry fluorescence resonance energy transfer (FRET) studies have shown that Vpr multimers self-assemble *in vivo* in cells and that this is dependent on a hydrophobic patch on the third  $\alpha$ -helix. G2 arrest was unaffected by mutations here. Arginine mutations such as R80A and R87/88A prevented Vpr induced G2 arrest but left oligomerization unaffected suggesting that this function is independent of oligomerization (421).

## **1.7.2 Functions**

### **1.7.2.1 Cell cycle arrest**

G2 cell cycle arrest is possibly the best studied effect of Vpr. Packaged Vpr induces cell cycle arrest (422). It was first observed in 1995 (423,424) when Vpr was seen to block proliferation of newly infected T lymphocytes which accumulated at G2 M phase with a 4N DNA content. Following cell division the cell undergoes a growth phase (G1) prior to DNA duplication (S phase) and then a second growth phase (G2). This comprises interphase and prepares the cell for mitosis. During G2 the DNA is checked for errors and mitosis is blocked by the G2 checkpoint mechanism if there is evidence of DNA damage. The 4 phases of mitosis or cell division follow G2: prophase, metaphase, anaphase and telophase.

Cell cycle arrest by Vpr is conserved (425) but it is unclear how this advantages the virus. Unexpectedly, in view of its effect on the cell cycle, several studies have described Vpr as enhancing replication in fully differentiated non-dividing macrophages but having no effect on replication in proliferating T cells (426–429). It may inhibit early steps in immune response activation and create a favorable cellular environment for viral replication since proviral transcription is higher during G2 (430,431). As this is more active in the G2 phase it may be through epigenetic control of the HIV-1 LTR promoter. Consistent with this, G2 arrest caused by Vpr correlates with efficient replication in primary human T cells (430,432).

Vpr has been shown to induce G2 cell cycle arrest and apoptosis in proliferating CCR5+ CD4+ T cells using a human hematopoietic stem cell-transplanted humanized mouse model. Since these cells are mainly CD4+ T cells it may explain their depletion in infected patients (433).

The mechanism by which Vpr induces G2 arrest has not been entirely elucidated but hypotheses have been advanced regarding nuclear envelope integrity, and induction of a DNA damage response either through degradation of a specific repair factor or through direct effects of DNA or chromosomal structure. Vpr localises to the nuclear envelope and has been shown to induce herniations of the nuclear membrane (434). This could redistribute nuclear proteins to the cytoplasm including the cyclins involved in the cell cycle regulation, thus contributing to arrest at G2. Studies using video fluorescence microscopy to monitor the movement of the proteins that regulate CDC-2 showed prominent transient nuclear envelope herniations in the presence of Vpr that were not formed by cell cycle arrest mutants (434) but this work has not been repeated or confirmed.

Vpr has been shown to activate DNA damage response pathways. It has multiple interactions with complexes that sense and repair damaged DNA, activating a major signalling pathway of the DNA damage response: ATR (ataxia-telangiectasia and Rad3-related) protein and its downstream target Chk1 (435–437). This in turn activates DNA damage response markers, such as replication protein A (RPA),  $\gamma$ H2AX and FANCD2 at nuclear foci and blocks the cell cycle at G2 (438). The interaction of Vpr with the host DCAF1 adaptor of the Cul4 E3 Ub ligase complex is required for these interactions and pathway activations (439) but the mechanism by which Vpr causes replication stress is unclear.

Vpr has epigenetic effects and can displace heterochromatin protein 1- $\alpha$  (HP1- $\alpha$ ) through acetylation of the histone H3 (440). This has been hypothesised to cause premature chromatid separation and G2 arrest through Vpr-induced activation of the DNA damage surveillance proteins ataxia-telangiectasia-mutated kinase (ATM) and ATM and Rad3-related kinase (ATR). These sense DNA damage and activate signalling pathways (422,436,441). Consistent with this, inhibition of ATR has been observed to disrupt Vpr dependent G2 arrest. ATR and ATM induce G2 arrest following DNA lesions but whether Vpr specifically causes DNA damage is not known (437,442).

Vpr expression correlates with hypo-phosphorylation and inactivation of the p34/CDC2 CDK1 kinase associated with cyclin B and a range of *in vitro* studies have examined proteins which regulate the cell cycle and found interactions with Vpr but detailed mechanistic insight is still lacking. The most promising recent evidence is that there is a target of Vpr caused to be degraded by the host proteasome machinery.

X-ray crystallography and increased understanding of the Vpr related protein, Vpx, provided an insight into the potential molecular mechanisms used by Vpr to recruit host cell ubiquitination machinery in order to inhibit host restriction factors or innate immune proteins. Like Vpr, Vpx comprises a zinc ion stabilised three-helix bundle. It recruits the E3 ligase substrate adaptor DCAF1 and SAMHD1 (discussed in detail in section 1.11.4). Studies of Vpx suggested how Vpr could hijack the proteosomal protein degradation pathway to inactivate innate immune components and several groups have shown that like Vif and Vpx, Vpr orchestrates a E3 Ub ligase complex composed of DCAF1, DDB1, Cul4 and Rbx1 (DDB1-Cullin4-associated factor 1; damage-specific DNA binding protein 1, cullin 4 and ring box protein 1 respectively) also named as the CRL4 complex. However the specific targets of Vpr have remained elusive (364,390). Vpr is proposed to interact with the DCAF1 adaptor of the Cul4 E3 Ub ligase. This is hypothesized to cause cell cycle arrest by causing the degradation of an unknown protein. It has been proposed that Vpr itself escapes proteosomal degradation by association with the Cul4-DDB1 ubiquitin ligase (443). It has been unclear whether it is the degradation of the host protein or the resulting G2 arrest that is the evolved purpose of Vpr. Belzile et al. have proposed a model where nuclear Vpr and specifically Vpr inside nuclear foci associates with DCAF1 and the DDB1-CuL4-E3 ubiquitin ligase. These co-localise with DNA repair foci which contain  $\gamma$ H2AX and RPA2. This may cause the K48-linked poly-ubiquitination induced degradation of a target bound to nuclear DNA. This in turn causes G2 arrest through ATR activation (439).

Interactions between Vpr and Cul 1 & 4 have been shown (444). DCAF1 was identified as a substrate specificity module in Cul4 and DDB1 based ubiquitin ligase E3 complexes (445,446). The DDB1-CuL4-E3 ubiquitin ligase complex is able to recruit various DCAFs and is hypothesized to have a role in maintenance of genome stability, DNA replication and cell cycle check point control (447). In 2007 DCAF1 was recognised as a host factor critical for Vpr induced cell cycle arrest (431,448). Vpr is proposed to use two separate interfaces for binding: the LR motif found between amino acids 60 and 68 binds to VprBP/DCAF1 while the flexible C-terminal region binds an unknown target for ubiquitination and degradation (390).

Laguet et al used tandem affinity purification, immunoprecipitation and mass spectrometry to identify the structure-specific endonuclease (SSE) regulator SLX4 complex (SLX4com) as a target of Vpr using proteomic analysis and showed that it is crucial for the G2-arrest activity. Glycerol gradient sedimentation and co-immunoprecipitation studies suggested that SLX4 subunits, DCAF1 and Vpr assemble into a single complex.

The SLX4 complex is comprised of 12 proteins that together resolve DNA lesions formed during DNA replication stress and/or homologous recombination repair. SLX4 itself acts as

molecular platform for a SLX4 complex comprising several structure specific endonucleases (SSEs) including ERCC1-ERCC4/XPF, MUS81-EME1 and SLX1. The SLX4 complex is suggested to repair the structures resulting from homologous recombination repair: double strand breaks and collapsed replication forks. (449,450). MUS81-EME1 and SLX1 repair X-Holliday Junctions, caused by replication, during homologous recombination (451,452). They are strictly regulated during the cell cycle to ensure removal of inadequate DNA recombination intermediates before chromosome segregation. Laguette et al. showed a slight Vpr dependent reduction in expression of EME1 and MUS81. Levels of polo-like kinase 1 (PLK1) and phospho-PLK1 which activates the endonuclease activity of EME1 were shown to increase. They also observed Vpr dependent remodelling of SLX4 complex following binding to phospho-EME1 and the DCAF1 ubiquitin ligase. Following time course experiments they concluded that activation of SLX4 complex by Vpr occurs prior to G2/M arrest rather than being a consequence of it. Additionally they suggested that silencing of subunits of the SLX4 complex (SLX4, EME1 or MUS81) prevented induction of G2 arrest by Vpr. This was confirmed by Berger et al. (44). Berger et al also showed that Vpr proteins from lentiviruses infecting African green monkeys and related primates also interact with African green monkey SLX4, suggesting that this is a conserved function for Vpr(453). Laguette *et al* also hypothesise that the active SLX4 complex being targeted by Vpr may enable evasion of innate immune detection of DNA damage though do not elaborate on the details of how this could work (389). This work could be combined with the model proposed by Belzile so that the activation of SLX4 complex would cause replication stress leading to creation of FANCD2 foci and cleavage of DNA replication intermediates. This would induce G2 arrest.

Contrasting with these reports a 2016 study from the Emerman lab expressed Vprs from HIV-1 and HIV-2 using an adeno-associated virus vector system in U2OS cells and found that while DNA damage response is conserved, the interaction of Vpr and SLX4 is variable among HIV-1 and HIV-2 isolates. Using clustered regularly interspaced short palindromic repeat (CRISPR)/Cas9 to knockout U2OS and 293T cells for SLX4 they observed that the DNA damage response and cell cycle arrest induced by Vpr are not dependent on the interactions of Vpr and SLX4 and argue that the mechanisms by which Vpr induces a DNA damage response have yet to be elucidated.

### **1.7.2.2 Vpr induced apoptosis**

The role of Vpr in apoptosis is unclear. Vpr has been observed to induce apoptosis in many cell types, however, the proposed mechanisms vary and both the phenotype and mechanisms are often cell-type specific and may be a feature of overexpression.

Apoptosis is a cell death mechanism which avoids damage to nearby cells and inflammation through the controlled degradation of cellular components. Upstream signalling events induce dimerization and activation of initiator caspases 8 and 9 which activate executioner caspases-3, -6, and -7. These orchestrate the degradation structural proteins and the activation of apoptotic enzymes. There are intrinsic and extrinsic pathways. The extrinsic pathway is activated through death receptor ligand binding. Caspase-8 is then recruited and activated and subsequently initiates apoptosis directly, by activating executioner caspases, or indirectly, through activation of the intrinsic pathway.

The intrinsic or mitochondrial apoptosis pathway is initiated via a range of cellular stresses all of which cause cytochrome *c* release from mitochondria and subsequent formation of the apoptosome. This is a complex composed of APAF1, cytochrome *c*, ATP, and caspase-9. Caspase-9 is activated and then cleaves and activates executioner caspases instigating apoptosis (454).

Various studies have suggested that treatment of cells with soluble Vpr induces caspase-dependent apoptosis in CD4+ T cell lines, neurons, hepatocytes, fibroblasts, and primary peripheral blood lymphocytes with both caspase-8 and caspase-9 mediated mechanisms having been implicated (455–457). Vpr has been observed to be a cell-penetrating protein and is also detected in the fluids of HIV-infected patients. It is therefore a potential cause of bystander cell death (414) though it is unclear also how these observations fit in with the mechanism of cell death for CD4 T cells proposed by Doitsch et al (62) who showed that most quiescent lymphoid CD4 cells die by caspase-1-mediated pyroptosis initiated through inflammatory signals.

Other models of Vpr induced apoptosis have been proposed. Jacotot et al determined that the apoptotic functions of Vpr appear to localise to a C-terminal domain which binds to the adenine nucleotide translocator (ANT) component of the mitochondrial permeability transition pore complex (PTPC). Mutations in this domain of Vpr (e.g., R73A, R77A, and R80A) diminish the ability of Vpr to induce apoptosis in T lymphocytes (458,459).

Some studies have proposed that apoptosis results from G2 arrest (460) whilst others have shown these effects to be independent (461).

Apoptosis may be linked to HIV related neurocognitive disorders. Jones et al determined that neuronal Vpr could cause apoptosis and suggested that Vpr may mediate neuron death through the release of Il-6 by astrocytes (462).

### 1.7.2.3 Vpr effects on reverse transcription

Vpr was used as bait in a yeast two-hybrid screen of a human cDNA library. This identified cellular uracil DNA glycosylase (UDG) UNG as a possible binding partner suggesting that Vpr might enable UNG incorporation into virions. (386).

The subsequent finding that the cytidine deaminase APOBEC3Gs generates cytidine to uracil changes in viral genomes which are degraded before being integrated, lead to the hypothesis that Vpr might have evolved to deliberately encapsidate UNG. There are two forms of UNG with different amino terminals: UNG1 is mitochondrial while UNG2 localises to the nucleus. Both are base excision repair system enzymes that remove uracil bases from DNA thus preventing mutagenesis (463). These initial findings have led to a series of contradictory studies some showing that UNG is incorporated and others showing that UNG is degraded by Vpr. It is possible to imagine UNG2 advantaging the virus by repairing uracil sites induced by APOBEC3 mediated deamination of cytidine.

Mansky et al. demonstrated that Vpr reduces the rate of mutation during reverse transcription by recruiting UNG. They measured *in vivo* rate of forward virus mutations per replication cycle and showed a 4-fold increase in mutation rate without Vpr expression (464). A 16-fold increase was seen in primary MDMs (465).

The association of Vpr with UNG2 may allow Vpr to decrease the mutation rate but other studies have shown Vpr can induce the proteasomal degradation of UNG2. This may prove to be an artefact of suppression of expression from overexpression assays (444,466). Other studies indicate that endogenous UNG2 being reduced by Vpr is not mediated by degradation at the proteasome (467,468). A decrease in replication was shown with virus produced from cells which had been depleted for UNG2, assessed by demonstrating a reduced number of viral transcripts measured (469). It may be that incorporated UNG2 reduces uracil accumulation in the viral genome when virions infect non-dividing cells as these usually have reduced amounts of UNG and with increases in dUTP levels (470). This however is at odds with the studies that show that Vpr causes degradation of UNG (444). That UNG2 has a role in HIV-1 infection seems likely but whether that role is as a co-factor (469,471) or as a restriction factor (472) is not clear.

Wu et al determined the crystal structure of HIV-1 Vpr in complex with human UNG2 and the CRL4 acceptor-receptor proteins DDB1-DCAF1 demonstrating that Vpr and Vpx both bind DCAF at a similar site through the N-terminal tail and  $\alpha$ -helix  $\alpha$ 3. Vpr interacts with the DNA-binding region of UNG2 by mimicking DNA using a cleft between helices  $\alpha$ 1 and  $\alpha$ 2 (384). This serves to further illustrate the similarities between Vpr and Vpx which have similar helices

for binding DCAF but which are able to adapt other molecular regions to determine substrate specificity. It also illustrates a central problem of our understanding of the biology of Vpr – that even detailed structural information can fail to shed light on biological functions and the advantages conferred through interaction with particular proteins.

#### **1.7.2.4 Vpr effects on nuclear import**

Vpr has been identified as promoting nuclear localisation of the pre-integration complex or the delivery of capsid to the nuclear pore. Additionally, nuclear localisation of Vpr has been reported as increasing infection of primary CD4 cells (473,474). Other findings however show that Vpr is not required for nuclear transport of the PIC (184). Given the intra-capsid localisation of Vpr and the increasingly prevailing hypothesis that capsid remains intact until nuclear docking it may prove that Vpr acts at the nuclear pore but only once capsid disassembly starts.

Vpr localises both to the nuclear rim and inside the nucleus but there is no canonical or M9-dependant nuclear localisation signal (475–477). Several arginine residues in the C-terminus of Vpr resemble a basic NLS but do not appear to function as one; instead it is the N-terminus that is required for protein–protein interactions (416,478). Vpr seems to use a non-classical pathway for nuclear entry through direct binding to importin- $\alpha$  (475,479). It has been hypothesised that Vpr may transport viral DNA to the nucleus (480,481). Vpr has been described as being able to bind to nuclear pore structures such as p54 and p58 and the hCG1 nucleoporin and this may cause Vpr accumulation at the nuclear envelope (482,483).

There are two classical pathways enabling transport of proteins across the nuclear pore complex (NPC): The NLS and M9-dependent pathways (484). The NLS pathway requires binding of an NLS to importin- $\alpha$ . This then binds importin- $\beta$  and this protein complex then binds the NPC. Both systems depend on the GTPase Ran/TC4 (485,486). Vpr localisation seems to be independent of either of these pathways and is unaffected by peptides which block the NLS, dominant negative importin- $\alpha$  or dominant negative Ran or Ran inhibitors.

Nuclear localisation of Vpr has been shown to involve all three helices (416). There have been conflicting studies about Vpr importin- $\alpha$  binding with some groups finding only a weak interaction (487) while others found stronger interactions (488). Miyatake et al made a complex crystal of Vpr C-terminal residues 85–96 (Vpr85–96) with a mouse importin- $\alpha$ 2 protein lacking the IBB domain ( $\Delta$ IBB-m-importin- $\alpha$ 2). They used X-ray crystallography to investigate the interaction between the Vpr C terminus and importin- $\alpha$  and suggested that Vpr may modify the aggregation state of importin- $\alpha$ . They also suggested that Vpr binds the minor NLS-binding site of importin- $\alpha$  as well as the major site but with lower affinity. The biological

significance of these studies conducted on peptide fragments from different species remains to be determined.

#### **1.7.2.5 Modulation of gene expression by Vpr**

There is evidence suggesting that Vpr may regulate transcription from the HIV-1 LTR as well as other host genes. Candidates include *ung2*, *nbp2* and *nhe1* which may increase viral replication *in vivo* (467,489–491).

Langevin et al 2009 re-examined the influence of Vpr on the amount of endogenous UNG2 and found that it did weakly reduce the UNG2 isoform by regulating transcription but used overexpression reporter assays to confirm this phenotype. As with the studies reported in this PhD they determined that this was independent of proteosomal degradation and cell cycle arrest, since it was observed mutants unable to induce G2 arrest, including the VprQ65R mutant (467).

Liu et al (2015) found that HIV-1 M Vpr suppressed transcription from the promoter of cytomegalovirus (CMV) (492) They showed that Vpr-mediated inhibition of the transcription of both CMV and the host gene *ung2* was dependent on sites in helix 1 of Vpr. Surprisingly they hypothesised that suppression of CMV promoter activation would provide a survival benefit to the host (and thus the virus) through reduction of opportunistic infections. This study lacked robust negative controls to demonstrate specificity at the promoter.

Weak transactivation activity at the HIV-1 LTR, as well as other heterologous promoter elements has been ascribed to Vpr (493). Transcription may be mediated via both *cis* elements and *trans*-acting factors. The U3 region of the LTR contains known *cis* elements for HIV-1 expression including NF-AT, glucocorticoid response element (GRE), NRF, NF $\kappa$ B, and Sp1 binding sites, the TATA box and the tat-responsive RNA element, TAR. Agostini et al mapped this Vpr phenotype with truncated HIV-1 LTR-CAT constructs locating it to a region (2278 to 2176) containing the GRE sequences in the HIV-1 LTR.

Hogan et al used electrophoretic mobility shift analysis (EMSA) to show that Vpr and HIV-1 LTR sequences that span the adjacent C/EBP site I, the NF $\kappa$ B site II, and the ATF/CREB binding site associate. They also showed that over 90% of LTRs isolated from peripheral blood contained C/EBP site I variants with a high Vpr binding affinity suggesting that cis-acting elements with high affinity for Vpr are maintained and provide some evidence that Vpr may act to regulate C/EBP transcription factor/LTR interactions.

Additionally, Vpr is found in sera and CSF of AIDS patients likely as a result of breakdown of viral particles. Levy et al found that purified serum HIV-1 M Vpr activated HIV expression from latently infected cell lines and from PBMCs of infected individuals and hypothesised this was due to direct, or indirect, activation of proviral transcription (494).

Kichler et al, reasoning that Vpr could interact with nucleic acids and enter the nucleus, either independently or in the context of a pre-integration complex, tested whether Vpr could be used as a plasmid DNA delivery system in mammalian cells (415). They used synthetic Vpr and reported that the C-terminal domain of Vpr (52-96) interacts with plasmid DNA and enables efficient transfection comparable to the best transfection reagents. They used SMD2 Luc and PCIneo-Luc which both have CMV promoters and a GFP also with a CMV promoter. Follow up studies by the same group showed using electron microscopy and transfection experiments that a Vpr C-terminal peptide can transfect plasmid DNA and that the entry pathway is endocytic. Vpr has not been pursued as a potential transfection reagent in the last decade or so since these studies (415,495).

#### **1.7.2.6 Clinical effects of Vpr**

A number of animal studies have demonstrated clinical effects of Vpr expression which appear to mimic observed effects in humans.

Whether they express the Vpr transgene or are infused with synthetic Vpr, mice recapitulate the adipose dysfunction, altered metabolic parameters and hepatic defects found in HIV patients. These include increased lipolysis, diminished fat and insulin resistance mass (496–498). Vpr was seen to block pre-adipocyte differentiation via cell cycle arrest, whilst increasing lipolysis in mature adipocytes and reducing peroxisome proliferator-activated receptor  $\gamma$  (PPAR $\gamma$ ) and glucocorticoid receptors (GR). This is presumed to be the same mechanisms which underlie the adipose tissue dysfunction characteristic of HIV-1 patients (499).

Hoch et al. (1995) showed that infection of rhesus macaques with SIVmac without the Vpr gene has diminished viral loads and disease progression (500).

Goh and colleagues (1998), analysed Vpr sequence changes over time in an individual accidentally infected during laboratory work with a virus containing mutations in *vpr*. These encoded an unstable and non-functional Vpr because of the insertion of a single thymidine resulting in a premature truncation of the protein. They found positive selection for Vpr function *in vivo* in both human and chimpanzees: within 2 years the protein lost the thymidine insertion and reverted back to an intact Vpr open reading-frame (501).

Additionally, Vpr mutations are associated with the clinical phenotype of long-term non-progression (LTNPs). Some HIV patients have detectable HIV replication yet do not progress to immunosuppression even without treatment. There is a higher frequency of R77Q Vpr mutations in patients with LTNP than in patients with progressive disease (457).

Jacquot et al sequenced Vpr from a long term non-progressor (LTNP) patient. Vpr proteins were observed to accumulate at the nuclear envelope and showed cytostatic and pro-apoptotic activities. An LTNP Vpr allele, harbouring the Q65R substitution, was unable to bind DCAF1 and no longer exhibited nuclear envelope localisation, possibly indicating a functional link between localisation and cytostatic activity. Contradicting other published results, the R77Q substitution, found in LTNP alleles, was not observed to affect pro-apoptotic activity (429).

### 1.7.2.7 Vpr and cyclophilin

While the interaction of Vpr with the peptidyl prolyl isomerase cyclophilin A (CypA) (502–504) has been characterised the *in vivo* relevance of the interaction remains unclear.

CypA is a dispensable cellular protein (505) but HIV-1 replication is inhibited by CypA inhibitors which has made it a potential drug target (506,507). Capsid (CA) mutants N74D and P90A, which are unable to bind cofactors Cleavage and Polyadenylation Specificity Factor subunit 6 (CPSF6) and cyclophilins (Nup358 and CypA) respectively, are defective for replication in human monocyte derived macrophages (MDM) putatively due to triggering of cytosolic DNA sensors and subsequent induction of an interferon response and antiviral state (165,174,325).

CypA has been shown to catalyse prolyl cis/trans isomerization of conserved Vpr proline residues 5, 10, 14, 35 at low relative concentrations of both CypA and the Vpr (508). Only N-terminal peptides containing Pro-35 (which has shown to be involved in multiple functions of Vpr) are able to bind to CypA as measured by surface plasmon resonance (SPR) implying that P35 is important for CypA binding (508).

There is consensus in the literature that N-terminal residues from 30-34, which overlap the N-terminal binding region of Vpr to CypA, are required for Vpr induced G2 arrest (478,509). There is also consensus that Pro-35 mutations disrupt the interaction with CypA (411,502) but Ardon et al also observed that an Arg-80 Ala mutant inhibited co-immunoprecipitation with CypA. Solbak et al studied the interaction of Vpr with CypA and suggest the presence of a novel specific non-Pro-containing C-terminal binding region comprising the 16 residues <sup>75</sup>GCRHSRIGVTRQRRAR<sup>90</sup>. They found a dissociation constant of Vpr to CypA was of 320 nM. This may indicate stronger binding than that of the well described interaction of

CypA capsid interaction (503). Whether the inhibition of HIV-1 replication by cyclosporine and SDZ-NIM811, specific inhibitors of the isomerase activity of CypA, is due to the disruption of interactions with Vpr seems unlikely since the P90A capsid mutant is known to be sensitive to cyclosporine.

#### **1.7.2.8 Degradation of DICER by Vpr**

The endoribonuclease Dicer has also been identified as a target for Vpr-mediated degradation via DDB1-CuL4-E3 ubiquitin ligase. Klocklow et al identified human Dicer as assembling in a complex with HIV-1 Vpr by immunoprecipitation of Myc-tagged Dicer which resulted in the co-purification of HIV-1 Vpr. They did not perform the appropriate reverse immunoprecipitation of Vpr to look for Dicer co-purification though and, while they consistently observed lower Dicer levels in lysates from cells co-expressing Vpr their observation that Dicer is “degraded by Vpr” is consistent with the expression defects observed from co-transfected plasmids that form the core of this PhD. Since there was a lack of adequate negative control plasmids it is hard to conclude that they demonstrated a specific degradation of DICER.

## **2 Chapter 2: Materials and Methods**

### **2.1 DNA preparation and manipulation**

#### **2.1.1 Preparation of plasmid DNA - Small scale**

Following transformation, plasmid DNA was purified from amplified bacterial clones by alkaline lysis using the QIAprep Spin Miniprep Kit (Qiagen). For small-scale preps, single colonies were picked from agar plates and used to inoculate 5ml of ampicillin-containing LB media which were grown in a shaker at 250rpm for 16-18 h at 37 °C. Plasmid DNA concentration was measured using Nanodrop NDW1000 (Thermo Fischer Scientific Inc.).

#### **2.1.2 Preparation of plasmid DNA - Large Scale**

5ml LB was inoculated with a single colony as above and agitated and incubated at 37°C for 6-8 hours. 200µl of this starter culture was then used to inoculate 200ml LB, which was incubated, shaking, at 37°C for approximately 18 hours. Cultures were centrifuged at 4000g, at 4°C, for 20mins, and the supernatant was removed. Plasmid DNA was extracted using QIAfilter Plasmid Midi Kit (Qiagen).

#### **2.1.3 Agarose gel electrophoresis and purification of DNA**

Electrophoretic separation in 0.8 % agarose gel at 80-125mV in TAE buffer (40 mM Tris, 20 mM acetic acid, and 1 mM ethylenediaminetetraacetic acid (EDTA)) was used to separate and analyse PCR products and DNA from ligation or restriction digest reactions. SYBR® Safe (Invitrogen) and long wave UV illumination were used to visualise DNA. DNA products were excised in gel slices and purified using the QiaQuick Gel Extraction Kit (Qiagen) according to the manufacturer's protocol.

#### **2.1.4 Restriction enzyme digestion**

Plasmid vectors and PCR products were digested using restriction enzymes. Digestion mixes comprised 1.5µg of DNA, 0.5µl of the necessary restriction enzymes (New England Biolabs or Promega) and 1ul of the appropriate 10 x restriction enzyme buffer (New England Biolabs or Promega), and were made up to 10ul with water. Digests were incubated for 2 h at 37 °C and products were analysed by agarose gel electrophoresis and purified from the agarose gel as described above.

Each digestion contained 1.5 µg DNA, 1 µl appropriate 10 x restriction enzyme buffer (Roche), 0.5 µl of each restriction enzyme (Roche), and made up to 10 µl with water. Restriction digests

were incubated at 37 °C for 2 h. Digestion products were analysed by agarose gel electrophoresis (see 2.1.2) and the DNA was purified from the gel (see 2.1.3).

### **2.1.5 DNA ligation**

Ligation of digested PCR products or digestion products with desired digested plasmid backbones was performed at a 2:1 molar ratio of insert:vector and this ratio was varied depending on transformation efficiency. Each ligation reaction contained 100 ng digested vector, the appropriate ng of digested insert, 10 x T4 DNA ligase buffer (Promega) and 1 U T4 DNA ligase (Promega), made up to 10 µl with water. Reactions were incubated for 3-24hrs at room temperature.

### **2.1.6 Production of competent *E. coli* bacteria**

Chemically competent HB101 (F- mcrB mrr hsdS20(rB- mB-) recA13 leuB6 ara-14 proA2 lacY1 galK2 xyl-5 mtl-1 rpsL20(SmR) glnV44 +-, described in (510)): A single starter colony was cultured overnight in 3 ml LB broth without antibiotic and then inoculated into 200ml lysogeny broth (LB - tryptone 10 g/l, yeast extract 5 g/l, NaCl 5 g/l) which had been previously autoclaved at 121°C for 15 min. This suspension was grown at 30°C until OD550nm = 0.45-0.55, chilled at 0°C for 10 min, divided into 4x50 ml aliquots, and centrifuged 3500 rpm for 10 min at 4 °C (Sorvall Legend RT Centrifuge). Supernatant was discarded and pellets kept on ice at 0°C throughout further manipulations. Pellets were gently resuspended in 20 ml TFB1 buffer (30 mM KAc, 100 mM RbCl, 10 mM CaCl, 50 mM MnCl, 15% glycerol in dH2O, sterilised through a 0.45 µm filter), incubated at 0°C for 5 min, centrifuged at 3500 rpm for 10 min, the supernatant was discarded and the remaining pellets resuspended in 2 ml TFB2 buffer (10 mM PIPES, 75 mM CaCl<sub>2</sub>, 10 mM RbCl, 15% glycerol in dH2O, sterilised through a 0.45 µm filter). Bacteria were aliquoted at 50µl, and snap frozen in liquid nitrogen, stored at -80 °C. Competency was assessed by transforming 50µl HB101 with 10pg pUC19 >100 colonies indicated high transformation efficiency.

### **2.1.7 Transformation of *E. coli***

50µl of chemically competent HB101 *Escherichia (E.) coli* cells were transformed with 5µl of ligation reaction mixture and incubated on ice for 30 min. Bacteria were heat shocked at 42 °C for 1 min and returned to ice for a further 5 min. Transformed bacteria were then spread on Luria Broth (LB) agar plates containing ampicillin (100 µg/ml) using aseptic technique. Plates were incubated overnight at 37 °C to allow bacterial growth.

### 2.1.8 Bacterial colony screening

Screening of the transformed bacterial colonies was used to identify bacteria harbouring the desired plasmid. Individual colonies were transferred to 2 ml LB with ampicillin (100 µg/ml) and incubated for 1 h at 37 °C with shaking. 1 µl of this bacterial culture was then used in a PCR containing 10 x GoTaq buffer (Promega), 25 mM MgCl<sub>2</sub>, 10 mM dNTPs, 0.2 µM of the primers originally used to amplify the desired gene, 1 U GoTaq polymerase (Promega) and water up to a volume of 20 µl. DNA amplification was then performed in a thermocycler using the following programme. Following PCR amplification, DNA products were analysed by agarose gel electrophoresis.

Temperature (°C)	Time (min)	Repeat
95	5	X1
95	0.5	X5
50	0.5	
72	1 per kbp	
95	0.5	X 25
55	0.5	
72	1 per kbp	
72	5 per kbp	X1

Table 2.1 Bacterial colony screening

### 2.1.9 Vpr Plasmid construction

Codon optimised Vpr cDNA was synthesised by GeneArt® and designed to include BamHI and No1I sites. These were manufactured in a PMA vector and subsequently digested and ligated to pcDNA3.1, which contains a FLAG-epitope tag appended to the Vpr N-terminus. Correct insertion was checked through sequencing (Beckman Coulter Genomics). FLAG was excised with BamHI and XhoI.

### 2.1.10 Site directed mutagenesis (SDM)

Point mutations were introduced into plasmids using site directed mutagenesis with overlapping forward and reverse primers, each bearing the mutation. SDM primers were designed to be 30-45bp long, to begin and end in a G/C, to have 20-30bp overlap, 40-70% GC content, similar melting temperatures (TM) of 55 - 80°C, a maximum of 3 mismatches, and mutation/s were located toward the 3' end of the primer. The reaction mixture is described in table 2.2 Cycling parameters are described in table 2.3. A negative control consisted of the

same reaction mixture but without *PfuTurbo*. 5  $\mu$ l of the Control and SDM reaction products were separated by 1% agarose gel electrophoresis to confirm amplification. 45  $\mu$ l of the remaining reaction sample was mixed with 1  $\mu$ l DpnI (NEB) and 5 $\mu$ l Buffer 4 (NEB) and incubated at 37°C for 2hrs to digest any original methylated plasmid produced by bacteria whilst leaving the PCR-produced DNA intact. The QIAquick PCR purification kit (Qiagen) was used to clean up DpnI digested PCR product and 5  $\mu$ l was used to transform 50  $\mu$ l HB101. Lack of negative control PCR colonies indicated successful DpnI digest. Plasmids were then prepared and sent for sequencing (Beckman).

Component	Conc/Amt
Pfu Turbo DNA Polymerase 2.5U/ $\mu$ l Stratagene	2.5U / 1 $\mu$ l
Pfu Turbo 10x Buffer	1x / 5 $\mu$ l
dNTPs (Promega) 25mM each	250 $\mu$ M / 5 $\mu$ l
Primers (Sigma) 100 $\mu$ M	2 $\mu$ M / 1 $\mu$ l
Plasmid Template	50- 100ng
dH <sub>2</sub> O	To total
Final volume	50 $\mu$ l

Table 2.2 SDM PCR components

Step	Plasmid DNA <10kb		
	Temp (°C)	Time (secs)	No. of Cycles
Initial denaturing	95	30	1
Denaturing	95	30	12/16 for 1/2 mutations
Annealing	55	60	
Extension	72	60/kb	
Final extension	72	120/kb	1

Table 2.3 Cycling parameters

## **2.2 Cell culture**

### **2.2.1 Maintenance of cells**

HEK293T (human embryonic kidney cell lines) cells, BSC-1 (African green monkey epithelial cell line of kidney origin), CV-1 and Vero cells (both African green monkey kidney fibroblast cell lines) were maintained in Dulbecco's modified Eagle's medium (DMEM) with 10 % (v/v) foetal calf serum (FCS) and penicillin/streptomycin (P/S) (50 µg/ml). FCS was treated for 1 h at 56 °C to inactivate complement. HEK293T Luc cells (with an integrated NFκB sensitive reporter) were maintained in the same way with additional puromycin (50 µg/ml).

### **2.2.2 Fugene-6 transfection**

Cells were seeded a day prior to transfection such that they were 70 % confluent when transfected. Transfection mixes were prepared by combining DNA plasmids with OPTIMEM in a ratio of 50 µl per 1 µg of DNA. Fugene-6 reagent (Roche) was then added (2 µl per 1 µg DNA), vortexed briefly and incubated at room temperature for 20 min. DMEM (as above) was added to the transfection mixture at an appropriate volume (according to the cell culture plate being used) and this was used to replace the growth medium previously on the cells. Media was once more replaced at 24 hrs and cells were harvested after 24-48 h. See table appendix for a list of plasmids used in this study.

### **2.2.3 Generation of cell line with integrated NFκB sensitive reporter**

Ready-to-transduce, replication incompetent, HIV-based, VSV-G pseudotyped lentiviral particles (NFκB-luc lentivirus) at  $2 \times 10^7$  TU/ml was purchased from Qiagen. The NFκB-responsive luciferase construct encodes the firefly luciferase gene under the control of a minimal (m)CMV promoter and tandem repeats of the NFκB transcriptional response element. 50,000 cells were plated onto in 6 well plate in 2ml DMEM. 150ul of virus was added and the media was changed at 24hrs. Spinoculation was not performed. At 48 hrs the media was replaced with media containing 2.5ug/ml puromycin. When cells were stable at 2.5 µg/ml puromycin, the drug concentration was increased to 7.5 µg/ml. Single cell clones were prepared by limiting dilution and stored in liquid nitrogen.

## **2.3 Reporter gene assays**

HEK293T cells (50,000 cells/well) were seeded into 48-well plates 24 h prior to transfection. Cells were transfected with 2.5ng of the indicated firefly luciferase reporter plasmids, 5ng of GL3-renilla luciferase (TK- renilla) plasmid, and titration series or single doses of expression

plasmids for the proteins of interest as indicated in figures. For the reporter gene assays, to determine the effect on varying promoters only the firefly reporter plasmids and Vpr expression plasmids were transfected. For the reporter gene assays testing transfected vs integrated NF $\kappa$ B reporter, a titration series of transfected reporter was performed to establish the dose of transfected reporter with the same baseline luciferase expression as the integrated reporter. This was found to be 55ng of the NF $\kappa$ B firefly luciferase plasmid. The total DNA in all wells was always made up to the same amount using EV. Transfection was performed using Fugene-6. Cells were 70 % confluent when transfected. Following transfection media was once more replaced at 24 hrs and cells were harvested after 24-48 h. See table appendix for a list of plasmids used in this study. Following the transfections and treatments described in figure legends, cells were washed once with PBS (150  $\mu$ l per well) and harvested in passive lysis buffer (Promega, 100  $\mu$ l/well) followed by freeze-thawing of cells to aid cell lysis and firefly and renilla luciferase activity measurement of 20  $\mu$ l in a 96Wwell GloMax Luminometer Light Plate (Promega). 30 $\mu$ l of Dual-Glo<sup>®</sup> Luciferase Assay Reagent was then added to each well and incubated for 10 minutes. The number of relative light units (RLU) were read 3 times using a GloMax 96 Microplate Luminometer (Promega) and a mean was taken. Except where indicated the same procedure was then followed after the addition of 30 $\mu$ l Dual-Glo Stop & Glo reagent and renilla luminescence was measured. The firefly-luciferase readings of each sample were normalised to the renilla-luciferase readings to account for cell number and transfection efficiency and fold inductions were calculated relative to the mock-stimulated controls as explained in figure legends.

## **2.4 RNA extraction and cDNA synthesis**

The QIAGEN RNeasy RNA extraction kit was used to extract RNA from cells using the manufacturer's protocols. For 24- and 6-well plates the cells were harvested in 350  $\mu$ l buffer RNeasy lysis buffer (RLT). For reverse transcription to synthesize complementary DNA (cDNA), each reaction contained 1 $\mu$ g RNA, 2.5 $\mu$ M oligo dT, 500 $\mu$ M dNTP, made up to 13 $\mu$ l with nuclease-free water. These reactions were incubated at 65 $^{\circ}$ C for 5 min and then transferred directly to ice for 1 min. To each reaction 4  $\mu$ l 5x First-strand buffer (Invitrogen), 5 mM DTT, 40 U RNase OUT (Invitrogen) and 50 U Superscript III reverse transcriptase (Invitrogen) was added, made up to a total of 20  $\mu$ l with nuclease-free water. The reactions were incubated at 50 $^{\circ}$ C for 1 h, followed by 70 $^{\circ}$ C for 15 min. cDNA was diluted 1:2 in nuclease-free water before quantitative reverse transcription-polymerase chain reaction (qRT-PCR) analysis or array.

## 2.5 qRT-PCR

Each qRT-PCR, performed in 96-well plates, in duplicate, contained 2  $\mu$ l cDNA, 10  $\mu$ l 2x SYBR® Green PCR master mix (Applied Biosystems), 0.5  $\mu$ M of each primer, made up to 20  $\mu$ l with water per well. A  $\Delta\Delta$ Ct relative quantity assay was then performed where the amplification of genes of interest was normalised to an endogenous control (GAPDH) on a 7900HT Real-Time PCR machine (Applied Biosystems) using the following programme: 2 min at 50°C; 10 min at 95°C; 15 s 95°C; 1 min at 60°C X 40 cycles. Data were analysed using the RQ Manager 1.2 software (Applied Biosystems).

## 2.6 Preparing short hairpin RNA (shRNA)-expressing MLV vectors

Potential 19mer RNAi sequences were selected using online Clontech RNAi algorithms (<http://bioinfo.clontech.com/rnaidesigner/sirnaSequenceDesignInit.do>). BLAST was used to check target sequences in cyclophilin A and Nup358 for complementarity to human genome transcripts. Three target oligonucleotides incorporating the 19mer per for each of CypA and Nup358 were designed using online Clontech designer tools. Oligonucleotides were annealed by mixing 10  $\mu$ l of each stock (previously made to 1  $\mu$ g/ml in water). Then 2.5  $\mu$ l of 2 M NaCl was added, and the reaction mixture was heated at 98 °C for 5 min and cooled slowly (~0.1 °C/sec), to 4 °C. 350  $\mu$ l DNase-free water, 40  $\mu$ l of 3 M NaAc (to reduce DNA interaction with dH<sub>2</sub>O) and 1.1 ml 100% EtOH were then added, mixed and stored at -80 °C overnight. Centrifugation at 13,000 rpm at 4 °C for 45 min was used to pellet DNA. The EtOH was removed and the pellet was air dried and resuspended in 50  $\mu$ l DNase-free water. 3  $\mu$ l annealed oligonucleotides were ligated with 1  $\mu$ l pSIREN-RetroQ vector (~50 ng) digested *EcoRI/BamHI*. Colonies were screened by *MluI* digest as inserts (annealed oligonucleotides) contain unique *MluI* sites. Pseudotyped, retroviral-based vectors incorporating shRNA-encoding transcripts were produced by three plasmid transfection of HEK293T cells. MoMLV GagPol particles were produced by co-transfection of: i) pSIREN-RetroQ encoding shRNA transcripts (the vector without viral genes, encoding a transgene under an internal constitutive CMV promoter, flanked by the *cis*-acting viral elements required for RNA packaging, reverse transcription and integration in target cells); ii) pCMVi packaging plasmid (contains retroviral genes required for enzymatic activity (*pol*) and particle formation (*gag*) under control of a CMV promoter, such that they are constitutively expressed in HEK293T cells); and iii) a VSV-G expression plasmid, pMD-G (encoding the envelope glycoprotein) as described by Naldini et al in 1996 (511). A 10 cm<sup>2</sup> dish of the same HEK293T cells used in transfection experiments was co-transfected just before at 80% confluency with 1 $\mu$ g GagPol expressor plasmid, 1  $\mu$ g

VSV-G expressing plasmid and 1.5µg retroviral vector was made to ~15µl with water. 12µl Fugene 6 (Roche) was then added to 200µl Opti-Mem without allowing Fugene 6 to touch the sides of the tube and mixed. The DNA mix was then added to this mixture, spun briefly to remove drops from the sides of the tube and incubated at room temperature for 20 min. Cell culture media was replaced with 8 ml fresh DMEM, 15% FCS, Penicillin and Streptomycin (as in previously) and the transfection mixture was added drop by drop to the replaced media. The media was replaced at 24hrs and vector containing supernatant was harvested at 48 and 72 hrs, filtered through a 0.45µm filter, aliquoted in 1.5 ml tubes and stored at -80 °C. 1 ml viral supernatant was used to transduce ~2 x 10<sup>5</sup> cells. At 48hrs cells were transferred to a 10 cm<sup>2</sup> dish in DMEM with 2.5µg/ml puromycin. As a control, non-transduced cells were also treated with puromycin. Transduced cells were plated for infection assays or frozen for storage. When cells were stable at 2.5µg/ml puromycin, the drug concentration was increased to 7.5µg/ml. Single cell clones were prepared by limiting dilution. 100 cells were suspended in 50 ml of DMEM (10% FCS, 100 U/ml penicillin, 100µg/ml streptomycin) with 10µg/ml puromycin and plated at 500µl/well in 4 x 48 well plates. Wells containing multiple colonies were discarded. Once single colonies had reached 50% confluency they were transferred to 6 well plates.

## **2.7 Protein analysis**

### **2.7.1 SDS-PAGE**

For sodium dodecyl sulphate (SDS) – polyacrylamide gel electrophoresis (SDS-PAGE) analysis cells were collected in 80ul Passive Lysis Buffer (Promega) and 30ul was used for luminometry analysis. The remaining 50 was centrifuged at 4°C, the cellular debris discarded, the supernatant removed and heated at 100°C for 5 min in 6x protein loading buffer (β-mercaptoethanol (BME) (50 mM Tris-HCl (pH 6.8), 2 % (w/v) SDS, 10% (v/v) glycerol, 0.1% (w/v) bromophenol blue, 100 mM BME) prior to loading on a 10 % or 12 % polyacrylamide gel. The proteins were separated by electrophoresis at 120 V in SDS running buffer (25 mM Tris-HCl, 250 mM glycine, 0.1 % (w/v) SDS).

### **2.7.2 Nu-PAGE**

For the analysis of proteins using the Invitrogen Nu-PAGE system, proteins were heated at 100°C for 5 min in 4x Nu-PAGE protein loading buffer (Invitrogen). The proteins were then separated on a 4-12 % Bis-Tris polyacrylamide gradient gel (Invitrogen) at 120 V in MES buffer (Invitrogen).

## 2.8 Immunoblotting

After PAGE, proteins were transferred to a Hybond nitrocellulose membrane (Amersham biosciences) in transfer buffer (25 mM Tris-HCl, 250 mM glycine, 20 % (v/v) methanol) using a semi-dry transfer system (Biorad) and blocked by incubation for 1 h at room temperature in 5 % (w/v) milk proteins + 0.01 % (v/v) Tween-20 in PBS (PBST). The membranes were then incubated overnight at 4 °C with the primary antibody (Ab, see below) diluted in 5 % (w/v) milk proteins in PBST. Membranes were washed three times for 5 min in PBST and probed with IR-dye labeled secondary anti-rabbit or anti-mouse antibodies labelled for detection in the 700 or 800nm channel (LiCor, 1:10 000) in 5% (w/v) milk proteins in PBST for 1 h at room temperature. The membranes were rinsed three times for 15 min with PBST and briefly with deionized water. Images were made with the Odyssey Infrared Imaging System (LI-COR Biosciences). Blots were imaged at 169 µm. Quantification was performed with the analysis software provided. Tubulin, Beta-actin or Valosin-containing protein (VCP) were used as loading controls. VCP is a 97 kDa ATPase involved in the ubiquitin-proteasome degradation pathway, membrane fusion, transcription activation, cell cycle control, apoptosis, and molecular chonng (522).

## 2.9 Silver staining of proteins

Proteins separated by PAGE were silver stained using the Invitrogen SilverQuest silver staining kit according to the manufacturer's protocol.

## 2.10 Immunofluorescence and Confocal Microscopy

For immunofluorescence assays, glass coverslips were placed in a 24 well plate and incubated with poly-L-lysine (Sigma) for 12hrs at 37°C. Coverslips were washed 3 time with PBS and cells were seeded the day before transfection at 50,000 cells per well. Cells were transfected as previously described and at 72hrs cells were washed three times with cold PBS and fixed in 4 % (v/v) paraformaldehyde in PBS containing 250 mM HEPES (pH 7.4) by incubation on ice for 5 min and then at room temperature for 15 min. The cells were then washed three times with PBS, incubated in 50 mM ammonium chloride in PBS for 5 min to quench free aldehyde autofluorescence, washed three times in PBS, and permeabilised with 0.1 % (v/v) Triton X-100 in PBS for 5 min. The cells were again washed three times in PBS then blocked in 5 % (v/v) FBS in PBS (blocking buffer) for 30 min at room temperature. The coverslips were then inverted and incubated on a 70 µl drop of primary anti-FLAG Ab diluted

in blocking buffer for 90 min. The coverslips were washed three times in blocking buffer followed by incubation on a 70  $\mu$ l drop of secondary Ab (see below) diluted in blocking buffer for 90 min. The coverslips were then washed twice with blocking buffer and once with PBS. Finally, the coverslips were dipped in distilled water to prevent the formation of PBS crystals, placed on to a slide prepared with a 30  $\mu$ l drop of mounting medium (Mowiol 4-88, containing 4',6-diamidino-2-phenylindole (DAPI)) and allowed to set before storing at 4°C. The cells were visualised using a Leica SPE1 Confocal Microscope at 63X magnification with an oil immersion lens and images were collected using Leica Image Browser.

## 2.11 Immunoprecipitation assays

Prior to harvesting, the cells were washed twice on ice with ice-cold PBS followed by scraping in an appropriate volume of immunoprecipitation (IP) buffer (NP40 0.5% in PBS, supplemented with protease inhibitors (Roche)). The cells were collected in Eppendorf tubes, slowly rotated at 4°C to allow lysis, and then the cell debris was collected by centrifugation at 14,000 x *g* for 20 min, 4°C. 50 $\mu$ l of the lysate supernatant was transferred to a tube (input) and the remainder transferred to another tube for the IP assay. 30 $\mu$ l of anti-FLAG M2 agarose beads (Sigma-Aldrich) were prepared per IP protocol by washing once with 1 ml water and twice with 1 ml IP buffer (centrifuging at 600 x *g* for 1 min per wash). The beads were resuspended in an appropriate volume of IP buffer and added directly to the cell lysates. The lysates were incubated with the beads by rotation at 4°C for 2 h and then washed three times in pre-chilled IP buffer (centrifuging at 600 x *g* for 1 min per wash). Finally, they were resuspended in 20  $\mu$ l 6x protein sample buffer for analysis by SDS-PAGE and immunoblotting.

## 2.12 Transcriptional Profiling

12 samples were prepared for array analysis: 3 replicates each of 4 conditions (SIVmon, SIVgsn, SIVmonS40N and empty vector). RNA was extracted as described previously using the QIAGEN RNeasy RNA extraction kit with the manufacturer's protocols. Genomic DNA was removed with the TURBO DNA-free kit (Ambion). RNeasy MinElute Cleanup kit (QIAGEN) was used to concentrate the RNA. RNA quality control was assessed with the Agilent 2100 Bioanalyzer (Agilent Technologies). Range of RNA was determined to be 56-179 ng/u with RNA integrity numbers (RIN) of: 7.2-10. The sample with the lowest integrity number of 7.2 was discarded. cRNA from all samples was fluorophore-labelled. with the Low Input QuickAmp labelling kit, and hybridized to SurePrint G3 Human Gene Expression v3 8  $\times$  60K or Human Gene Expression v2 4  $\times$  44K whole-genome microarrays (Agilent Technologies). Array images were acquired with Agilent's dual-laser microarray scanner G2565BA and analyzed with Agilent Feature Extraction software (v9.5.1). This extracts raw data from the scanner

output files, log<sub>2</sub>-transforms median Cy3 and Cy5 signal intensities and normalises these intensities using LOESS local linear regression to the mean signal of all the samples using the R package *agilp* (512)(513). Analysis of all microarray data was conducted on log<sub>2</sub>-transformed data and restricted to gene symbol–annotated probes expressed above background negative-control levels in at least one sample. Significant gene expression differences between datasets were identified using Mann-Whitney *U* tests for nonparametric data in MultiExperiment Viewer v4.9 (<http://www.tm4.org/mev.html>) with a false discovery rate of 0.05 and a filter for greater than 2-fold differences in median normalised expression values. Gene ontology and pathway analyses were performed in InnateDB, which identifies biological pathways that are statistically over-represented in a given gene list. Network graphics of gene and pathway association were generated using Gephi (<http://gephi.github.io/>). A principle component analysis (PCA) was performed in R and one SIVgsn sample did not cluster with other replicates of the same condition and was excluded from further analysis. Significant gene expression differences between datasets were identified. There were 30 transcripts with increased expression and 29 with reduced expression in the SIVmon samples. Gene ontology (GO) and pathway analyses were performed in innateDB (514). InnateDB incorporates pathway annotation (all pathways not just immune relevant ones) from major public databases including KEGG, Reactome, NetPath, INOH, BioCarta and PID. GO over-representation analysis (ORA) examines a gene/protein list for the occurrence of GO annotation terms, which are more prevalent in the dataset than expected by chance. Annotations that occur more frequently than expected in a gene list can be identified and may point towards a biological process or pathway that is being differentially regulated in the condition of interest, in this case SIVmon. GO ORA is restricted to biological processes. A second analysis was performed restricted to the “reactome”. Then, a transcription factor binding site analysis was performed using online software oPOSSUM to detect over-represented conserved transcription factor binding sites and binding site combinations in sets of genes or sequences but there were no results with a Z score of >10, which would indicate significance. These analyses were performed comparing SIVmon Vpr to all controls and an Ingenuity pathway analysis was performed using IPA (<http://www.ingenuity.com>), which applies causal networks that integrate previously observed cause–effect relationships reported in the literature. IPA® is a web-based software application that enables researchers to analyze data derived from expression and SNP microarrays, RNA-sequencing, proteomics and metabolomics experiments, and small-scale experiments (such as PCR) that generate gene or protein lists and enables understanding of the significance of data or targets of interest in relation to larger biological or chemical systems. The causal analysis is derived from a structured repository of biological and chemical “findings” curated from various sources including the literature.

## 2.13 Phylogenetic analysis

Vpr sequences obtained from the Los Alamos database were manually aligned using the Se-  
Al sequence editor (<http://tree.bio.ed.ac.uk/software/seal/>). Whilst Vpr and Vpx are extremely  
diverse proteins and not amenable to consistent alignment, multiple strategies consistently  
give the clades of interest strong support. A maximum-likelihood phylogeny structure was  
reconstructed by using the General Time-Reversible model of nucleotide substitutions and  
adjusting evolution rates across sites (GTR+CAT) and FastTree v2.1.5 software (515). Branch  
support was calculated by Shimodaira-Hasegawa-like local branch support (SH-like test), as  
implemented in FastTree. The phylogeny was edited with the program FigTree  
(<http://tree.bio.ed.ac.uk/software/seal/>). The tree was artificially rooted and branch lengths  
indicate the number of nucleotide substitutions per site.

## 2.14 Structural alignments

To guide a mutagenesis strategy, a structural alignment was made using the online T-Coffee  
multiple alignment software. This uses an algorithm combining progressive and consistency-  
based alignment, and is available for online usage and is considered to be useful for  
alignments of more divergent sequences and which also incorporates three-dimensional  
structural information for the alignment of protein sequences  
(<http://www.ch.embnet.org/software/TCoffee.html>) (516,517). The ESPript (*Easy Sequencing  
in PostScript*) online software was then used, a program that renders sequence similarities  
and secondary structure information from aligned sequences (518).

### 3 Chapter 3 Antagonism of reconstituted innate immune sensing in 293 cells with lentiviral Vprs

#### 3.1 HIV-1 M Vpr is able to rescue a spreading infection in monocyte derived macrophages from addition of cGAMP

Unpublished data from our lab (Jane Rasaiyaah) show that HIV-1 M Vpr is able to rescue a spreading infection in monocyte derived macrophages from inhibition by addition of cGAMP, the second messenger released by cGAS following activation by a dsDNA ligand, which activates STING (figure 3.1). This initiates a signalling cascade culminating in the production of type I interferon (IFN) and pro-inflammatory genes via IRF3 and NF- $\kappa$ B transcription factors. We hypothesised that Vpr has evolved to antagonise these signalling pathways to protect viral replication from antiviral responses induced by DNA sensing.

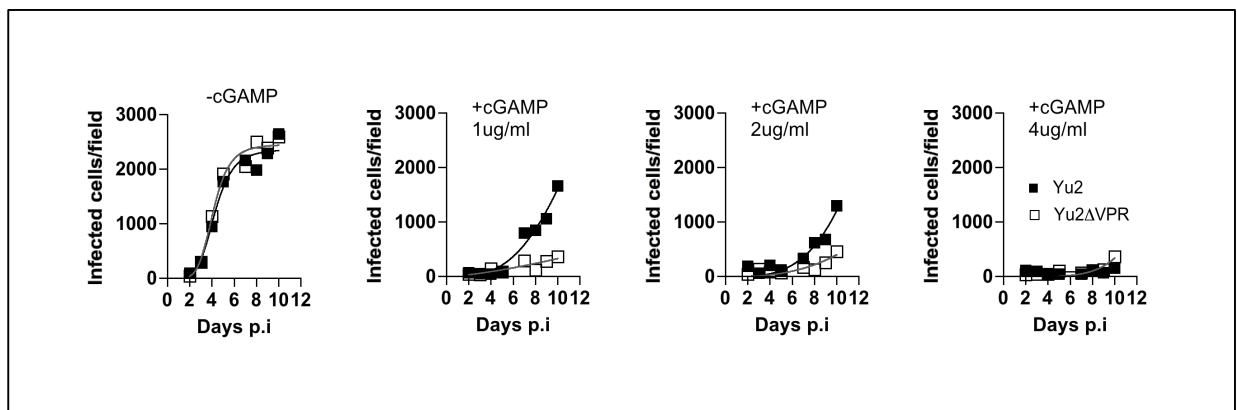


**Figure 3.1** HIV-1 M Vpr is able to rescue a spreading infection in monocyte derived macrophages from addition of cGAMP. Replication of HIV-1 YU2 WT or a Vpr-null mutant measured over 11 days with 0ng, 1ng, 2ng or 4ug/ml (L to R) of cGAMP added on day 1 post infection.

#### 3.2 Co-expression of cGAS/STING activates an NF $\kappa$ B-sensitive promoter

In order to investigate the effect of HIV-1 M Vpr, this signalling pathway was reconstituted in HEK293T cells using transfected expression plasmids. HEK293T cells have been reported to deficient in cGAS and STING signalling (326) and indeed this may underlie their utility as transfectable cells. Being unable to detect and respond appropriately to cytosolic DNA may be central to the poorly understood mechanisms of transfection. Absence of these proteins was demonstrated on immunoblot (figure 3.2) and a transfection assay to recapitulate cGAS/STING activation using a NF $\kappa$ B-promoter firefly luciferase reporter was optimised.

HEK293T cells were transfected in 48-well plates with 0, 1 or 3ng of expression vectors for cGAS and/or STING to activate NF $\kappa$ B signalling (figure 3.2A). Simultaneously, a firefly luciferase reporter plasmid was transfected, where the expression of firefly luciferase is under the control of a synthetic NF $\kappa$ B sensitive promoter. This promoter contains five copies of an NF- $\kappa$ B response element (NF- $\kappa$ B-RE) that drives transcription of the luciferase reporter (Promega).

Early experiments were duplicated with a reporter plasmid under control of the natural promoter of the *immunoglobulin kappa light chain* gene which is also sensitive to NF $\kappa$ B subunits p50 and p65 and contains three repeat  $\kappa$ B sequences. The binding sequence is 5'-GGGRNYYYCC-3', where R is a purine, Y is a pyrimidine, and N is an unspecified base (personal communication Andrew McDonalds and 523–525). No significant differences were seen in either NF $\kappa$ B activation or antagonism between the synthetic and natural promoters. Where NF $\kappa$ B activity is shown it is from the synthetic promoter. This was chosen as it is identical to the integrated reporter in figures 4.7, 4.10 and 5.3.

7.5ng of a transfection control reporter plasmid was also co-transfected to confirm consistency between transfections and lack of toxicity (figure 3.2B). This plasmid contained a minimal promoter fragment from the HSV thymidine kinase (TK) promoter adjacent to a reporter gene, the secreted luciferase from the anthozoan coelenterate *Renilla reniformis* (Promega). At 48 hours post transfection cells were harvested for immunoblot. Firefly and renilla luciferase activity were measured 48 hours after transfection by luminometry (Fig 2 A & B). The firefly luciferase activity was then normalised to renilla luciferase activity (Fig 3.2 C).

Whereas ectopic cGAS expression alone failed to activate NF $\kappa$ B signalling, in support of the notion that there is no endogenous STING in these cells, transfection of STING alone was able induce NF $\kappa$ B promoter activity possibly because of low levels of endogenous cGAS able to sense the transfected DNA (figure 3.2A&C)). This would be consistent with previous published data reporting very low levels of cGAS RNA in HEK293T cells (293).

STING induced NF $\kappa$ B promoter activity is augmented ~10 fold by simultaneous transfection of cGAS in a 1:1 ratio and further augmentation of signal was achieved by increasing the dose of each molecule and adding 100ng more of empty expression vector (pcDNA.3) (figure 3.2 A&C). This may act as a substrate for cGAS, triggering the production of cyclic GMP-AMP (cGAMP). This observation supports the notion that cGAS/STING mediated NF $\kappa$ B activation may be mediated by cGAS sensing the transfected DNA itself as well as being a feature of overexpression.

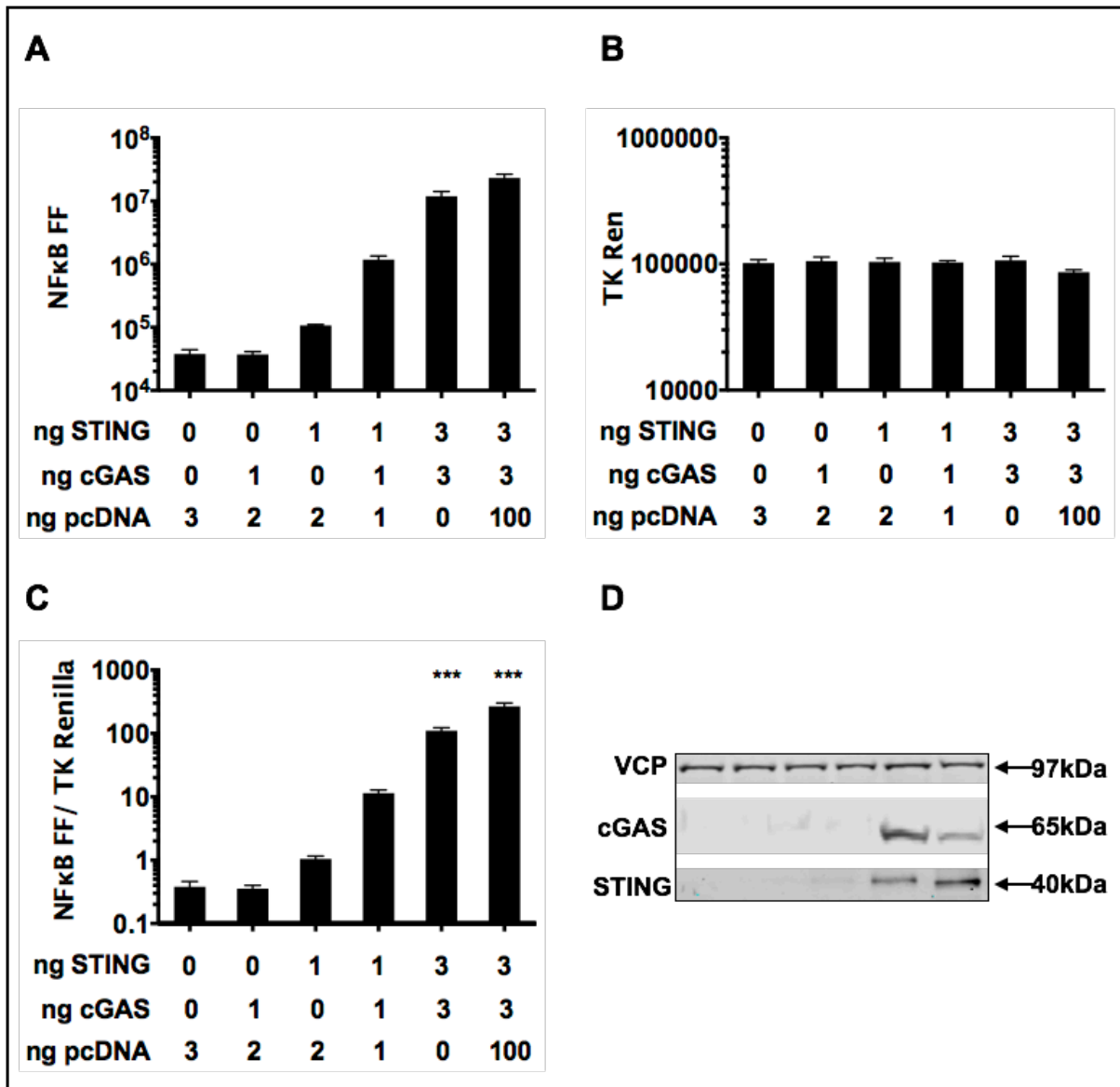


**Figure 3.2 Co-expression of cGAS/STING activates NFκB-sensitive promoter driven luciferase expression.** Firefly (FF) and renilla (Ren) luciferase signals were quantified with luminometry (A & B, respectively), with renilla fluorescence acting as a transfection control. Firefly luciferase activity was normalised to renilla luciferase activity (C). Data are from three independent experiments and represented as mean ± SEM. (D) A representative immunoblot shows relative expression of HA-cGAS and HA-STING with VCP as a loading control. \*\*\*:  $P < 0.001$  compared to 0ng STING, 0ng cGAS, one-way ANOVA with Dunnett's post-hoc test. Valosin-containing protein (VCP) is a 97 kDa protein used as a loading control. VCP is an ATPase involved in the ubiquitin-proteasome degradation pathway, membrane fusion, transcription activation, cell cycle control, apoptosis, and molecular choning (522).

### 3.3 Co-expression of cGAS/STING induces expression of endogenous NF $\kappa$ B genes

To confirm stimulation of endogenous gene expression following ectopic expression of cGAS and STING, mRNA levels for three different genes, all sensitive to NF $\kappa$ B, were quantified with qRT-PCR: ISG56, CXCL-10 and IFIT-2 (figure 3.3A&B).

ISG56: IFNAR (IFN- $\alpha/\beta$  receptor) is common surface receptor for all type I IFNs. It activates the JAK-STAT signalling pathway. This leads to transcription of more than 200 IFN-stimulated genes (ISGs) (309). IFN-stimulated gene 56 (ISG56) was one of the first interferon (IFN)-inducible genes to be cloned almost 3 decades ago (523). It is one of a family of viral stress-inducible genes (VSIG) with high sensitivity to IFN treatment and activation of innate immune signalling pathways. VSIGs are induced by activation of IFN regulatory factors (IRFs) which initiate transcription following recognition of the IFN-stimulated response elements or ISREs - cis-acting elements found approximately 200 bp upstream of the TATA box in the VSIG promoters. IRF-3, is activated by dsRNA (via TLR3 or RIG-I/MDA-5), by lipopolysaccharides (via TLR4) or by dsDNA (via cGAS and STING), potently induces ISG56 family genes, and ISG56 expression is frequently used as the readout for IRF-3 transcriptional activity (524).

CXCL10 is a CXC chemokine which chemo-attracts activated T cells and myeloid cells through CXCR3 receptor binding. Its expression is controlled by multiple transcription factors including IRF3 and NF $\kappa$ B (525).

IFIT2 is part of the *Ifit* family of ISGs which are strongly induced by type I IFNs and by many signalling pathways that activate IRF-3 or IRF-7 (526).

RNA was extracted from HEK293T cells 48 hrs post transfection with a 5 point titration series of cGAS and STING in a 1:1 ratio and used for qRT-PCR analysis to examine the expression of ISG mRNAs. cGAS and STING robustly stimulated the tested genes in a dose dependent manner (figure 3.3). STING levels were measured by immunoblot (figure 3.3A)

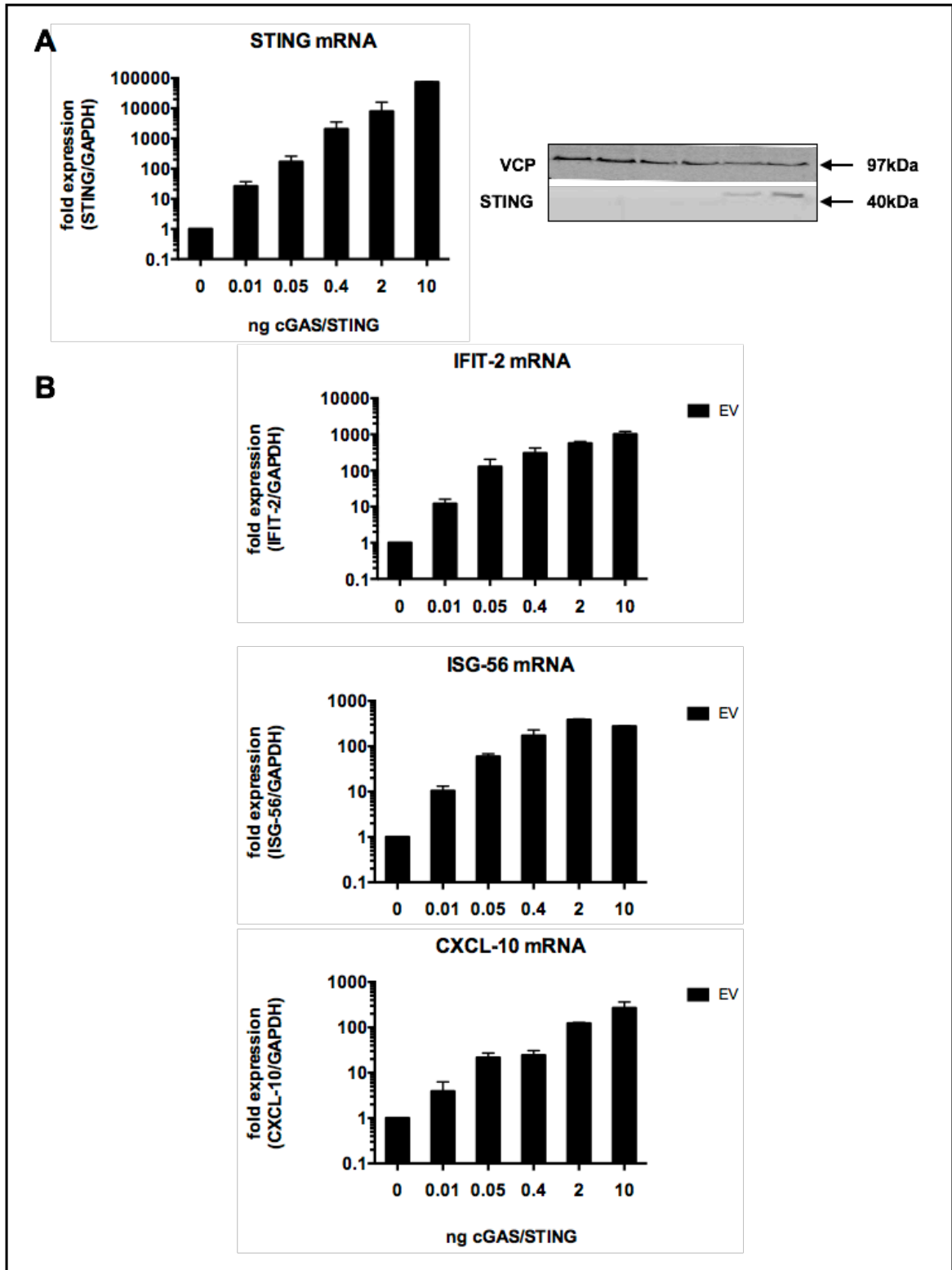


**Figure 3.3 Co-expression of cGAS/STING activates endogenous NF $\kappa$ B sensitive genes.** qRT-PCR analysis of ISG expression for presence of STING mRNA (3.3 A) and induction of ISG56, CXCL-10 and IFIT-2 (3.3 B). Data are presented as the mean (of three separate experiments) fold induction relative to the unstimulated control of each cell line  $\pm$  SEM. The whole cell lysates were separated by SDS-PAGE and analysed by immunoblot with anti-HA antibodies for detection of STING. Protein molecular mass is indicated (kDa) (A).

### **3.4 Co-expression of HIV-1 YU2 Vpr selectively antagonises NF- $\kappa$ B induced expression of luciferase**

To test the effect of HIV-1 M Vpr on the dsDNA sensing pathway a plasmid expressing HIV-1 YU2 Vpr was transfected at 0, 50 or 150ng with the cGAS, STING and reporter plasmids. The plasmid used in this experiment was the first Vpr construct tested and was codon optimised at Blue Heron Bio. Subsequent Vprs were codon optimised by another proprietary algorithm (Geneart) which caused them to have far greater expression levels. At 48hrs post transfection luminometry and immunoblots were performed on cell lysates. The HIV-1 M YU2 Vpr was found to antagonise luciferase expression from the NF $\kappa$ B sensitive promoter, and from the promoter of the IFN $\beta$  gene which contains binding sites for the NF- $\kappa$ B, IRF3 and AP-1 transcription factors (527,528) (figure 3.4 A and B).

An ISG56-promoter firefly luciferase reporter was used to test the effect of Vpr on IRF3 signalling (figure 3.4C). Transcription of this gene is highly dependent on, and specific for the IRF3 transcription factor (529) and was unaffected by transfection of even high doses of Vpr. The constitutively expressed TK renilla control reporter was not significantly affected.

Interestingly there was a reduction in levels of STING detected on immunoblot observed in all three experimental conditions (Fig 3.4 A, B & C). This was unexpected: luciferase expression from the IRF3 sensitive reporter was unaffected by HIV-1 M Vpr, despite the loss of the STING which was stimulating activation at this promoter, presumably by nuclear translocation of IRF3. I hypothesised that Vpr was causing STING to be degraded but that there were potentially two pools of STING, one causing IRF3 activation and one causing NF $\kappa$ B activation. If this was the case and one of these pools (leading to NF $\kappa$ B signalling) was selectively degraded then the other (leading to IFR3) might remain unaffected. There could also be a distal block to signalling in the pathway specific for NF $\kappa$ B but which left IFR3 signals unaffected. This is in contrast to a study by Vermeire et al which found a weakly stimulatory effect of Vpr on NF $\kappa$ B signalling (530). Given the centrality of NF $\kappa$ B signalling in the up regulation of antiviral genes and the known sensitivity of HIV-1 to interferon a selective advantage to antagonising NF $\kappa$ B signalling in early infection is biologically plausible. It is subsequently shown in this study that the apparently specific effect on NF $\kappa$ B signalling is in fact due to the weak codon optimization of this Vpr gene causing it to be relatively poorly expressed combined with the greater sensitivity of the ISG56 promoter to low levels of IRF3 (see figure 3.6).

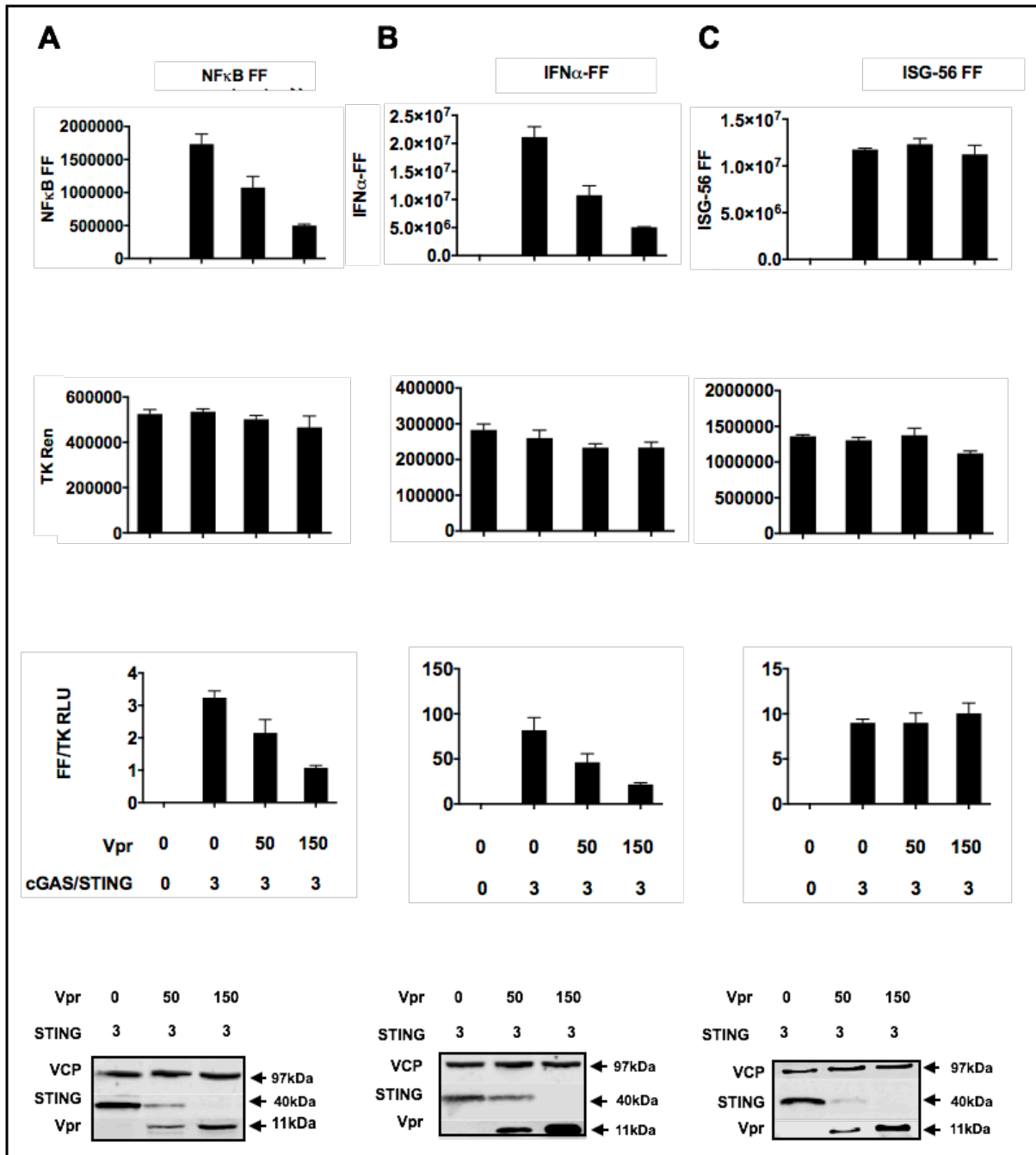


**Figure 3.4 Co-expression of HIV-1 YU2 Vpr antagonises expression from NFκB sensitive promoters but not IRF3 sensitive promoters.** HA epitope tagged cGAS and STING expression plasmids were transfected into HEK293T cells at a constant dose of 3ng simultaneously with transfection of firefly luciferase reporters and 7.5ng of TK renilla luciferase and with either an NFκB sensitive promoter (A), the IFNβ promoter (B) or the ISG56 promoter. HIV-1 M YU2 Vpr was co-transfected at 150 or 50ng. Cells lysates were assessed with luminometry. Firefly luciferase (top row) and renilla luciferase (middle row) are presented. Firefly luciferase was normalised to the renilla (bottom row). Data are from three separate experiments and are represented as mean ± SEM. Whole cell lysates were separated by SDS-PAGE and immunoblotted with anti-HA antibodies and anti-Vpr antibodies. The location of protein molecular mass markers is indicated (kDa).

### **3.5 Expression of HIV-1 M Vpr does not cause an increase in LIVE/DEAD cell staining**

Vpr has been widely reported to cause apoptosis in a number of different cell lines and types (460,462,531,532). To ensure that the phenotype of antagonism of NF $\kappa$ B signal was could not be attributed to cell death cells were transfected with Vpr up to a dose of 300ng/50,000 cells, a far higher dose than was used in any other experiment reported. Cells were then stained with a viability dye (LIVE/DEAD Aqua, Invitrogen) at 48hrs post transfection then fixed and analyzed on a BD FACSCalibur (Figure 3.5 A&B). Cells were gated by structure, size, and LIVE/DEAD stain. Representative plots at 48hrs are shown.

A number of additional checks were made to ascertain that cell viability was not compromised by the transfection. pH indicators in the DMEM culture medium showed identical colour change across wells with increasing doses of Vpr. Subjective observations of cell viability as well as Trypan Blue exclusion dye counting gave no indication of cell death, changes in adherence or morphological changes. Finally, the consistency of loading controls on immunoblot (figure 3.5B), the maintenance of expression of renilla luciferase from the control plasmid and the specificity of the phenotype for NF $\kappa$ B inhibition all support the notion that the effect of Vpr expression is not an artifact of toxicity.

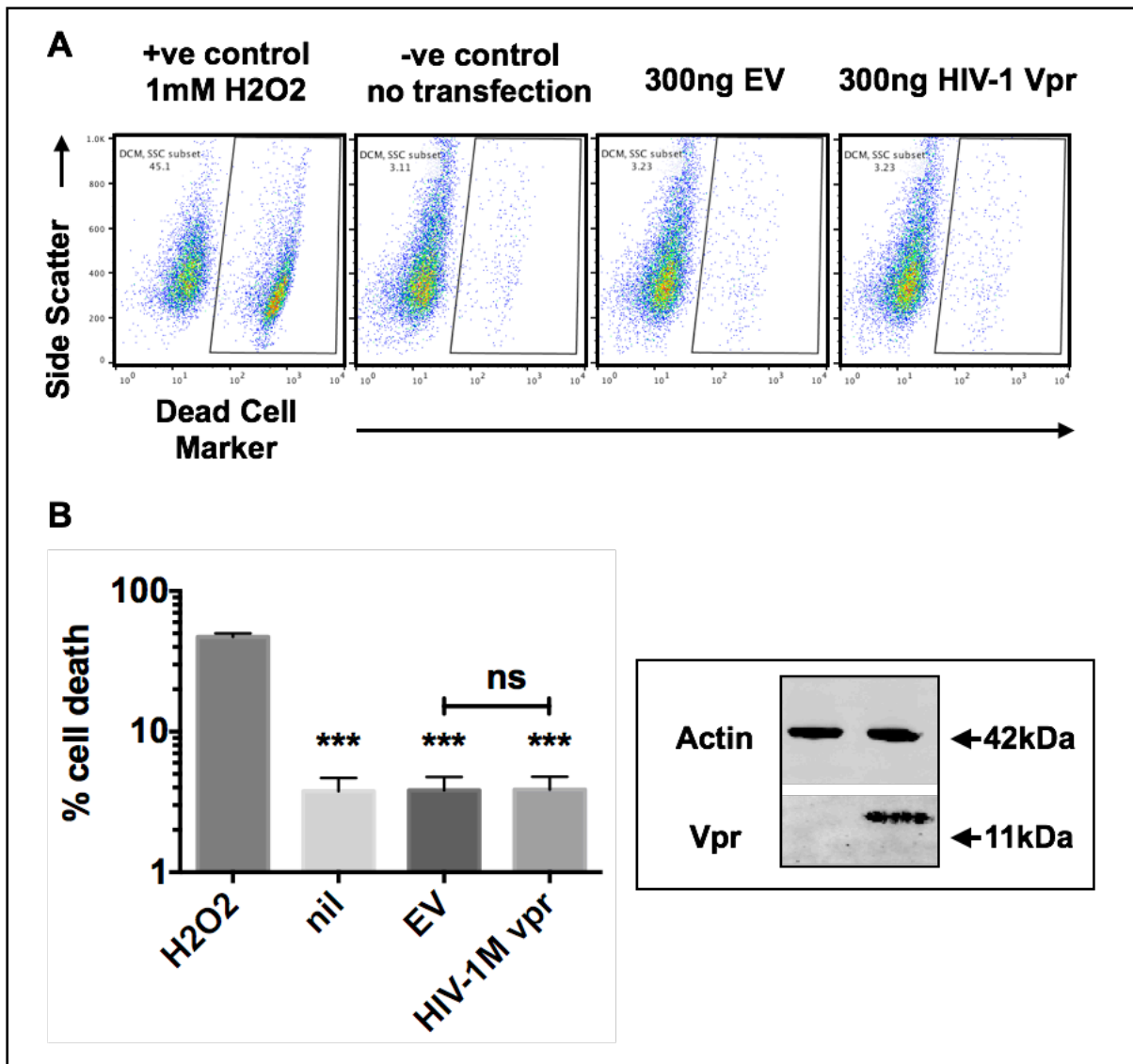


**Figure 3.5 Ectopic expression of Vpr does not cause an increase in LIVE/DEAD cell staining** (A) Cells were transfected as previously with either Vpr empty vector (EV). For a negative control cells were left untransfected (nil). Hydrogen Peroxide treatment (H<sub>2</sub>O<sub>2</sub> 1mM for 3hrs at 37°C) was used to kill cells as a positive control. Cells were harvested at 48hrs and stained with a viability dye (LIVE/DEAD Aqua, Invitrogen), then fixed and analyzed on a BD FACSCalibur. Cells were gated by structure, size, and LIVE/DEAD. Representative plots at 48hrs are shown for the highest dose of Vpr. Cell death induced by hydrogen peroxide was used as a positive control and untransfected cells as a negative control. (B) Presence of Vpr was confirmed on immunoblot. Statistical analysis was performed using a paired t-test. \*\*\*= p<0.001.

### 3.6 Primate Vprs exhibit differential antagonism of cGAS/STING induced NF- $\kappa$ B promoter driven expression of luciferase

Previous studies of cellular restriction factors for HIV and their antagonism by viral accessory proteins have provided evolutionary and mechanistic insight into host virus interactions and transmission events. The species specific degradation of tetherin by either Nef or Vpu being prototypical examples (533,534).

To determine whether the observed signalling antagonism is species specific, or conserved, a panel of primate lentiviral Vprs were tested against NF $\kappa$ B activity stimulated by cGAS/STING transfection (as in the assay described in figure 3.4A). This panel represented HIV-1 M group (YU2 primary isolate) and HIV-2 A, two SIVcpz (both from central chimpanzees, *Pan troglodites troglodites*), SIVsmm (Sooty mangabey *Chlorocebus pygerythrus*) SIVtal (Talapoin, *Miopithecus ogouensis*) and SIVver (Vervet monkey *Chlorocebus pygerythrus*). The HIV-1 YU2 construct was codon optimized with a proprietary algorithm for protein expression optimization from Blue Heron Bio whereas the other constructs were designed and codon optimized for these experiments by Geneart. FLAG-epitope tags were cloned into the open reading frame at the N terminus for detection on Western blot. HEK293T cells were co-transfected with the Vprs as in figure 3.4A and expression was normalised to a control transfected with empty vector (Figure 3.6 A).

Antagonism of cGAS/STING signalling, compared to transfection of an empty vector, was observed with Vpr from both human viruses and the parental primate lineages from which they originated. Interestingly the most effective antagonists were the SIVcpz $_{ptt}$  Vprs from the western Chimpanzee subspecies *pan troglodytes troglodytes*. It was hypothesised that this was due to poor codon optimisation of the HIV-1 M which had undetectable expression levels and yet was still able to significantly antagonise.

Importantly this antagonism matched the reduction in STING intensity on western blot with an  $R^2$  of 0.73. (Figure 3.6 B&C). Vif, Vpu, and Vpx all link to cullin-RING finger ubiquitin ligases to induce the polyubiquitination and proteasomal degradation of their cellular targets and it was hypothesised that the reduction of STING on immunoblot by Vpr could be enabled by a similar mechanism. With the exception of the comparison of SIVcpz Vprs and HIV-1 M Vpr the degree of antagonism was independent of levels of expression of Vpr indicating this phenotype may be due to structural differences between Vprs rather than as a product of expression levels (Figure 3.6D).

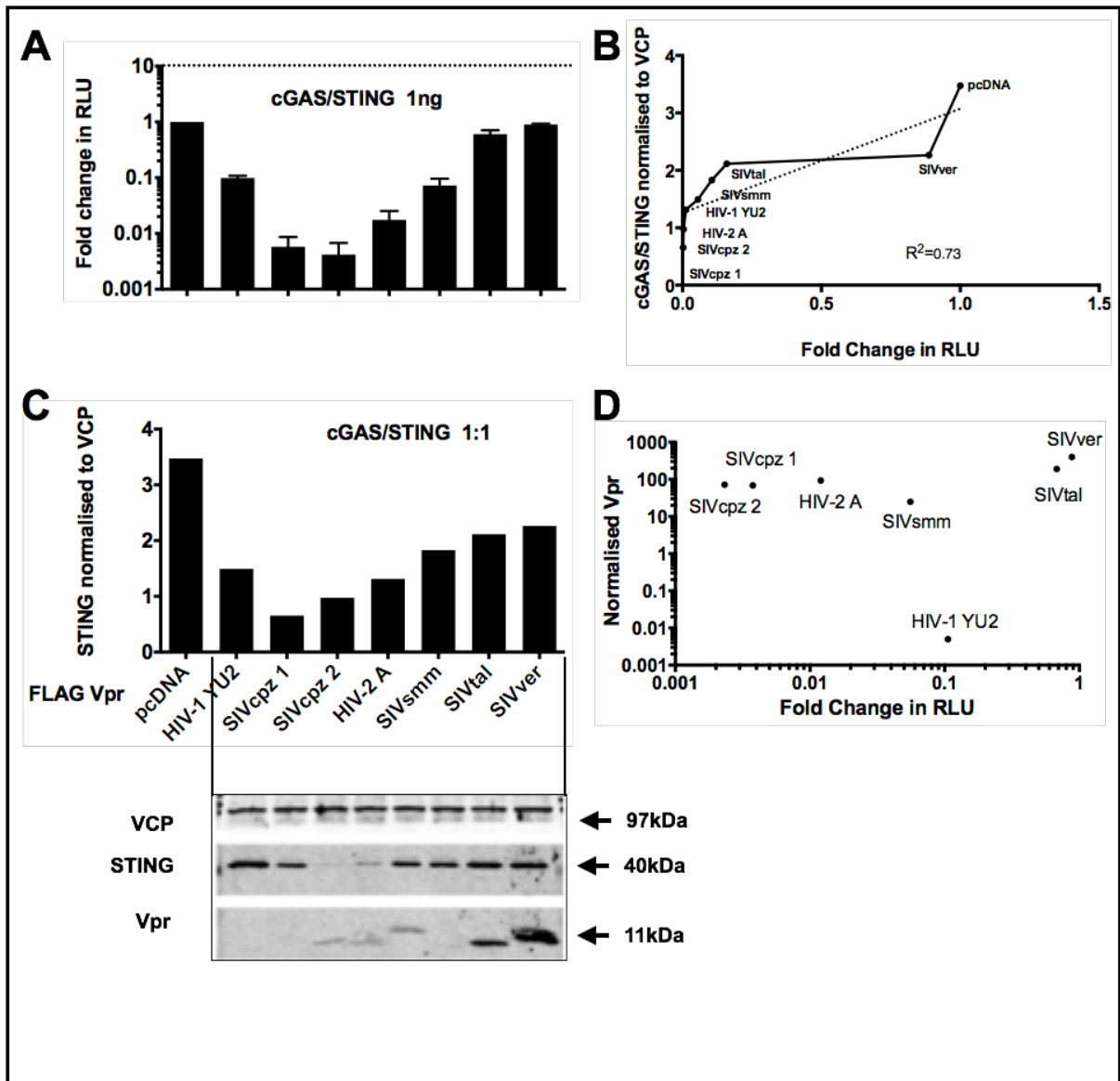


**Figure 3.6 Differential antagonism of NF- $\kappa$ B activity by primate lentiviral Vpr proteins.** (A) HEK293T cells were transfected as previously described with reporter plasmids, cGAS and STING and HIV or SIV Vprs or an empty vector control. NF $\kappa$ B activation was determined as previously described (by luminometry) 48 h post-transfection. Data are presented as the fold induction relative to an identical dose of cGAS/STING transfected with an empty expression vector. The mean values of three transfections  $\pm$ SEM are shown. (C) Immunoblotting was used to confirm expression of proteins with anti-HA and anti FLAG antibodies and anti VCP as a loading control. Molecular mass markers in kDa are shown. (B) relationship between loss of STING on immunoblot and RLU. (D) differential expression levels of Vpr plotted against RLU.

### **3.7 Codon optimised HIV-1 M Vpr shows greater antagonism of cGAS/STING mediated NFκB promoter activation than HIV-2**

To investigate whether HIV-1 M is able to antagonise NFκB signalling more effectively than other Vprs at a given level of expression, a panel of HIV-1 and HIV-2 Vpr expression vectors was constructed.

Vpr sequences were chosen from viruses isolated within the first weeks or months following clinical infection which may have unique properties compared to viruses derived from cell culture amplification (535). Many HIV-1 clones come from virus produced in cell culture. While this process selects for strains with an *in vitro* growth advantage, these strains may not represent the virus present *in vivo*. For this reason clinical sample clones were used including HIV-1 YU2, SUMA, WITO and CH77.

HIV-1 M YU2 was cloned directly from uncultured brain tissue of a patient with AIDS dementia complex (536,537). HIV-1 M CH77, SUMA and WITO are infectious molecular clones (IMCs) representing transmitted/founder (T/F) viruses. The sequence of the complete T/F virus genomes used here were inferred from subjects with early/acute clade B infection, the dominant HIV subtype in the Americas, Western Europe and Australasia, using viral RNA (vRNA) obtained early during infection, as well as sequencing of single-genome amplicons (SG amplicons) and phylogenetic inference based on a model of random virus evolution (535). These techniques have been used to show that in nearly 80% of the cases of HIV-1 sexual transmission, viral sequences came from a single ancestral sequence, the T/F sequence (538,539).

All constructs in this experiment were codon-optimised using the Genearth proprietary algorithm. This increased the expression levels of the HIV-1 M YU2. As in figure 3.6, a directly proportional relationship between loss of STING and loss of NFκB driven luciferase expression was seen (figure 3.7A&B). However, whereas previously HIV-2 was seen to be a more effective antagonist of cGAS/STING mediated signalling than HIV-1 M, in this panel the HIV-1 constructs were up to 10 fold more effective (figure 3.7A). The SUMA Vpr T/F clone was the most effective. This was probably attributable to small differences in expression or transfection as detected on immunoblot (figure 3.7B).

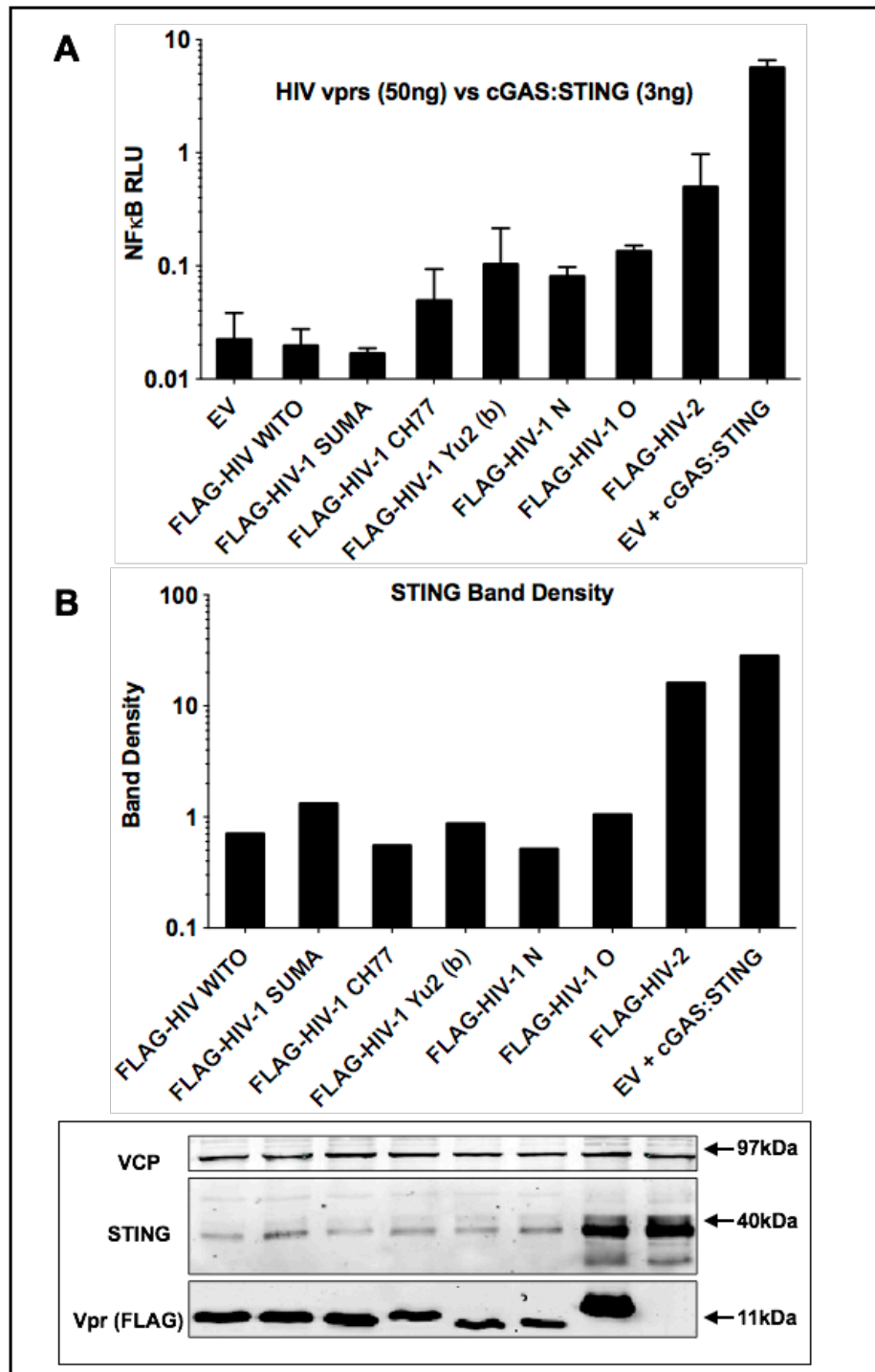


**Figure 3.7 Transmitted/founder isolates of HIV-1 M Vpr antagonise cGAS/STING induced NF-κB activation more effectively than HIV-2 Vpr.** (A) HEK293T cells were transfected as previously with reporter plasmids, cGAS and STING and HIV Vprs or an empty vector control. NFκB activation was determined as previously described (by luminometry) 48 h post-transfection. Data are presented as the fold induction relative to an identical dose of cGAS/STING transfected with an empty expression vector. The mean values of three transfections  $\pm$ SEM are shown. (B) Immunoblotting from the same 48-well plates was used to confirm expression of proteins. Molecular mass markers in kDa are shown.

### 3.8 NFκB signal inhibition by Vpr is unaffected by FLAG epitope tags at the Vpr N-terminal

To confirm that the phenotype was not influenced by the FLAG epitope tag a panel of Vpr expression vectors were cloned without the tag and then tested in parallel with a wider panel of HIV and SIV Vprs (figure 3.8). This panel represents viruses from all families of human and non-human primates infected with lentiviruses including the African apes and the old world monkeys (Cercopithecidae). *Cercopithecidae* monkeys are divided into two subfamilies named *Colobinae* (which include the African colobus monkeys and the Asian genera which do not naturally carry lentiviruses and have only forced zoonotic infections) and *Cercopithecinae* (mainly African, but includes the diverse genus of macaques, which are Asian and North African). *Cercopithecinae* monkeys, from which most non-human primate lentiviruses have been isolated, are categorized in two tribes (Cercopithecini and Papionini) as well as many species and subspecies found across sub-Saharan Africa (540).

There are six approximately equidistant groups of primate lentiviruses, classified, using phylogenetic analysis. The tested range of Vprs represent all of six (541,542).

- (i) SIVcpz/HIV-1 lineage from chimpanzees (*Pan troglodytes*) and humans human immunodeficiency virus type 1 (HIV-1) and SIVgor (*Gorilla gorilla gorilla*).
- (ii) SIVsm lineage from sooty mangabey (*Cercocebus atys*) together with HIV-2.
- (iii) SIVagm lineage from the four main species of African green monkeys, i.e., grivet, sabeus, vervet, and tantalus (members of the genus *Chlorocebus*).
- (iv) SIVsyk lineage from Sykes' monkeys (*Cercopithecus mitis albogularis*), SIVmon from mona monkeys (*Cercopithecus mona*), SIVgsn from greater spot-nosed guenons (*Cercopithecus nictitans*), SIVmus from mustached monkeys (*Cercopithecus cephus*), and SIVdeb from De Brazza's monkeys (*Cercopithecus neglectus*).
- (v) The SIVlhoest lineage, composed of SIVlhoest from L'Hoest monkeys (*Cercopithecus lhoesti*), SIVsun from sun-tailed monkeys (*Cercopithecus solatus*), and SIVmnd-1 from mandrills (*Mandrillus sphinx*);
- (vi) SIVcol lineage from black, white and olive colobus (*Colobus guereza*).

As more sequences have been analyzed the phylogeny has been complicated with discordant viruses from SIVrcm, gsn and mnd2 which change phylogeny according to the gene region analyzed (26–28) and SIVrcm and gsn sequences were included. The panel included the original sequences in figures 3.6 and 3.7 with further sequences from the eastern chimpanzee (*Pan troglodytes schweinfurthii*), the western gorilla (*Gorilla gorilla gorilla*) the SIVagm group, SIVtan (Tantalus *Cercopithecus tantalus*), SIVrcm (Red Capped Mangabey, *Cercocebus torquatus*), SIVdeb (De Brazza's monkeys, *Cercopithecus neglectus*), SIVsyk (Sykes' monkey, *Cercopithecus mitis*), 2 Vprs from SIVmon (Mona Monkey *Cercopithecus mona*), SIVmus, mustached monkey (*Cercopithecus cephus*); greater spot-nosed monkey (*Cercopithecus nictitans*); SIVolc (Olive Colobus, *Procolobus verus*) and SIVlst (L'Hoest's Guenon, *Cercopithecus lhoesti*). In no case did the tag significantly affect the phenotype antagonism of sensing.

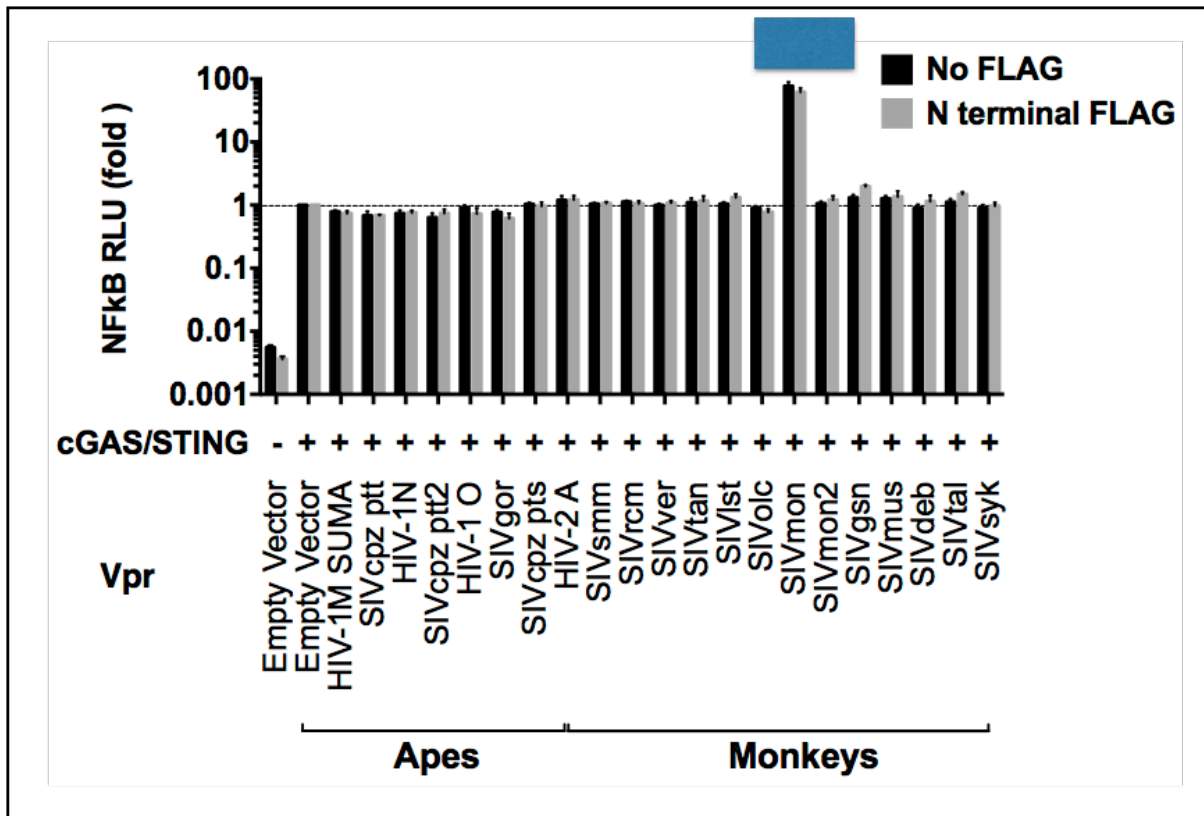


**Figure 3.8 Inhibition of cGAS/STING induced NFκB signalling is unaffected by a FLAG epitope tag at the N-terminal of the Vpr.** HEK293T cells were transfected as previously with an NFκB sensitive reporter, cGAS and STING (3ng) and HIV or SIV Vprs or an empty vector control. NFκB activation was determined by luminometry 48 h post-transfection. The mean fold change in RLU (relative light units – firefly luciferase normalised to renilla) relative to a control with no Vpr (empty vector + cGAS:STING) is displayed. Data are presented as the fold induction relative to an identical dose of cGAS/STING transfected with an empty Vpr expression vector. The mean values of three transfections ±SEM are shown. Data were analysed for the effect of the FLAG epitope tag using a two way ANOVA (analysis of variance) test and no statistically significant difference was found between tagged and untagged Vprs. Western blot data for this experiment are shown in figure 3.9)

### **3.9 Inhibition of NF $\kappa$ B induced signalling is not conserved across all Vprs from different primate lineages.**

When the effects on NF $\kappa$ B sensitive promoter expression are compared with immunoblot data from the full panel of Vprs there is an overall correlation between loss of STING and loss of NF $\kappa$ B sensitive luciferase expression (figure 3.9A&B). The luminometry data represent 4 separate experiments whereas the immunoblot data is from a single representative experiment. The Vpr effect is not binary but there is a clear pattern of variable antagonism across species. HIV-1 viruses and their parent species inhibit >10X. HIV-2 and its parent species along with other mangabeys show reduced inhibition. The African Green Monkey SIVs (SIVver, SIVtan from the *Chlorocebus* Genus), the guenon SIVs (L'Hoest's, De Brazza's, Moustached, Great-spot nosed and 2 sequences of Mona), the Talapoin and the Colobus (Olive) showed variably reduced inhibition of luciferase activation and loss of STING (figure 3.9B).

Of particular interest, I noted that the SIVcpzpts showed diminished ability to antagonise signalling compared to other ape viruses. Only 3 lineages of SIV have transmitted to humans from non-human primates. SIVcpz, SIVgor and SIVmm. Statistically significant antagonism of sensing was observed in all lineages which have transmitted to human beings but the parent species of HIV-1 were able to antagonise more robustly than either HIV-2 or SIVsmm. No lineage assessed that failed to antagonise has transmitted to humans suggesting that the observed effect (subsequently shown in chapter 4 to be inhibition of cGAS and STING expression) may be necessary for zoonotic transmission to humans.

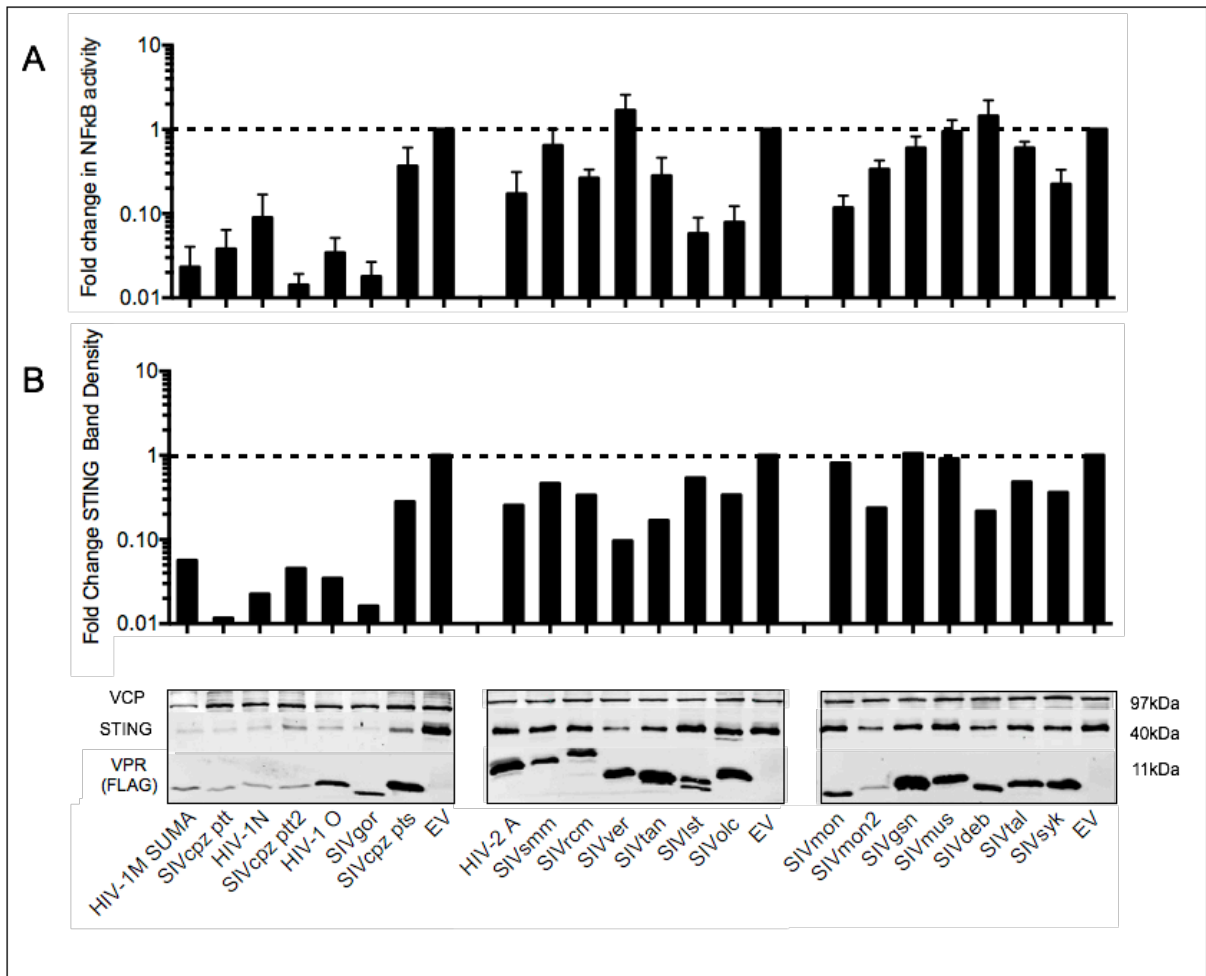


**Figure 3.9 Inhibition of NFκB induced signalling is not conserved across Vprs from different primate lineages.** (A) HEK293T-cells were transfected as previously described. NFκB induced firefly luciferase expression was normalised to a thymidine kinase promoter-driven renilla luciferase reporter. Data are presented as the fold induction relative to an identical dose of cGAS/STING transfected with an empty expression vector  $-/+$  SEM.(B) Immunoblotting from the same plates was used to confirm expression of proteins and calculate relative quantities of STING. Molecular mass markers in kDa are shown.

### 3.10 NF $\kappa$ B signal inhibition and Vpr phylogeny

To better understand the relationships between NF $\kappa$ B signal inhibition and host species a phylogenetic tree of Vpx and Vpr alignments was constructed using sequences from the Los Alamos database including the sequences cloned into expression vectors. Sequences were manually aligned and validated using PRANK online software. An 'approximate maximum likelihood' algorithm was used to generate phylogeny structure with online software FastTree (515). Branch support was calculated by Shimodaira-Hasegawa-like local branch support (SH-like test) and the nodes with SH-test p-values < 0.1 noted with a black rectangle (figure 3.10A). The tree is mid-point rooted and branch lengths indicate the number of nucleotide substitutions per site. The scale bars represent 0.2 substitutions per site.

This tree enabled examination of the relationship between antagonism and cross species transmission of SIV to humans: clades with transmission to humans have appreciably greater inhibition of signalling with the clade including HIV-1 M Vpr, the only pandemic primate lentivirus, inhibiting most strongly (figure 3.10B).

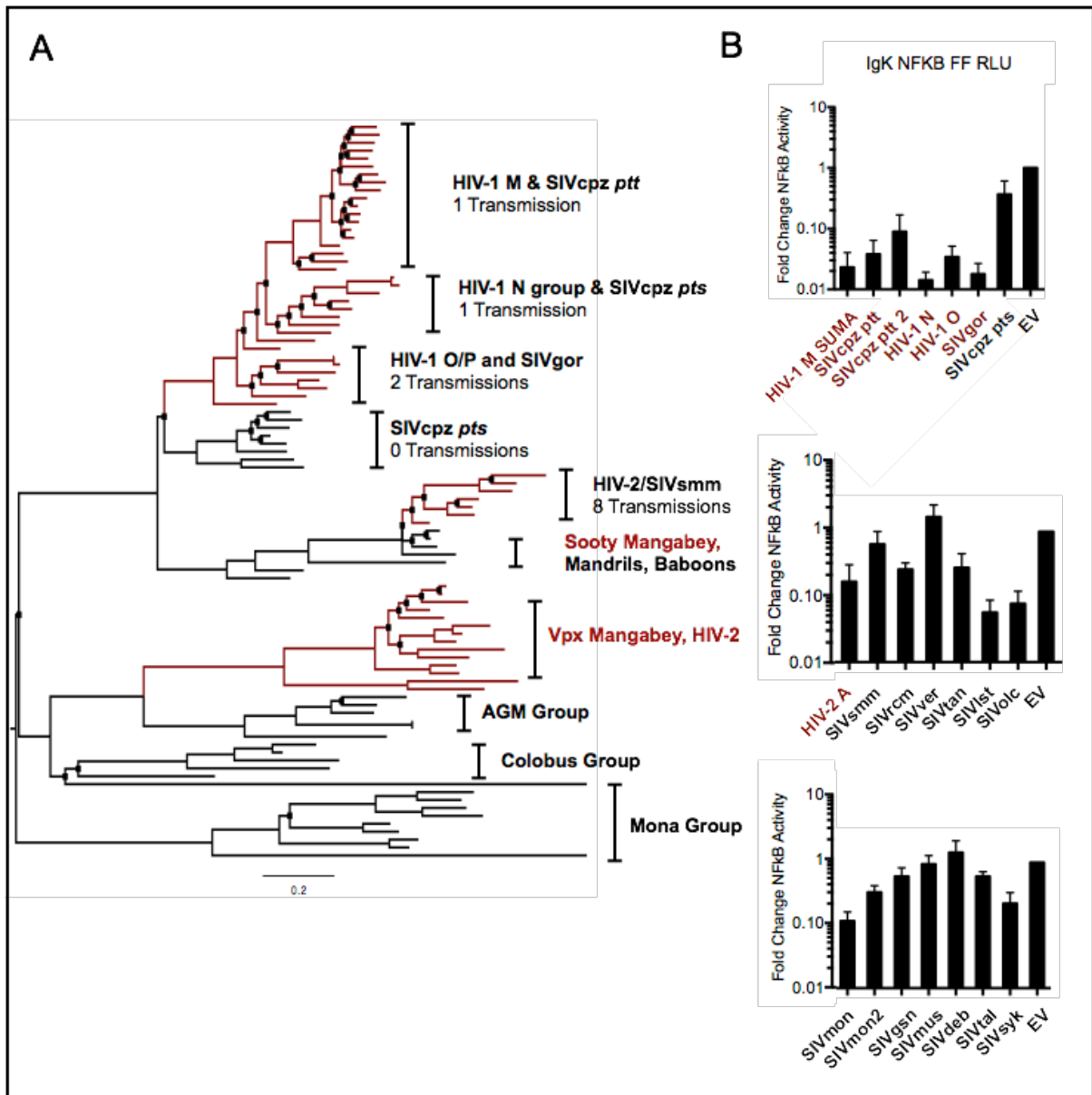


**Figure 3.10 NFκB signal inhibition and Vpr phylogeny.** (A) Phylogenetic analysis of Vpr sequences from SIV and HIV. The lentiviral Vpr from viruses that have had zoonotic transmission to humans species are coloured red. Sequences were manually aligned and validated using PRANK online software. An 'approximate maximum likelihood' algorithm was used to generate phylogeny structure with online software FastTree (515). Branch support was calculated by Shimodaira-Hasegawa-like local branch support (SH-like test), and the nodes with SH-test p-values < 0.1 noted with a black rectangle. The tree is artificially rooted and branch lengths indicate the number of nucleotide substitutions per site. The scale bars represent 0.2 substitutions per site. (B) NFκB activation data from figure 3.9 are presented next each clade.

### **3.11 SIVcpz Vpr from the eastern chimpanzee does not antagonise cGAS/STING stimulated NF $\kappa$ B signalling.**

The only chimpanzee subspecies with a lentivirus that has failed to transmit between species, the eastern chimpanzee (*Pan troglodytes schweinfurthii*) (543), was noted to lack significant inhibition despite >5 fold increased expression levels compared to HIV-1 or SIVcpz $ptt$  Vprs (see immunoblot figure 3.9B). A phylogenetic analysis of Vpr sequences from HIV-1 and its ancestor viruses was constructed using the same methods as the tree in figure 3.10A. A further sequence was cloned and compared with HIV-1 M and SIVcpz $ptt$  sequences and this finding was confirmed (figure 3.11B). Given that SIVcpz $ptt$  strains have been transmitted to humans and gorillas at least 5 times the lack of evidence of similar transmission SIVcpz $pts$  is striking especially since infection rates determined by field sampling seem to be very similar to those found in *P. t. troglodytes* (544–546). Whilst it is possible that there are social and cultural determinants of cross species transmission between humans and great apes in east and west Africa I hypothesised that the apparent inability of Vpr to antagonise NF $\kappa$ B signalling (in fact the inability to inhibit expression of cGAS/STING – see chapter 4) may provide an extra barrier.

A sequence alignment of all available HIV-1, SIVcpz and SIVgor Vprs was constructed which shows an 11-18 residue deletion at the C-terminal end (figure 3.11C). The only other uniquely different residue in SIVcpz $pts$  Vpr is a tryptophan at position 102 which aligns with tyrosines, phenylalanines or leucines in HIV-1, SIVgor or SIVcpz $ptt$  Vprs all of which have hydrophobic side chains and may, therefore, not be significant substitutions.

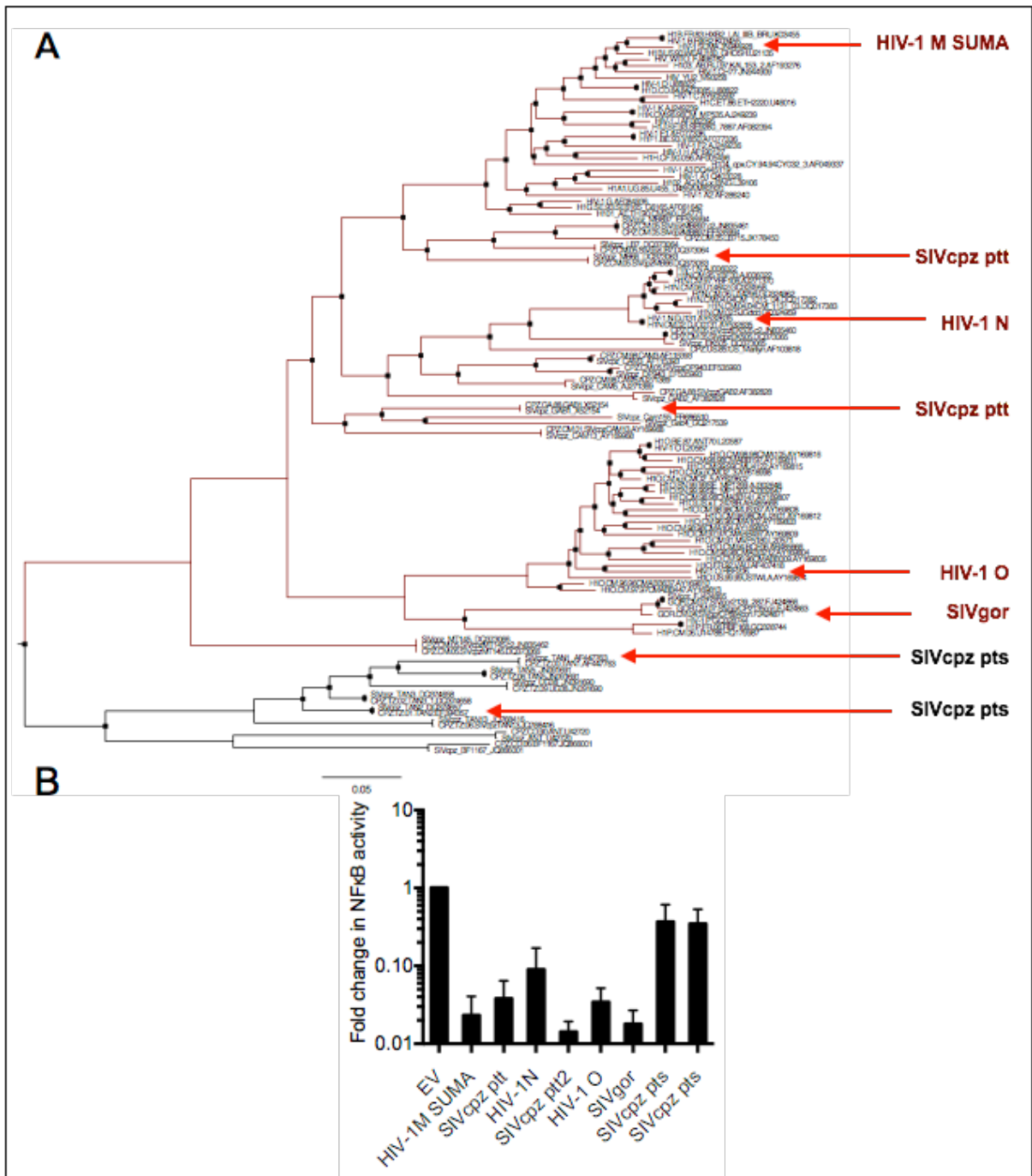


**Figure 3.11 A&B SIVcpz Vprs from eastern and western Chimpanzees differentially antagonise NFκB mediated signalling** (A) Phylogenetic analysis of Vpr sequences from HIV-1 and its ancestor viruses SIVcpz and SIVgor. Tree branches from viruses that have had zoonotic transmission to humans species are coloured red. Sequences were aligned and a phylogeny was generated as in figure 3.10. The tree is artificially rooted and branch lengths indicate the number of nucleotide substitutions per site. The scale bars represent 0.2 substitutions per site. (B) Fold change in NFκB induced firefly luciferase expression. Cells were transfected as before with cGAS and STING and one of HIV-1 M SUMA, 2 different SIVcpz<sub>ptt</sub>, HIV-1 N, SIVgor, HIV-1 O and 2 different SIVcpz<sub>pts</sub> Vprs. Data are presented as the fold induction relative cGAS/STING transfected with an empty expression vector. The mean values of three transfections ±SEM are shown.

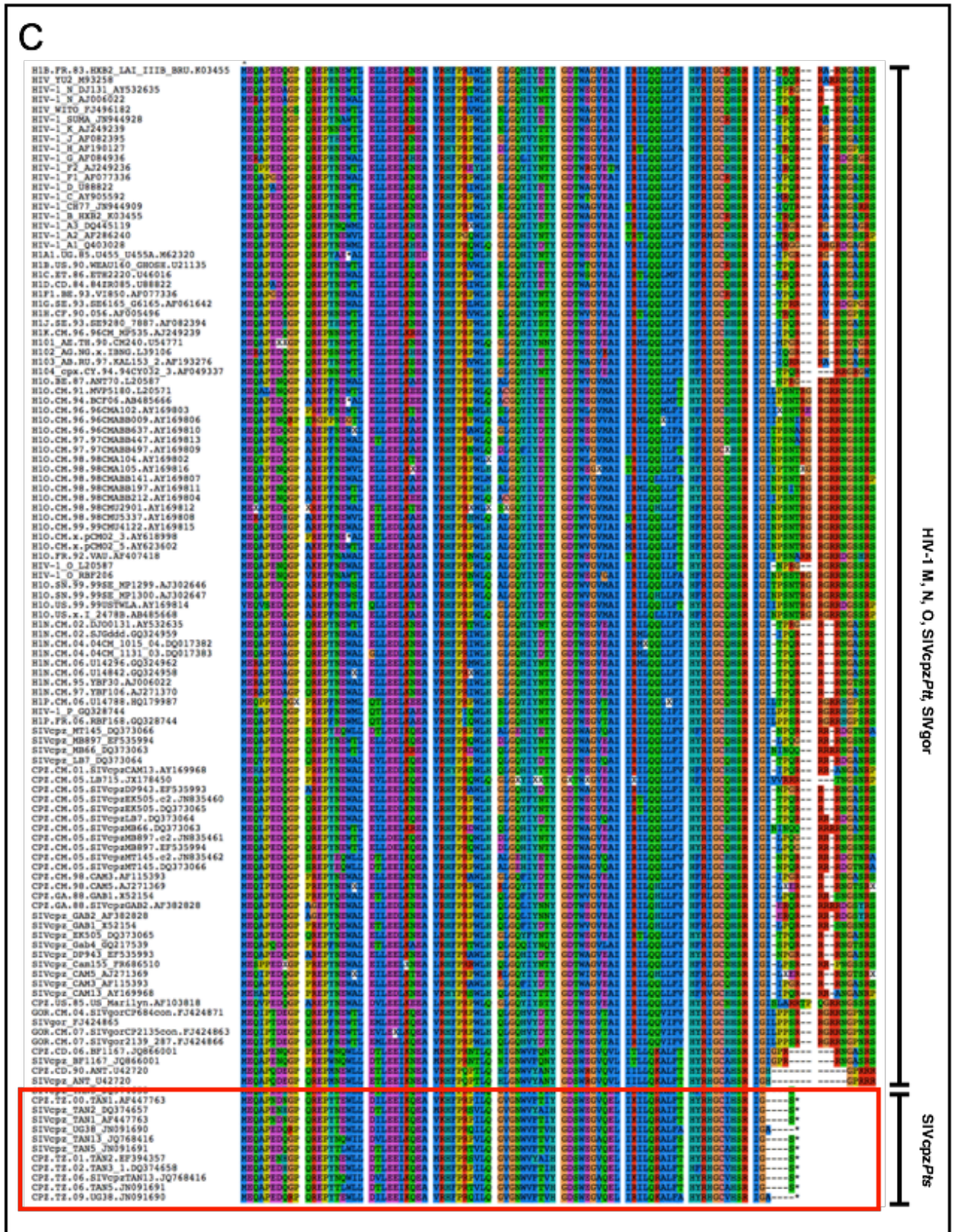


**Figure 3.11 C Vpr alignment** 160 full-length Vpr nucleotide sequences derived from 24 HIV/SIV strains from the Los Alamos HIVSequence Database (<http://www.hiv.lanl.gov>) manually aligned using the Se-AL sequence editor (<http://tree.bio.ed.ac.uk/software/seal/>) showing the deletion in the strains derived from the eastern *Pan troglodytes Schweinfurthii* subspecies



### 3.12 Inhibition of differentially activated NF $\kappa$ B signalling by Vpr

In order to investigate the level at which Vpr is inhibiting the pathway, innate immune molecules capable of stimulating NF $\kappa$ B signalling were ectopically expressed with HIV-1 M YU2. Five different stimuli were used: cGAS/STING as previously; a constitutively active mutant of the canonical IKK, IKK $\beta$ ; the non-canonical IKK, TBK1 (known also to activate IRF3 signalling); MAVS (mitochondrial antiviral signalling adaptor) and TNF $\alpha$ . Significant inhibition of signalling by Vpr was seen with signalling mediated by IKK $\beta$  and TBK1 but not with MAVS or TNF $\alpha$  (figure 3.12). Additionally IKK $\beta$  and TBK1 showed reduced expression on immunoblot as had been shown previously with STING (figure 3.12B&C). Considering the convergence of signalling pathways on TBK1 and IKK $\beta$ , and the loss of both IKK $\beta$  and TBK1 on immunoblot the lack of effect on TNF $\alpha$  and MAVS mediated signalling was unexpected.

NF- $\kappa$ B is activated downstream of the TLRs, RLRs, some NLRs and DNA sensors, as well as the TNF $\alpha$  receptor (TNFR) and IL-1 receptor (IL-1R). NF- $\kappa$ B-activating signalling converges on the IKK complex, consisting of the canonical IKKs (IKK $\alpha$  and IKK $\beta$  and NF- $\kappa$ B essential modulator (NEMO) (547)) or IKK $\gamma$ , a non-enzymatic regulatory component (548). The IKKs phosphorylate members of the inhibitor of  $\kappa$ B (I $\kappa$ B) family directly inducing proteosomal degradation (549) and NF- $\kappa$ B is then free to translocate to the nucleus.

Signalling pathways leading to IRF3 activation downstream of TLRs, RLRs and cytoplasmic DNA sensors converge on the non-canonical IKKs; These PRRs utilise various adaptors like MAVS but generally require TRAF3 to co-ordinate upstream signalling events and activate TBK1 and IKK $\epsilon$  which phosphorylate IRF3 causing it to dimerise and translocate to the nucleus (282,550,551).

I hypothesised that TNF $\alpha$  and MAVS mediated NF $\kappa$ B signalling in HEK293T cells is mediated via unknown pathway members unaffected by YU2 Vpr. I also hypothesized that IKK $\beta$  and TBK1 were being degraded in complex with STING since these molecules are known to associate(290). It became clear after completing the experiments presented in chapter 4 that the HIV-1 M YU2 tested was insufficiently expressed to show an effect on MAVS mediated signalling and the lack of effect on TNF $\alpha$  signalling was because the molecule was added to the transfected cells rather than being transfected as a plasmid (see chapter 4).

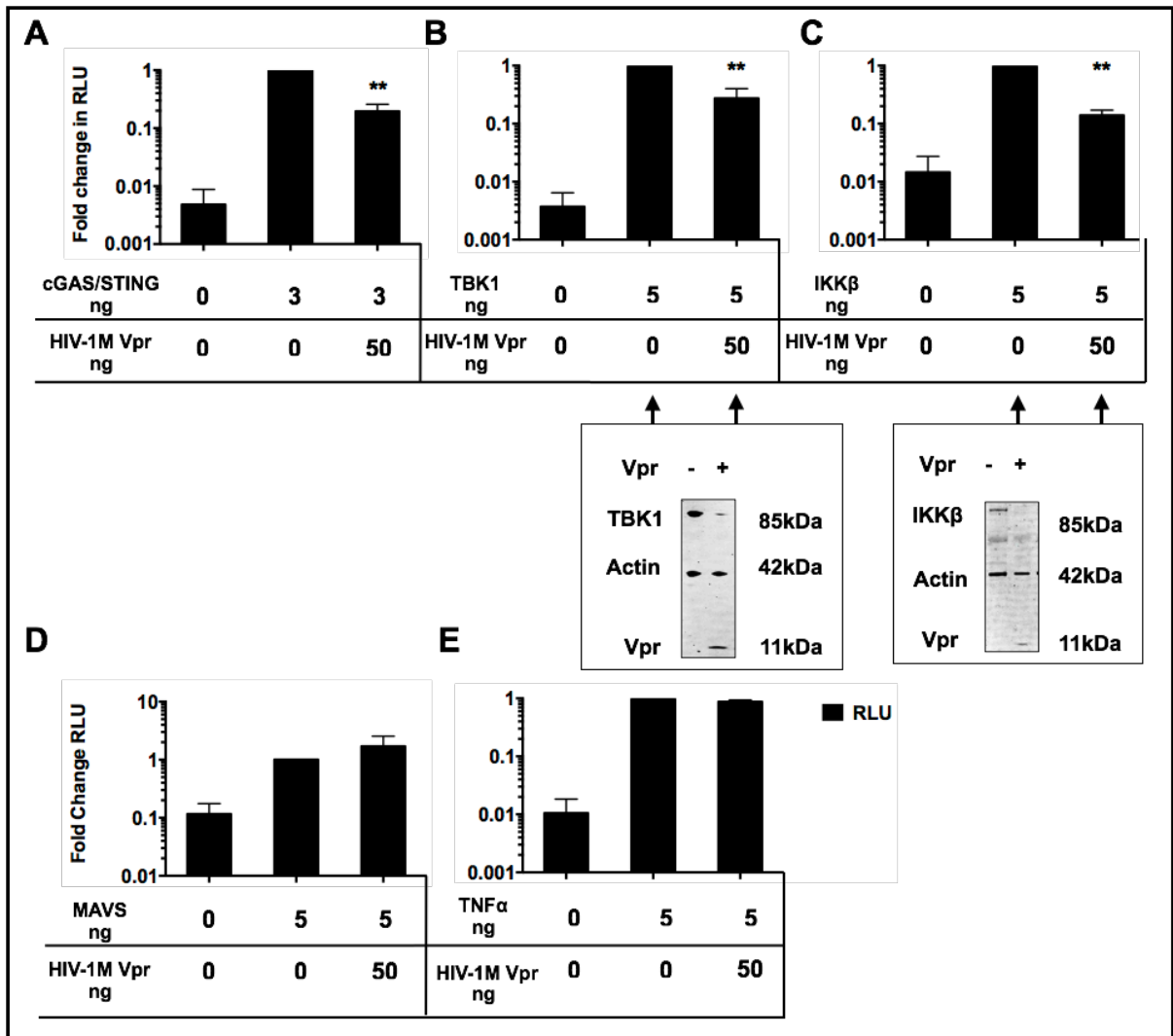


**Figure 3.12 Differential antagonism of NFκB signalling when activated by different stimuli.** HEK293T cells were transfected as previously with an NFκB sensitive reporter, and HIV-1 M YU2 Vpr or an empty vector control. NFκB signalling was activated by transfection of one of HA epitope tagged cGAS and STING (A) IKKβ (B), TBK1 (C), or untagged MAVS (D) or addition of TNFα (E). NFκB activation was determined by luminometry, as previously described, 48 h post-transfection. The mean fold change in RLU (relative light units – firefly luciferase normalised to renilla) relative to a control with no Vpr (empty vector + cGAS:STING) is displayed. The mean values of three transfections ±SEM are shown. The whole cell lysates for (B) IKKβ and (C) TBK1 were separated by SDS-PAGE and analysed by immunoblotting with anti-HA antibodies. The location of protein molecular mass markers is indicated (kDa). \*\*=P<0.01 one-way ANOVA with Dunnett’s post-hoc test.

### **3.13 The pattern of species specific antagonism by primate lentiviral Vprs is preserved across different NFκB activating stimuli**

A similar pattern of species specific activity is observed with a panel of different species' Vprs co-transfected with different NFκB activating stimuli. The panel of Vprs used in figures 3.8 & 3.9 was tested against these different NFκB activating proteins (figure 3.13 A-D). This revealed a conserved differential effect against MAVS, IKKβ and TBK1 across all Vprs (figure 3.13 A-D).

The clinical isolates with improved expression over YU2 all antagonised MAVS-mediated signalling robustly >10 fold (figure 3.13 D). Expression of Vprs following addition of TNFα was confirmed with immunoblot. It was hypothesised that Vpr was acting distally in an NFκB pathway common to TBK1, IKK, cGAS/STING and MAVS but that the TNFα activated pathway converged on a different point. It was also hypothesised that Vpr caused the degradation of a putative complex containing the activating molecules. Conceivably, given the viral LTR's sensitivity to NFκB and the role of NFκB in an inflammatory response, the virus could have evolved to modulate NFκB signalling with great sensitivity. At this point it was not considered that the observed effects could be explained by inhibition of activator molecule (TBK1, IKKβ, cGAS/STING) expression since from the data in figure 3.4 IRF3 signalling appeared to be unaffected.

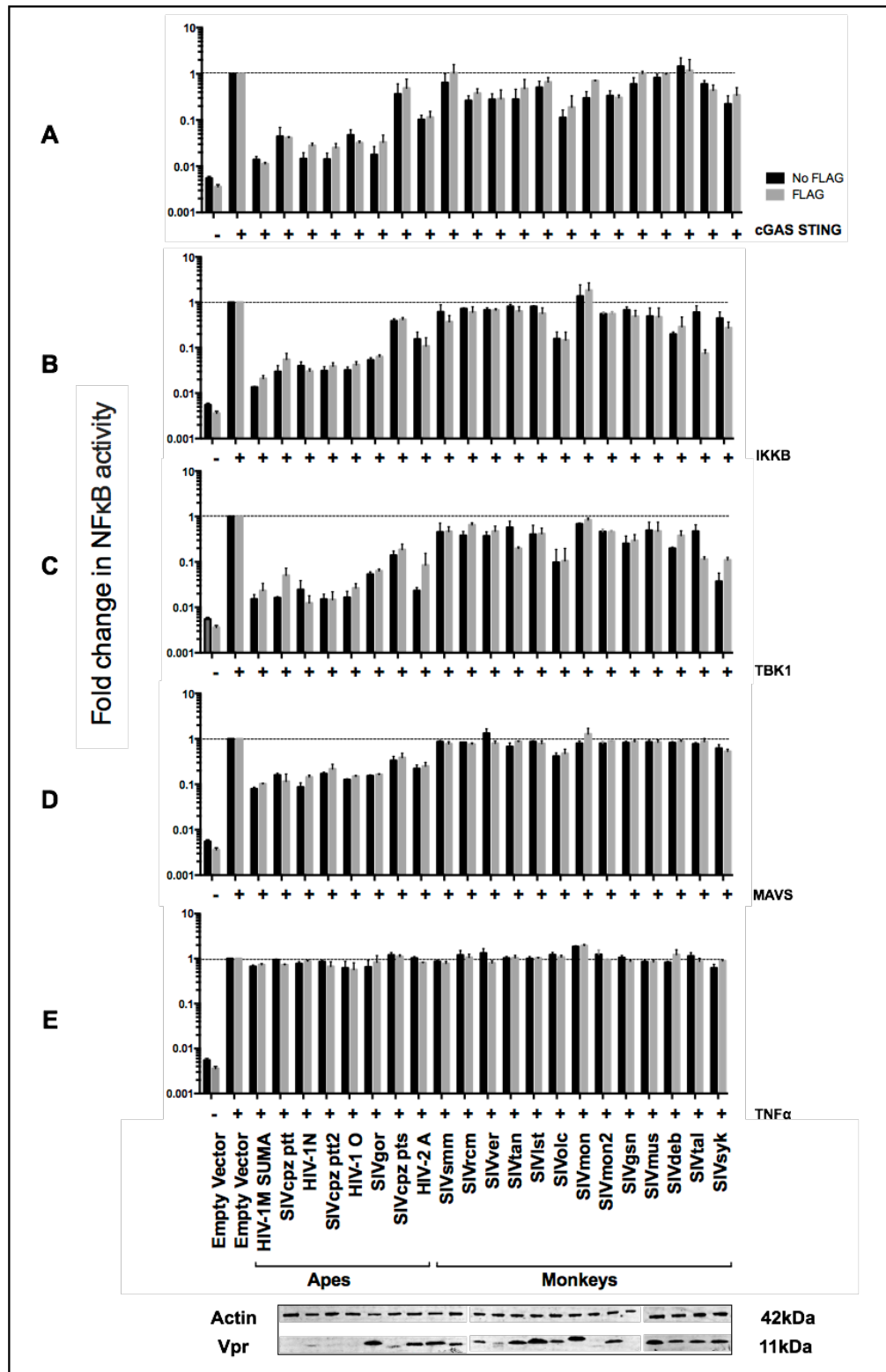


**Figure 3.13 Preserved pattern of antagonism across a panel of primate lentiviral Vprs co-transfected with different NFκB activating stimuli** HEK293T cells were transfected as in figure 3.8. NFκB signalling was activated by transfection of one of HA epitope tagged cGAS and STING (A) IKKβ (B), TBK1 (C), or untagged MAVS (D) or addition of TNFα (E). The mean fold change in RLU relative to a control with no Vpr is displayed. The mean values of three transfections ±SEM are shown. The cell lysates were analysed by immunoblotting to confirm expression of Vpr from the TNFα experiment (E).

### **3.14 HIV-1 M Vpr causes loss of TRAF2 & TRAF6 on immunoblot**

Co-transfection of Tumor necrosis factor receptor-associated factors (TRAFs) 3 and 6 also activated NF $\kappa$ B signalling and unexpectedly the Vpr also caused a dose dependent loss of TRAF3 and TRAF6 expression measured by immunoblot and a proportional loss of NF $\kappa$ B signalling (figure 3.14 B&C). cGAS and STING were co-transfected as a positive control (figure 3.14A).

With the exception of TLR3, all TLRs recruit myeloid differentiation factor 99 (MyD88) to activate a signalling complex that interacts with TNF receptor-associated factor 6 (TRAF6) which then promotes the downstream activation of the IKK complex (550,552). TLR3 recruits the non-canonical IKKs via an adaptor molecule TRAF3 (551). TRAF3 also links signalling downstream of the RLRs to the non-canonical IKKs by interacting with MAVS.

From the published literature on NF $\kappa$ B signalling pathways it was hard to conceive of a mechanism by which Vpr could specifically antagonise NF $\kappa$ B signalling when stimulated by STING/TBK/IKK/MAVS/TRAF3 and TRAF6 whilst leaving signalling stimulated via TNF $\alpha$  unaffected and IRF3 signalling unaffected.

Additionally, whilst the putative degradation of multiple signalling molecules as part of a complex is in theory possible, the range of molecules that showed reduced expression on immunoblot are not known to associate. Subsequent experiments detailed in chapter 4 demonstrated that Vpr was not causing a complex to be degraded but was in fact inhibiting expression from the transfected plasmids.

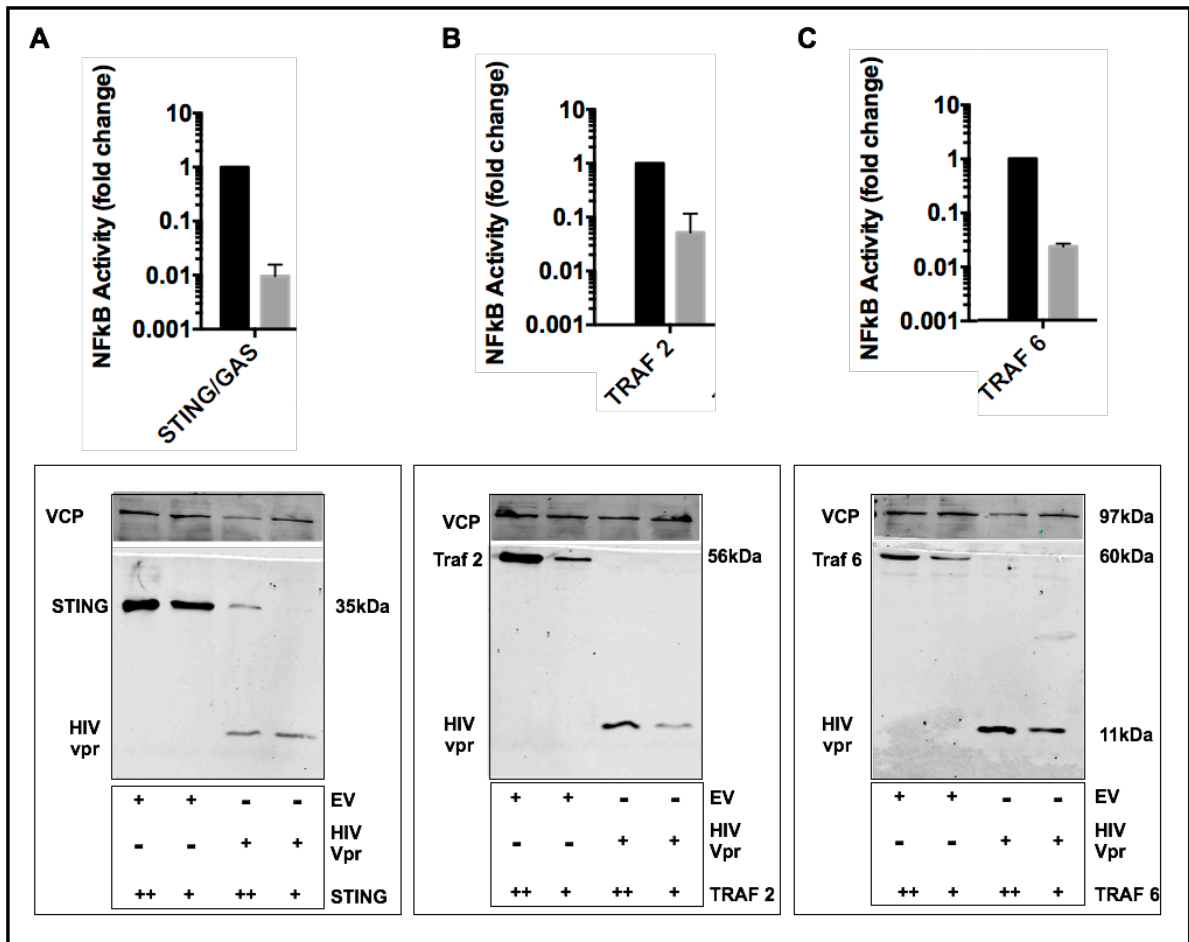


**Figure 3.14 Co-transfected HIV-1 M Vpr causes loss of HA-TRAF2 & HA-TRAF6 on immunoblot** Two doses of expression plasmids encoding HA epitope tagged TRAF 2 and 6 were transfected into HEK293T cells together with reporter plasmids and either HIV-1 M Vpr as previously. 48 hours post transfection the cells were harvested for luminometry. Firefly luciferase activity was measured and normalised to the renilla luciferase activity. Data from three experiments are represented as the fold induction relative to an identical dose of activating molecule with an empty expression vector  $\pm$  SEM. The whole cell lysates were separated by SDS- PAGE and analysed by immunoblotting with anti-FLAG and anti-HA antibodies.

## **4 Chapter 4 - HIV Vpr non-specifically suppresses expression from co-transfected plasmids**

It was noticed in untransfected experimental controls that even without co-transfection of an NF $\kappa$ B signal activating molecule (e.g. IKK $\beta$ , TBK1 etc) one of the two Vprs from SIVmon (infecting the mona monkey species) specifically stimulated NF $\kappa$ B signalling ~100fold both with and without a FLAG epitope tag compared to empty vector (see chapter 5, figure 5.1). It was hypothesised that SIVmon Vpr could provide a useful reagent to determine putative interaction partners for HIV-1 M Vpr and the stimulation of NF $\kappa$ B signalling by SIVmon Vpr was characterized (see chapter 5). In the course of characterizing the SIVmon Vpr activation of NF $\kappa$ B it was determined that HIV-1 M Vpr was able to inhibit this NF $\kappa$ B signal and caused loss of SIVmon Vpr on immunoblot.

However whilst conducting these experiments it was noted that HIV-1 M Vpr additionally caused loss on immunoblot of two other Vprs, inactive for NF $\kappa$ B signalling: SIVgsn Vpr and SIVmon2 Vpr (figure 4.1A). Whilst loss of SIVmon Vpr could be hypothesised to be due to the degradation of a large signalling complex that it had joined, it seemed less probable that these inactive Vprs were part of the same signalling complex. This observation needed to be reconciled with the observation that HIV-1 M Vpr seemed able to specifically antagonise NF $\kappa$ B signalling from all co-transfected molecules. Indeed, the only signalling stimulus that had been tried which was not inhibited was TNF $\alpha$ , but this cytokine had been added to cells post transfection rather than being a cDNA transfected simultaneously with Vpr (figure 3.13 & 4.1B).

### **4.1 HIV-1 M Vpr antagonism of NF $\kappa$ B signalling requires transfection of the activating stimulus**

To test the hypothesis that the inhibition of the NF $\kappa$ B signal was a transfection dependent phenotype HEK293T cells were transfected with a plasmid encoding TNF $\alpha$  (figure 4.1B). This recapitulated the same pattern of inhibition across the panel of FLAG epitope tagged and untagged Vprs that was seen in figure 3.13. Thus, inhibition of signal appeared to be dependent on a property of the transfected plasmid rather than being dependent on the molecule encoded.

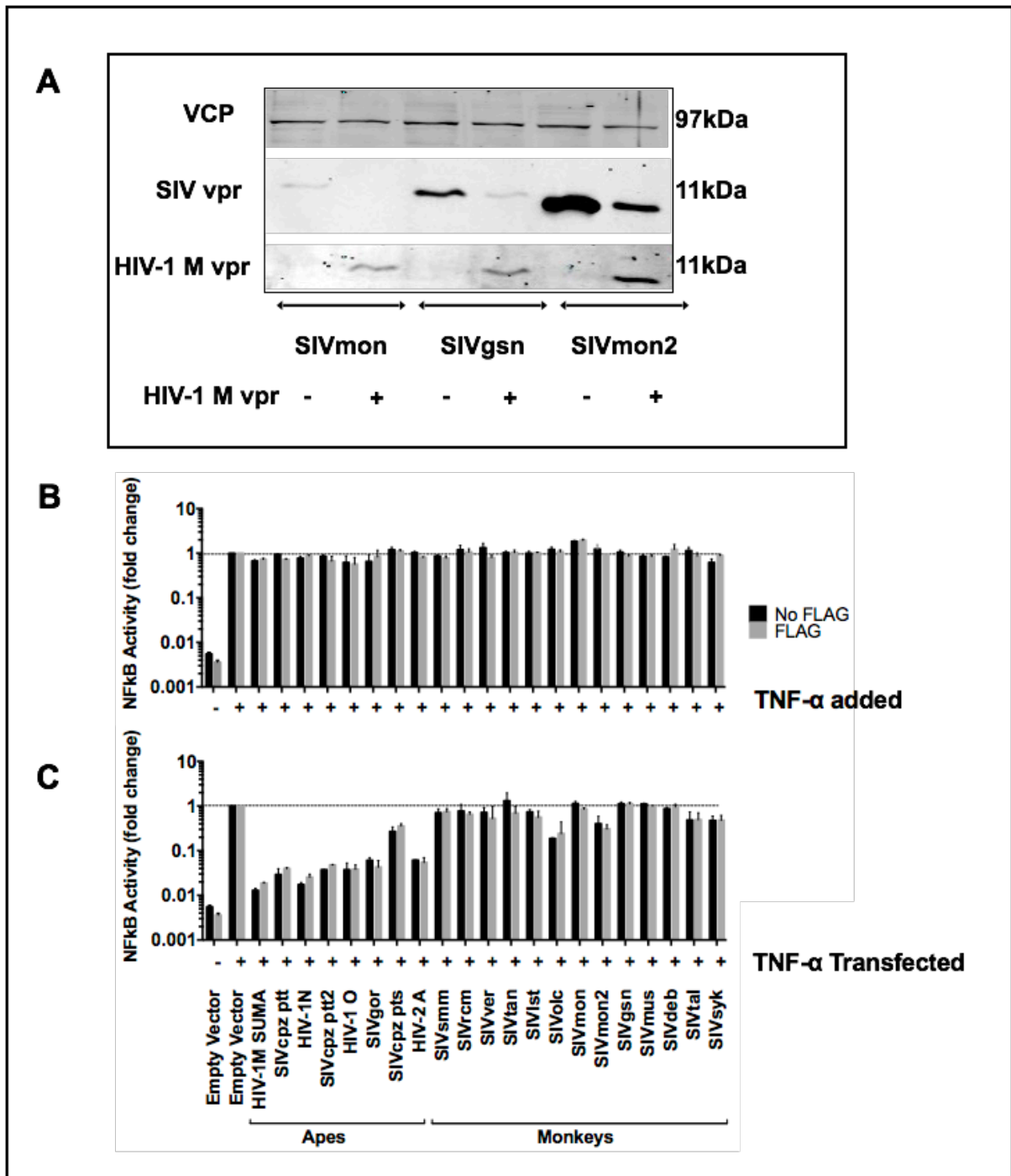


**Figure 4.1 Transfected HIV-1 M Vpr antagonises NF $\kappa$ B signalling depending on whether the activating molecule is added or transfected.** (A) FLAG tagged SIVmon group SIV Vprs were transfected with untagged HIV-1 M Vpr or empty vector. Cell lysates analysed by immunoblot with anti-FLAG anti-HIV-Vpr, for loading, anti-VCP. (B) NF $\kappa$ B signalling was stimulated as previously with added TNF $\alpha$  or with an expression plasmid for TNF $\alpha$  under the control of a CMV promoter and tested against the panel of tagged and untagged Vprs as used previously. The mean fold change in RLU (relative light units – firefly luciferase normalised to renilla) relative to a control with no Vpr (empty vector + cGAS:STING) is displayed. The mean values of three transfections  $\pm$ SEM are shown.

## 4.2 HIV-1 M Vpr inhibits expression from a co-transfected GFP encoding plasmid

To test whether only transfected molecules involved in innate immune signalling pathways showed reduced expression when co-transfected with HIV-1 Vpr, a pcDNA.3 expression vector (identical to the vector used for the Vprs) encoding GFP under the control of a CMV promoter was transfected. Both GFP positive cell number and mean fluorescence intensity were both significantly reduced at 48 hr post transfection (figure 4.2).

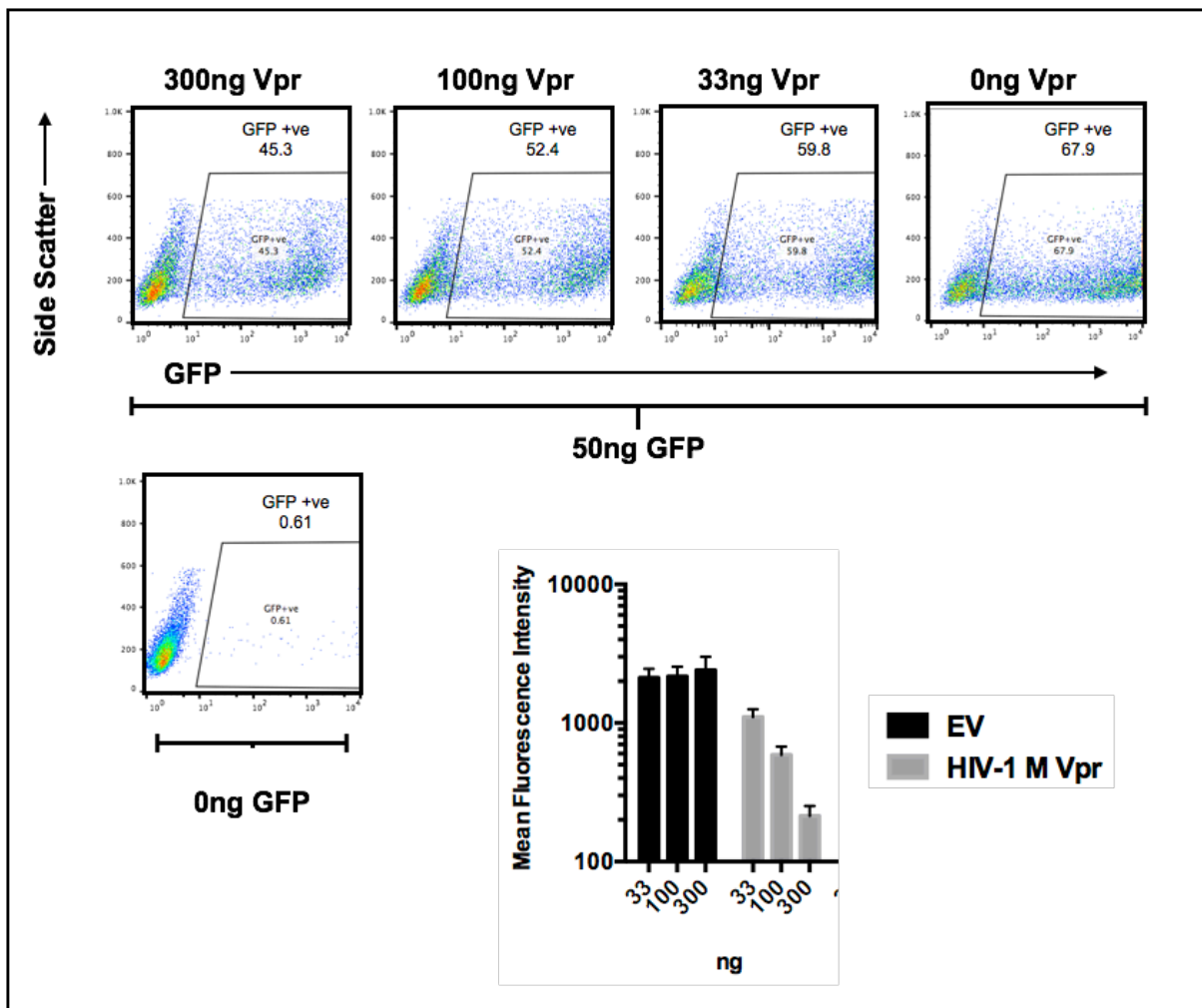


**Figure 4.2 HIV-1 M Vpr inhibits expression from a co-transfected plasmid encoding GFP driven by a CMV promoter.** HIV-1 M Vpr or empty vector was transfected from 0-300ng with a pcDNA.3 plasmid encoding GFP. 48 hours after transfection the cells were collected for and analysed by FACS. Data are from one representative experiment of two.

### **4.3 HIV-1 M Vpr inhibits mRNA expression from co-transfected cGAS and STING encoding plasmids.**

I hypothesised that rather than specifically inhibiting NFκB signalling pathways HIV-1M Vpr inhibited expression from the co-transfected activating plasmids possibly in a promoter dependent fashion. To confirm this effect of HIV-1 M Vpr on cGAS and STING mRNA levels was tested by qRT-PCR. HEK293T cells were transfected in triplicate in 48 well plates with a 5 fold dilution series of cGAS and STING plasmids in a 1:1 ratio between 0.01ng and 10ng and simultaneously transfected with either HIV-1M Vpr at a constant dose of 50ng or the same dose of an empty expression vector. For qRT-PCR analysis the cells were harvested 48hr post transfection, the RNA was extracted, cDNA was synthesized and used for qRT-PCR analysis using primers specific for human cGAS and STING. HIV-1 M Vpr reduced mRNA levels of cGAS and STING by >10 fold (figure 4.3 A and B).

To investigate the previously unexplained specificity for NFκB signalling (figure 3.12) qRT-PCR was also performed to measure transcription of ISG-56 mRNA. It was observed that maximal expression of ISG56 could be induced with between 0.4 and 2ng of cGAS/STING. Co-transfection of HIV-1M Vpr with 10ng of cGAS/STING reduced the cGAS and STING expression levels to the equivalent of 2ng of transfected plasmid i.e. still enough to maximally induce ISG56 (figure 4.3C). So even though the activating molecules (STING and cGAS) had reduced expression when co-expressed with Vpr, this was not detected by RT PCR for ISG mRNA or by the IRF3 sensitive ISG56 luciferase reporter construct.

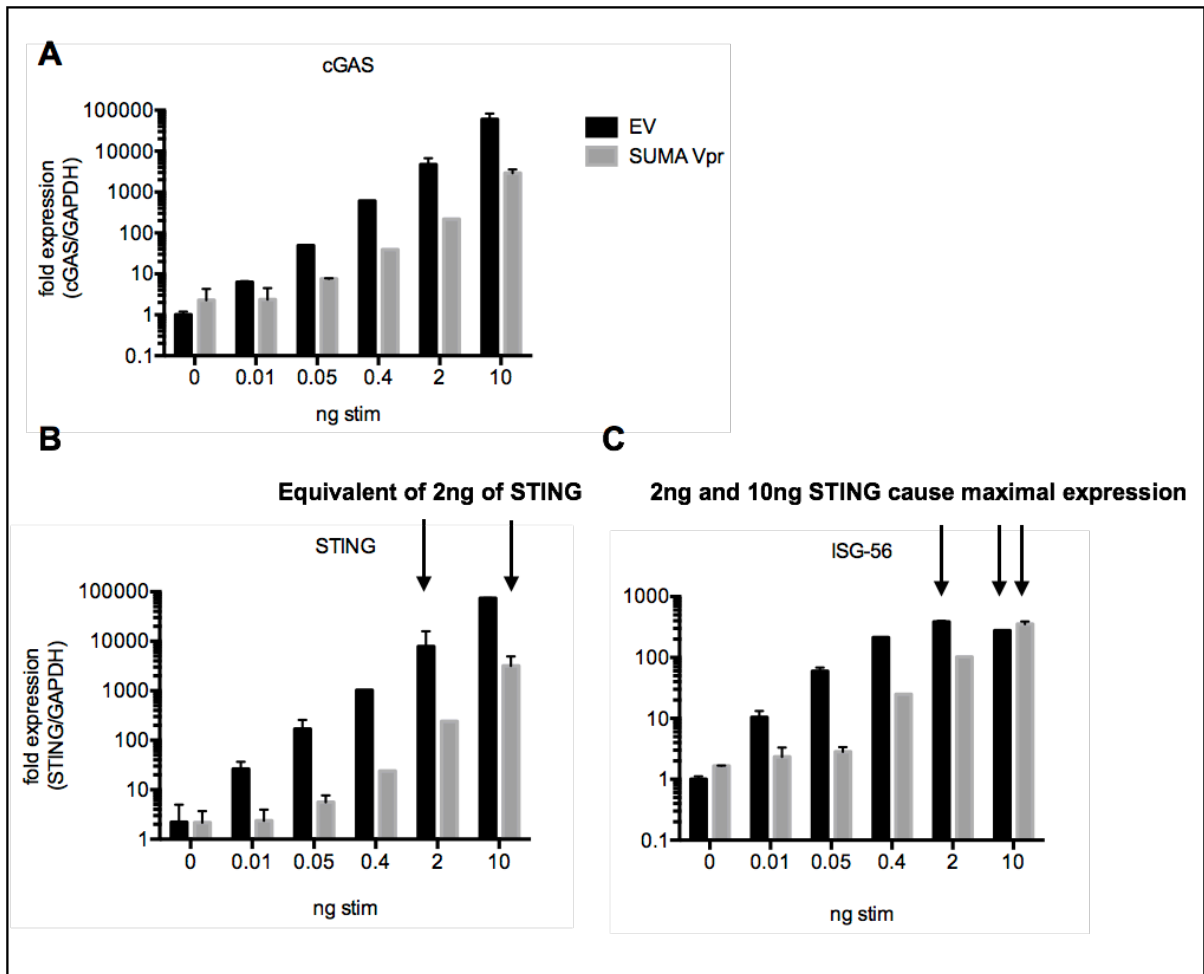


**Figure 4.3** HIV-1 M Vpr inhibits mRNA expression from co-transfected cGAS and STING. HEK293T cells were transfected in triplicate in 48-well plates with HIV-1 M Vpr at 50ng or empty vector control (EV) expression plasmid per well and increasing doses of cGAS and STING in a 1:1 ratio between 0.01ng and 10ng. After 48 hrs the cells were lysed and RNA was extracted from the cells, cDNA was synthesized and used for qRT-PCR analysis in duplicate using primers specific for human *cGAS*, *STING* and *ISG56*. Data are represented as mean  $\pm$  SD stimulation relative to sample one of the mock-treated EV control. Arrows indicate left to right i) mRNA level of 2ng transfected STING without Vpr ii) the level of STING mRNA detected when Vpr is transfected with STING iii) and iv) that 2ng and 10ng STING respectively stimulate ISG56 mRNA transcription to the same maximal level.

## **4.4 HIV-1 M Vpr inhibits luciferase expression from different promoter constructs**

To further investigate the effect of Vpr on co-transfected plasmids, site directed mutagenesis was used to create Q65R and F34I/P35N mutants of HIV-1M Vpr which have been reported previously as DCAF and cyclophilin binding mutants respectively. Neither have any effect on Vpr induced cell cycle arrest (431). Together with HIV-1 M Vpr (from the SUMA clonal isolate) these were tested against a variety of reporter constructs with differing promoters.

All the pathway activating proteins in these studies were expressed from a pcDNA.3 expression vector i.e. under the control of a CMV promoter. A report by Liu et al in 2015 indicated that Vpr could have a slight inhibitory effect on expression of GFP from a CMV promoter (492). They found that there was no defect in this inhibition using the Q65R binding mutant or in cells depleted of DCAF using RNAi. They also found that the proteasome inhibitor MG132 did not alter the efficiency of Vpr inhibition. They did not test transfected plasmids with expression from other promoters.

I confirmed dose dependent inhibition of expression of luciferase from CMV promoters with constructs expressing both firefly and renilla luciferase over a titration series (figure 4.4 A&B). The CMV promoter contains multiple transcription factor binding sites; two AP2, AP1, four NF- $\kappa$ B, and five CREB binding sites, SP1 (Promega) (553).

The Q65R mutant did retain some ability to antagonise signalling but also demonstrated greater expression on immunoblot at a lower dosage – putatively due to reduced degradation. If normalised to expression level the DCAF mutant is a less effective antagonist. The F34i, P35N mutant showed markedly reduced inhibition.

Immunoblot confirmed greater levels of the expressed mutant Vprs. This is likely due to reduced auto-inhibition of the transfected plasmid (figure 4.4C). The greater the antagonism of the reporter the greater the antagonism of expression of Vpr itself.

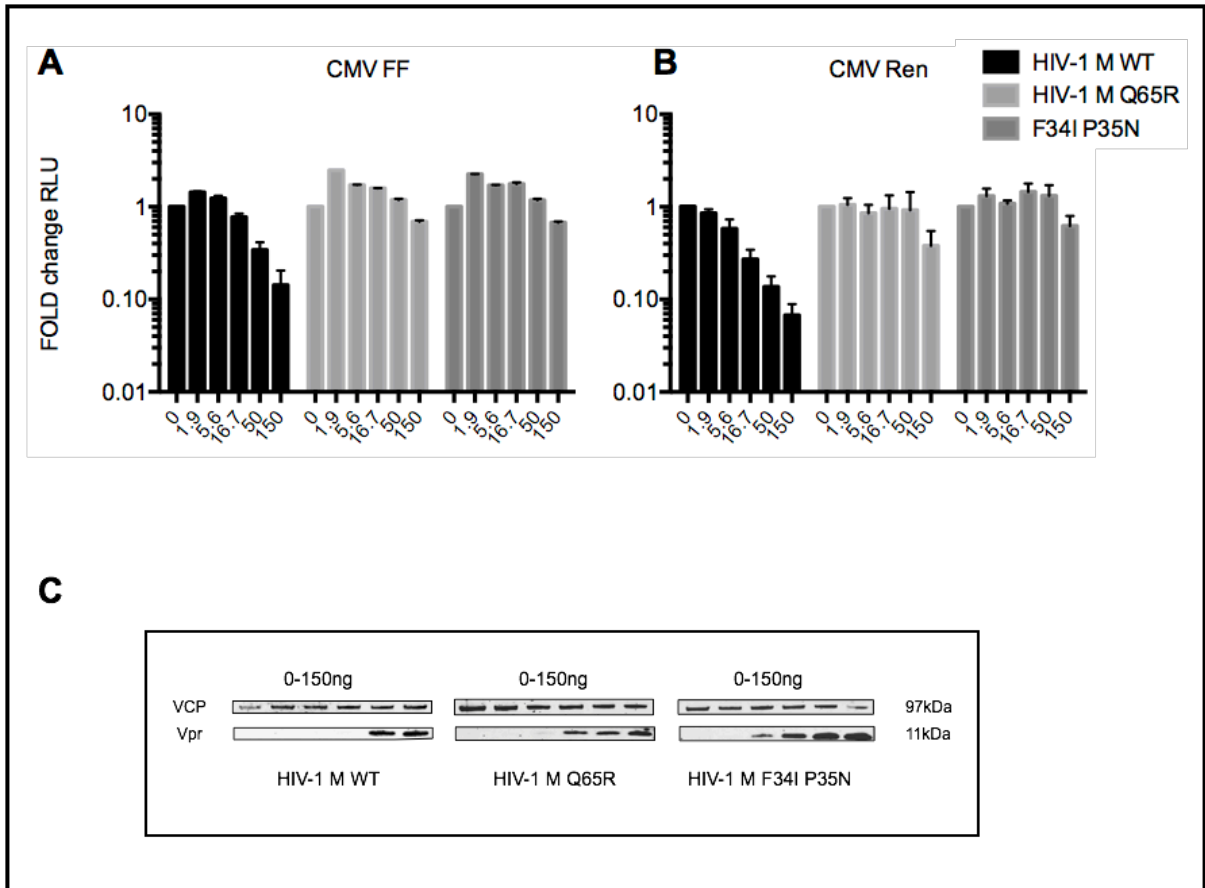


**Figure 4.4 HIV-1 M Vpr inhibits expression from the CMV promoter.** HEK293T cells were transfected with increasing doses of HIV-1 M Vpr WT or Q65R or F34I/P35N mutants together with 2.5ng of (A) CMV firefly or (B) renilla reporter constructs. Cell lysates were analysed by luminometry at 48hrs. Data are represented as mean  $\pm$  SEM stimulation relative to sample one of the mock-treated EV control. (C) 48 hours after transfection cell lysates were analysed by immunoblotting with anti-FLAG anti-HIV-Vpr, and for the loading control anti-VCP.

## 4.5 HIV-1 M Vpr inhibits expression from a panel of viral promoters

Further viral promoter constructs were then tested including the HSV TK (Herpes Simplex Virus Thymidine Kinase) promoter; the M5P LTR (from Murine Leukaemia virus); the SFFV (spleen focus forming virus ) promoter and the SV40 (Simian vacuolating virus 40) promoters (figure 4.5 A, B, C&D respectively). The same patterns of inhibition were seen as with the CMV promoters. The HSV-1 *thymidine kinase* promoter binds Sp1, CCAAT-enhancer-binding proteins CCAAT-TF (C/EBPs) (554,555). The Simian vacuolating virus 40 (SV40) promoter binds SP1, AP1 and AP2 (Promgea) (553,556). The Spleen focus-forming virus (SFFV) promoter and the M5P promoter are both from murine leukaemia viruses; since gene transfer vectors derived from the Moloney murine leukemia virus (MLV) have been used in gene therapy clinical trials since 1991 (557) these promoters are well characterized. Multiple members of the Ets family of transcription factors bind to two sites and the core-binding factor (CBF) is a heterodimeric binding protein that recognizes the enhancer core region (558,559). I confirmed dose dependent inhibition of expression of luciferase from all these plasmids including the TK renilla plasmid used previously as a control. I had not observed an effect on the renilla previously as the control dose used (7.5ng) was much higher than the dose tested here (2.5ng) and so the effect was minimalized. Also intital experiments optimizing the assay had used the poorly expressed Blue Heron Bio codon optimized HIV-1M YU2 Vpr.

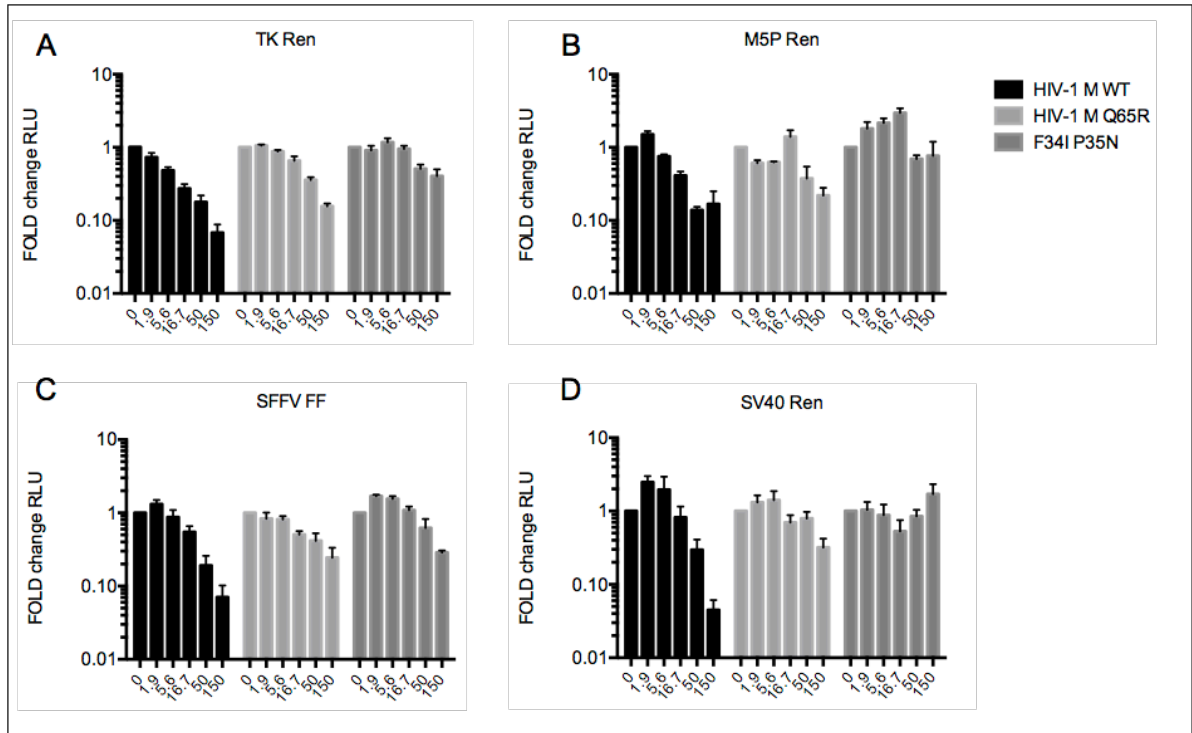


**Figure 4.5** HIV-1 M Vpr inhibits expression from a panel of viral promoters. HEK293T cells were transfected increasing doses of HIV-1 M Vpr, its Q65R mutant or the F34I/P35N double mutant with firefly or renilla reporter constructs with 2.5ng of (A) HSV TK, (B) MLV LTR (M5P), (C) SFFV or (D) SV40 promoters. Data are represented as mean  $\pm$  SEM stimulation relative to sample one of the mock-treated EV control.

## 4.6 HIV-1 M Vpr inhibits expression from two human promoters

To test whether viral promoters were specifically inhibited human promoters for IgK and Ubiquitin B were tested and the same pattern of inhibition was observed (figure 4.6 A&B). The natural promoter of the *immunoglobulin kappa light chain* gene sensitive to NF $\kappa$ B subunits p50 and p65 contains three repeat kB sequences. The binding sequence is 5'-GGGRNYYYCC-3' (where R is a purine, Y is a pyrimidine, and N is an unspecified base). (personal communication Andrew McDonalds, (519–521). The SFXU construct with a Ubiquitin B promoter has binding sites for HSF, NF $\kappa$ B, AP-1(c-jun), NF-IL6 and Sp1 CEBP/B, CREB, GATA-2 and Sp1(560,561).

With such a diverse range of transcriptional activators required across these promoters I hypothesised that this indicated that inhibition of expression is a feature of transfection rather than being promoter dependent.

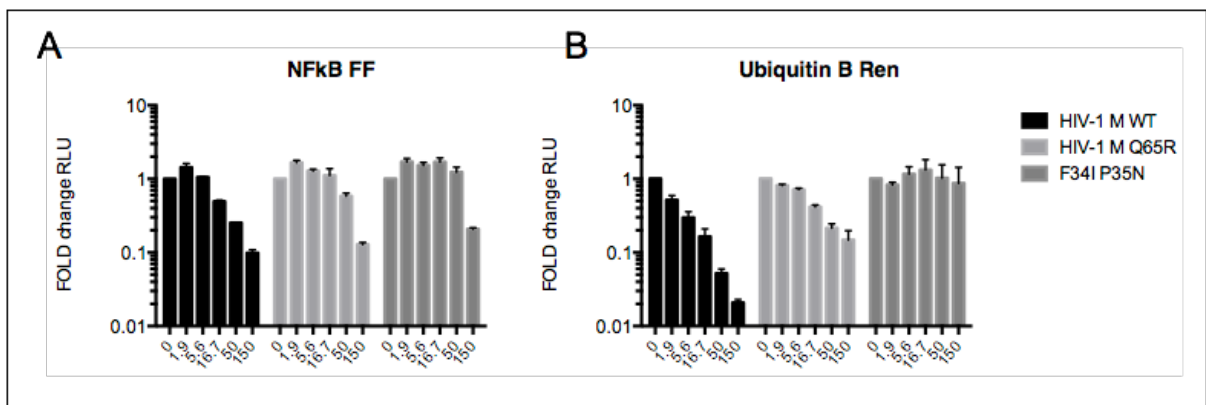


**Figure 4.6 HIV-1 M Vpr inhibits expression from two human promoters.** HEK293T cells were transfected with a 5 point dilution series of HIV-1 M Vpr, its Q65R mutant or the F34I/P35N double mutant together with constant doses of with firefly or renilla reporter constructs with either the human (A) IgK or (B) Ubiquitin B promoters. Data are represented as mean  $\pm$  SEM stimulation relative to sample one of the mock-treated EV control.

## 4.7 HIV-1 M Vpr inhibits expression from a transfected NF $\kappa$ B promoter but not from the same promoter when it is integrated into the cell genome using a retrovirus

Background luciferase expression from an integrated reporter in HEK293Ts is unaffected by HIV-1 M Vpr. However, when the NF $\kappa$ B sensitive reporter plasmid with the same promoter region is co-transfected with HIV-1 Vpr in the absence of any NF $\kappa$ B activating stimulus the background expression of luciferase is inhibited >10fold providing further evidence of a transfection specific inhibition (figure 4.7). The dose of the reporter plasmid was adjusted so that the basal expression level was the same as the integrated reporter. This provides evidence that there is not a detectable effect of Vpr on basal NF $\kappa$ B activity but rather the effect is on transfected plasmids irrespective of promoter or expressed gene.

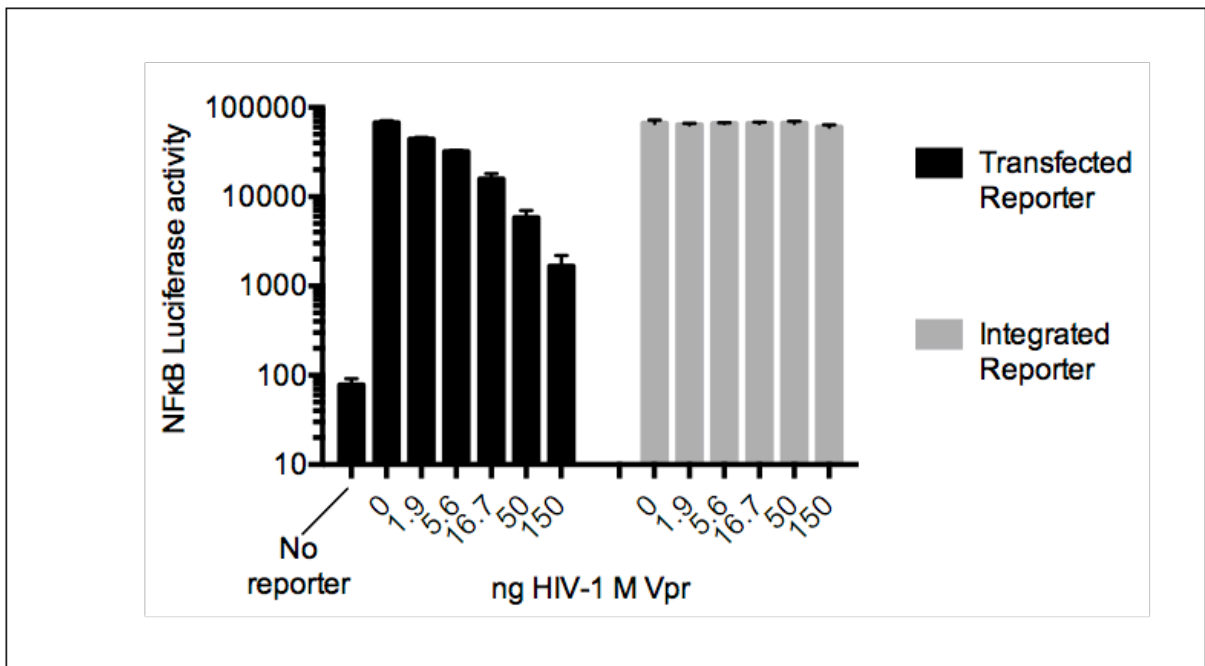


**Figure 4.7 HIV-1 M Vpr inhibits unactivated expression of a transfected NF $\kappa$ B promoter but not from the same integrated promoter** HEK293T cells or HEK293T-Luc cells (with an integrated NF $\kappa$ B sensitive luciferase reporter) were transfected with a 5 point dilution series of HIV-1 M Vpr. The cells without an integrated reporter were also transfected with a dose of NF $\kappa$ B sensitive luciferase reporter plasmid. Cells were harvested for luminometry at 48hrs. Data are represented as mean  $\pm$  SEM stimulation relative to sample one of the mock-treated EV control

## 4.8 Nuclear localisation and inhibition of expression

Previous observations have shown that Vpr localizes to the nuclear rim although the details of the pathway and interacting partners for this localisation have not been described (476,478,562). In order to investigate the relationship between intracellular localisation and the inhibition of expression from co-transfected plasmids immunofluorescence confocal microscopy was used to measure nuclear rim localisation of HIV-1 M Vpr. I found minimal cytoplasmic or intranuclear expression (figure 4.8A). HEK293T cells were fixed and stained for imaging at 48hrs post transfection. While the wild type HIV-1M Vpr localized to the nuclear rim, by contrast the Q65R and F34I/P35N mutants showed expression in both nuclear and cytoplasmic regions on cross-sectional images indicating that Vpr induced inhibition of expression from transfected plasmids may be dependent on nuclear rim localisation (figure 4.8 B&C). Further evidence for this was provided by work done with a collaborator in our lab (Hataf Khan – PhD student) who showed that the phenotype of inhibition of expression from co-transfected plasmids correlated exactly with nuclear rim localisation (table 4.1). A table of phenotypes associated with Vpr mutants is provided on page 150 (table 4.2).

Vpr residue	Nuclear rim localisation	Inhibition
WT	Yes	Yes
A30S	Yes	Yes
V31S	Yes	Yes
A30S+V31S	Yes	Yes
F34I	No	No
P35N	No	No
F34I+P35N	No	No
W54R	Yes	Yes
Q65R	No	No
H71R	No	No
R73S	Yes	Yes
S79A	Yes	Yes
R80A	Yes	Yes
R90A	Yes	Yes

**Table 4.1** Correlation between rim localisation and inhibition of expression – work on mutants other than HIV-1 M Vpr WT, and the two mutants Q65R and F34I/P35N was undertaken by H. Khan.

Vpr residue	Biological Function	Inhibition
F34	Importin alpha interaction (563)	No
P35	Cyclophilin interaction (411)	No
W54	UNG2 interaction (509)	Not tested
Q65	DCAF1 complex recruitment (370)	No
H71	Dimer formation (563)	No
R73	LTR transcription(564)	Yes
S79	TAK1 interaction (565)	Yes
R80	Cell cycle mutant (431)	Yes
R90	Vpr suppression of IL-12 in DC (566)	Yes
WT		Yes

**Table 4.2** Vpr mutant phenotypes

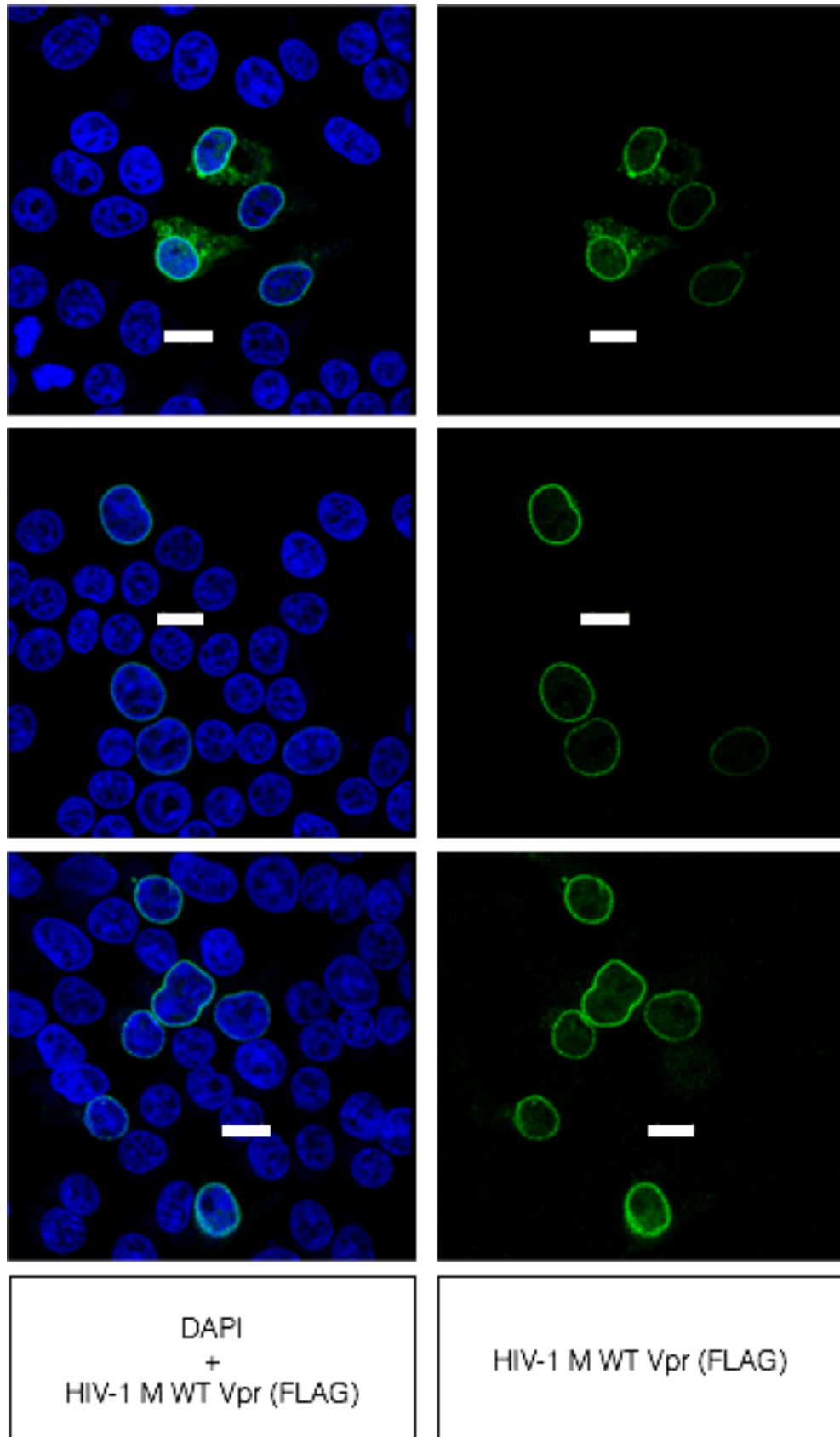


Fig 4.8 A Transfected HIV-1 M Vpr localises to the nuclear rim in HEK293T cells

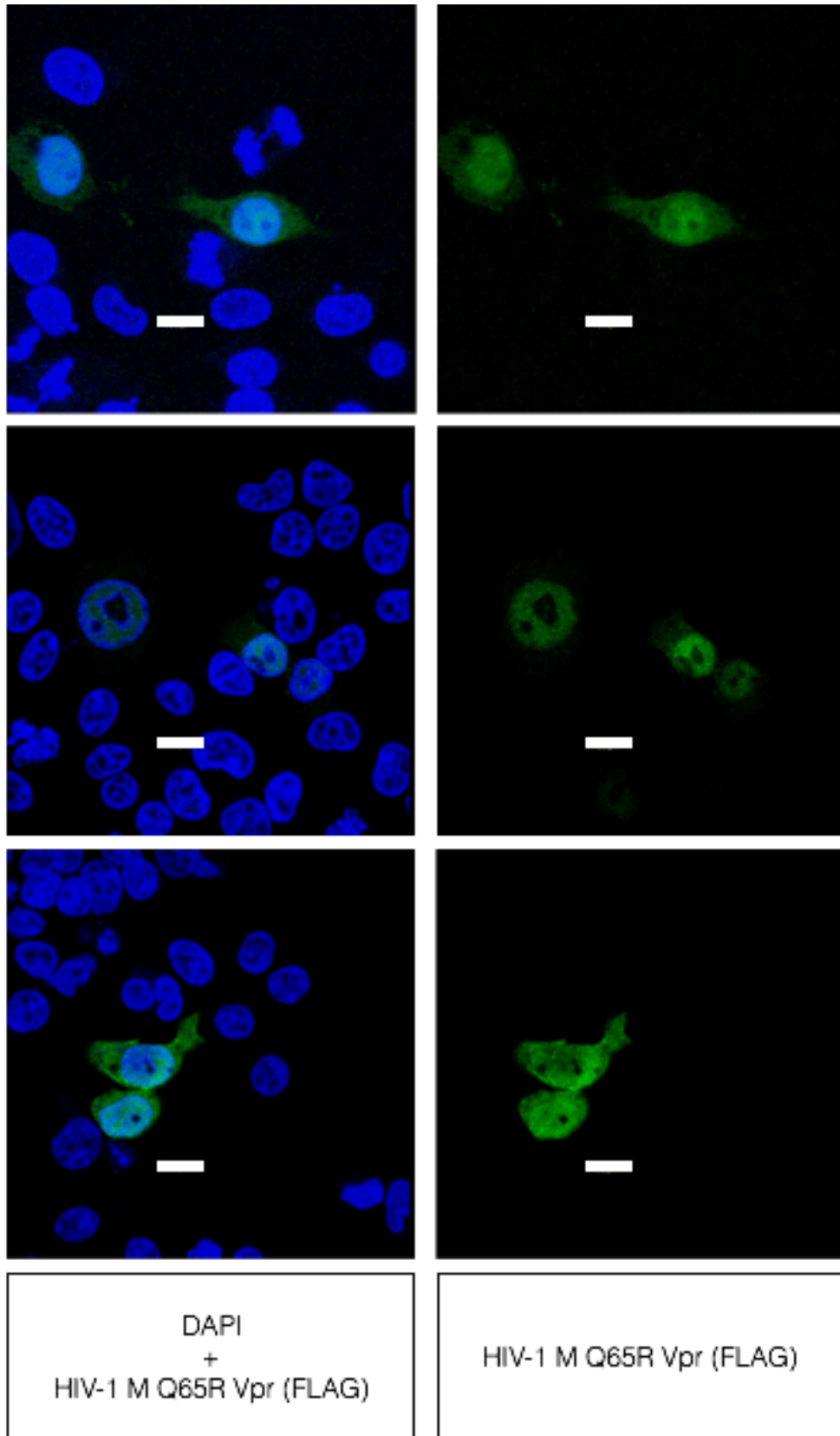
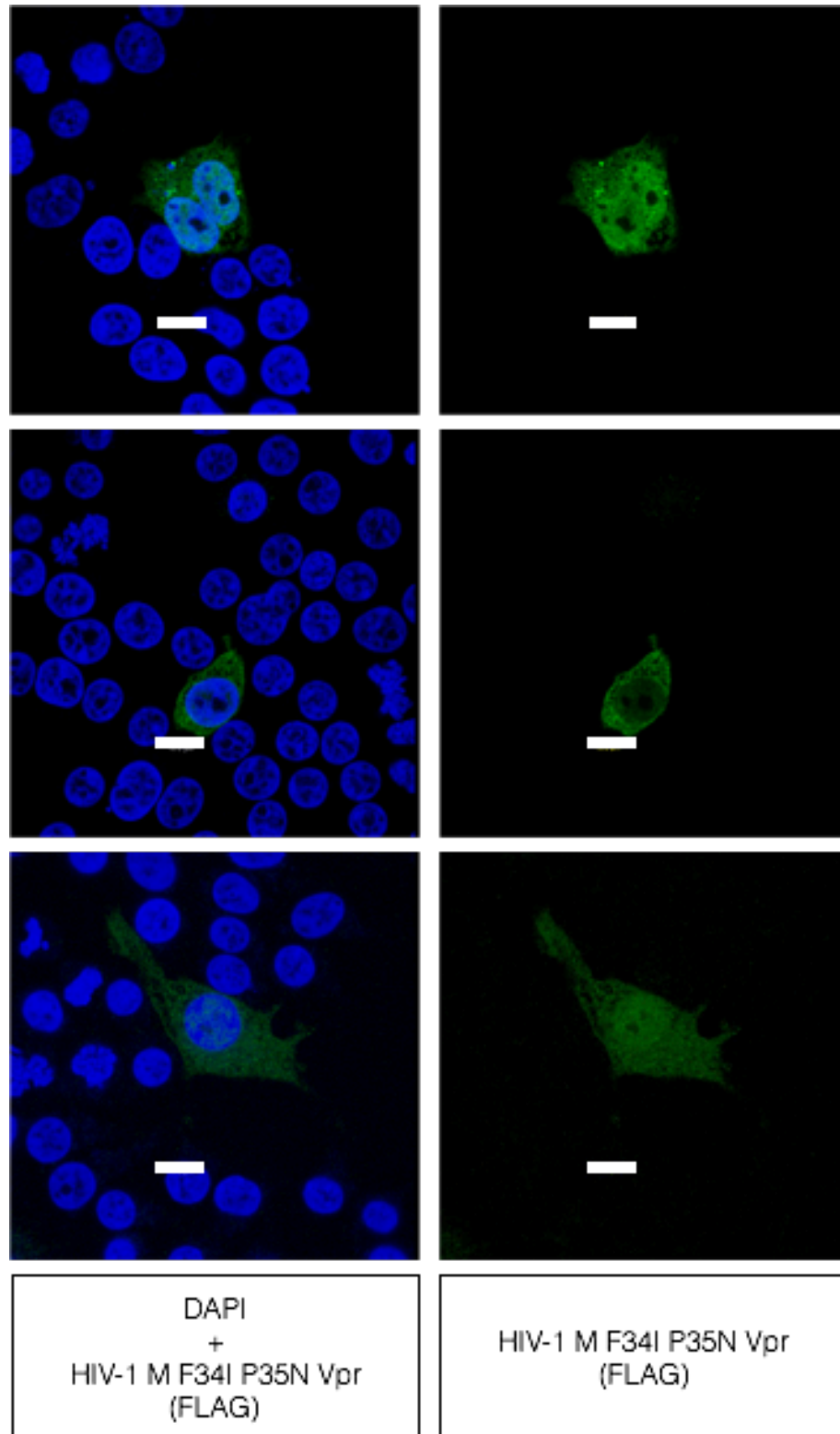


Fig 4.8 B Transfected HIV-1 M Vpr Q65R mutant does not localise to the nuclear rim in HEK293T cells



**Figure 4.8 C Localisation of Vpr and mutants** HEK293T cells were transfected with HIV-1 M Vpr (A), its Q65R mutant (B) or the F34I/P35N double mutant (C). Cells were then fixed, permeabilised and stained for FLAG epitope tags and with DAPI nuclear stain. Confocal microscopy was used to analyse the localisation of Vpr in these cells. White lines indicate scale (10  $\mu$ M).

## **4.9 Visualisation of co-transfected stained expression vector**

Following these observations, I hypothesised that Vpr may be creating a block to nuclear entry by either 1) binding the cyclophilin domain of Nup358 through its cyclophilin binding domain or 2) binding another region of the nuclear pore complex or 3) binding the nuclear envelope. To investigate whether expression of Vpr altered the intracellular localisation of transfected plasmids a GFP encoding pcDNA.3 plasmid was labelled with LabelIT intracellular nucleic acid tracker Cy5 and was co transfected into HEK293T cells with HIV-1M Vpr or empty vector. Stained plasmid localisation and GFP expression were visualised using the automated WiScan Hermes high resolution microscopy platform.

The cells expressing Vpr showed a reduction in GFP expression as expected: both the number of green cells and the mean fluorescence intensity of those cells were reduced at 48hrs in cells. Stained plasmid was clearly visualized (figure 4.9). The images show that whilst every cell contains stained plasmid DNA not every cell is expressing GFP. This is consistent with the notion that the rate limiting step in expression from transfected plasmids is nuclear entry and raises the possibility that Vpr is manipulating this step.

It was not possible to quantitatively detect changes in cytoplasmic or nuclear plasmid localisation due to lack of resolution – plasmid at the edge of the nucleus could not be distinguished from plasmid inside the nucleus. Additionally, since the automated platform is not confocal and cross-sectional imaging is not possible. Since the cells used are more disc-like than sphere-like it was assumed that stained plasmid over lying the nucleus would be inside it but this would need to be confirmed using confocal microscopy.

The quantity of plasmid DNA required to express visible GFP may be invisible to detection using this microscope and there may be more appropriate techniques to visualize specific sequences (like fluorescence in-situ hybridization (FISH)) that could be combined with immunofluorescence and depletion of nuclear rim proteins to test the hypothesis that Vpr prevents nuclear entry of transfected plasmid DNA (see discussion chapter 6.1.1).

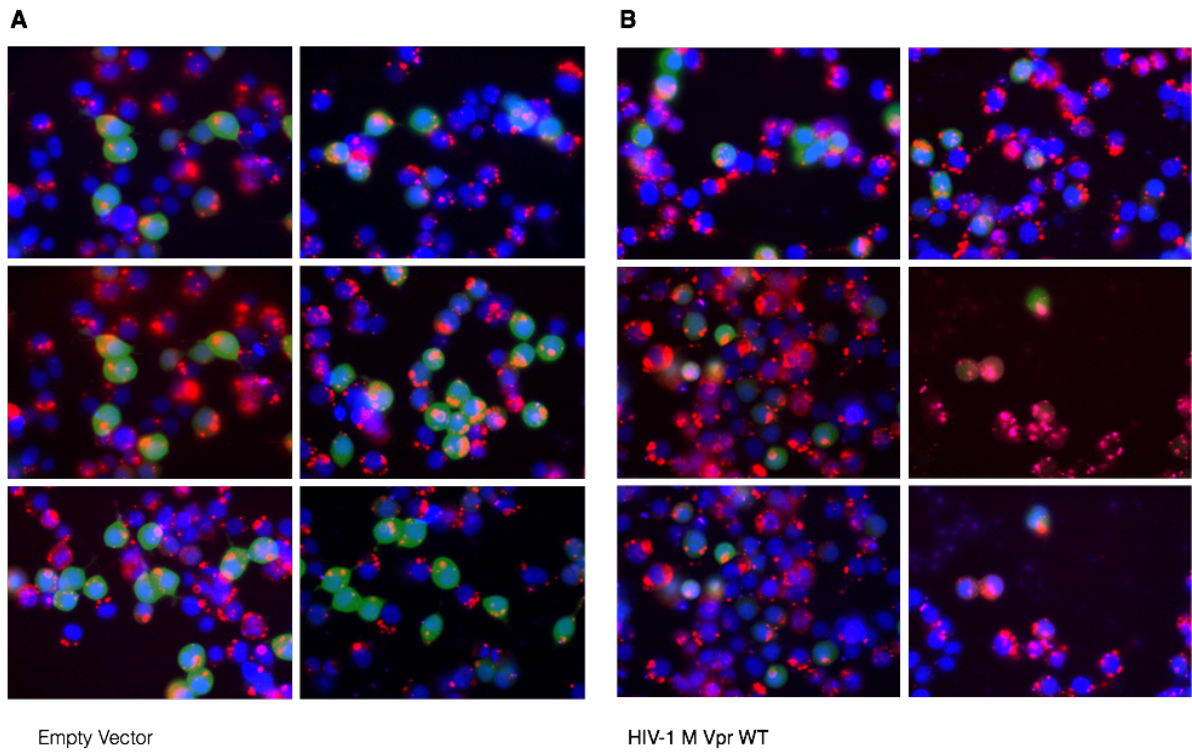


**Figure 4.9 Transfected HIV-1 M Vpr with Label-IT stained GFP expression vector.** HEK293T cells were transfected overnight with a plasmid expressing empty vector (A) or HIV-1 M Vpr (B) at 150ng/well. 50ng of a plasmid encoding GFP, labelled with Rhodamine Cx, was simultaneously transfected. At 48hrs post transfection cells were then fixed and stained with DAPI nuclear dye. The localisation of GFP (green), nuclear DNA (blue) and stained plasmids (red) is shown.

## **4.10 Transfected HIV-1 M Vpr antagonises NF $\kappa$ B luciferase expression stimulated by added TNF $\alpha$ at an integrated reporter**

Intriguingly, a final experiment did show HIV-1 M Vpr inhibition of expression from an integrated NF $\kappa$ B sensitive luciferase reporter. Soluble TNF $\alpha$  (rather than transfected plasmid encoding TNF $\alpha$ ) was used to activate the same integrated NF $\kappa$ B sensitive promoter as used figure 4.7. Vpr was transfected 24hrs prior to addition of TNF $\alpha$ .

Luciferase expression stimulated by TNF $\alpha$  was antagonised up to 5 fold over a titration series and this inhibition of signal was diminished with the Q65R DCAF mutant and the F34I/P35N cyclophilin mutant (figure 4.10). This antagonism was not observed previously (in figure 3.13 E) most likely because the doses of both soluble TNF $\alpha$  stimulation and NF $\kappa$ B reporter were too high to detect any antagonism.

This assay, measuring the effect of Vpr on an NF $\kappa$ B signaling induced by a soluble cytokine at an integrated reporter may be more physiologically relevant than the assays measuring the effect on expression from co-transfected plasmids - in the body soluble cytokines initiate signaling cascades but there is no known physiological process closely equivalent to transfection. However, since the effect of Vpr on integrated NF $\kappa$ B reporter activity stimulated by soluble TNF $\alpha$  is abrogated in the same way by the Q65R and F34I/P35N mutants as the effect on expression from co-transfected plasmids, I hypothesise that both effects are mediated by the same mechanism – putatively through the regulation of nuclear import by Vpr (see discussion chapter 6).

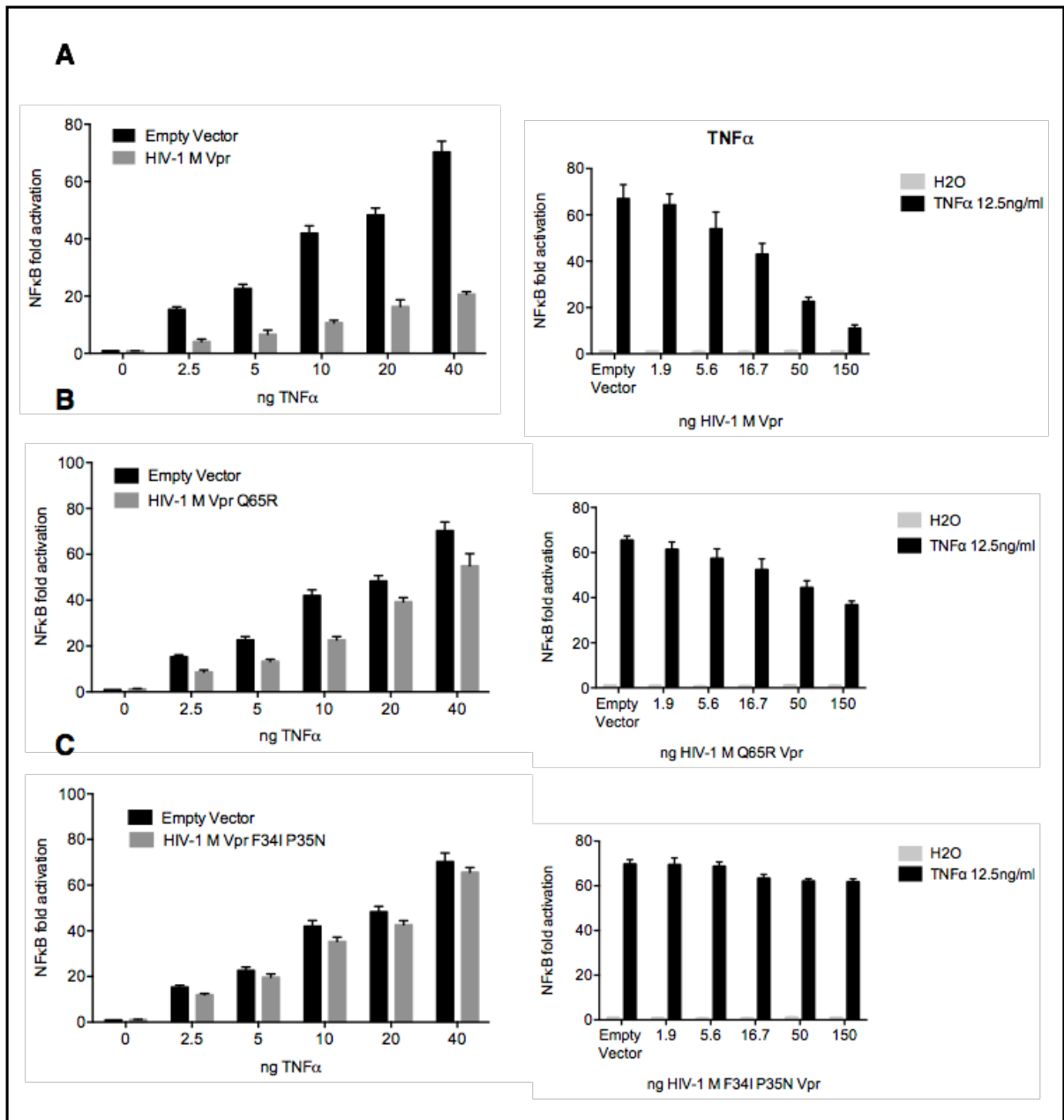


**Figure 4.10 Transfected HIV-1 M Vpr antagonises NFκB luciferase expression stimulated by added TNFα at an integrated reporter.** NFκB signalling in HEK293T-Luc cells (with an integrated NFκB sensitive luciferase reporter) was activated with a dilution series of added TNFα with a constant dose of Vpr (left column) or a constant dose of TNFα, with a dilution series of Vpr (right column). HIV-1 M WT (A), Q65R (B) and (C) F34i/P35N were tested. Data are represented as mean ± SEM stimulation relative to sample one of the mock-treated EV control.

## **5 Chapter 5: Characterisation of SIVmon (mona monkey) Vpr to identify determinants of block to sensing**

### **5.1 SIVmon Vpr activates NF $\kappa$ B signalling**

In experiments using the panel of primate species' Vprs it was noticed in the untransfected experimental control wells that even without co-transfection of an NF $\kappa$ B signal activating molecule (e.g. cGAS/STING, IKKB, TBK1 etc) one of the two Vprs from the mona monkey stimulated luciferase expression driven by an NF $\kappa$ B sensitive promoter ~100 fold compared to empty vector. This stimulation was unaffected by an N-terminal FLAG epitope tag (figure 5.1).

Prior to the characterization of HIV-1 M Vpr's inhibitory effects on transcription from all tested transfected plasmids I hypothesised that SIVmon Vpr may be activating the NF $\kappa$ B signalling pathway by joining the same cellular signalling complex as the HIV-1 M Vpr but activating it rather than inhibiting it. I sought to characterize this stimulatory activity of SIVmon Vpr to see if it could provide a useful experimental reagent to better understand NF $\kappa$ B signalling and Vpr antagonism, and to help identify binding partners.

These studies on SIVmon Vpr were started prior to determining the effect of HIV-1 M Vpr on transcription. Their relevance to illuminating our understanding of the function and mechanism of HIV Vpr is perhaps less clear but since there seems to be a true effect on NF $\kappa$ B signalling as well as suppression of transfected NF $\kappa$ B activation molecule expression, SIVmon Vpr may yet prove useful as an experimental reagent both for understanding HIV-1 M Vpr and for understanding NF $\kappa$ B signalling.

Previous studies have used tandem affinity purification to identify SAMHD1 and SLX4 as a binding partner for Vpr but since the HEK293T cells seem to constitutively lack many of the putative binding partners involved in the inhibition of NF $\kappa$ B signalling (i.e. the co-transfected molecules that show reduced expression on immunoblot when co-transfected with HIV-1 M Vpr) this technique seemed unlikely to be successful in this cell line (438).

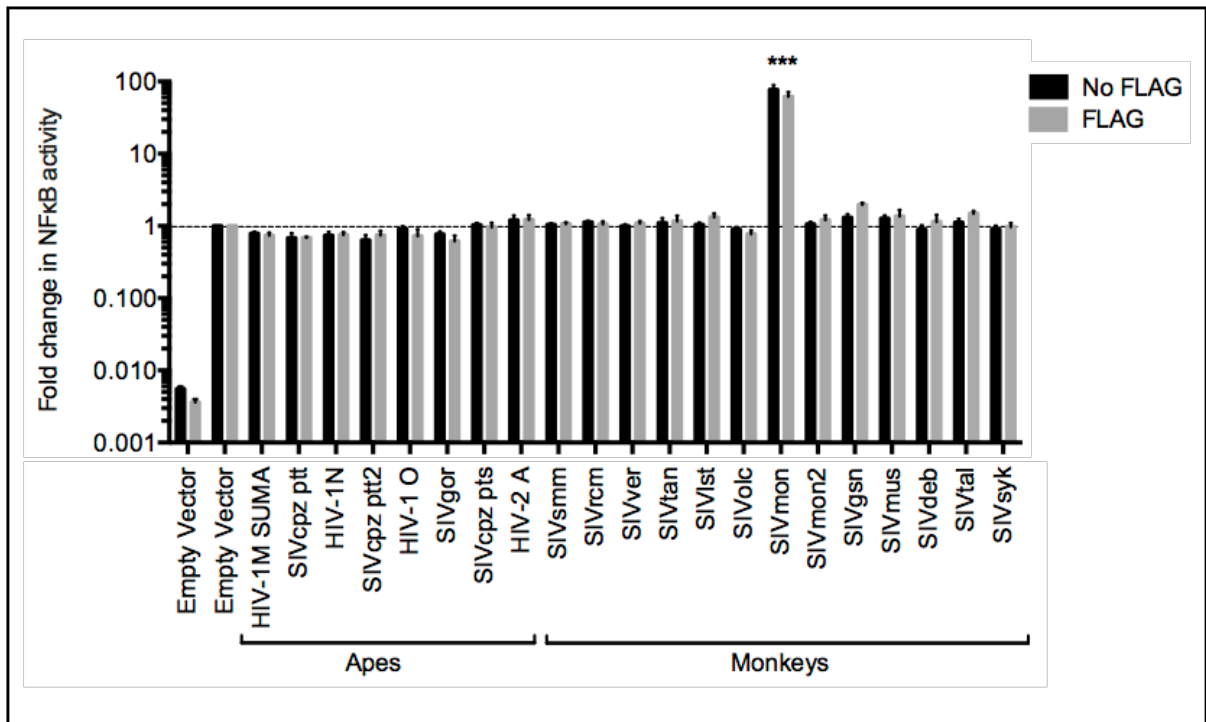


**Figure 5.1 SIVmon Vpr stimulates an NFκB sensitive promoter luciferase construct in the absence of transfected innate immune molecules** HEK293T cells were transfected as previously with expression plasmids for Vpr and two reporter plasmids (sensitive to NFκB and constitutively expressed respectively). Cells were harvested for luminometry at 48hrs. Firefly luciferase activity was measured and normalised to the renilla luciferase activity. Data are presented as the fold induction relative to an identical dose an empty expression vector. The mean values of three transfections ±SEM are shown. \*\*\*=P<0.001 one-way ANOVA with Dunnett's post-hoc test.

## **5.2 SIVmon Vpr expression activates a co-transfected NF $\kappa$ B reporter and SIVmon Vpr expression is suppressed by co-transfection of HIV-1M Vpr**

A three-fold dilution series of SIVmon Vpr with only reporter plasmids indicated SIVmon Vpr robustly stimulated signalling from the NF $\kappa$ B sensitive reporter but in a non dose dependent fashion with 1.9ng activating the pathway more than 150ng (figure 5.2A). This is not unusual for signalling activation and may imply that over-expression titrates a signalling molecules out of a complex leading to reduced activation (567,568). As with other stimulatory molecules SIVmon Vpr showed reduced expression on immunoblot and inhibition of the NF $\kappa$ B signal with addition of increasing doses of HIV-1 M Vpr (figure 5.2B). Prior to the realization that HIV-1 M Vpr inhibits expression from all co-transfected plasmids this was interpreted as a potential indication of an effect on a common pathway. In fact, expression of SIVmon Vpr was being inhibited in the same way as the plasmids in chapters 3 and 4.

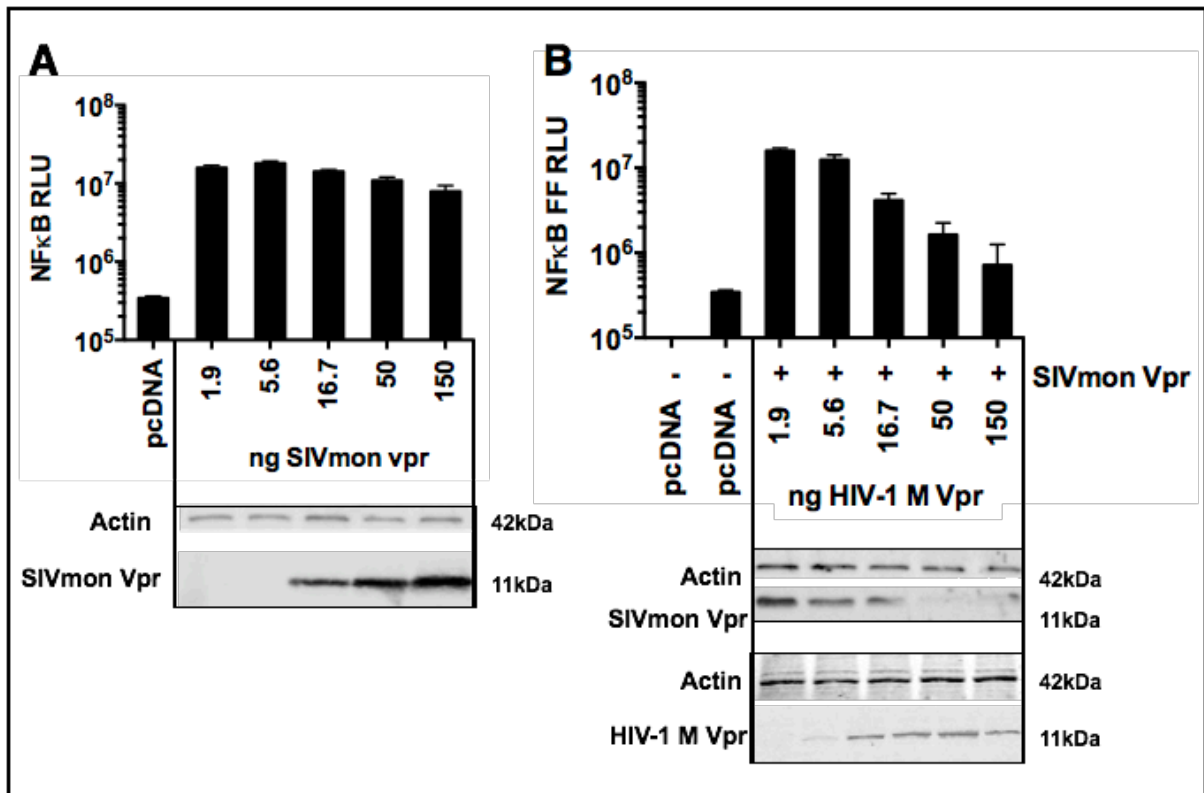


**Figure 5.2 Ectopic expression of SIVmon Vpr activates a co-transfected NFκB reporter and is inhibited by co-transfection of HIV-1M Vpr.** (A) SIVmon Vpr was transfected in a five point dilution series together with luciferase reporters. (B) SIVmon Vpr was transfected at a constant dose of 5.6ng and HIV-1M Vpr was added in a five point three fold dilution series. 48 hours after transfection the cells were harvested for luminometry. Firefly luciferase activity was measured and normalised to the renilla luciferase activity. Data from three experiments are represented as the fold induction relative to an identical dose of activating molecule with an empty expression vector  $\pm$  SEM. Cell lysates were analysed by immunoblot with anti-FLAG antibodies and actin as a loading control.

### 5.3 SIVmon Vpr activates NFκB signalling from an integrated reporter

To investigate whether the stimulatory activity of SIVmon Vpr was an effect confined to transfected reporter plasmids a HEK293T cell line was transduced with VSV-G pseudotyped lentiviral particles with a reporter encoding for a mammalian codon-optimized, non-secreted form of the firefly luciferase under the control of a minimal CMV promoter and tandem repeats of the NFκB transcriptional response element (TRE) i.e. the same promoter used in the transfected reporter plasmids. Here the activation of NFκB signalling by SIVmon Vpr was linearly dose dependent compared to the transfection where an attenuation of signal was seen at higher doses indicating possible antagonism of expression from a co-transfected plasmid by SIVmon Vpr. HIV-1 M Vpr did not affect basal NFκB signal whereas co-transfected cGAS and STING acting as a positive control activated the pathway as in figure 4.7.

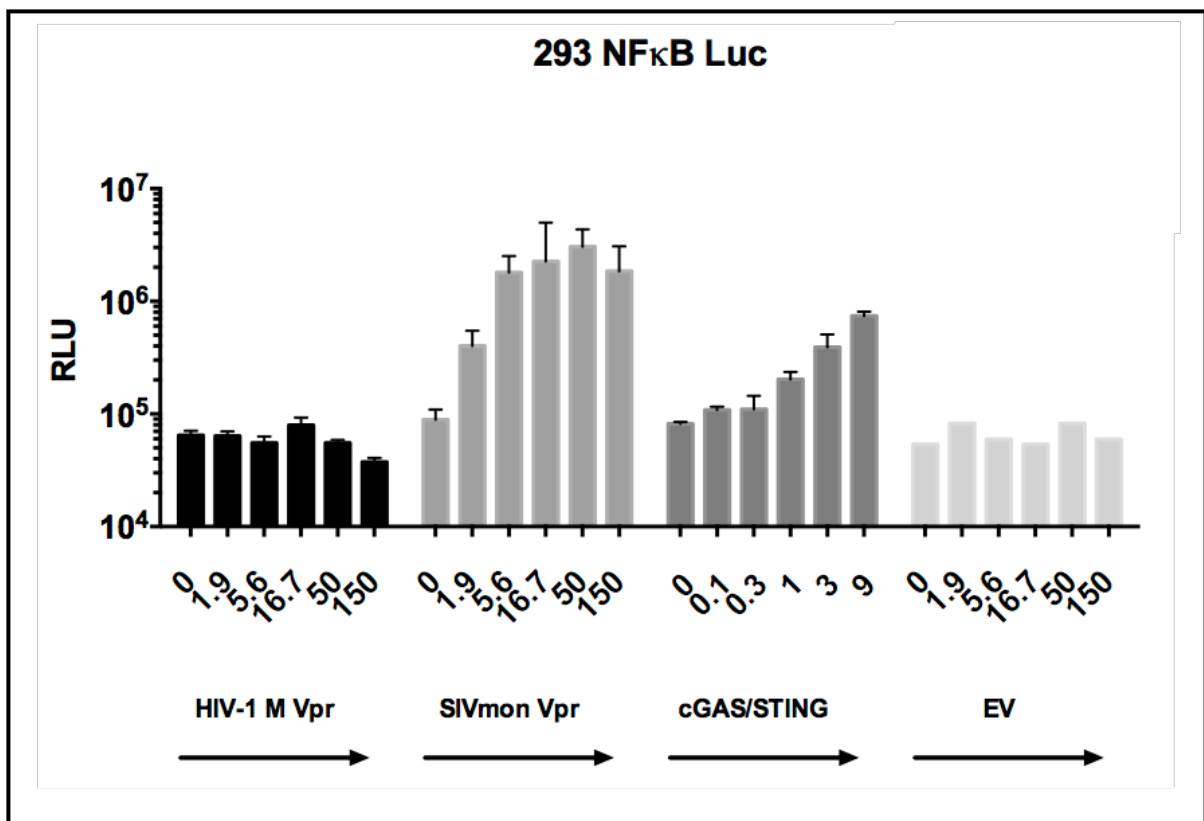


**Figure 5.3 SIVmon Vpr activates expression from an integrated NFκB sensitive luciferase reporter** HEK293T cells with an integrated luciferase gene under the control of the NFκB promoter were transfected in a titration series with SIVmon Vpr, HIV-1 M Vpr, cGAS /STING or an empty expression plasmid. Luciferase activity was measured at 48hrs post transfection. Data from three independent experiments are represented as the fold induction relative to an identical dose of empty expression vector +/- SEM.

## 5.4 Mutagenesis of SIVmon Vpr

Experiments on the HIV-1 M Vpr had shown that a cyclophilin binding mutant P35N is defective for nuclear localisation (fig 4.8B) and the phenotype of signal antagonism. To guide a mutagenesis strategy for testing the SIVmon Vpr, a structural alignment was generated with T-Coffee multiple alignment software which can incorporate three-dimensional structural information for the alignment of protein sequences (516,517). The ESPrnt (*Easy Sequencing in PostScript*) online software was then used, a program which renders sequence similarities and secondary structure information from aligned sequences (518) (figure 5.4).

The Serine at position 40 aligned consistently with the Proline and was mutated to Asparagine using site directed mutagenesis (SDM). We hypothesised that this might disrupt the same binding site and allow us to infer potential binding partners.

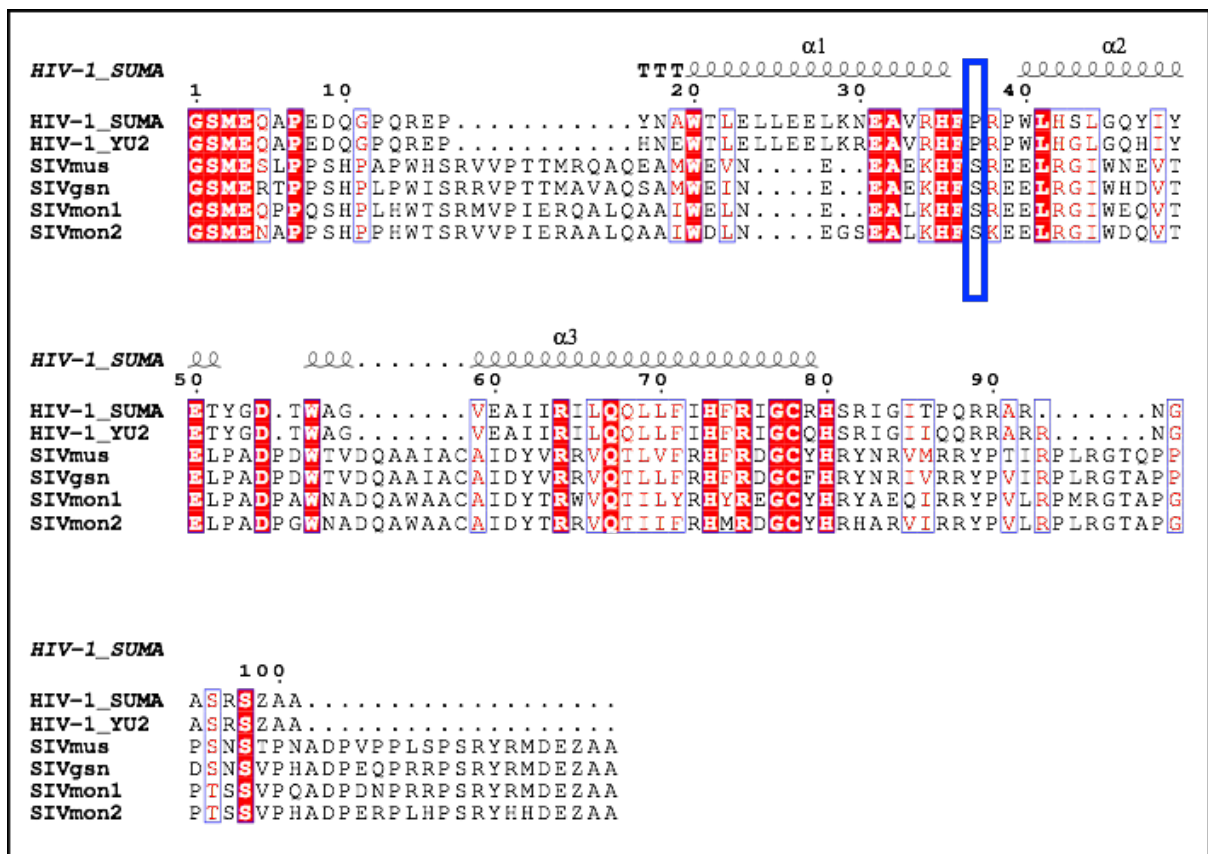


Figure 5.4 Alignment of Mona monkey group SIV, HIV\_YU2 and SIVcpz Vprs. Primary and secondary structures and sequence data were aligned using the webserver program ESPrnt3.0

## 5.5 SIVmon Vpr specifically activates NF $\kappa$ B signalling

To characterize the ability of SIVmon Vpr, its S40N mutant and the SIVgsn Vpr from the same group, the effect of ectopic expression of these proteins on transcriptional reporters in HEK293T cells was examined across a range of immune related promoters with cGAS and STING acting as a positive control (figure 5.5 A-F). They were tested over a three fold dilution series against six separate luciferase promoter constructs including the IFN $\beta$  promoter which contains binding sites for the NF- $\kappa$ B, IRF3 and AP-1 transcription factors (527,528); the ISG56 promoter sensitive to IRF3 (524,529); an Interferon Sensitive Response Element (ISRE) sensitive to the ISGF3 complex and IRF1&3 (569,570); an AP-1 sensitive promoter encoding the firefly luciferase reporter gene under the control of a minimal (m)CMV promoter and tandem repeats of the TPA-induced transcriptional response element (TRE) (QIAGEN); the synthetic NF $\kappa$ B sensitive promoter as used as the reporter throughout chapter 3; and the HSV Thymidine Kinase (TK) promoter Renilla luciferase construct with binding sites described for TFIID, Spl, and CCAAT-binding proteins (Promega) (555). This was the same construct used as a transfection control throughout chapter 3.

Data in figure 5.5 are presented as the raw values from the luminometer of relative light units (RLU) for the firefly luciferase expression to show the basal activation level of each promoter. Both the S40N mutant and the SIVgsn Vpr showed little or no effect on luciferase expression from any plasmid. However the wild type SIVmon Vpr increased transcription from the NF $\kappa$ B promoter whilst dramatically suppressing expression from the ISG56 and TK promoters >10fold (figure 5.5).

This is hard to explain in terms of known transcription factors but there is “cross talk” between the NF $\kappa$ B and IRF3 signalling pathways; NF- $\kappa$ B p65 and IRF3 can form stable complexes that can be recruited through an interferon-response element (IRE) or a  $\kappa$ B site (571). Additionally NF- $\kappa$ B target genes can be IRF dependent and this is determined by an IRE in close proximity to the  $\kappa$ B site (572). Glucocorticoid receptors inhibit a subset of NF- $\kappa$ B-dependent transcriptional responses following ligand binding and can directly displace IRF3 from p65 (573). Assembly of NF- $\kappa$ B, IRF and ATF-c-Jun transcription factors at the enhancer of the gene encoding interferon- $\beta$ , occurs after viral infection (574). Additionally p50 homodimers repress a subset of interferon-inducible genes through direct binding to guanine-rich IRE sequences and probably through direct competition with IRF3 (575).

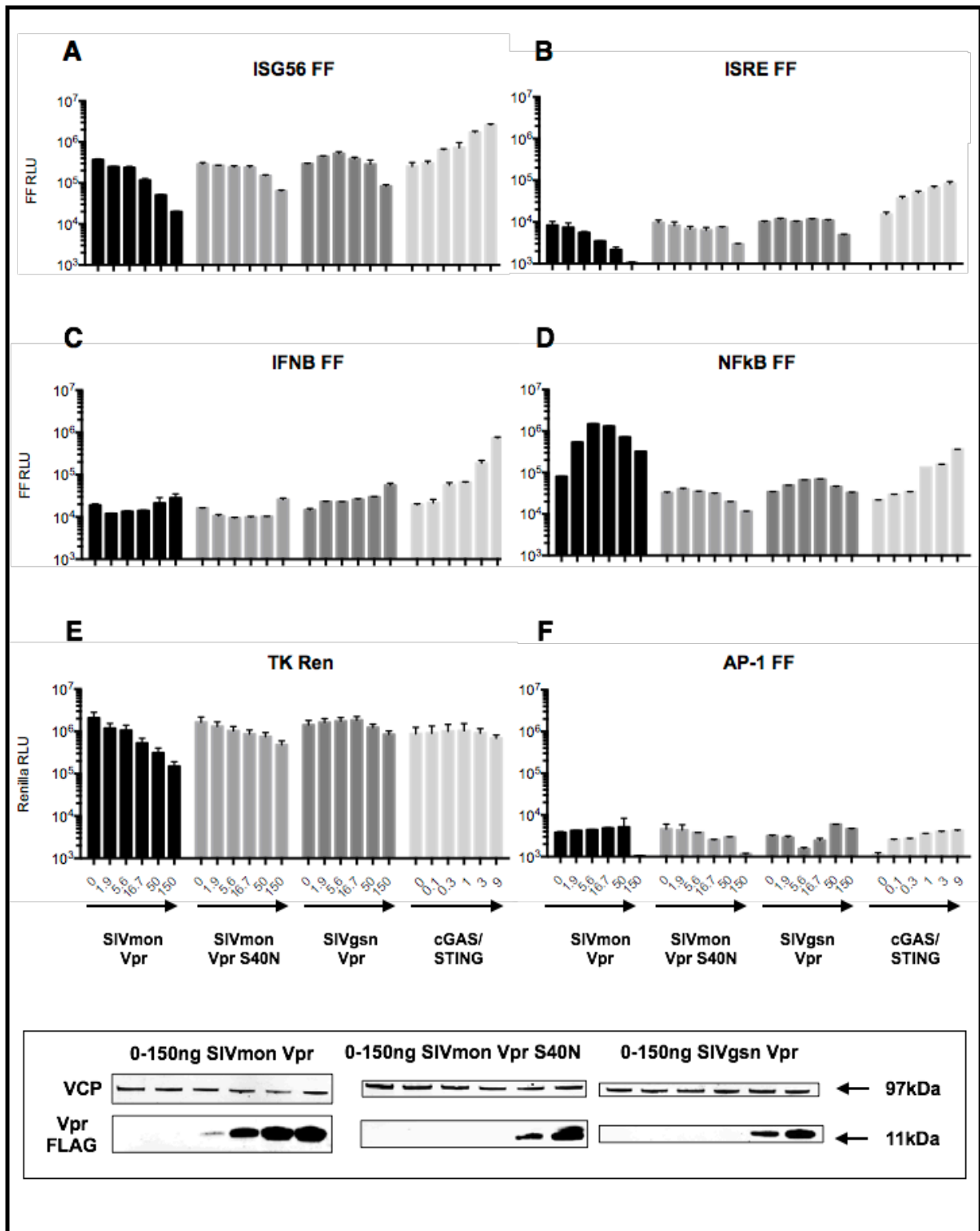


**Figure 5.5 SIVmon Vpr specifically activates NFκB signalling** HEK293T cells were transfected with luciferase reporter plasmids with the indicated promoters and then a dilution series of either SIVmon WT Vpr, SIVmon S40N Vpr, SIVgsn Vpr, or cGAS/STING. Cells were harvested for luminometry and immunoblot at 48hrs. Data are presented as the mean raw relative light unit (RLU) value for the firefly luciferase substrate from three experiments +/- SEM.

## 5.6 Depletion of Nup358 reduces SIVmon Vpr NF $\kappa$ B signalling

HIV-1 M, like Nup385, localises to the nuclear rim (see figure 4.8) and is known to have a cyclophilin (cyp) binding domain previously described by numerous previous studies (408,502,503,508,576,577). Nup358 has a cyclophilin homology domain and has been described as a co-factor for HIV-1 M nuclear entry (164,165,167,331,332). While the cyclophilin binding domain of SIVmon Vpr has not been studied the putative S40N mutant with diminished function aligns with the P35 in HIV-1 M Vpr believed to be central to binding of cyclophilin.

I hypothesised that SIVmon and HIV-1 M Vprs could be binding to cyclophilin A and the cyclophilin homology domain of Nup358 through their putative cyclophilin binding domains and through this binding could be modulating nuclear entry of NF $\kappa$ B subunits or transfected DNA.

To test this hypothesis initially, Nup358 was depleted with short hairpin RNA (shNup358) in HEK293T cells and these cells were transfected with either empty vector (with and without HIV-1 M Vpr) or cGAS and STING in a 1:1 ratio (with and without HIV-1 M Vpr) (figure 5.6A). As expected HIV-1 M Vpr reduced cGAS/STING induced NF $\kappa$ B driven luciferase expression in both the shControl and the shNup358 cells (figure 5.6A). But determining the effect of Nup358 depletion on HIV-1 M Vpr inhibition of NF $\kappa$ B activation was complicated by the fact that depletion of Nup358 reduced the NF $\kappa$ B activation induced by cGAS and STING transfection (figure 5.6A). This makes it difficult to determine any further effect of Nup358 depletion on HIV-1 M Vpr on signal reduction. This difficulty was one of the main reasons for investigation and characterization of the SIVmon Vpr: to identify binding partners of HIV-1 M Vpr that could be further investigated.

NF $\kappa$ B activation was then tested in the same shNup358 or shControl HEK293T cells using either transfected SIVmon Vpr or soluble TNF $\alpha$ . TNF $\alpha$  induced NF $\kappa$ B signalling was not significantly affected but there was a small reduction in SIVmon Vpr induced NF $\kappa$ B driven luciferase expression. Nup358 depletion left TNF $\alpha$  mediated NF $\kappa$ B signalling unaffected, but signalling activated by SIV mon was significantly antagonised potentially indicating an interaction between these proteins or a dependency on Nup358 for SIVmon Vpr, but not TNF $\alpha$ , mediated NF $\kappa$ B signalling (figure 5.6B) although the observed inhibition of the SIVmon Vpr NF $\kappa$ B signal was not large.

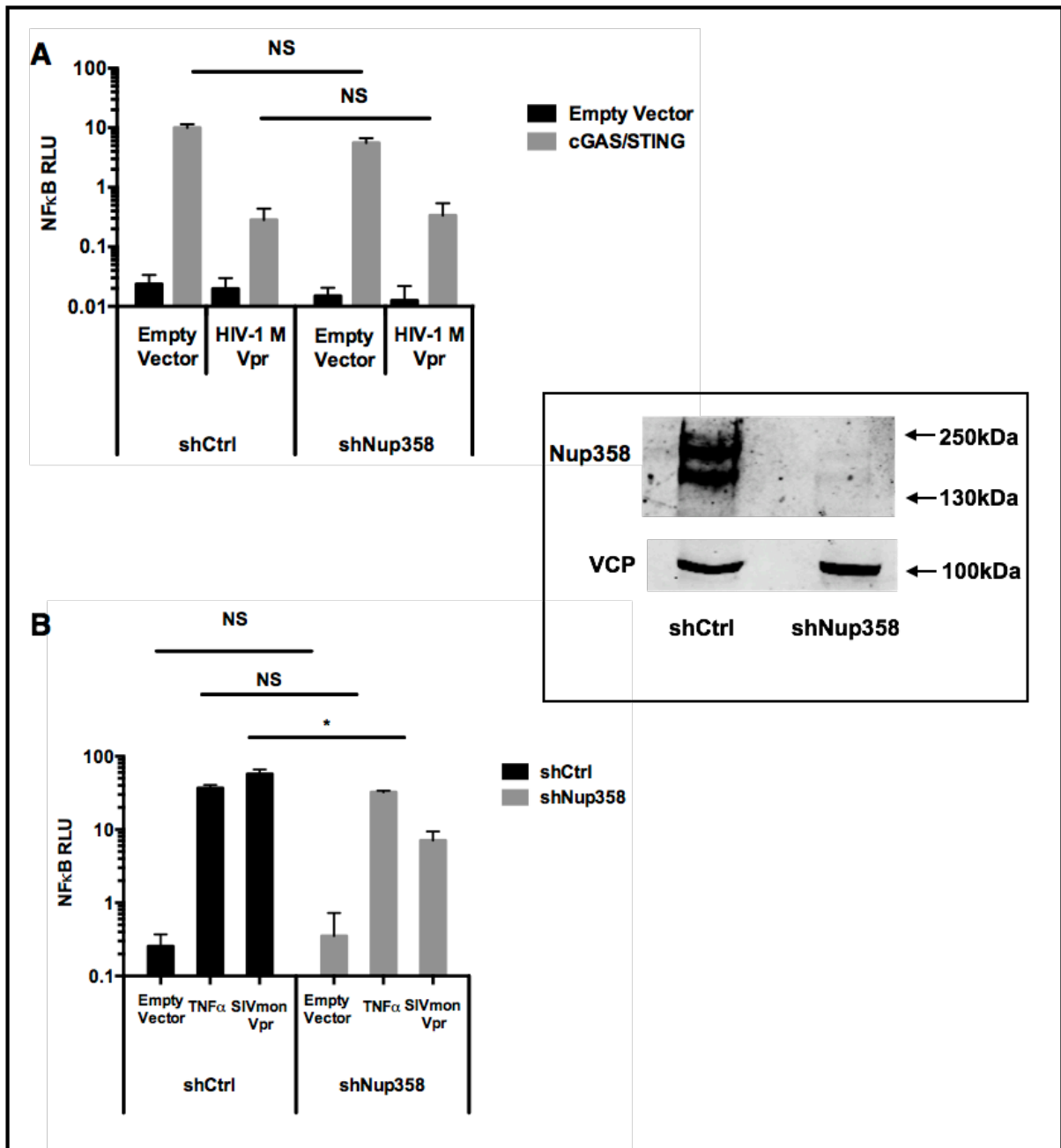


**Figure 5.6 Depletion of Nup358 reduces SIVmon Vpr NFκB signalling.** Depletion of Nup358 in HEK293T cells using shRNA lentiviral vector transduction followed by transfection with (A) cGAS/STING +/- HIV-1M Vpr and an NFκB luciferase reporter. (B) Depleted cells were also either transfected with SIVmon Vpr or TNFα was added. Luminometry was performed at 48hrs. Data from three experiments are represented as the fold induction relative to an identical dose of empty expression vector +/- SEM. Cell lysates were then analyzed by immunoblotting with anti-Nup358. \* $P < 0.05$  one-way ANOVA with Dunnett's post-hoc test.

## **5.7 Depletion of cyclophilin A reduces SIVmon Vpr NF $\kappa$ B signalling**

In order to determine whether the observed SIVmon Vpr activation of an NF $\kappa$ B reporter was dependent on cyclophilin A, short hairpin RNA was used to deplete cyclophilin A in HEK293T cells. These cells were then transfected with empty vector, SIVmon Vpr or cGAS and STING in a 1:1 ratio in order to stimulate NF $\kappa$ B signalling and NF $\kappa$ B promoter activity was measured at 48 hours post transfection by luminometry. Cyp A depletion was confirmed using an immunoblot. Since it has overlap with SIVmon Vpr FLAG on immunoblot the empty vector lysate was tested for depletion (figure 5.7 B).

Cyp A depletion inhibited SIVmon Vpr induced expression of luciferase driven by an NF $\kappa$ B promoter approximately 2 fold whilst cGAS/STING induced reporter expression was left unaffected (figure 5.7A). While the effect is not large it is statistically significant potentially indicating cyp A as a co-factor for SIVmon Vpr NF $\kappa$ B activation.

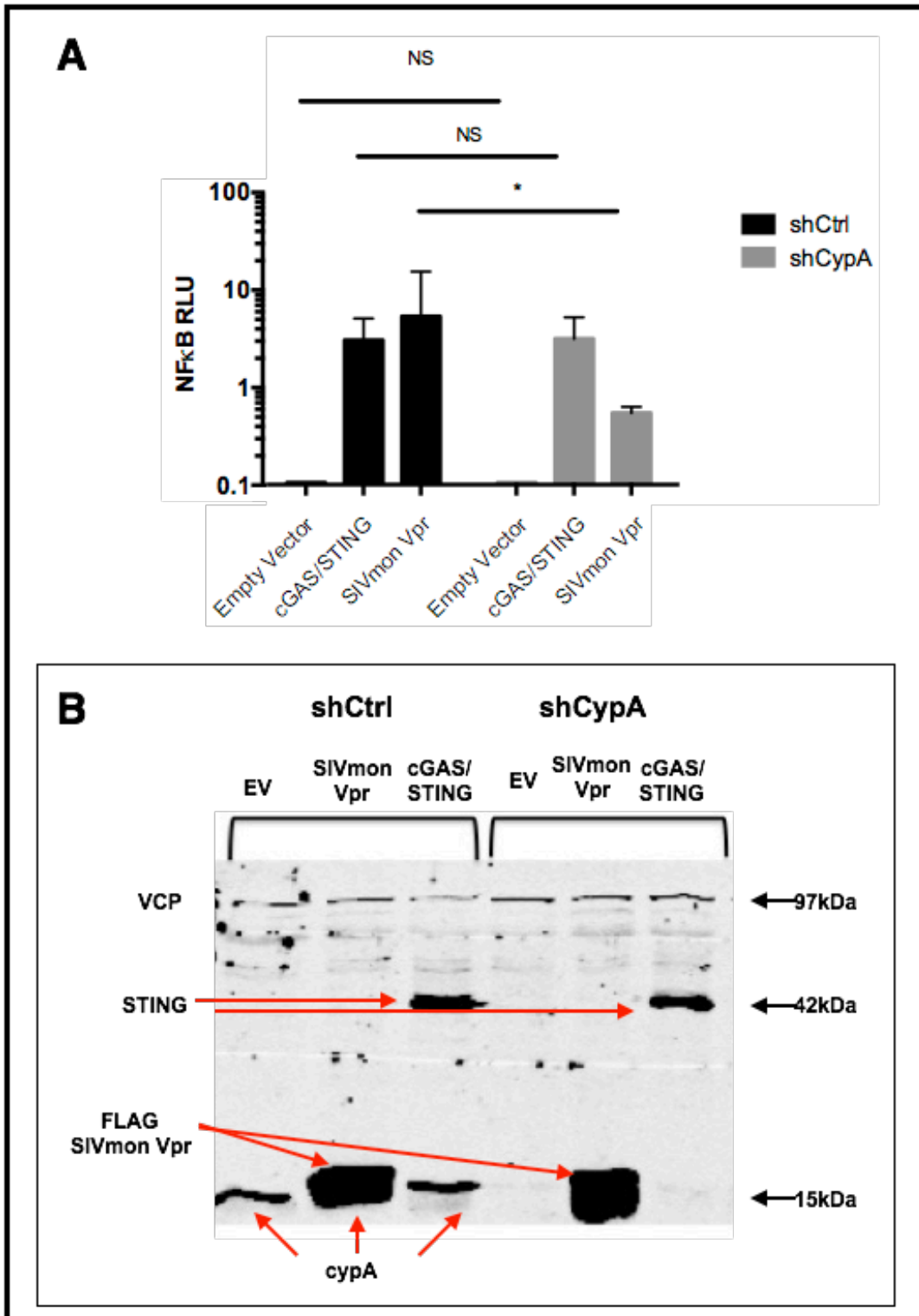


**Figure 5.7 Depletion of CypA reduces activation of an NFκB reporter by SIVmon Vpr** CypA was depleted in HEK293T cells using shRNA lentiviral vector transduction followed by transfection with cGAS/STING or SIVmon Vpr and an NFκB luciferase reporter. Data from three experiments are represented as the fold induction relative to an identical dose of empty expression vector ± SEM. Cell lysates were analyzed by Western blotting with anti FLAG, anti CypA and, as a loading control, anti-VCP. \* $P < 0.05$  one-way ANOVA with Dunnett's post-hoc test.

## 5.8 Overexpression of CypA or Nup358cyp leaves SIVmon Vpr activated NFκB signalling unaffected.

To test whether overexpression of CypA or the cyclophilin homology domain of Nup358 has any effect on SIVmon Vpr induced NFκB sensitive reporter activation both molecules were expressed in HEK293T cells with co-transfection of cGAS and STING in a 1:1 ratio or SIVmon Vpr (figure 5.8 A for CypA and B for 358cyp). NFκB signalling was left unaffected by either molecule. Additionally, unpublished data from our lab indicate that overexpression of CypA and Nup358 also leave NFκB signal antagonism by HIV-1 M Vpr unaffected (personal communication, Lucy Thorne).

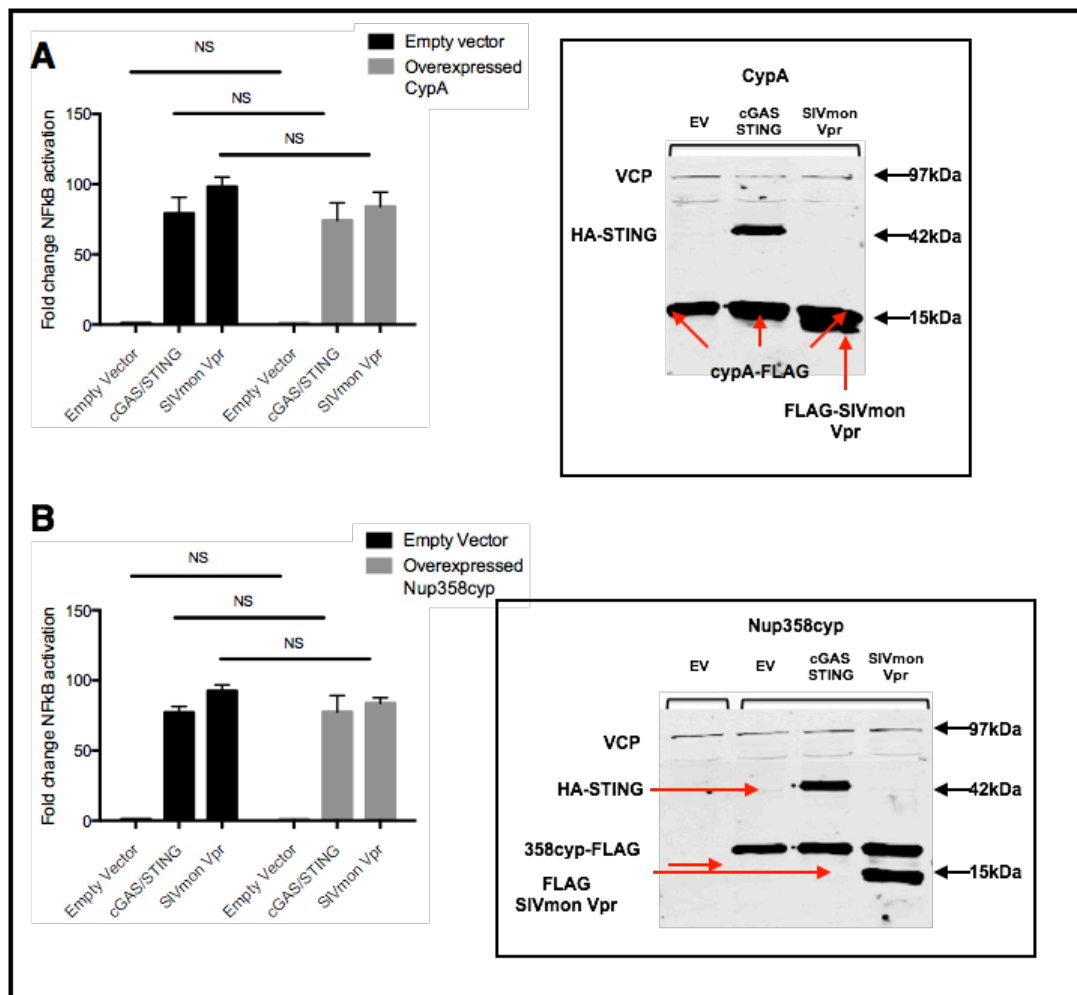


**Figure 5.8 Overexpression of CypA or Nup358cyp leaves SIVmon Vpr activated NFκB signalling unaffected.** CypA (A) and 358cyp (B) were overexpressed in HEK293T cells with either empty vector, cGAS/STING or SIVmon Vpr and an NFκB luciferase reporter. Data from three experiments are represented as the fold induction relative to an identical dose of empty expression vector +/- SEM. Cell lysates were analysed by Western blotting with anti FLAG, anti HA and as a loading control anti-VCP. NS=non-significant, one-way ANOVA with Dunnett's post-hoc test.

## 5.9 SIVmon Vpr does not co-immunoprecipitate with co-transfected members of the pathway

As well as being a useful reagent for understanding of NF $\kappa$ B signaling I hypothesised that the SIVmon Vpr may help to identify the binding partner of HIV-1 Vpr since it was able to activate signalling without co-transfection of any signalling molecules (e.g. cGAS/STING). To investigate whether if SIVmon Vpr binds specific members of the NF $\kappa$ B signalling pathway, I attempted to immunoprecipitate FLAG-tagged SIVmon Vpr from the cleared cell lysates of cells expressing HA tagged IKK, TBK, cGAS, STING, p50, p65 or 358cyp using a mouse-anti-HA Ab coupled to protein agarose beads following co-transfection with FLAG SIVmon Vpr (figure 5.9). The transfected molecules were detected in the whole cell lysates but the SIVmon Vpr was not found to co-immunoprecipitate, indicating that as had been hypothesised for HIV-1 M the binding site was not in any transfected molecule.

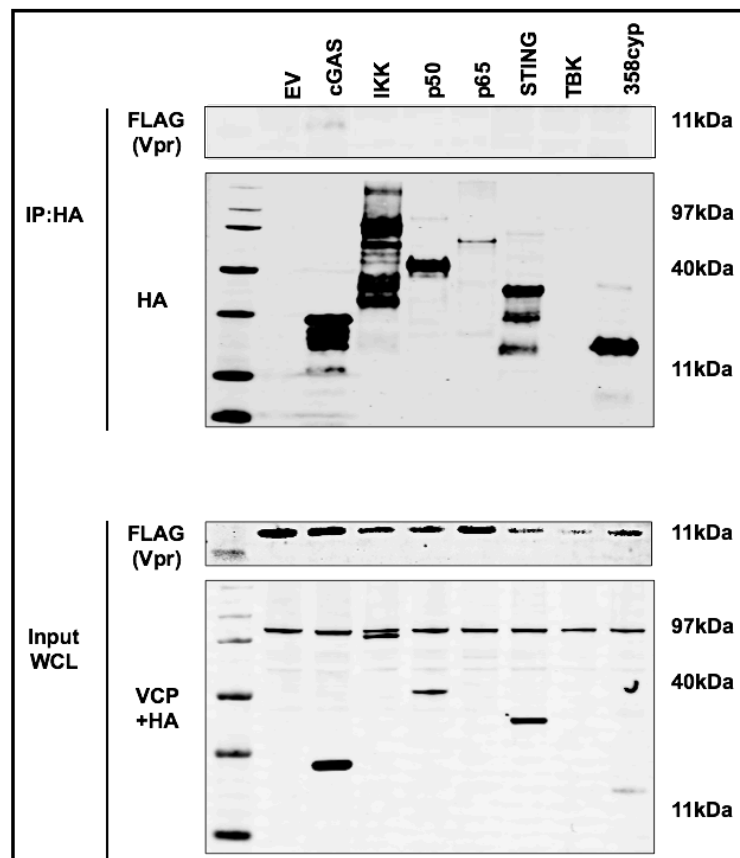


**Figure 5.9 SIVmon Vpr does not co-immunoprecipitate with co-transfected members of the pathway.** HEK293T cells were transfected with empty vector, HA tagged IKK, TBK, cGAS, STING, p50, p65 and 358cyp together with FLAG SIVmon Vpr. At 48hrs cell lysates were incubated with mouse-anti-HA Ab coupled to agarose beads. Whole cell lysates (Input WCL) and immunoprecipitated proteins (IP) were separated by SDS-PAGE and analysed by immunoblotting with mouse-anti-HA, mouse-anti-FLAG and rabbit-anti-VCP antibodies. The locations of protein molecular mass markers are indicated (kDa).

## 5.10 SIVmon localises to the nucleus

I hypothesised that if SIVmon Vpr was acting at the same binding site in the pathway as HIV-1 M Vpr then it might show the same pattern of intracellular localisation. Cellular localisation of SIVmon Vpr, SIVgsn Vpr and SIVmon S40N was studied by immunofluorescence in HEK293T cells 48hrs post transfection all three molecules being detected using a rabbit-anti-FLAG polyclonal antibody and DAPI nuclear stain. All three localised to the nucleus but with differing distributions (figure 5.10A, B&C).

SIVmon Vpr localised to discrete puncta or “dots” within the nucleus (figure 5.10A). The localisation pattern resembled that of the promyelocytic leukaemia (PML) nuclear bodies first identified in the nuclei of malignant cells in the early 1960s (578). PML bodies measure 0.1-1.0um and are found in the nuclear matrix a poorly defined structural component of the nucleus believed to regulate many nuclear functions including transcription and epigenetic modification (579). They sequester an expanding number of partner proteins but many details of their function remain unclear. PML bodies have been linked to regulation of apoptosis and senescence but a mechanism by which SIVmon Vpr might bind to these subnuclear structures and active NF $\kappa$ B signalling is not obvious from previous studies of PML nuclear bodies. Indeed, the mere similarity between PML body appearance and SIVmon Vpr localisation does not confirm a link between these proteins and there are other nuclear dots which have a similar appearance (580).

The SIVmon Vpr S40N mutant, putatively analogous to the P35N cyclophilin binding mutant in HIV-1 M had a markedly different distribution to the wild type SIVmon Vpr (figure 5.10B). It was evenly distributed in the nucleus with some cytoplasmic expression. The SIVgsn Vpr from the other Mona Group monkey which is defective for NF $\kappa$ B signal activation localised inside the nucleus but with a tendency to collect around the inside of the nuclear envelope (figure 5.10C). None of these Vpr proteins contain a classic nuclear localisation signal or a known DNA binding region was assessed using NucPred (581) and PredictProtein (582).

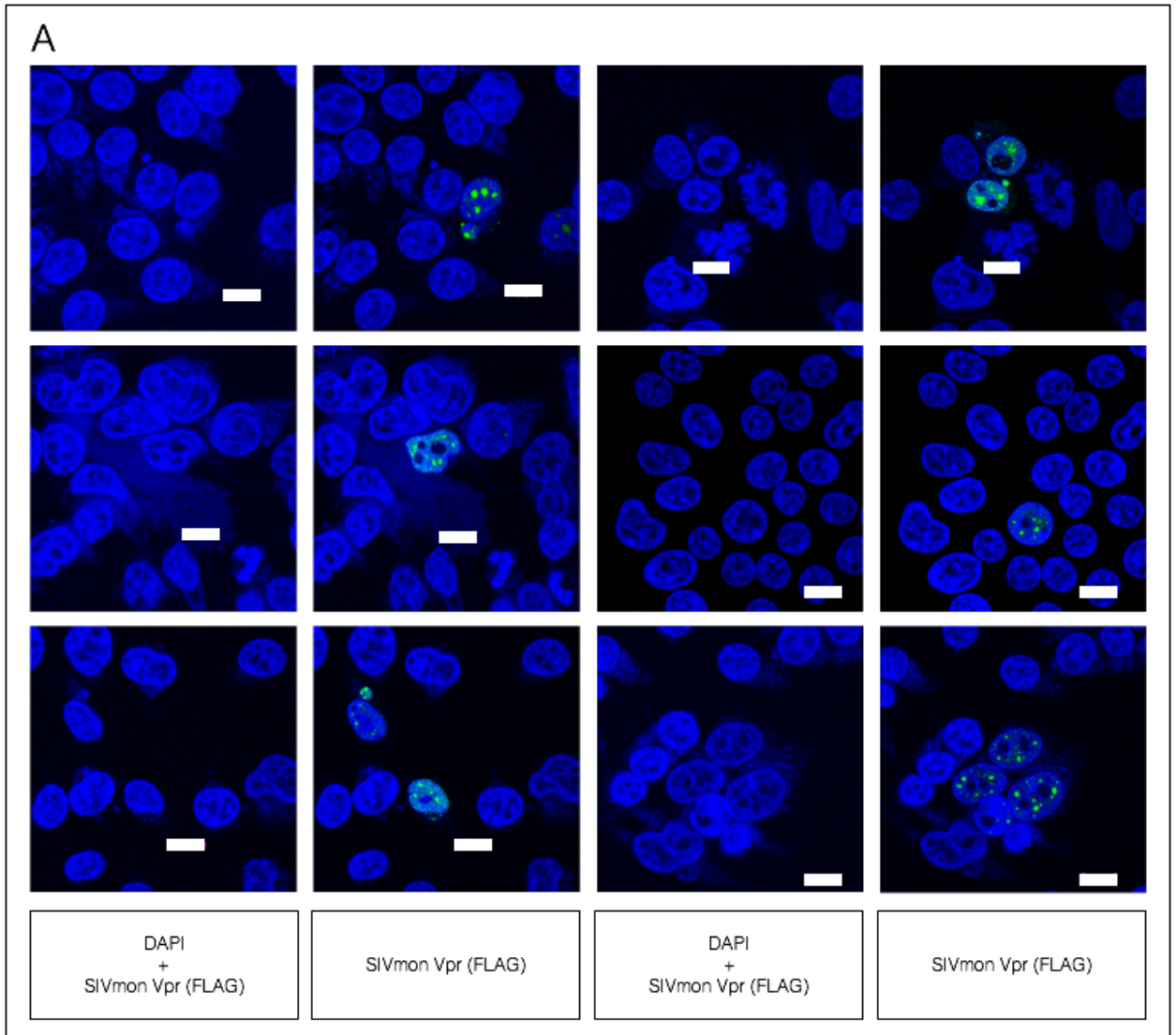


**Figure 5.10 A Localisation of SIVmon**

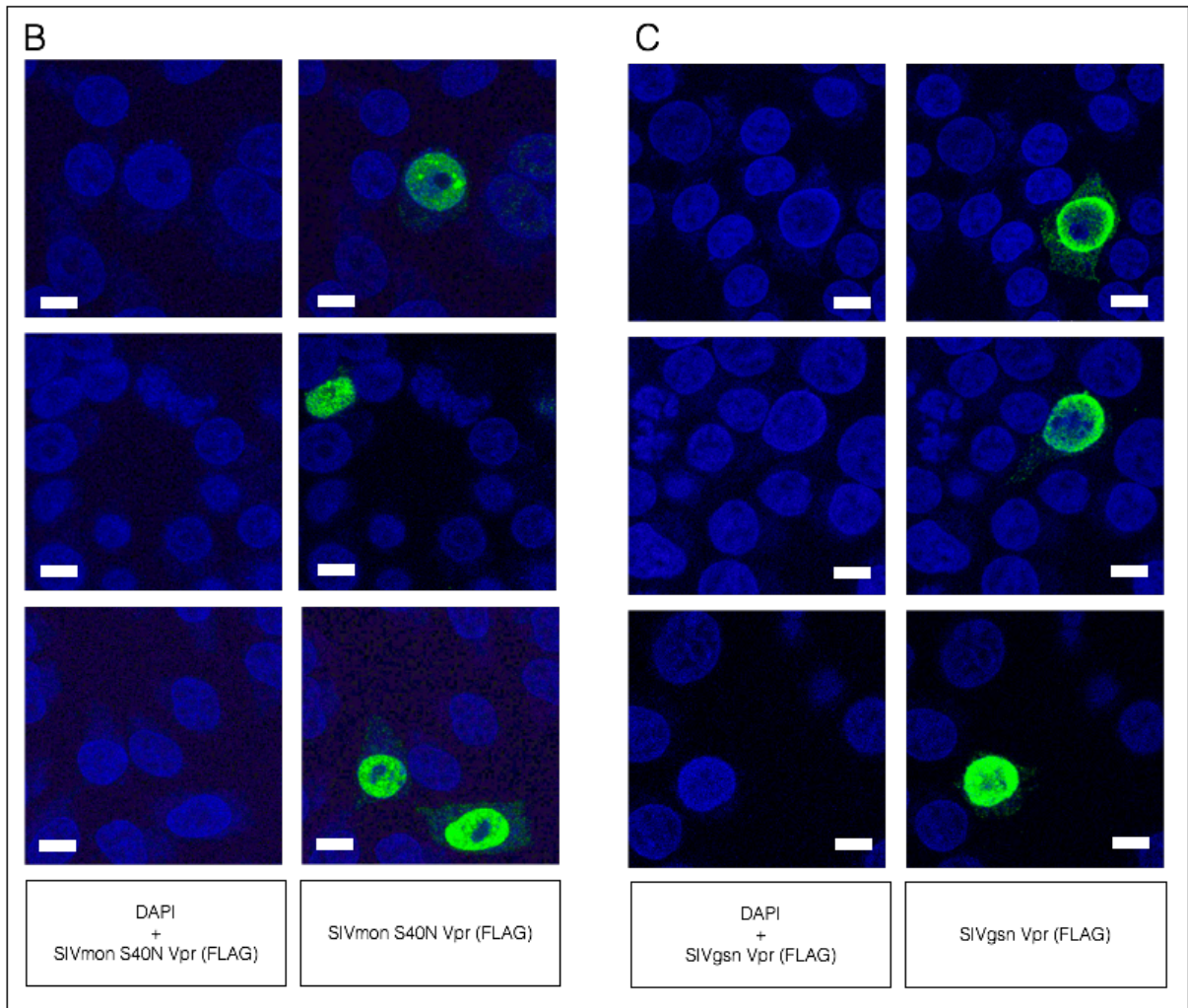


**Figure 5.10 B and C Localisation of SIVmon Vpr by immunofluorescence.** HEK293T cells were transfected overnight with a plasmid expressing FLAG epitope tagged SIVmon Vpr (A), its S40N mutant (B) or the SIVgsn Vpr (C). Cells were then fixed and stained with an anti-FLAG antibody. The localisation of Vpr (green), nuclear DNA stained with DAPI (blue), and merged images are shown.

## 5.11 Optimization of SIVmon Vpr expression for determination of binding partner by SILAC

Since SIVmon Vpr is observed to differ markedly in localisation compared to HIV-1 M Vpr, and the evidence for a common binding partner seems inconclusive, its utility as a reagent for understanding the function and mechanism of HIV-1 M Vpr may be through its use in dissecting NF $\kappa$ B signaling pathways: since it has a specific effect on NF $\kappa$ B signalling it may prove to be a useful reagent to further characterise this signalling pathway. With this in mind preparations were made to identify relevant interacting proteins using affinity purification followed by quantitative mass spectrometry using stable isotope labeling of amino acids in cell culture (SILAC) (583) (figure 5.11A&B are replicates).

In the SILAC experiment, three cell populations are generated in media with light, medium and heavy isotopes conditions. This allows for direct comparison of protein expression levels by mixing the non-labeled “light” and the labeled “medium” and “heavy” cell populations. Each peptide appears as a pair in MS analysis with a difference in mass, and the relative peak intensities reflect the abundance ratios (584).

HEK293T cells were transfected overnight with plasmids expressing either empty vector, FLAG epitope tagged SIVmon Vpr, FLAG epitope tagged SIVmon Vpr S40N mutant or FLAG epitope tagged SIVgsn Vpr. The expressed proteins were then immunoprecipitated using mouse-anti-FLAG antibody coupled agarose beads and detected in both the input lysate samples and the immunoprecipitate using mouse anti-FLAG antibodies. The light and heavy chains from the mouse anti FLAG immunoglobulin on the beads are also visible on the immunoblot since the secondary antibody used for detection of the anti-FLAG antibody was a fluorophore coupled to an anti-mouse antibody (figure 5.11 A&B).

The main aims of the optimization experiment were to ensure that the protein of interest could be expressed and would immunoprecipitate. Coomassie staining was used as an indicator to determine that enough protein and putative interacting partners immunoprecipitate for mass spectrometry analysis. Additionally, the amount of each Vpr expressed and immunoprecipitated was optimized to have them as similar as possible in order to enable a comparative mass spectrometry analysis and ensure that if a cellular binding partner is found it is not an artifact of better expression and immunoprecipitation. FLAG immunoprecipitation was performed and proteins were stained by coomassie blue after SDS-PAGE but cell populations were not labeled at this stage.

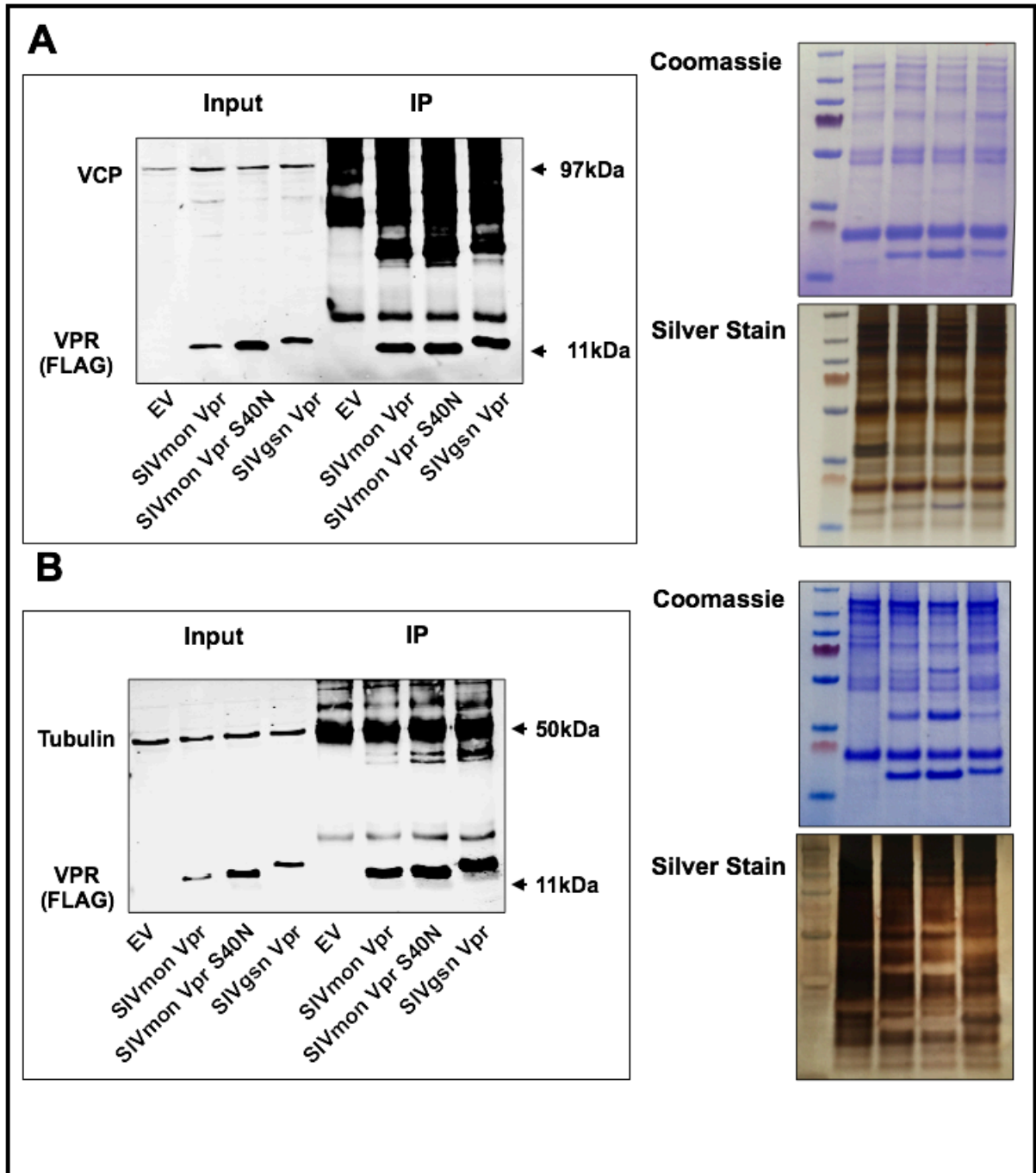


**Figure 5.11 Optimization of expression and immunoprecipitation for SILAC.** (A&B are replicates) HEK293T cells were transfected overnight with a plasmid expressing FLAG epitope tagged SIVmon Vpr, its S40N mutant or the SIVgsn Vpr or an empty vector control. At 48 hrs the cells were harvested in IP buffer (see chapter 2) and the cleared lysates were incubated with mouse-anti-FLAG antibody coupled to agarose beads to immunoprecipitate the epitope-tagged proteins. Whole cell lysates (INPUT) and immunoprecipitated proteins (IP) were separated by SDS-PAGE and analysed by immunoblotting with mouse-anti-FLAG, and rabbit-anti-tubulin antibodies as a loading control. The location of protein molecular mass markers is indicated (kDa). IP samples were run on a pre-cast gradient PAGE gel and stained with Coomassie blue and then silver stain.

## 5.12 Transcriptional signature of SIVmon Vpr

To attempt to characterise the transcriptional signature activated by SIVmon Vpr transfection HEK293T cells were transfected with plasmids expressing SIVmon Vpr, its S40N mutant, the SIVgsn Vpr or an empty vector (pcDNA.3). Cells were harvested for RNA extraction at 48hrs. 12 samples were analysed, 3 replicates each of 4 conditions (SIVmon Vpr, SIVgsn Vpr, SIVmon S40N Vpr, and pcDNA.3). One sample of the SIVgsn Vpr was degraded and excluded. All samples were labeled for gene expression microarrays with fluorophores Cy3 and Cy5 and array images were acquired with Agilent's dual-laser microarray scanner G2565BA. The Agilent Feature Extraction software was used to extract raw data from the scanner output file and log<sub>2</sub>-transform median Cy3 and Cy5 signal intensities. These were normalised and only gene symbol-annotated probes expressed above background negative-control levels in at least one sample were analysed.

An initial comparison of SIVmon Vpr to empty vector showed only 126 genes with a >2 fold change in expression (figure 5.12A). This is unlikely to be compatible with a significant activation of NF $\kappa$ B signalling pathways which are central to the regulation of many thousands of genes by many more than 2 fold. Of these only 102 were annotated and of these 102 only 52 showed increased expression (30 had a refseq ID), the remaining 50 showed reduced expression (of which 29 had a refseq ID). These 59 genes were analyzed using gene ontology enrichment analysis, pathway analysis, Transcription binding factor site analysis and Ingenuity pathway analysis (see chapter 2) none of which showed any evidence of NF $\kappa$ B regulatory gene enrichment.

The experiment lacked a technical positive control but more significantly the plasmids were transfected at a dose (16.7ng) that likely only stimulated a small percentage of the cells (figure 5.12B). Early experiments had showed a maximal activation of NF $\kappa$ B signal at low doses with a co-transfected plasmid and so these doses were used in the array. Whilst when using a luciferase assay even a small amount of secreted luciferase may be detected if a gene expression change is seen in only a small number of cells then the change in mRNA signal may be lost in background noise. This hypothesis was tested by transfecting cells with a titration of GFP under control of the same promoter in the same plasmid vector and showing that at the dose used in the array experiment only <20% of cells were likely to be transfected. At the time when the array results were analysed further data on the phenotype of HIV-1M Vpr including nuclear localisation and the effect on co-transfected plasmids called into question the validity of using SIVmon Vpr as an experimental tool to identify the binding partner for HIV-

1 M and so considering the lack of clarity regarding a hypothesis another array was not attempted.

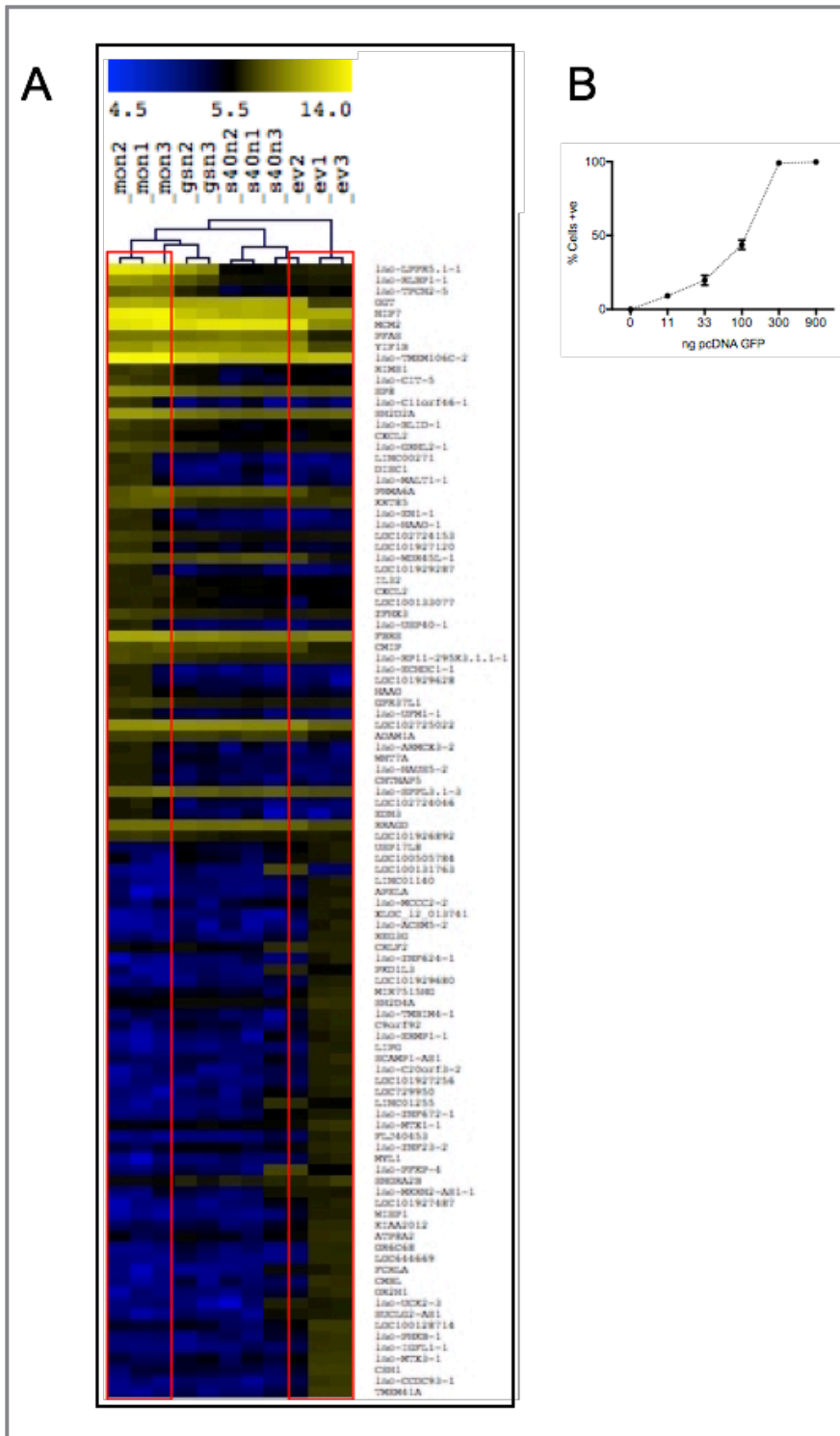


**Figure 5.12 Comparison of relative gene expression changes following transfection of SIVmon Vpr (A)126 genes with a >2 fold change in expression in HEK293T cells following SIVmon Vpr transfection compared to empty vector. (B) % cells transfected at different doses of the expression vector used to express SIVmon Vpr.**

## 6 Chapter 6: Discussion

The evasion of host cellular innate immune responses is a requirement that shapes the structure and lifecycle of all viruses. The investigation of the wide variety of strategies that viruses employ to achieve this improves both clinical understanding and treatment of agents of disease, as well as enabling deeper understanding of cellular immune processes since, through a process of real world combinatorial optimisation, viruses have a deep “understanding” of our immune system and how to subvert it.

All primate lentiviruses encode the Vpr accessory protein and, while a number of binding partners and *in vivo* and *in vitro* phenotypes have been observed, an explanation for the universal conservation of Vpr remains elusive. It has proved hard to reconcile, for example, the most biochemically investigated property of Vpr, that it causes G2 arrest (44,438,585–588), with the observation that it enhances a spreading infection in non-dividing cells (428,465,589).

Data from our lab (figure 3.1, Jane Rasaiyaah, unpublished, personal communication) indicate that Vpr is able to rescue a spreading infection in macrophages from the addition of cGAMP, the second messenger in the cGAS mediated cytosolic DNA sensing pathway. It may be that inadvertent activation of this or a related pathway in published experiments accounts for previous published observations that Vpr is able to improve infection efficiency (428,589,590). It was therefore hypothesised that Vpr was antagonising this pathway. Vpr, like other accessory proteins is able to recruit cellular ubiquitin ligases and is packaged inside the virion, both features that would be consistent with it functioning as an early antagonist of innate immune signalling or pattern recognition. An experimental transfection assay was developed to test this.

The cGAS/STING mediated cytosolic DNA sensing pathway was reconstituted in HEK293T cells and was shown to activate NF $\kappa$ B and IRF3 sensing using luciferase reporters and qRT-PCR of endogenous genes. Initial experiments were undertaken with a Vpr from the HIV-1 M YU2 used in the spreading infection experiment. The *Vpr* gene was codon-optimised using a proprietary algorithm for protein expression optimization from Blue Heron Bio and expressed relatively weakly. It was observed to specifically antagonise NF $\kappa$ B without affecting IRF3 signalling which appeared to indicate a specificity of effect (Fig 3.4). Additionally, loss of stimulatory molecules on immunoblot was observed and interpreted as Vpr induced possible degradation. This was a plausible hypothesis in view of published observations that Vpr is able to degrade host proteins SLX4 and UNG (44,384,387,438). However subsequent titration experiments with a re-codon-optimised Vpr gene showed that this was not the case. The much

higher sensitivity of IRF3 sensitive endogenous and reporter genes to activation by low doses of transfected cGAS and STING (or to cGAS and STING reduced to a low dose by Vpr) disguised the fact that the effect on IRF3 signalling was identical to the effect on NF $\kappa$ B signalling. Loss of both signals was subsequently shown to be due to suppression of expression from the co-transfected stimulatory molecules (Figure 4.3).

## 6.1 Function and Mechanism of HIV-1 M Vpr

There are three main findings of this thesis which have implications both for the potential function and mechanism of Vpr *in vivo* and for future experimental work.:

- 1) **Antagonism of expression from co-transfected plasmids:** The observation that ectopically expressed Vpr inhibits expression from all tested co-transfected plasmids encoding a variety of gene products (GFP, cGAS, IKK, TKB1, STING, MAVS, TNF $\alpha$ , renilla luciferase, firefly luciferase and SIV Vpr molecules). This antagonism correlates with localisation to the nuclear rim: breaking nuclear rim localisation breaks the inhibitor activity consistent with an effect regulating nuclear transport.
- 2) **Antagonism of NF $\kappa$ B activation by TNF $\alpha$  at an integrated reporter:** The observation that HIV-1 M Vpr inhibits TNF $\alpha$  mediated NF $\kappa$ B signalling from an integrated luciferase reporter and that this inhibition is rescued in the same way as the inhibition of expression from transfected plasmids by the Q65R and F34I /P35N mutagenized Vpr.
- 3) **Activation of NF $\kappa$ B signaling by SIVmon Vpr:** the observation that one of the two sequenced Vprs from the SIVmon lentivirus is able to stimulate NF $\kappa$ B signalling and that this appear to be dependent on the formation of intranuclear puncta.

It may prove possible to reconcile these findings with a single hypothesis – that Vpr regulates nuclear transport. This, in turn, may give insight into both the *in vivo* function of Vpr and mechanisms of nuclear import.

### 6.1.1 Antagonism of expression from co-transfected plasmids

The effect of Vpr on transcription does not seem to be promoter specific. Vpr antagonises expression of various genes, encoded by various expression plasmids with varied promoters with sensitivities to different transfection factors. Detailed descriptions of the transcriptional regulation of all the promoters used are not available but transcription factor binding information has been demonstrated experimentally and inferred for most of these promoters

and indicates a wide range of transcription factors. An attempt to investigate the effect of co-transfected Vpr on a luciferase construct with an HIV-1 M LTR was considered but previous use of similar constructs requires the co-expression of Tat the expression of which would be suppressed by Vpr (591,592). The range of transcription factors acting at these promoters of diverse origins makes it seem unlikely that the effect of Vpr is due to degradation or inhibition of a specific transcription factor or factors and there was no evidence of a global impairment of transcription (by either objective measurements like Live/Dead stain and trypan blue uptake or more subjective observations like media colour or cell appearance under the microscope). Additionally, the lack of effect on baseline transcription of an integrated reporter of NF $\kappa$ B compared to the >10 fold effect on a co-transfected reporter (fig 4.7) provides evidence that the inhibition of expression is unique to co-transfected DNA.

Remarkably little is known about cellular or nuclear entry of co-transfected DNA despite chemical transfection of nucleic acid into cultured mammalian cells having been first reported over 50 years ago (593,594). A number of different chemical methods have been used for transfection including DEAE-dextran (a cationic polymer), calcium phosphate and synthetic cationic lipids. All chemical transfection methods involve complexes of positively charged chemicals with negatively charged nucleic acids. The negative cell membrane then attracts these positive complexes but precisely how they traverse the membrane is not known. Endocytosis and phagocytosis may be required. Intranuclear localisation is required for transfected DNA to be expressed but this mechanism is also not known (595). This may be due to the proprietary nature of many of the current technologies. The FuGENE® HD transfection reagent (Promega) was used in these assays which has a proprietary non-liposomal formulation. It is hypothesized that the ability of Vpr to block expression from transfected plasmids relates interference with nuclear entry.

### **6.1.2 Antagonism of NF $\kappa$ B activation by TNF $\alpha$ at an integrated reporter**

These effects on transcription would ideally be reconciled with the effect on TNF $\alpha$  signalling at an integrated reporter. The only transfected plasmid in the experiments in figure 4.10 is the Vpr. It is assumed that, since the cells are identical to the other assays, that the previous observations regarding lack of toxicity hold true (and indeed subjective observations showed no indication of toxicity) and so this appears to be a true effect of Vpr on signalling. Importantly the phenotype is abrogated in the same way by the mutants Q65R and F34I/ P35N as the effect on expression from transfected plasmids. This is perhaps the most tantalising finding with relevance to *in vivo* studies indicating a true specificity of effect on NF $\kappa$ B signalling that

appears to be independent of toxicity and transfection. It is possible that there is a common mechanism for inhibiting nuclear import of transfected DNA.

### **6.1.3 Reconciling the effects on co-transfected plasmids and TNF $\alpha$ signalling**

Following observations that Vpr localises to the nucleus, much of the literature describes Vpr as being a regulator of nuclear import of the “pre-integration complex”. It has been proposed that it does this in an importin independent way (405), an importin dependent way (488) or in an importin- $\beta$  independent way (479). Vpr has also been implicated in import of proviral DNA into the nucleus of macrophages using biochemical techniques (596).

A model is proposed here where the defining selection force on many aspects of the viral life cycle is avoidance and suppression of innate immunity. Increasingly the viral capsid core is believed to have a vital role in these functions, concealing reverse transcription, and the nascent genome produced, in a closed environment, shielding it from host factors such as cGAS and TREX1 (see 1.10.1.2). The main evidence for this role of the capsid core comes from the observation that cytosolic DNA sensors are not activated by viral cDNA (170,597) unless there are capsid mutations which disrupt the interaction of capsid with cellular factors (165).

As evidence mounts that the capsid core remains intact until arrival at the nuclear pore the role of Vpr should also be reconsidered. Rather than being part of a “pre-integration complex” it may be that it has a highly local and specific effect at the NPC during or following uncoating. Three proteins involved in nuclear import, transportin-3 (TNPO3), Nup153 and Nup358, have been identified as co-factors for HIV-1 infection in genome wide small interfering RNA (siRNA) or yeast two-hybrid screens (333,598,599) but the mechanism by which the HIV capsid core or pre-integration complex engages these proteins remains unclear. Intriguingly both CA and Vpr have cyclophilin binding domains (165,411,502,503). CypA is has been shown to catalyse the cis/trans isomerisation of the Gly89-Pro90 peptide bond of CA (600) and while the exact effect that this has on the stability of the core has not been elucidated, CypA knockdown, deletion and inhibition all partially restrict infection (506,601). Vpr has also been shown to bind cyclophilin *in vitro* but the link between CypA binding and any of the many observed phenotypes of Vpr remains to be determined. While Vpr and CA have cyclophilin binding domains, Nup358 has a cyclophilin homology domain which has been shown in some studies to interact with CA and induce isomerisation and thus been linked to uncoating (602). Other studies have shown that the Nup358 cyclophilin homology domain is not a requirement for infectivity although this study was in mice and it's not clear that co-factor usage is the same in

mouse cells (603). A 2011 study determined that Vpr CypA binding was stronger than that of CA and CypA (503). Whilst it is not possible at this stage to form a fully coherent hypothesis about the mechanism of Vpr function there are several observations consistent with a role in nuclear transport including the localisation to the nuclear rim, the interactions with known nuclear import pathways and the cyclophilin binding. These all provide further avenues for investigation.

## **6.2 Future work on HIV-1 M Vpr**

An important consideration in the planning and interpretation of future experiments is that Vpr may have an extremely localized effect on a cell. It may be that Vpr works in small doses at highly specific regions of the nuclear rim proximate to an infecting virion core; so its localisation all around the nuclear rim is only seen when it is present in large quantities following over expression. It is possible to imagine a scenario where virion associated Vpr is released in a 'cloud' at the nuclear pore, and prevents signal transduction in close proximity to that particle at the nuclear rim but has no effect on overall nuclear transduction. In this case it would be extremely hard to measure a signal (or loss of signal) that would not be lost in noise. A hint at this idea comes from observations from our lab (unpublished) that whilst Vpr is able to rescue from addition of soluble cGAMP it does not seem to be able to rescue infected cells from capsid mutants believed to trigger DNA sensing (P90A, N74D).

Considering the effect on all tested co-transfected plasmids observed in these studies and in these cells it might be expected that only a limited amount more information could be gained from future co-transfection work that would provide insight into Vpr function.

### **6.2.1 Transfection Assays**

Further investigation of Vpr function would benefit from approaches more closely related to *in vivo* function but stimulated by the exciting finding that HIV-1 M Vpr does seem able to modulate an integrated NF $\kappa$ B reporter following activation mediated by TNF $\alpha$ . I would like to characterize in detail the effect of HIV-1 M Vpr and a series of mutants (described in table 4.2) on the stimulatory effect of a variety of added, soluble stimuli on a range of integrated reporters in transfectable cells lines. Integrated reporters in HEK293T cells could be tested using a variety of stimuli including RNA viruses, IFN- $\beta$  and cGAMP.

### **6.2.2 Vpr expressing lentiviral vectors**

To investigate the effect of Vpr on primary cells or non-transfectable cell lines it may be possible to make vesicular stomatitis virus glycoprotein (VSV G) pseudotyped lentiviral vectors

containing a genome encoding Vpr driven by a strong promoter. This process may be complicated by the effect of Vpr on co-transfected plasmids as it would be expressed from the genome construct to be packaged in the vector.

VLPs bearing Vpr could be used to take the same approach as was used to investigate the mechanism of action of Vpx (368,369). The effect on a variety of integrated reporters using a variety of stimuli in a range of less transfectable cell lines (pIFIT1-GLuc THP-1 reporter cells for example) and possibly primary cells could be studied. This approach would have the advantage of being quantifiable in terms of the numbers of cells infected with VLPs and might this make experiments examining effects on phosphorylation or translocation of transcription factors or other signalling molecules possible.

It would also be possible to assess the effect of transfected Vpr on vector transduction – whether Vpr blocks a transduced genome expression in the same way as it blocks expression from transfected DNA for example. As well as giving insight into the function of Vpr this approach might also contribute understanding to mechanisms of nuclear import in transfection.

These experiments would help to inform other studies using full length virus in primary cells including CD4+ T cells and monocyte derived macrophages. Previously published experiments have not focussed on the ability of Vpr to rescue infection from innate immune stimuli. An approach where cells are activated with a range of PAMPS or immune stimuli and Vpr is tested for an ability to rescue infection could be followed by genetic depletion studies to identify the partner molecules following an unbiased approach using SILAC.

### **6.2.3 Microscopy**

Optimisation of confocal microscopy of stained DNA plasmids might enable detection of differences in localisation that could be quantified. Use of the existing automated platform microscopes is complicated by the need to determine whether a stained plasmid is intra-nuclear or merely “in front of” or “behind” the nucleus. Automated high resolution microscopy platforms were tried including the WiScan Hermes and the Perkin Elmer Operetta but these both proved unable to resolve localisation of stained DNA. In order to measure whether Vpr had an effect on the physical localisation of transfected DNA a number of variables in this experiment would need to be optimised including use of confocal microscopy, Vpr expression labelling and changes in dose and intensity of plasmid dyes in order to get useful information about the effect of Vpr.

Whilst the observations of stained plasmid after transfection (figure 4.9) were not able to resolve a difference in the intracellular position of stained plasmid when expressed with either HIV-1 M Vpr or empty vector they did imply that every cell contained plasmid although not every cell was expressing GFP. This is consistent with the notion that transfection efficiency may have nuclear entry as the rate limiting step. A technique like fluorescence *in situ* hybridization (FISH), using a labelled probe to identify nuclear plasmid might give greater resolution.

#### **6.2.4 Reporter plasmid circularisation assay**

Biochemical techniques might prove more successful. A linearised plasmid with a promoter separated from a reporter would be expected to be circularised on entry to the nucleus by the cellular non-homologous end joining pathway. A reduction in re-circularised plasmids and thus reporter expression on co-transfection of Vpr would provide evidence of a block to nuclear entry of transfected DNA.

#### **6.2.5 Effects on NF $\kappa$ B subunit localisation**

It has not proved possible to observe effects on NF $\kappa$ B subunit translocation or phosphorylation in HEK293T cells using either immunoblotting or confocal microscopy. This is possibly due to difficulty in timing these experiments: transfected cells do not seem to have NF $\kappa$ B stimulation activated simultaneously. A luciferase assay works because of the relatively stable nature of luciferase which therefore accumulates but the translocation of NF $\kappa$ B subunits may be transient and thus impossible to capture by fixing cells at a particular time point (either in a lysate or on a microscope slide) when those cells are asynchronously expressing the stimulating protein. Luciferase assays are further complicated by the fact that it is not possible to tell how many cells are taking part in the experiment except by indirect means. If only a small number of cells are taking part then it may be that effects on activation of signalling molecules are lost in background noise as is hypothesised to have been the case with the micro-array investigation of SIVmon Vpr.

#### **6.2.6 Future species specificity characterisation**

A panel of Vprs representing all six major primate lentiviral lineages was constructed and tested against a variety of expression vectors encoding differing signalling molecules and luciferase reporters with differing promoters. It was observed that there was a conserved pattern of inhibition (or lack of inhibition) across all pathway stimulating molecules (cGAS/STING, MAVS, IKK and TBK-1) apart from TNF $\alpha$  signalling which was unaffected. The

significance of this being an added rather than a transfected molecule did not become apparent immediately.

These experiments were designed to identify the level in the pathway at which Vpr is acting and, while with hindsight they were unable to do this, they are not uninformative, acting essentially as replicates of a single experiment. The differential phenotype observed between each species' Vpr is not of course related to specific degradation of signalling molecules but reduced expression from the transfected plasmids however the same approximate pattern is seen across the Vpr panel with each stimulatory molecule.

The high sequence variability of Vpr together with the lack of a binary phenotype mean it is not possible to make inferences from examination of any single primate Vpr. An alignment shows there to be no specific region or site, no deletion or insertion that confers or abrogates the phenotype.

The analysis is further complicated by the number of plasmids in the experiments in figures 3.6-3.14 that are affected. At the doses of Vpr and the renilla luciferase reporter that were used, the effects on renilla luciferase expression were small but present nonetheless present. As well as the loss of expression of the molecules which are activating NF $\kappa$ B signalling there is also a direct effect on the NF $\kappa$ B sensitive luciferase reporter itself as can be seen in figure 4.6.

Further insights into species specificity will be gained using non-human primate cell lines. African green monkeys (*Chlorocebus*) are the only genus of non-human primates naturally infected with SIV for which laboratory cell lines are readily available and commonly used and as such provide an opportunity for molecular investigation of this phenotype. Accordingly, an attempt was made to reconstitute the signalling pathway described in figure 3.2 in 4 separate cell lines derived from African green monkeys (Vero, BSC-1, COS-1, MA104). Despite attempts with a matrix of different stimulatory molecules, transfection reagents and reporter genes no luciferase or PCR signal could be activated against which to test an antagonism by Vpr. Part of this lack of signal was attributable to lower transfection efficiency of AGM cell lines than the HEK293T cells. Transfection of the AGM cell lines with a plasmid encoding GFP indicated an 10-20 fold reduced expression of GFP compared with HEK293T as indicated by both mean fluorescence intensity and transfected cell number. But it is also possible that the lack of detectable signal was due to incompatibility of human innate immune signalling proteins with other pathway molecules in AGM cells although these proteins are generally well conserved. Members of pathways involved in detection and restriction of microorganism infection are likely to be under strong selection pressure and it may be that the ~30 million

year evolutionary distance between African green monkeys and humans would prevent interaction between human and monkey pathway molecules (604). At the time that these studies were being performed a complete genome of an African green monkey species was not available but had it been possible to identify the binding partner or partner of HIV-1 M Vpr then it would have been possible to sequence and clone pathway members from these cells. Although it is now understood that the tested innate immune molecules were not being specifically degraded this approach could still be used in order to test species specificity following the identification of a putative nuclear rim binding partner. This will be facilitated by the publication of a complete genome from *Chlorocebus aethiops* has now been published (604).

If AGM cell lines prove sufficiently transfectable then a transfection assay using constitutively expressed luciferase reporter constructs could be used to determine differential antagonism of expression by SIVagm Vpr and HIV-1 M Vpr. It might also prove possible to visualise FLAG tagged Vpr at the nuclear rim using confocal microscopy and assess species specific nuclear localisation of HIV and SIVagm in AGM cells and human cells. Since the SIVagm Vprs tested (SIVver, SIVtan) fail to antagonise expression from co-transfected plasmids in human cells it could be hypothesised that they would not be expected to localise to the nuclear envelope. Conversely if this localisation of Vpr is linked to an evolved function of Vpr then it would be expected to be observed in AGM cells. Further mutational analyses could be combined with biased and unbiased immunoprecipitation approaches to try to identify a binding partner in cell lines of green monkey origin.

### **6.3 SIVmon Vpr**

Studies on the SIVmon Vpr were undertaken to provide insight into both the function and mechanism of HIV-1 M Vpr, and also to characterize the NF $\kappa$ B signalling pathway. It was hypothesised that it would show the same intracellular localisation, and similar responsiveness to co-factor depletion and that this might enable determination of a binding partner for HIV-1 M Vpr. Using the HIV-1 M Vpr itself was complicated by the requirement for overexpression of stimulatory molecules none of which it seemed to associate with.

SIVmon Vpr was observed to activate NF $\kappa$ B dependent luciferase expression >10 fold whilst suppressing expression from an ISG56 promoter and a HSV thymidine kinase promoter >10 fold. These effects are unique to the SIVmon AY340701. The only other SIVmon sequence (AJ549283) and the other Vprs from the mona monkey group (SIVgsn and SIVmus) are inactive for signalling. This would seem to make it unlikely that the observed effect has been selected for – there is no reason to suppose that SIVmon Vpr has been under a selection

pressure in humans or other apes to activate NF $\kappa$ B signalling. Although SIVcpz is likely a recombinant of SIVrcm and SIVgsn (from the mona group) the Vpr in SIVcpz appears to have greater sequence homology with SIVrcm. It is therefore hypothesised that SIVmon Vpr may provide a useful experimental reagent rather than providing insight into the *in vivo* effects of SIVmon Vpr in its host species.

The activation of luciferase expression from an NF $\kappa$ B sensitive promoter is abrogated by an S40N mutant which, in a structural alignment, appears analogous to the residue of the P35N cyclophilin binding mutant in HIV-1 M Vpr. This initially appeared to bolster the hypothesis that SIVmon was acting at the same site in the pathway. However, despite a small but significant effect observed following depletion of CypA, overexpression and depletion studies using Nup358cyp, CypA and Nup358 were inconclusive. Immunoprecipitation experiments also failed to produce a binding partner using a biased overexpression approach.

Confocal microscopy showed a clear difference in localisation of SIVmon compared to HIV-1 M Vpr and the SIVmon S40N mutant and SIVgsn. SIVmon Vpr forms discrete intranuclear puncta or dots. This localisation pattern resembles that of promyelocytic leukaemia protein nuclear bodies (PML-NBs). These are nuclear structures which have been implicated in a range of nuclear functions including the activation of NF $\kappa$ B signalling pathways via the DNA damage response (DDR) pathway (605,606): following DNA damage, DNA double strand breaks (DSBs) increase the number and size of PML-NBs. They have been proposed to function as DNA damage sensors (607) and both DNA repair and checkpoint proteins dynamically co-localise with PML-NBs potentially enabling them to function as catalytic surfaces (605). Several kinases which trigger NF $\kappa$ B activation following DNA damage localise to the PML-NBs including ataxia telangiectasia-mutated protein kinase (ATM) and Rad3 related kinase (ATR) (608,609).

As discussed in section 1.9.2.5, NF $\kappa$ B acts as a cellular stress sensor. It can be activated by a wide range of cellular stresses (610,611) but the details of the signalling pathways which activate NF $\kappa$ B following activation of the DNA damage response remain poorly defined. In all NF $\kappa$ B signalling pathways the activating stimulus activates an IKK complex (IKK $\beta$ , IKK $\alpha$ , and NEMO), which phosphorylates I $\kappa$ B proteins. Phosphorylation of I $\kappa$ B leads to its ubiquitination and proteasomal degradation, freeing NF- $\kappa$ B/Rel subunit complexes. These subunits undergo further modification by phosphorylation, acetylation and ubiquitination then translocate to the nucleus to induce target gene expression. Activation of NF $\kappa$ B by the DNA damage response requires activation of ATM and nuclear accumulation of the adaptor protein NF $\kappa$ B essential modulator (NEMO) in PML-NBs (611,612). Here NEMO associates in a complex with ATM

and subsequently translocates to the cytoplasm allowing activation of the I $\kappa$ B kinase (IKK) complex. This in turn mediates phosphorylation and subsequent proteasomal degradation of I $\kappa$ B and NF $\kappa$ B subunit release (613).

Localisation of SIVmon Vpr to PML-NBs could be confirmed using microscopy in HELA cells expressing PML-YFP. If it is shown that there is co-localisation then the studies of the DNA damage response and PML dependent NF $\kappa$ B activation provide a useful starting point for potential SIVmon VPr interaction.

The low doses used for these confocal microscopy pictures were the same as activated the maximum amount of expression from a co-transfected reporter. Addition of more plasmid reduced image quality due to excessive staining in cells. Additionally, the signal from the reporter plasmid was diminished at higher doses (see figure 5.2 and 5.5). If SIVmon Vpr is directly binding NF $\kappa$ B promoters then it may be that it activates in a non-linear fashion. When an integrated reporter was tested the NF $\kappa$ B response is dose dependent. Remarkably little is known about the mechanics of transfection but it is believed that DNA forms complexes with transfection reagents such that each transfected cell gets all co-transfected plasmids. Therefore the mathematical relationship between the number of SIVmon Vpr molecules expressed “per reporter” may be very different between integrated vs co-transfected reporters.

The relatively low dose of Vpr (16.7ng – a number arrived at by using a three fold dilution series starting at 150ng)) that maximally activated a co-transfected NF $\kappa$ B reporter gene was used for confocal microscopy and also in the expression array in figure 5.12. Following the lack of changes in gene expression seen with the array it was subsequently determined that while a dose of 16.7ng maximally activated a co-transfected reporter it in fact meant that <20% of cells were transfected – few enough that even large changes in gene expression might not have been detected. Repetition of this array with a positive control (say TNF $\alpha$  stimulation) and a higher dose of Vpr ensuring transfection of close to 100% of cells (150-300ng) would be the first step in determining the gene expression profile change induced by SIVmon Vpr. Following this, unbiased quantitative mass spectrometry using SILAC may be used to identify a binding partner.

## 6.4 Conclusion

This thesis presents evidence for two effects of HIV-1 M Vpr. Firstly, it inhibits expression from co-transfected plasmids in HEK293T cells, independent of promoter or the gene being expressed (likely by inhibiting plasmid nuclear transport). Secondly it inhibits NF $\kappa$ B signalling from an integrated reporter in HEK293T cells following addition of soluble TNF $\alpha$ . Both effects are dependent on nuclear rim localisation and are partially abrogated by Q65R mutants and completely abrogated by the double mutant F34I/P35N. They may stem from an interaction which implicates Vpr as having a role in innate immune signalling. Work to further characterise species specificity and the phenotype outside of a transfection assay may provide insights into the function of Vpr *in vivo* and provide 'drugable' targets in this universally conserved lentiviral accessory protein.

## 7 Appendix of tables

Table 7.1 Plasmids used in this study

Plasmid name	Description
IFN $\beta$ -LUC	IFN $\beta$ promoter fused with firefly luciferase, AmpR, obtained from A. Bowie
ISG 56 LUC	ISG-56 promoter fused with firefly luciferase, AmpR, obtained from A. Bowie
ISRE-LUC	ISRE responsive promoter fused with firefly luciferase, AmpR, obtained from A. Bowie (Trinity College Dublin)
M5P Ren LUC	MLV LTR promoter fused with renilla luciferase obtained from R.Sumner
NF- $\kappa$ B-LUC	NF- $\kappa$ B responsive promoter fused with firefly luciferase, AmpR (Promega)
pcDNA +/- FLAG HIV-1 M CH77 Vpr	Accession No JN944909 (535) constructed by C. van Tulleken
pcDNA +/- FLAG HIV-1 M SUMA Vpr	Accession No JN944928 (535) constructed by C. van Tulleken
pcDNA +/- FLAG HIV-1 M SUMA Vpr F34I P35N	Accession No JN944928 (535) bearing F34I P35N mutations
pcDNA +/- FLAG HIV-1 M SUMA Vpr Q65R	Accession No JN944928 (535) bearing Q65R mutation
pcDNA +/- FLAG HIV-1 M WITO Vpr	Accession No AY835451(614) constructed by C. van Tulleken
pcDNA +/- FLAG HIV-1 M YU2(a+b) Vpr	Accession No M93258 (615) constructed by C. van Tulleken
pcDNA +/- FLAG HIV-1 N Vpr	Accession No AY532635 (616) constructed by C. van Tulleken
pcDNA +/- FLAG HIV-1 O Vpr	Accession No AB485666 constructed by C. van Tulleken

pcDNA +/- FLAG HIV-2 A Vpr	Accession No PJK7312AS constructed by C. van Tulleken
pcDNA +/- FLAG SIVcpzPts1 Vpr	Accession No AF447763 (38) constructed by C. van Tulleken
pcDNA +/- FLAG SIVcpzPts2 Vpr	Accession No DQ374658 (38) constructed by C. van Tulleken
pcDNA +/- FLAG SIVcpzPtt1 Vpr	Accession No: DQ373063 (617) constructed by C. van Tulleken
pcDNA +/- FLAG SIVcpzPtt2 Vpr	Accession no. X52154 (39) constructed by C. van Tulleken
pcDNA +/- FLAG SIVdeb Vpr	Accession No AY523866 (618) constructed by C. van Tulleken
pcDNA +/- FLAG SIVden Vpr	Accession No AJ580407 (619) constructed by C. van Tulleken
pcDNA +/- FLAG SIVgor Vpr	Accession No FJ424865(620) constructed by C. van Tulleken
pcDNA +/- FLAG SIVgsn Vpr	Accession No AF468658 (32) constructed by C. van Tulleken
pcDNA +/- FLAG SIVlst Vpr	Accession No AF188115 constructed by C. van Tulleken
pcDNA +/- FLAG SIVmon1 Vpr	Accession No AY340701 (32) constructed by C. van Tulleken
pcDNA +/- FLAG SIVmon1 Vpr S40N	Accession No AY340701 (32) bearing S40N mutation
pcDNA +/- FLAG SIVmon2 Vpr	Accession No AJ549283 (619) constructed by C. van Tulleken
pcDNA +/- FLAG SIVmus Vpr	Accession No AY340700 (32) constructed by C. van Tulleken
pcDNA +/- FLAG SIVolc Vpr	SIVolc Vpr Accession No FM165200 constructed by C. van Tulleken
pcDNA +/- FLAG SIVrcm Vpr	Accession No AF3496801(542) constructed by C. van Tulleken
pcDNA +/- FLAG SIVsmm Vpr	SIVsmm Vpr Accession No AF077017 constructed by C. van Tulleken
pcDNA +/- FLAG SIVsyk Vpr	Accession No AY523867 (618) constructed by C. van Tulleken

pcDNA +/- FLAG SIVtal Vpr	Accession No AY655744 (621) constructed by C. van Tulleken
pcDNA +/- FLAG SIVtan Vpr	Accession No U58991(425) constructed by C. van Tulleken
pcDNA +/- FLAG SIVver Vpr	Accession No DJ048201 (622) constructed by C. van Tulleken
pcDNA3 MAVS	MAVS with no tag constructed by C.P. Tan
pcDNA3.1 FLAG	CMV promoter, SV40 origin for episomal replication, Ampicillin resistance gene and pUC origin for selection and maintenance in <i>E. coli</i> . (Thermo-Fisher), FLAG epitope tag inserted by C.P.Tan.
pcDNA3.1 FLAG IKK $\beta$	IKK $\beta$ with N-terminal FLAG tag, AmpR. via R. Sumner (623)
pcDNA3.1 FLAG TBK1	TBK1 with N-terminal HA tag, AmpR, constructed by C. van Tulleken
pcDNA3.1 FLAG TNF $\alpha$	TNF $\alpha$ with N-terminal FLAG tag from Made by C.P. Tan
pcDNA3.1 FLAG-TRAF3	TRAF-3 with N-terminal FLAG tag, AmpR, constructed by R. Sumner
pcDNA3.1 GFP	GFP untagged. Constructed by C.P.Tan
pcDNA3.1 HA cGAS	Human cGAS with N-terminal FLAG tag, AmpR. Made by C.P.Tan
pcDNA3.1 HA STING	Human STING with N-terminal FLAG tag, AmpR. Made by C.P.Tan
pCSGW	pHR'SIN-cPPT-SGW, self-inactivating HIV-1-derived vector encoding GFP from an SFFV promoter
pDUAL SFXU Luc	HIV-1 vector construct with a Ubiquitin B promoter fused with Renilla luciferase constructed by David Stirling/Yasu Takeuchi
pGL4 CMV LUC	CMV promoter fused with firefly luciferase obtained from R.Sumner
pGL4 NF $\kappa$ B LUC	5 copies of an NF- $\kappa$ B response element in promoter fused to firefly luciferase (Promega).

pGL4 SV40 Ren LUC	SV40 promoter fused with Renilla luciferase obtained from R.Sumner
PLG4 CMV Ren LUC	CMV promoter fused with Renilla luciferase obtained from R.Sumner
pMD.G	Encodes envelope protein G of the vesicular stomatitis virus under control of CMV promoter (511)
SFFV LUC	MLV LTR promoter fused with renilla luciferase obtained from R.Sumner
TK-Renilla-LUC	TK promoter fused with renilla luciferase, AmpR, (Promega)

Table 7.2 Primers for qRT-PCR

Primer	Sequence 5'-3'
Human GAPDH FWD	5' ACCCAGAAGACTGTGGATGG 3'
Human GAPDH REV	5' TTCTAGACGGCAGGTCAGGT 3'
Human CCL-5 FWD	5' CCCAGCAGTCGTCTTTGTCA 3'
Human CCL-5 REV	5' TCCCGAACCCATTTCTTCTCT 3'
Human IFIT-2 FWD	5' GGAGGGAGAAAACCTCCTTGGGA 3'
Human IFIT-2 REV	5' GGCCAGTAGGTTGCACATTGT 3'
Human CXCL-10 FWD	5'-GAACTGTACGCTGTACCTGCA-3'
Human CXCL-10 REV	5'-TTGATGGCCTTCGATTCTGGA-3'
Human ISG-56 FWD	5'-CCTGGAGTACTATGAGCGGGC-3'
Human ISG-56 REV	5'-TGGGTGCCTAAGGACCTTGTC-3'
Human STING FWD	5'- AACACCGGTCTAGGAAGCAG-3'
Human STING REV	5'-CATATTTGGAGCGGTGACCT-3'
Human cGAS FWD	5' GGGAGCCCTGCTGTAACACTTCTTAT 3'
Human cGAS REV	5' CCTTTGCATGCTTGGGTACAAGGT 3'

Table 7.3 SDM primer sequences

Vpr Mutation	Plasmid	Sequence 5'-3'
SIVmon S40N FWD	pcDNA3	CATCCTGTACCGGCGGTACAGAGAGGGCTG
SIVmon S40N REV	pcDNA3	CAGCCCTCTCTGTACCGCCGGTACAGGATG
HIV-1 M Q65R FWD	pcDNA3	GTACCGGCACTACAGCGAGGGCTGCTACCAC
HIV-1 M Q65R REV	pcDNA3	GTGGTAGCAGCCCTCGCTGTAGTGCCGGTAC
HIV-1 M F34I P35N	pcDNA3	CAGTAAGACATTTCTCGAGACCCTGGCTTC
HIV-1 M F34I P35N	pcDNA3	GAAGCCAGGGTCTCGAGAAATGTCTTACTG

Table 7.4 Antibodies used in this study

Antibody	Source	Dilution
Rabbit-anti- $\beta$ -actin	Sigma (A2066)	1:1000
Mouse-anti-FLAG	Sigma (F1804)	1:1000
Rabbit-anti-HA	Sigma (H6908)	1:1000
Mouse-anti-HA	Cambridge Bioscience (MMS-101P)	1:200
Rabbit-anti-VCP	Ab109240 Abcam®	1:1000
Mouse-anti-Actin	Ab6276 Abcam®	1:20,000
Rabbit-anti-Nup358	C288 Catavas.E	1:2000
Mouse-anti-STING	Ab92605	1:1000

## Bibliography

1. Vallée H, Carré H. Sur la nature infectieuse de l'anémie du cheval. *Comp Rend Acad Sci.* 1904;139:331–333.
2. Ellerman V, Bang O. Experimentelle Leukämie bei Hühnern. *Zentralbl. Bakteriol. Zentralbl Bakteriol Parasitenkd Infect Hyg Abt.* 1908;46:595–609.
3. Rous P. A SARCOMA OF THE FOWL TRANSMISSIBLE BY AN AGENT SEPARABLE FROM THE TUMOR CELLS. *J Exp Med* [Internet]. The Rockefeller University Press; 1911 Apr 1 [cited 2017 Mar 14];13(4):397–411. Available from: <http://www.ncbi.nlm.nih.gov/pubmed/19867421>
4. Baltimore D. Viral RNA-dependent DNA Polymerase: RNA-dependent DNA Polymerase in Virions of RNA Tumour Viruses. *Nature* [Internet]. Nature Publishing Group; 1970 Jun 27 [cited 2017 Mar 14];226(5252):1209–11. Available from: <http://www.nature.com/doi/10.1038/2261209a0>
5. Temin HM, Mizutani S. Viral RNA-dependent DNA Polymerase: RNA-dependent DNA Polymerase in Virions of Rous Sarcoma Virus. *Nature* [Internet]. Nature Publishing Group; 1970 Jun 27 [cited 2017 Mar 14];226(5252):1211–3. Available from: <http://www.nature.com/doi/10.1038/2261211a0>
6. Freed E, Martin MA. *Field's Virology*. 4th. Vol. 2; HIVs and Their Replication. 2001. 1971–2041 p.
7. Coffin JM, Hughes SH, Varmus HE. *Retroviruses* [Internet]. Retroviruses. Cold Spring Harbor Laboratory Press; 1997 [cited 2017 Feb 11]. Available from: <http://www.ncbi.nlm.nih.gov/pubmed/21433340>
8. Gifford RJ, Katzourakis A, Tristem M, Pybus OG, Winters M, Shafer RW. A transitional endogenous lentivirus from the genome of a basal primate and implications for lentivirus evolution. *Proc Natl Acad Sci U S A* [Internet]. National Academy of Sciences; 2008 Dec 23 [cited 2017 Mar 16];105(51):20362–7. Available from: <http://www.ncbi.nlm.nih.gov/pubmed/19075221>
9. Gilbert C, Maxfield DG, Goodman SM, Feschotte C, Marx P, Vences M. Parallel Germline Infiltration of a Lentivirus in Two Malagasy Lemurs. Malik HS, editor. *PLoS Genet* [Internet]. Los Alamos National Laboratory, Theoretical Biology and Biophysics; 2009 Mar 20 [cited 2017 Mar 16];5(3):e1000425. Available from: <http://dx.plos.org/10.1371/journal.pgen.1000425>
10. Sharp PM, Rayner JC, Hahn BH. Great Apes and Zoonoses. *Science* (80- ). 2013;340(6130).
11. Gottlieb MS, Schroff R, Schanker HM, Weisman JD, Fan PT, Wolf RA, et al. *Pneumocystis carinii* pneumonia and mucosal candidiasis in previously healthy homosexual men: evidence of

- a new acquired cellular immunodeficiency. Vol. 305, The New England journal of medicine. 1981. p. 1425–31.
12. Barre-Sinoussi F, Chermann J, Rey F, Nugeyre M, Chamaret S, Gruest J, et al. Isolation of a T-lymphotropic retrovirus from a patient at risk for acquired immune deficiency syndrome (AIDS). *Science* (80- ). 1983;220(4599).
  13. Patterson S, Cescon A, Samji H, Chan K, Zhang W, Raboud J, et al. Life expectancy of HIV-positive individuals on combination antiretroviral therapy in Canada. *BMC Infect Dis* [Internet]. BioMed Central; 2015 Jul 17 [cited 2017 Feb 13];15:274. Available from: <http://www.ncbi.nlm.nih.gov/pubmed/26183704>
  14. Antiretroviral Therapy Cohort Collaboration. Life expectancy of individuals on combination antiretroviral therapy in high-income countries: a collaborative analysis of 14 cohort studies. *Lancet* [Internet]. 2008 Jul 26 [cited 2017 Feb 13];372(9635):293–9. Available from: <http://www.ncbi.nlm.nih.gov/pubmed/18657708>
  15. De Leys R, Vanderborght B, Vanden Haesevelde M, Heyndrickx L, van Geel A, Wauters C, et al. Isolation and partial characterization of an unusual human immunodeficiency retrovirus from two persons of west-central African origin. *J Virol* [Internet]. American Society for Microbiology (ASM); 1990 Mar [cited 2017 Mar 16];64(3):1207–16. Available from: <http://www.ncbi.nlm.nih.gov/pubmed/2304140>
  16. Plantier J-C, Leoz M, Dickerson JE, De Oliveira F, Cordonnier F, Lemée V, et al. A new human immunodeficiency virus derived from gorillas. *Nat Med* [Internet]. Nature Publishing Group; 2009 Aug [cited 2015 Apr 3];15(8):871–2. Available from: <http://dx.doi.org/10.1038/nm.2016>
  17. Gao F, Bailes E, Robertson DL, Chen Y, Rodenburg CM, Michael SF, et al. Origin of HIV-1 in the chimpanzee *Pan troglodytes troglodytes*. *Nature* [Internet]. Nature Publishing Group; 1999 Feb 4 [cited 2016 Dec 4];397(6718):436–41. Available from: <http://www.nature.com/doi/10.1038/17130>
  18. Sharp PM, Hahn BH. Origins of HIV and the AIDS pandemic. *Cold Spring Harb Perspect Med* [Internet]. 2011 Sep [cited 2014 Jul 19];1(1):a006841. Available from: <http://www.pubmedcentral.nih.gov/articlerender.fcgi?artid=3234451&tool=pmcentrez&rendertype=abstract>
  19. Silvestri G, Sodora DL, Koup RA, Paiardini M, O'Neil SP, McClure HM, et al. Nonpathogenic SIV Infection of Sooty Mangabeys Is Characterized by Limited Bystander Immunopathology Despite Chronic High-Level Viremia. *Immunity* [Internet]. 2003 Mar [cited 2015 Apr 12];18(3):441–52. Available from: <http://www.sciencedirect.com/science/article/pii/S1074761303000608>

20. De Cock KM, Adjorlolo G, Ekpini E, Sibailly T, Kouadio J, Maran M, et al. Epidemiology and transmission of HIV-2. Why there is no HIV-2 pandemic. *JAMA* [Internet]. 1993 Nov 3 [cited 2017 Mar 21];270(17):2083–6. Available from: <http://www.ncbi.nlm.nih.gov/pubmed/8147962>
21. Heuverswyn F Van, Li Y, Bailes E, Neel C, Lafay B, Keele BF, et al. Genetic diversity and phylogeographic clustering of SIVcpzPtt in wild chimpanzees in Cameroon. 2007;
22. Keele BF, Van Heuverswyn F, Li Y, Bailes E, Takehisa J, Santiago ML, et al. Chimpanzee reservoirs of pandemic and nonpandemic HIV-1. *Science* [Internet]. 2006;313(5786):523–6. Available from: <http://www.pubmedcentral.nih.gov/articlerender.fcgi?artid=2442710&tool=pmcentrez&rendertype=abstract>
23. Wertheim JO, Worobey M. Dating the age of the SIV lineages that gave rise to HIV-1 and HIV-2. *PLoS Comput Biol*. 2009;5(5).
24. Hemelaar J, Gouws E, Ghys PD, Osmanov S, WHO-UNAIDS Network for HIV Isolation and Characterisation. Global trends in molecular epidemiology of HIV-1 during 2000–2007. *AIDS* [Internet]. 2011 Mar 13 [cited 2017 Mar 21];25(5):679–89. Available from: <http://www.ncbi.nlm.nih.gov/pubmed/21297424>
25. Guindon S, Gascuel O. A simple, fast, and accurate algorithm to estimate large phylogenies by maximum likelihood. *Syst Biol* [Internet]. 2003 Oct [cited 2017 Apr 2];52(5):696–704. Available from: <http://www.ncbi.nlm.nih.gov/pubmed/14530136>
26. Souquiere S, Bibollet-Ruche F, Robertson DL, Makuwa M, Apetrei C, Onanga R, et al. Wild *Mandrillus sphinx* Are Carriers of Two Types of Lentivirus. *J Virol* [Internet]. 2001 Aug 1 [cited 2017 Mar 16];75(15):7086–96. Available from: <http://jvi.asm.org/cgi/doi/10.1128/JVI.75.15.7086-7096.2001>
27. Takehisa J, Kraus MH, Decker JM, Li Y, Keele BF, Bibollet-Ruche F, et al. Generation of Infectious Molecular Clones of Simian Immunodeficiency Virus from Fecal Consensus Sequences of Wild Chimpanzees. *J Virol* [Internet]. 2007 May 9 [cited 2015 Apr 11];81(14):7463–75. Available from: <http://www.pubmedcentral.nih.gov/articlerender.fcgi?artid=1933379&tool=pmcentrez&rendertype=abstract>
28. Courgnaud V, Salemi M, Pourrut X, Mpoudi-Ngole E, Abela B, Auzel P, et al. Characterization of a novel simian immunodeficiency virus with a vpu gene from greater spot-nosed monkeys (*Cercopithecus nictitans*) provides new insights into simian/human immunodeficiency virus phylogeny. *J Virol* [Internet]. American Society for Microbiology (ASM); 2002 Aug [cited 2017 Mar 5];76(16):8298–309. Available from: <http://www.ncbi.nlm.nih.gov/pubmed/12134035>

29. Beer BE, Bailes E, Sharp PM, Hirsch VM. Diversity and Evolution of Primate Lentiviruses. [cited 2017 Mar 24]; Available from: <http://www.cbs.dtu.dk/courses/27622/2009/exercises/ExMulPhyl/beer.pdf>
30. Aghokeng AF, Ayoub A, Ahuka S, Liegoies F, Mbala P, Muyembe J-J, et al. Genetic diversity of simian lentivirus in wild De Brazza's monkeys (*Cercopithecus neglectus*) in Equatorial Africa. *J Gen Virol* [Internet]. Microbiology Society; 2010 Jul [cited 2017 Mar 16];91(Pt 7):1810–6. Available from: <http://www.ncbi.nlm.nih.gov/pubmed/20219893>
31. Aghokeng AF, Mpoudi-Ngole E, Dimodi H, Atem-Tambe A, Tongo M, Butel C, et al. Inaccurate Diagnosis of HIV-1 Group M and O Is a Key Challenge for Ongoing Universal Access to Antiretroviral Treatment and HIV Prevention in Cameroon. Pai NP, editor. *PLoS One* [Internet]. Public Library of Science; 2009 Nov 6 [cited 2017 Mar 16];4(11):e7702. Available from: <http://dx.plos.org/10.1371/journal.pone.0007702>
32. Bailes E, Gao F, Bibollet-Ruche F, Cournaud V, Peeters M, Marx PA, et al. Hybrid Origin of SIV in Chimpanzees. *Science* (80- ). 2003;300(5626).
33. Leendertz SAJ, Locatelli S, Boesch C, Kücherer C, Formenty P, Liegeois F, et al. No evidence for transmission of SIVwrc from western red colobus monkeys (*piliocolobus badius badius*) to wild west african chimpanzees (*pan troglodytes verus*) despite high exposure through hunting. *BMC Microbiol* [Internet]. BioMed Central; 2011 [cited 2016 Dec 4];11(1):24. Available from: <http://bmcmicrobiol.biomedcentral.com/articles/10.1186/1471-2180-11-24>
34. Gagneux P, Wills C, Gerloff U, Tautz D, Morin PA, Boesch C, et al. Mitochondrial sequences show diverse evolutionary histories of African hominoids. *Proc Natl Acad Sci U S A* [Internet]. National Academy of Sciences; 1999 Apr 27 [cited 2016 Dec 4];96(9):5077–82. Available from: <http://www.ncbi.nlm.nih.gov/pubmed/10220421>
35. Peeters M, Delaporte E. Simian retroviruses in African apes. *Clin Microbiol Infect* [Internet]. Blackwell Publishing Ltd; 2012 Jun [cited 2016 Dec 3];18(6):514–20. Available from: <http://linkinghub.elsevier.com/retrieve/pii/S1198743X14641434>
36. Fischer W, Apetrei C, Santiago ML, Li Y, Gautam R, Pandrea I, et al. Distinct evolutionary pressures underlie diversity in simian immunodeficiency virus and human immunodeficiency virus lineages. *J Virol* [Internet]. 2012 Dec 15 [cited 2016 Feb 26];86(24):13217–31. Available from: <http://jvi.asm.org/cgi/content/long/86/24/13217>
37. Keele BF, Jones JH, Terio KA, Estes JD, Rudicell RS, Wilson ML, et al. Increased mortality and AIDS-like immunopathology in wild chimpanzees infected with SIVcpz. *Nature* [Internet]. Nature Publishing Group; 2009 Jul 23 [cited 2016 Dec 4];460(7254):515–9. Available from: <http://www.nature.com/doi/10.1038/nature08200>

38. Etienne L, Nerrienet E, LeBreton M, Bibila GT, Foupouapouognigni Y, Rousset D, et al. Characterization of a new simian immunodeficiency virus strain in a naturally infected Pan troglodytes troglodytes chimpanzee with AIDS related symptoms. *Retrovirology* [Internet]. BioMed Central; 2011 Jan 13 [cited 2017 Mar 23];8:4. Available from: <http://www.ncbi.nlm.nih.gov/pubmed/21232091>
39. Sharp PM, Shaw GM, Hahn BH. Simian immunodeficiency virus infection of chimpanzees. *J Virol* [Internet]. American Society for Microbiology; 2005 Apr [cited 2016 Dec 3];79(7):3891–902. Available from: <http://www.ncbi.nlm.nih.gov/pubmed/15767392>
40. Keele BF, Heuverswyn F Van, Li Y, Bailes E, Santiago ML, Bibollet-ruche F, et al. Chimpanzee Reservoirs of Pandemic and Nonpandemic HIV-1 Chimpanzee Reservoirs of Pandemic and Nonpandemic HIV-1 Chimpanzee Reservoirs of Pandemic and Nonpandemic HIV-1. *Science* (80- ). 2006;(May):1–8.
41. Worobey M, Santiago ML, Keele BF, Ndjango J-BN, Joy JB, Labama BL, et al. Origin of AIDS: contaminated polio vaccine theory refuted. *Nature* [Internet]. 2004 Apr 22 [cited 2015 Apr 11];428(6985):820. Available from: <http://dx.doi.org/10.1038/428820a>
42. Tristem M, Marshall C, Karpas A, Hill F, Klug A. Evolution of the primate lentiviruses: evidence from vpx and vpr. *EMBO J* [Internet]. 1992 [cited 2017 Mar 21];1(19):3405–341. Available from: <https://www.ncbi.nlm.nih.gov/pmc/articles/PMC556875/pdf/emboj00094-0250.pdf>
43. Sharp PM, Bailes E, Stevenson M, Emerman M, Hahn BH. Gene acquisition in HIV and SIV. *Nature* [Internet]. Nature Publishing Group; 1996 Oct 17 [cited 2017 Mar 21];383(6601):586–7. Available from: <http://www.nature.com/doifinder/10.1038/383586a0>
44. Berger G, Lawrence M, Hué S, Neil SJD. G2/M cell cycle arrest correlates with primate lentiviral Vpr interaction with the SLX4 complex. *J Virol* [Internet]. 2015 Jan 1 [cited 2015 Apr 12];89(1):230–40. Available from: <http://jvi.asm.org/content/89/1/230.long>
45. UNAIDS. Fact sheet 2016 | UNAIDS [Internet]. UNAIDS. 2016. Available from: <http://www.unaids.org/en/resources/fact-sheet>
46. UN General Assembly. Political Declaration on HIV and AIDS: On the Fast-Track to Accelerate the Fight against HIV and to End the AIDS Epidemic by 2030 | UNAIDS [Internet]. 2016 [cited 2017 Mar 22]. Available from: <http://www.unaids.org/en/resources/documents/2016/2016-political-declaration-HIV-AIDS>
47. Degenhardt L, Mathers B, Vickerman P, Rhodes T, Latkin C, Hickman M. Prevention of HIV infection for people who inject drugs: why individual, structural, and combination approaches are needed. *Lancet* [Internet]. VU University Medical Center, Amsterdam; 2010 Jul 24 [cited 2017 Mar 21];376(9737):285–301. Available from:

<http://www.ncbi.nlm.nih.gov/pubmed/20650522>

48. Birrell PJ, Gill ON, Delpech VC, Brown AE, Desai S, Chadborn TR, et al. HIV incidence in men who have sex with men in England and Wales 2001–10: a nationwide population study. *Lancet Infect Dis* [Internet]. 2013 Apr [cited 2017 Mar 21];13(4):313–8. Available from: <http://www.ncbi.nlm.nih.gov/pubmed/23375420>
49. Beyrer C, Sullivan P, Sanchez J, Baral SD, Collins C, Wirtz AL, et al. The increase in global HIV epidemics in MSM. *AIDS* [Internet]. 2013 Nov 13 [cited 2017 Mar 21];27(17):2665–78. Available from: <http://www.ncbi.nlm.nih.gov/pubmed/23842129>
50. Mayer KH, Mimiaga MJ. Past as Prologue: The Refractory and Evolving HIV Epidemic Among Men Who Have Sex With Men. *Clin Infect Dis* [Internet]. Oxford University Press; 2011 Jun 1 [cited 2017 Mar 21];52(11):1371–3. Available from: <https://academic.oup.com/cid/article-lookup/doi/10.1093/cid/cir206>
51. Ortblad KF, Lozano R, Murray CJL. The burden of HIV: insights from the Global Burden of Disease Study 2010. *AIDS* [Internet]. 2013 Aug 24 [cited 2017 Mar 22];27(13):2003–17. Available from: <http://www.ncbi.nlm.nih.gov/pubmed/23660576>
52. UNAIDS. HIV estimates with uncertainty bounds 1990-2015 | UNAIDS [Internet]. USAIDS. 2016. Available from: [http://www.unaids.org/en/resources/documents/2016/HIV\\_estimates\\_with\\_uncertainty\\_bounds\\_1990-2015](http://www.unaids.org/en/resources/documents/2016/HIV_estimates_with_uncertainty_bounds_1990-2015)
53. Chen P, Chen BK, Mosoian A, Hays T, Ross MJ, Klotman PE, et al. Virological Synapses Allow HIV-1 Uptake and Gene Expression in Renal Tubular Epithelial Cells. *J Am Soc Nephrol* [Internet]. 2011 Mar 1 [cited 2017 Mar 22];22(3):496–507. Available from: <http://www.ncbi.nlm.nih.gov/pubmed/21335514>
54. Liu Y, Liu H, Kim BO, Gattone VH, Li J, Nath A, et al. CD4-independent infection of astrocytes by human immunodeficiency virus type 1: requirement for the human mannose receptor. *J Virol* [Internet]. 2004 Apr [cited 2017 Mar 22];78(8):4120–33. Available from: <http://www.ncbi.nlm.nih.gov/pubmed/15047828>
55. McMichael AJ, Borrow P, Tomaras GD, Goonetilleke N, Haynes BF. The immune response during acute HIV-1 infection: clues for vaccine development. *Nat Rev Immunol* [Internet]. Nature Publishing Group; 2010 Jan [cited 2015 Mar 16];10(1):11–23. Available from: <http://dx.doi.org/10.1038/nri2674>
56. Stacey AR, Norris PJ, Qin L, Haygreen E a, Taylor E, Heitman J, et al. Induction of a striking systemic cytokine cascade prior to peak viremia in acute human immunodeficiency virus type 1 infection, in contrast to more modest and delayed responses in acute hepatitis B and C virus

infections. *J Virol*. 2009;83(8):3719–33.

57. de Wolf F, Spijkerman I, Schellekens PT, Langendam M, Kuiken C, Bakker M, et al. AIDS prognosis based on HIV-1 RNA, CD4+ T-cell count and function: markers with reciprocal predictive value over time after seroconversion. *AIDS* [Internet]. 1997 Dec [cited 2017 Mar 22];11(15):1799–806. Available from: <http://www.ncbi.nlm.nih.gov/pubmed/9412697>
58. Fraser C, Lythgoe K, Leventhal GE, Shirreff G, Hollingsworth TD, Alizon S, et al. Virulence and pathogenesis of HIV-1 infection: an evolutionary perspective. *Science* [Internet]. Europe PMC Funders; 2014 Mar 21 [cited 2016 Dec 3];343(6177):1243727. Available from: <http://www.ncbi.nlm.nih.gov/pubmed/24653038>
59. Pilcher CD, Eron JJ, Galvin S, Gay C, Cohen MS. Acute HIV revisited: new opportunities for treatment and prevention. *J Clin Invest* [Internet]. 2004 Apr 1 [cited 2017 Mar 23];113(7):937–45. Available from: <http://www.ncbi.nlm.nih.gov/pubmed/15057296>
60. Trautmann L, Janbazian L, Chomont N, Said EA, Gimmig S, Bessette B, et al. Upregulation of PD-1 expression on HIV-specific CD8+ T cells leads to reversible immune dysfunction. *Nat Med* [Internet]. 2006 Nov 20 [cited 2017 Mar 22];12(10):1198–202. Available from: <http://www.ncbi.nlm.nih.gov/pubmed/16917489>
61. Cooper A, García M, Petrovas C, Yamamoto T, Koup R a, Nabel GJ. HIV-1 causes CD4 cell death through DNA-dependent protein kinase during viral integration. *Nature* [Internet]. 2013 Jun 20 [cited 2013 Dec 16];498(7454):376–9. Available from: <http://www.ncbi.nlm.nih.gov/pubmed/23739328>
62. Doitsh G, Galloway NLK, Geng X, Yang Z, Monroe KM, Zepeda O, et al. Cell death by pyroptosis drives CD4 T-cell depletion in HIV-1 infection. *Nature* [Internet]. 2014;505(7484):509–14. Available from: <http://dx.doi.org/10.1038/nature12940>
63. Richman DD, Wrin T, Little SJ, Petropoulos CJ. Rapid evolution of the neutralizing antibody response to HIV type 1 infection. *Proc Natl Acad Sci U S A* [Internet]. 2003 Apr 1 [cited 2017 Mar 22];100(7):4144–9. Available from: <http://www.ncbi.nlm.nih.gov/pubmed/12644702>
64. Walker LM, Huber M, Doores KJ, Falkowska E, Pejchal R, Julien J-P, et al. Broad neutralization coverage of HIV by multiple highly potent antibodies. *Nature* [Internet]. 2011 Sep 22 [cited 2017 Mar 22];477(7365):466–70. Available from: <http://www.ncbi.nlm.nih.gov/pubmed/21849977>
65. Liao H-X, Lynch R, Zhou T, Gao F, Alam SM, Boyd SD, et al. Co-evolution of a broadly neutralizing HIV-1 antibody and founder virus. *Nature* [Internet]. 2013 Apr 25 [cited 2017 Mar 22];496(7446):469–76. Available from: <http://www.ncbi.nlm.nih.gov/pubmed/23552890>
66. Mehandru S, Poles MA, Tenner-Racz K, Manuelli V, Jean-Pierre P, Lopez P, et al. Mechanisms

- of Gastrointestinal CD4+ T-Cell Depletion during Acute and Early Human Immunodeficiency Virus Type 1 Infection. *J Virol* [Internet]. 2007 Jan 15 [cited 2017 Mar 22];81(2):599–612. Available from: <http://www.ncbi.nlm.nih.gov/pubmed/17065209>
67. Brenchley JM, Price DA, Schacker TW, Asher TE, Silvestri G, Rao S, et al. Microbial translocation is a cause of systemic immune activation in chronic HIV infection. *Nat Med* [Internet]. 2007 Jan 19 [cited 2017 Mar 22];12(12):1365–71. Available from: <http://www.ncbi.nlm.nih.gov/pubmed/17115046>
  68. Meier A, Chang JJ, Chan ES, Pollard RB, Sidhu HK, Kulkarni S, et al. Sex differences in the Toll-like receptor–mediated response of plasmacytoid dendritic cells to HIV-1. *Nat Med* [Internet]. 2009 Aug 13 [cited 2017 Mar 22];15(8):955–9. Available from: <http://www.ncbi.nlm.nih.gov/pubmed/19597505>
  69. Hsue PY, Hunt PW, Sinclair E, Brecht B, Franklin A, Killian M, et al. Increased carotid intima-media thickness in HIV patients is associated with increased cytomegalovirus-specific T-cell responses. *AIDS* [Internet]. 2006 Nov 28 [cited 2017 Mar 22];20(18):2275–83. Available from: <http://www.ncbi.nlm.nih.gov/pubmed/17117013>
  70. Prendergast A, Prado JG, Kang Y-H, Chen F, Riddell LA, Luzzi G, et al. HIV-1 infection is characterized by profound depletion of CD161+ Th17 cells and gradual decline in regulatory T cells. *AIDS* [Internet]. 2010 Feb 20 [cited 2017 Mar 22];24(4):491–502. Available from: <http://www.ncbi.nlm.nih.gov/pubmed/20071976>
  71. J Buzón M, Massanella M, Llibre JM, Esteve A, Dahl V, Puertas MC, et al. HIV-1 replication and immune dynamics are affected by raltegravir intensification of HAART-suppressed subjects. *Nat Med* [Internet]. 2010 Apr 14 [cited 2017 Feb 12];16(4):460–5. Available from: <http://www.ncbi.nlm.nih.gov/pubmed/20228817>
  72. Terrence Higgins Trust. What are HIV and AIDS? | Terrence Higgins Trust [Internet]. 2016. [cited 2017 Mar 23]. Available from: [http://www.tht.org.uk/sexual-health/About-HIV/What-are-HIV-and-AIDS\\_qm\\_](http://www.tht.org.uk/sexual-health/About-HIV/What-are-HIV-and-AIDS_qm_)
  73. WHO. INTERIM WHO CLINICAL STAGING OF HIV/AIDS AND HIV/AIDS CASE DEFINITIONS FOR SURVEILLANCE AFRICAN REGION. 2005 [cited 2017 Mar 23]; Available from: <http://www.who.int/hiv/pub/guidelines/clinicalstaging.pdf>
  74. Rodger AJ, Lodwick R, Schechter M, Deeks S, Amin J, Gilson R, et al. Mortality in well controlled HIV in the continuous antiretroviral therapy arms of the SMART and ESPRIT trials compared with the general population. *AIDS* [Internet]. 2013 Mar 27 [cited 2017 Mar 22];27(6):973–9. Available from: <http://www.ncbi.nlm.nih.gov/pubmed/23698063>
  75. Helleberg M, Kronborg G, Larsen CS, Pedersen G, Pedersen C, Gerstoft J, et al. Causes of

death among Danish HIV patients compared with population controls in the period 1995–2008. *Infection* [Internet]. 2012 Dec 12 [cited 2017 Mar 22];40(6):627–34. Available from: <http://www.ncbi.nlm.nih.gov/pubmed/22791407>

76. Kulkarni SP, Shah KR, Sarma K V., Mahajan AP. Clinical Uncertainties, Health Service Challenges, and Ethical Complexities of HIV “Test-and-Treat”: A Systematic Review. *Am J Public Health* [Internet]. 2013 Jun [cited 2017 Mar 22];103(6):e14–23. Available from: <http://www.ncbi.nlm.nih.gov/pubmed/23597344>
77. Chair DC, Waters L, Chair V, Ahmed N, Angus B, Boffito M, et al. BHIVA guidelines for the treatment of HIV---1---positive adults with antiretroviral therapy 2015 Writing Group. 2015 [cited 2017 May 7]; Available from: [www.nice.org.uk/accreditation](http://www.nice.org.uk/accreditation)
78. World Health Organization. WHO HIV drug resistance report, 2012 [Internet]. World Health Organization; 2012 [cited 2017 Mar 22]. 78 p. Available from: <http://www.who.int/hiv/pub/drugresistance/report2012/en/>
79. Cohen MS, Chen YQ, Mccauley M, Gamble T, Hosseinipour MC, Kumarasamy N, et al. Prevention of HIV-1 Infection with Early Antiretroviral Therapy. *n engl j med* [Internet]. 2011 [cited 2017 Mar 22];365(11):493–505. Available from: <http://www.nejm.org/doi/pdf/10.1056/NEJMoa1105243>
80. Rodger AJ, Cambiano V, Bruun T, Vernazza P, Collins S, van Lunzen J, et al. Sexual Activity Without Condoms and Risk of HIV Transmission in Serodifferent Couples When the HIV-Positive Partner Is Using Suppressive Antiretroviral Therapy. *JAMA* [Internet]. American Medical Association; 2016 Jul 12 [cited 2017 Mar 22];316(2):171. Available from: <http://jama.jamanetwork.com/article.aspx?doi=10.1001/jama.2016.5148>
81. Thigpen MC, Kebaabetswe PM, Paxton LA, Smith DK, Rose CE, Segolodi TM, et al. Antiretroviral Preexposure Prophylaxis for Heterosexual HIV Transmission in Botswana. *N Engl J Med* [Internet]. Massachusetts Medical Society ; 2012 Aug 2 [cited 2017 Mar 22];367(5):423–34. Available from: <http://www.nejm.org/doi/abs/10.1056/NEJMoa1110711>
82. Plazy M, Farouki K El, Iwuji C, Okesola N, Orne-Gliemann J, Larmarange J, et al. Access to HIV care in the context of universal test and treat: challenges within the ANRS 12249 TasP cluster-randomized trial in rural South Africa. *J Int AIDS Soc* [Internet]. 2016 [cited 2017 Mar 22];19(1):20913. Available from: <http://www.ncbi.nlm.nih.gov/pubmed/27258430>
83. Connor EM, Sperling RS, Gelber R, Kiselev P, Scott G, O’Sullivan MJ, et al. Reduction of Maternal-Infant Transmission of Human Immunodeficiency Virus Type 1 with Zidovudine Treatment. *N Engl J Med* [Internet]. Massachusetts Medical Society ; 1994 Nov 3 [cited 2017 Mar 22];331(18):1173–80. Available from: <http://www.nejm.org/doi/abs/10.1056/NEJM199411033311801>

84. Townsend CL, Cortina-Borja M, Peckham CS, de Ruiter A, Lyall H, Tookey PA. Low rates of mother-to-child transmission of HIV following effective pregnancy interventions in the United Kingdom and Ireland, 2000-2006. *AIDS* [Internet]. 2008 May 11 [cited 2017 Mar 22];22(8):973–81. Available from: <http://www.ncbi.nlm.nih.gov/pubmed/18453857>
85. McCormack S, Dunn DT, Desai M, Dolling DI, Gafos M, Gilson R, et al. Pre-exposure prophylaxis to prevent the acquisition of HIV-1 infection (PROUD): effectiveness results from the pilot phase of a pragmatic open-label randomised trial. *Lancet* [Internet]. 2016 Jan 2 [cited 2017 Mar 22];387(10013):53–60. Available from: <http://www.ncbi.nlm.nih.gov/pubmed/26364263>
86. Grant RM, Lama JR, Anderson PL, McMahan V, Liu AY, Vargas L, et al. Preexposure chemoprophylaxis for HIV prevention in men who have sex with men. *N Engl J Med* [Internet]. NIH Public Access; 2010 Dec 30 [cited 2017 Mar 22];363(27):2587–99. Available from: <http://www.ncbi.nlm.nih.gov/pubmed/21091279>
87. Baeten JM, Donnell D, Ndase P, Mugo NR, Campbell JD, Wangisi J, et al. Antiretroviral prophylaxis for HIV prevention in heterosexual men and women. *N Engl J Med* [Internet]. NIH Public Access; 2012 Aug 2 [cited 2017 Mar 22];367(5):399–410. Available from: <http://www.ncbi.nlm.nih.gov/pubmed/22784037>
88. NHS England. NHS England » Prep Statement [Internet]. 2016 [cited 2017 Mar 22]. Available from: <https://www.england.nhs.uk/2016/12/hiv-prevention-preprogramme/>
89. Muesing MA, Smith DH, Cabradilla CD, Benton C V., Lasky LA, Capon DJ. Nucleic acid structure and expression of the human AIDS/lymphadenopathy retrovirus. *Nature* [Internet]. Nature Publishing Group; 1985 Feb 7 [cited 2017 Feb 11];313(6002):450–8. Available from: <http://www.nature.com/doi/10.1038/313450a0>
90. Krebs FC, Hogan TH, Quiterio S, Gartner S, Wigdahl B. Lentiviral LTR-directed Expression, Sequence Variation, and Disease Pathogenesis.
91. Kurth R, Bannert N. *Retroviruses : molecular biology, genomics, and pathogenesis* [Internet]. Caister Academic Press; 2010 [cited 2017 Mar 14]. 454 p. Available from: [https://books.google.co.uk/books/about/Retroviruses.html?id=Vx3HbMRDj11C&redir\\_esc=y](https://books.google.co.uk/books/about/Retroviruses.html?id=Vx3HbMRDj11C&redir_esc=y)
92. Mishra SH, Shelley CM, Barrow DJ, Darby MK, Germann MW. Solution structures and characterization of human immunodeficiency virus Rev responsive element IIB RNA targeting zinc finger proteins. *Biopolymers* [Internet]. 2006 Nov [cited 2017 Feb 11];83(4):352–64. Available from: <http://www.ncbi.nlm.nih.gov/pubmed/16826557>
93. Jablonski JA, Buratti E, Stuanis C, Caputi M. The secondary structure of the human immunodeficiency virus type 1 transcript modulates viral splicing and infectivity. *J Virol* [Internet].

- American Society for Microbiology; 2008 Aug [cited 2017 Feb 11];82(16):8038–50. Available from: <http://www.ncbi.nlm.nih.gov/pubmed/18550660>
94. Harrison GP, Lever AM. The human immunodeficiency virus type 1 packaging signal and major splice donor region have a conserved stable secondary structure. *J Virol* [Internet]. American Society for Microbiology (ASM); 1992 Jul [cited 2017 Feb 11];66(7):4144–53. Available from: <http://www.ncbi.nlm.nih.gov/pubmed/1602537>
  95. Jacks T, Power MD, Masiarz FR, Luciw PA, Barr PJ, Varmus HE. Characterization of ribosomal frameshifting in HIV-1 gag-pol expression. *Nature* [Internet]. 1988 Jan 21 [cited 2017 Jan 14];331(6153):280–3. Available from: <http://www.ncbi.nlm.nih.gov/pubmed/2447506>
  96. Freed EO. HIV-1 replication. *Somat Cell Mol Genet* [Internet]. 2001;26(1–6):13–33. Available from: <http://www.ncbi.nlm.nih.gov/pubmed/12465460>
  97. Freed EO. HIV-1 assembly, release and maturation. *Nat Rev Microbiol* [Internet]. Nature Research; 2015 Jun 29 [cited 2017 Feb 10];13(8):484–96. Available from: <http://www.nature.com/doi/10.1038/nrmicro3490>
  98. Karn J, Stoltzfus CM. Transcriptional and posttranscriptional regulation of HIV-1 gene expression. *Cold Spring Harb Perspect Med* [Internet]. Cold Spring Harbor Laboratory Press; 2012 Feb [cited 2016 Dec 30];2(2):a006916. Available from: <http://www.ncbi.nlm.nih.gov/pubmed/22355797>
  99. Sundquist WI, Kräusslich H-G. HIV-1 assembly, budding, and maturation. *Cold Spring Harb Perspect Med* [Internet]. 2012 Jul [cited 2013 Mar 11];2(7):a006924. Available from: <http://www.pubmedcentral.nih.gov/articlerender.fcgi?artid=3385941&tool=pmcentrez&rendertype=abstract>
  100. Kramer A, Schwebke I, Kampf G. How long do nosocomial pathogens persist on inanimate surfaces? A systematic review. *BMC Infect Dis* [Internet]. BioMed Central; 2006 Aug 16 [cited 2017 Mar 23];6:130. Available from: <http://www.ncbi.nlm.nih.gov/pubmed/16914034>
  101. Wilen CB, Tilton JC, Doms RW. Molecular Mechanisms of HIV Entry. In Springer US; 2012 [cited 2016 Dec 30]. p. 223–42. Available from: [http://link.springer.com/10.1007/978-1-4614-0980-9\\_10](http://link.springer.com/10.1007/978-1-4614-0980-9_10)
  102. Chan DC, Fass D, Berger JM, Kim PS. Core Structure of gp41 from the HIV Envelope Glycoprotein. *Cell*. 1997;89(2):263–73.
  103. Kwong PD, Wyatt R, Robinson J, Sweet RW, Sodroski J, Hendrickson W a. Structure of an HIV gp120 envelope glycoprotein in complex with the CD4 receptor and a neutralizing human antibody. *Nature*. 1998;393(June):648–59.

104. Engelman A, Cherepanov P. The structural biology of HIV-1: mechanistic and therapeutic insights. *Nat Rev Microbiol* [Internet]. NIH Public Access; 2012 Mar 16 [cited 2016 Dec 30];10(4):279–90. Available from: <http://www.ncbi.nlm.nih.gov/pubmed/22421880>
105. Hill CP, Worthylake D, Bancroft DP, Christensen AM, Sundquist WI. Crystal structures of the trimeric human immunodeficiency virus type 1 matrix protein: implications for membrane association and assembly. *Proc Natl Acad Sci U S A* [Internet]. National Academy of Sciences; 1996 Apr 2 [cited 2016 Dec 30];93(7):3099–104. Available from: <http://www.ncbi.nlm.nih.gov/pubmed/8610175>
106. Pornillos O, Ganser-Pornillos BK, Kelly BN, Hua Y, Whitby FG, Stout CD, et al. X-Ray Structures of the Hexameric Building Block of the HIV Capsid. *Cell* [Internet]. 2009 Jun 26 [cited 2016 Dec 9];137(7):1282–92. Available from: <http://www.ncbi.nlm.nih.gov/pubmed/19523676>
107. Zhao G, Perilla JR, Yufenyuy EL, Meng X, Chen B, Ning J, et al. Mature HIV-1 capsid structure by cryo-electron microscopy and all-atom molecular dynamics. *Nature* [Internet]. NIH Public Access; 2013 May 30 [cited 2016 Dec 29];497(7451):643–6. Available from: <http://www.ncbi.nlm.nih.gov/pubmed/23719463>
108. Gitti RK, Lee BM, Walker J, Summers MF, Yoo S, Sundquist WI. Structure of the amino-terminal core domain of the HIV-1 capsid protein. *Science* [Internet]. 1996 Jul 12 [cited 2016 Dec 9];273(5272):231–5. Available from: <http://www.ncbi.nlm.nih.gov/pubmed/8662505>
109. Bhattacharya A, Alam SL, Fricke T, Zadrozny K, Sedzicki J, Taylor AB, et al. Structural basis of HIV-1 capsid recognition by PF74. 2014;1–6.
110. Ganser BK, Li S, Klishko VY, Finch JT, Sundquist WI. Assembly and Analysis of Conical Models for the HIV-1 Core. *Science* (80- ) [Internet]. 1999;283(5398):80–3. Available from: <http://www.sciencemag.org/content/283/5398/80%5Cnhttp://www.ncbi.nlm.nih.gov/pubmed/9872746%5Cnhttp://www.sciencemag.org.scd-rproxy.u-strasbg.fr/content/283/5398/80.long%5Cnhttp://www.sciencemag.org/content/283/5398/80.full.pdf>
111. Zhao G, Perilla JR, Yufenyuy EL, Meng X, Chen B, Ning J, et al. Mature HIV-1 capsid structure by cryo-electron microscopy and all-atom molecular dynamics. *Nature* [Internet]. NIH Public Access; 2013 May 30 [cited 2016 Dec 9];497(7451):643–6. Available from: <http://www.ncbi.nlm.nih.gov/pubmed/23719463>
112. D’Souza V, Summers MF. How retroviruses select their genomes. *Nat Rev Microbiol* [Internet]. Nature Publishing Group; 2005 Aug [cited 2016 Dec 29];3(8):643–55. Available from: <http://www.nature.com/doifinder/10.1038/nrmicro1210>
113. Kutluay SB, Bieniasz PD, Harrison G, Lever A, Lever A, Gottlinger H, et al. Analysis of the

- Initiating Events in HIV-1 Particle Assembly and Genome Packaging. Hope TJ, editor. PLoS Pathog [Internet]. Public Library of Science; 2010 Nov 18 [cited 2016 Dec 30];6(11):e1001200. Available from: <http://dx.plos.org/10.1371/journal.ppat.1001200>
114. Stockley PG, White SJ, Dykeman E, Manfield I, Rolfsson O, Patel N, et al. Bacteriophage MS2 genomic RNA encodes an assembly instruction manual for its capsid. Bacteriophage [Internet]. Taylor & Francis; 2016 [cited 2017 May 8];6(1):e1157666. Available from: <http://www.ncbi.nlm.nih.gov/pubmed/27144089>
  115. Johnson SF, Telesnitsky A. Retroviral RNA dimerization and packaging: the what, how, when, where, and why. PLoS Pathog [Internet]. Public Library of Science; 2010 Oct 7 [cited 2016 Dec 29];6(10):e1001007. Available from: <http://www.ncbi.nlm.nih.gov/pubmed/20949075>
  116. Lever AML. HIV-1 RNA Packaging. Adv Pharmacol. 2007;55:1–32.
  117. Kleiman L, Jones CP, Musier-Forsyth K. Formation of the tRNALys packaging complex in HIV-1. FEBS Lett [Internet]. NIH Public Access; 2010 Jan 21 [cited 2016 Dec 19];584(2):359–65. Available from: <http://www.ncbi.nlm.nih.gov/pubmed/19914238>
  118. Connell BJ, Lortat-Jacob H. Human Immunodeficiency Virus and Heparan Sulfate: From Attachment to Entry Inhibition. Front Immunol [Internet]. Frontiers; 2013 [cited 2017 Mar 16];4:385. Available from: <http://journal.frontiersin.org/article/10.3389/fimmu.2013.00385/abstract>
  119. Starling S, Jolly C. LFA-1 Engagement Triggers T Cell Polarization at the HIV-1 Virological Synapse. J Virol [Internet]. American Society for Microbiology (ASM); 2016 Nov 1 [cited 2017 Mar 14];90(21):9841–54. Available from: <http://www.ncbi.nlm.nih.gov/pubmed/27558417>
  120. Arrighi J-F, Pion M, Garcia E, Escola J-M, van Kooyk Y, Geijtenbeek TB, et al. DC-SIGN-mediated infectious synapse formation enhances X4 HIV-1 transmission from dendritic cells to T cells. J Exp Med [Internet]. 2004;200(10):1279–88. Available from: <http://www.pubmedcentral.nih.gov/articlerender.fcgi?artid=2211914&tool=pmcentrez&rendertype=abstract>
  121. Maddon PJJ, Dalgleish AGG, McDougal JSS, Clapham PRR, Weiss RAA, Axel R, et al. The T4 gene encodes the AIDS virus receptor and is expressed in the immune system and the brain. Cell [Internet]. Elsevier; 1986 Nov 7 [cited 2016 Dec 29];47(3):333–48. Available from: <http://www.ncbi.nlm.nih.gov/pubmed/3094962>
  122. Hartley O, Klasse PJ, Sattentau QJ, Moore JP. V3: HIV's Switch-Hitter. AIDS Res Hum Retroviruses [Internet]. Mary Ann Liebert, Inc. 2 Madison Avenue Larchmont, NY 10538 USA ; 2005 Feb [cited 2016 Dec 29];21(2):171–89. Available from: <http://www.liebertonline.com/doi/abs/10.1089/aid.2005.21.171>

123. McDougal JS, Nicholson JK, Cross GD, Cort SP, Kennedy MS, Mawle AC. Binding of the human retrovirus HTLV-III/LAV/ARV/HIV to the CD4 (T4) molecule: conformation dependence, epitope mapping, antibody inhibition, and potential for idiotypic mimicry. *J Immunol* [Internet]. 1986 Nov 1 [cited 2017 Jan 15];137(9):2937–44. Available from: <http://www.ncbi.nlm.nih.gov/pubmed/2428879>
124. Huang C, Tang M, Zhang M-Y, Majeed S, Montabana E, Stanfield RL, et al. Structure of a V3-containing HIV-1 gp120 core. *Science* [Internet]. 2005;310(5750):1025–8. Available from: <http://www.pubmedcentral.nih.gov/articlerender.fcgi?artid=2408531&tool=pmcentrez&rendertype=abstract>
125. Wu L, LaRosa G, Kassam N, Gordon CJ, Heath H, Ruffing N, et al. Interaction of chemokine receptor CCR5 with its ligands: multiple domains for HIV-1 gp120 binding and a single domain for chemokine binding. *J Exp Med* [Internet]. The Rockefeller University Press; 1997 Oct 20 [cited 2016 Dec 29];186(8):1373–81. Available from: <http://www.ncbi.nlm.nih.gov/pubmed/9334377>
126. Wilen CB, Tilton JC, Doms RW. HIV: cell binding and entry. *Cold Spring Harb Perspect Med* [Internet]. Cold Spring Harbor Laboratory Press; 2012 Aug 1 [cited 2016 Dec 29];2(8). Available from: <http://www.ncbi.nlm.nih.gov/pubmed/22908191>
127. Feng Y, Broder CC, Kennedy PE, Berger EA. HIV-1 Entry Cofactor: Functional cDNA Cloning of a Seven-Transmembrane, G Protein-Coupled Receptor. *Science* (80- ). 1996;272(5263).
128. Dragic T, Litwin V, Allaway GP, Martin SR, Huang Y, Nagashima KA, et al. HIV-1 entry into CD4+ cells is mediated by the chemokine receptor CC-CKR-5. *Nature* [Internet]. Nature Publishing Group; 1996 Jun 20 [cited 2016 Dec 30];381(6584):667–73. Available from: <http://www.nature.com/doifinder/10.1038/381667a0>
129. Doranz BJ, Rucker J, Yi Y, Smyth RJ, Samson M, Peiper SC, et al. A dual-tropic primary HIV-1 isolate that uses fusin and the beta-chemokine receptors CKR-5, CKR-3, and CKR-2b as fusion cofactors. *Cell* [Internet]. Elsevier; 1996 Jun 28 [cited 2016 Dec 30];85(7):1149–58. Available from: <http://www.ncbi.nlm.nih.gov/pubmed/8674120>
130. Deng H, Liu R, Ellmeier W, Choe S, Unutmaz D, Burkhart M, et al. Identification of a major co-receptor for primary isolates of HIV-1. *Nature* [Internet]. Nature Publishing Group; 1996 Jun 20 [cited 2016 Dec 29];381(6584):661–6. Available from: <http://www.nature.com/doifinder/10.1038/381661a0>
131. Choe H, Farzan M, Sun Y, Sullivan N, Rollins B, Ponath PD, et al. The  $\beta$ -Chemokine Receptors CCR3 and CCR5 Facilitate Infection by Primary HIV-1 Isolates. *Cell*. 1996;85(7):1135–48.
132. Alkhatib G, Combadiere C, Broder CC, Feng Y, Kennedy PE, Murphy PM, et al. CC CKR5: A

- RANTES, MIP-1 $\alpha$ , MIP-1 $\beta$  Receptor as a Fusion Cofactor for Macrophage-Tropic HIV-1. *Science* (80- ). 1996;272(5270).
133. Funke I, Hahn A, Rieber EP, Weiss E, Riethmüller G. The cellular receptor (CD4) of the human immunodeficiency virus is expressed on neurons and glial cells in human brain. *J Exp Med* [Internet]. The Rockefeller University Press; 1987 Apr 1 [cited 2016 Dec 29];165(4):1230–5. Available from: <http://www.ncbi.nlm.nih.gov/pubmed/3104529>
  134. Feng Y, Zhang F, Lokey LK, Chastain JL, Lakkis L, Eberhart D, et al. Translational suppression by trinucleotide repeat expansion at FMR1. *Science* [Internet]. 1995 May 5 [cited 2016 Dec 29];268(5211):731–4. Available from: <http://www.ncbi.nlm.nih.gov/pubmed/7732383>
  135. Melikyan GB, White J, Delos S, Brecher M, Schornberg K, Harrison S, et al. Common principles and intermediates of viral protein-mediated fusion: the HIV-1 paradigm. *Retrovirology* [Internet]. BioMed Central; 2008 [cited 2016 Dec 29];5(1):111. Available from: <http://retrovirology.biomedcentral.com/articles/10.1186/1742-4690-5-111>
  136. Dean M, Carrington M, Winkler C, Huttley GA, Smith MW, Allikmets R, et al. Genetic Restriction of HIV-1 Infection and Progression to AIDS by a Deletion Allele of the *CCR5* Structural Gene. *Science* (80- ). 1996;273(5283).
  137. Berger EA, Doms RW, Fenyö E-M, Korber BTM, Littman DR, Moore JP, et al. A new classification for HIV-1. *Nature* [Internet]. Nature Publishing Group; 1998 Jan 15 [cited 2016 Dec 29];391(6664):240–240. Available from: <http://www.nature.com/doi/10.1038/34571>
  138. Keele BF, Giorgi EE, Salazar-Gonzalez JF, Decker JM, Pham KT, Salazar MG, et al. Identification and characterization of transmitted and early founder virus envelopes in primary HIV-1 infection. *Proc Natl Acad Sci U S A* [Internet]. National Academy of Sciences; 2008 May 27 [cited 2016 Dec 29];105(21):7552–7. Available from: <http://www.ncbi.nlm.nih.gov/pubmed/18490657>
  139. Moore JP, Kitchen SG, Pugach P, Zack JA. The *CCR5* and *CXCR4* Coreceptors—Central to Understanding the Transmission and Pathogenesis of Human Immunodeficiency Virus Type 1 Infection. *AIDS Res Hum Retroviruses* [Internet]. 2004 Jan [cited 2016 Dec 29];20(1):111–26. Available from: <http://www.ncbi.nlm.nih.gov/pubmed/15000703>
  140. Hunt PW, Harrigan PR, Huang W, Bates M, Williamson DW, McCune JM, et al. Prevalence of *CXCR4* tropism among antiretroviral-treated HIV-1-infected patients with detectable viremia. *J Infect Dis* [Internet]. Oxford University Press; 2006 Oct 1 [cited 2016 Dec 29];194(7):926–30. Available from: <http://www.ncbi.nlm.nih.gov/pubmed/16960780>
  141. Regoes RR, Bonhoeffer S. The HIV coreceptor switch: a population dynamical perspective. *Trends Microbiol.* 2005;13(6):269–77.

142. Lehmann MJ, Sherer NM, Marks CB, Pypaert M, Mothes W. Actin- and myosin-driven movement of viruses along filopodia precedes their entry into cells. *J Cell Biol* [Internet]. The Rockefeller University Press; 2005 Jul 18 [cited 2017 Jan 17];170(2):317–25. Available from: <http://www.ncbi.nlm.nih.gov/pubmed/16027225>
143. Sloan RD, Kuhl BD, Mesplède T, Münch J, Donahue DA, Wainberg MA. Productive entry of HIV-1 during cell-to-cell transmission via dynamin-dependent endocytosis. *J Virol* [Internet]. American Society for Microbiology; 2013 Jul [cited 2016 Dec 9];87(14):8110–23. Available from: <http://www.ncbi.nlm.nih.gov/pubmed/23678185>
144. Murooka TT, Deruaz M, Marangoni F, Vrbanac VD, Seung E, von Andrian UH, et al. HIV-infected T cells are migratory vehicles for viral dissemination. *Nature* [Internet]. 2012 Aug 1 [cited 2016 Dec 9];490(7419):283–7. Available from: <http://www.ncbi.nlm.nih.gov/pubmed/22854780>
145. Jolly C, Booth NJ, Neil SJD. Cell-cell spread of human immunodeficiency virus type 1 overcomes tetherin/BST-2-mediated restriction in T cells. *J Virol* [Internet]. American Society for Microbiology (ASM); 2010 Dec [cited 2016 Dec 30];84(23):12185–99. Available from: <http://www.ncbi.nlm.nih.gov/pubmed/20861257>
146. Jolly C, Kashefi K, Hollinshead M, Sattentau QJ. HIV-1 cell to cell transfer across an Env-induced, actin-dependent synapse. *J Exp Med* [Internet]. The Rockefeller University Press; 2004 Jan 19 [cited 2016 Dec 9];199(2):283–93. Available from: <http://www.scopus.com/inward/record.url?eid=2-s2.0-1642540589&partnerID=tZOtx3y1>
147. Igakura T, Stinchcombe JC, Goon PK, Taylor GP, Weber JN, Griffiths GM, et al. Spread of HTLV-1 Between Lymphocytes by Virus-Induced Polarization of the Cytoskeleton. *Science* (80-) [Internet]. 2003;299(2003):1713–6. Available from: <http://science.sciencemag.org/content/299/5613/1713>
148. Sattentau QJ. Cell-to-Cell Spread of Retroviruses. *Viruses* [Internet]. Multidisciplinary Digital Publishing Institute (MDPI); 2010 Jun [cited 2017 Jan 18];2(6):1306–21. Available from: <http://www.ncbi.nlm.nih.gov/pubmed/21994681>
149. Martin N, Welsch S, Jolly C, Briggs JAG, Vaux D, Sattentau QJ. Virological synapse-mediated spread of human immunodeficiency virus type 1 between T cells is sensitive to entry inhibition. *J Virol* [Internet]. 2010;84(7):3516–27. Available from: <http://www.scopus.com/inward/record.url?eid=2-s2.0-77949412821&partnerID=tZOtx3y1>
150. Jolly C, Welsch S, Michor S, Sattentau QJ, Sattentau Q, Jolly C, et al. The Regulated Secretory Pathway in CD4+ T cells Contributes to Human Immunodeficiency Virus Type-1 Cell-to-Cell Spread at the Virological Synapse. Hope T, editor. *PLoS Pathog* [Internet]. Public Library of Science; 2011 Sep 1 [cited 2017 Jan 18];7(9):e1002226. Available from: <http://dx.plos.org/10.1371/journal.ppat.1002226>

151. Martin N, Welsch S, Jolly C, Briggs JAG, Vaux D, Sattentau QJ. Virological synapse-mediated spread of human immunodeficiency virus type 1 between T cells is sensitive to entry inhibition. *J Virol* [Internet]. American Society for Microbiology; 2010 Apr [cited 2017 Jan 18];84(7):3516–27. Available from: <http://www.ncbi.nlm.nih.gov/pubmed/20089656>
152. Cameron PU, Freudenthal PS, Barker JM, Gezelter S, Inaba K, Steinman RM. Dendritic cells exposed to human immunodeficiency virus type-1 transmit a vigorous cytopathic infection to CD4+ T cells. *Science* [Internet]. 1992 Jul 17 [cited 2017 Feb 11];257(5068):383–7. Available from: <http://www.ncbi.nlm.nih.gov/pubmed/1352913>
153. Bakri Y, Schiffer C, Zennou V, Charneau P, Kahn E, Benjouad A, et al. The Maturation of Dendritic Cells Results in Postintegration Inhibition of HIV-1 Replication. *J Immunol*. 2001;166(6).
154. Felts RL, Narayan K, Estes JD, Shi D, Trubey CM, Fu J, et al. 3D visualization of HIV transfer at the virological synapse between dendritic cells and T cells. *Proc Natl Acad Sci* [Internet]. 2010 Jul 27 [cited 2017 Jan 18];107(30):13336–41. Available from: <http://www.ncbi.nlm.nih.gov/pubmed/20624966>
155. McDonald D, Wu L, Bohks SM, KewalRamani VN, Unutmaz D, Hope TJ. Recruitment of HIV and Its Receptors to Dendritic Cell-T Cell Junctions. *Science* (80- ). 2003;300(5623).
156. Uchil PD, Mothes W. HIV Entry Revisited. *Cell* [Internet]. Elsevier; 2009 May 1 [cited 2017 Feb 11];137(3):402–4. Available from: <http://www.ncbi.nlm.nih.gov/pubmed/19410537>
157. Miyauchi K, Kim Y, Latinovic O, Morozov V, Melikyan GB. HIV enters cells via endocytosis and dynamin-dependent fusion with endosomes. *Cell* [Internet]. NIH Public Access; 2009 May 1 [cited 2016 Dec 30];137(3):433–44. Available from: <http://www.ncbi.nlm.nih.gov/pubmed/19410541>
158. Hübner W, McNerney GP, Chen P, Dale BM, Gordon RE, Chuang FYS, et al. Quantitative 3D video microscopy of HIV transfer across T cell virological synapses. *Science* [Internet]. NIH Public Access; 2009 Mar 27 [cited 2017 Jan 17];323(5922):1743–7. Available from: <http://www.ncbi.nlm.nih.gov/pubmed/19325119>
159. Thomas JA, Gorelick RJ. Nucleocapsid protein function in early infection processes. *Virus Res* [Internet]. NIH Public Access; 2008 Jun [cited 2016 Dec 30];134(1–2):39–63. Available from: <http://www.ncbi.nlm.nih.gov/pubmed/18279991>
160. Wu X, Liu H, Xiao H, Conway J, Hehl E, Kalpana G V., et al. Human immunodeficiency virus type 1 integrase protein promotes reverse transcription through specific interactions with the nucleoprotein reverse transcription complex. *J Virol* [Internet]. 1999;73(3):2126–35. Available from:

<http://www.pubmedcentral.nih.gov/articlerender.fcgi?artid=104457&tool=pmcentrez&rendertype=abstract>

161. McDonald D, Vodicka MA, Lucero G, Svitkina TM, Borisy GG, Emerman M, et al. Visualization of the intracellular behavior of HIV in living cells. *J Cell Biol* [Internet]. The Rockefeller University Press; 2002 Nov 11 [cited 2016 Dec 30];159(3):441–52. Available from: <http://www.ncbi.nlm.nih.gov/pubmed/12417576>
162. Hu W-S, Hughes SH. HIV-1 reverse transcription. *Cold Spring Harb Perspect Med* [Internet]. Cold Spring Harbor Laboratory Press; 2012 Oct 1 [cited 2016 Dec 29];2(10):a006882. Available from: <http://www.ncbi.nlm.nih.gov/pubmed/23028129>
163. Arhel N. Revisiting HIV-1 uncoating. *Retrovirology* [Internet]. BioMed Central; 2010 Nov 17 [cited 2017 Feb 12];7:96. Available from: <http://www.ncbi.nlm.nih.gov/pubmed/21083892>
164. Bichel K, Price AJ, Schaller T, Towers GJ, Freund SM V, James LC. HIV-1 capsid undergoes coupled binding and isomerization by the nuclear pore protein NUP358. *Retrovirology* [Internet]. 2013;10(1):81. Available from: <http://www.pubmedcentral.nih.gov/articlerender.fcgi?artid=3750474&tool=pmcentrez&rendertype=abstract>
165. Rasaiyaah J, Tan CP, Fletcher AJ, Price AJ, Blondeau C, Hilditch L, et al. HIV-1 evades innate immune recognition through specific cofactor recruitment. *Nature* [Internet]. Nature Publishing Group; 2013 Nov 21 [cited 2013 Dec 11];503(7476):402–5. Available from: <http://www.ncbi.nlm.nih.gov/pubmed/24196705>
166. Yang Y, Fricke T, Diaz-Griffero F. Inhibition of reverse transcriptase activity increases stability of the HIV-1 core. *J Virol* [Internet]. American Society for Microbiology; 2013 Jan [cited 2016 Dec 30];87(1):683–7. Available from: <http://www.ncbi.nlm.nih.gov/pubmed/23077298>
167. Dharan A, Talley S, Tripathi A, Mamede JI, Majetschak M, Hope TJ, et al. KIF5B and Nup358 Cooperatively Mediate the Nuclear Import of HIV-1 during Infection. *PLoS Pathog*. 2016;12(6):1–24.
168. Aiken C. Cell-free assays for HIV-1 uncoating. *Methods Mol Biol* [Internet]. NIH Public Access; 2009 [cited 2016 Dec 30];485:41–53. Available from: <http://www.ncbi.nlm.nih.gov/pubmed/19020817>
169. Thomas JA, Ott DE, Gorelick RJ. Efficiency of human immunodeficiency virus type 1 postentry infection processes: evidence against disproportionate numbers of defective virions. *J Virol* [Internet]. American Society for Microbiology (ASM); 2007 Apr [cited 2016 Dec 30];81(8):4367–70. Available from: <http://www.ncbi.nlm.nih.gov/pubmed/17267494>

170. Lahaye X, Satoh T, Gentili M, Cerboni S, Conrad C, Hurbain I, et al. The Capsids of HIV-1 and HIV-2 Determine Immune Detection of the Viral cDNA by the Innate Sensor cGAS in Dendritic Cells. *Immunity*. 2013;39(6):1132–42.
171. Kobiler O, Drayman N, Butin-Israeli V, Oppenheim A. Virus strategies for passing the nuclear envelope barrier. *Nucleus* [Internet]. Taylor & Francis; 2012 [cited 2017 Feb 6];3(6):526–39. Available from: <http://www.ncbi.nlm.nih.gov/pubmed/22929056>
172. Arhel NJ, Souquere-Besse S, Munier S, Souque P, Guadagnini S, Rutherford S, et al. HIV-1 DNA Flap formation promotes uncoating of the pre-integration complex at the nuclear pore. *EMBO J* [Internet]. EMBO Press; 2007 Jun 20 [cited 2016 Dec 30];26(12):3025–37. Available from: <http://www.ncbi.nlm.nih.gov/pubmed/17557080>
173. Lelek M, Di Nunzio F, Henriques R, Charneau P, Arhel N, Zimmer C. Superresolution imaging of HIV in infected cells with FIAsh-PALM. *Proc Natl Acad Sci U S A* [Internet]. National Academy of Sciences; 2012 May 29 [cited 2016 Dec 30];109(22):8564–9. Available from: <http://www.ncbi.nlm.nih.gov/pubmed/22586087>
174. Schaller T, Ocwieja KE, Rasaiyaah J, Price AJ, Brady TL, Roth SL, et al. HIV-1 capsid-cyclophilin interactions determine nuclear import pathway, integration targeting and replication efficiency. *PLoS Pathog*. 2011;7(12).
175. Matreyek KA, Yücel SS, Li X, Engelman A, Roe T, Reynolds T, et al. Nucleoporin NUP153 Phenylalanine-Glycine Motifs Engage a Common Binding Pocket within the HIV-1 Capsid Protein to Mediate Lentiviral Infectivity. Luban J, editor. *PLoS Pathog* [Internet]. Public Library of Science; 2013 Oct 10 [cited 2016 Dec 30];9(10):e1003693. Available from: <http://dx.plos.org/10.1371/journal.ppat.1003693>
176. Di Nunzio F, Fricke T, Miccio A, Valle-Casuso JC, Perez P, Souque P, et al. Nup153 and Nup98 bind the HIV-1 core and contribute to the early steps of HIV-1 replication. *Virology* [Internet]. NIH Public Access; 2013 May 25 [cited 2016 Dec 30];440(1):8–18. Available from: <http://www.ncbi.nlm.nih.gov/pubmed/23523133>
177. Price AJ, Jacques DA, McEwan WA, Fletcher AJ, Essig S, Chin JW, et al. Host Cofactors and Pharmacologic Ligands Share an Essential Interface in HIV-1 Capsid That Is Lost upon Disassembly. Cullen BR, editor. *PLoS Pathog* [Internet]. 2014 Oct 30 [cited 2016 Dec 9];10(10):e1004459. Available from: <http://dx.plos.org/10.1371/journal.ppat.1004459>
178. Jacques DA, McEwan WA, Hilditch L, Price AJ, Towers GJ, James LC. HIV-1 uses dynamic capsid pores to import nucleotides and fuel encapsidated DNA synthesis. *Nature* [Internet]. Nature Research; 2016 Aug 10 [cited 2016 Dec 9];536(7616):349–53. Available from: <http://www.nature.com/doi/10.1038/nature19098>

179. Stremlau M, Owens CM, Perron MJ, Kiessling M, Autissier P, Sodroski J. The cytoplasmic body component TRIM5 $\alpha$  restricts HIV-1 infection in Old World monkeys. *Nature* [Internet]. Nature Publishing Group; 2004 Feb 26 [cited 2016 Dec 30];427(6977):848–53. Available from: <http://www.nature.com/doi/10.1038/nature02343>
180. Hoelz A, Debler EW, Blobel G. The Structure of the Nuclear Pore Complex. *Annu Rev Biochem* [Internet]. Annual Reviews ; 2011 Jul 7 [cited 2016 Dec 30];80(1):613–43. Available from: <http://www.annualreviews.org/doi/10.1146/annurev-biochem-060109-151030>
181. Frey S, Richter RP, Gorlich D. FG-Rich Repeats of Nuclear Pore Proteins Form a Three-Dimensional Meshwork with Hydrogel-Like Properties. *Science* (80- ) [Internet]. 2006 Nov 3 [cited 2016 Dec 30];314(5800):815–7. Available from: <http://www.ncbi.nlm.nih.gov/pubmed/17082456>
182. Wente SR, Rout MP, Blobel G. A new family of yeast nuclear pore complex proteins. *J Cell Biol* [Internet]. 1992 Nov [cited 2017 Mar 14];119(4):705–23. Available from: <http://www.ncbi.nlm.nih.gov/pubmed/1385442>
183. Yamashita M, Emerman M, Weinberg J, Matthews T, Cullen B, Malim M, et al. The Cell Cycle Independence of HIV Infections Is Not Determined by Known Karyophilic Viral Elements. *PLoS Pathog* [Internet]. Public Library of Science; 2005 [cited 2016 Dec 30];1(3):e18. Available from: <http://dx.plos.org/10.1371/journal.ppat.0010018>
184. Yamashita M, Emerman M. Capsid Is a Dominant Determinant of Retrovirus Infectivity in Nondividing Cells. *J Virol* [Internet]. 2004;78(11):5670–8. Available from: <http://jvi.asm.org/cgi/doi/10.1128/JVI.78.11.5670-5678.2004>  
<http://www.ncbi.nlm.nih.gov/pubmed/15140964>  
<http://www.pubmedcentral.nih.gov/articlerender.fcgi?artid=PMC415837>
185. Sluis-Cremer N, Arion D, Abram ME, Parniak MA. Proteolytic processing of an HIV-1 pol polyprotein precursor: insights into the mechanism of reverse transcriptase p66/p51 heterodimer formation. *Int J Biochem Cell Biol*. 2004;36(9):1836–47.
186. Sarafianos SG, Das K, Tantillo C, Clark AD, Ding J, Whitcomb JM, et al. Crystal structure of HIV-1 reverse transcriptase in complex with a polypurine tract RNA:DNA. *EMBO J* [Internet]. European Molecular Biology Organization; 2001 Mar 15 [cited 2016 Dec 30];20(6):1449–61. Available from: <http://www.ncbi.nlm.nih.gov/pubmed/11250910>
187. Fields BN, Knipe DM (David M, Howley PM. *Fields virology*. Wolters Kluwer Health/Lippincott Williams & Wilkins; 2013. 82 p.
188. Acheson NH. *Fundamentals of molecular virology*. John Wiley & Sons; 2011. 500 p.

189. Arts EJ, Hazuda DJ. HIV-1 antiretroviral drug therapy. *Cold Spring Harb Perspect Med* [Internet]. Cold Spring Harbor Laboratory Press; 2012 Apr [cited 2016 Dec 29];2(4):a007161. Available from: <http://www.ncbi.nlm.nih.gov/pubmed/22474613>
190. Craigie R, Bushman FD. HIV DNA integration. *Cold Spring Harb Perspect Med* [Internet]. Cold Spring Harbor Laboratory Press; 2012 Jul 1 [cited 2016 Dec 19];2(7). Available from: <http://www.ncbi.nlm.nih.gov/pubmed/22762018>
191. Jeanson L, Subra F, Vaganay S, Hervy M, Marangoni E, Bourhis J, et al. Effect of Ku80 depletion on the preintegrative steps of HIV-1 replication in human cells. *Virology* [Internet]. Academic Press; 2002 Aug 15 [cited 2016 Dec 30];300(1):100–8. Available from: <http://www.ncbi.nlm.nih.gov/pubmed/12202210>
192. Venter JC, Adams MD, Myers EW, Li PW, Mural RJ, Sutton GG, et al. The Sequence of the Human Genome. *Science* (80- ). 2001;291(5507).
193. Lander ES, Linton LM, Birren B, Nusbaum C, Zody MC, Baldwin J, et al. Initial sequencing and analysis of the human genome. *Nature* [Internet]. Nature Publishing Group; 2001 Feb 15 [cited 2017 Feb 12];409(6822):860–921. Available from: <http://www.nature.com/doi/10.1038/35057062>
194. Schröder ARW, Shinn P, Chen H, Berry C, Ecker JR, Bushman F. HIV-1 Integration in the Human Genome Favors Active Genes and Local Hotspots. *Cell*. 2002;110(4):521–9.
195. Barr SD, Ciuffi A, Leipzig J, Shinn P, Ecker JR, Bushman FD. HIV Integration Site Selection: Targeting in Macrophages and the Effects of Different Routes of Viral Entry. *Mol Ther* [Internet]. 2006 Aug [cited 2016 Dec 30];14(2):218–25. Available from: <http://www.ncbi.nlm.nih.gov/pubmed/16647883>
196. Han Y, Lassen K, Monie D, Sedaghat AR, Shimoji S, Liu X, et al. Resting CD4+ T cells from human immunodeficiency virus type 1 (HIV-1)-infected individuals carry integrated HIV-1 genomes within actively transcribed host genes. *J Virol* [Internet]. American Society for Microbiology (ASM); 2004 Jun [cited 2016 Dec 30];78(12):6122–33. Available from: <http://www.ncbi.nlm.nih.gov/pubmed/15163705>
197. Wang GP, Ciuffi A, Leipzig J, Berry CC, Bushman FD. HIV integration site selection: Analysis by massively parallel pyrosequencing reveals association with epigenetic modifications. *Genome Res*. 2007;17(8):1186–94.
198. Stevens SW, Griffith JD. Sequence analysis of the human DNA flanking sites of human immunodeficiency virus type 1 integration. *J Virol* [Internet]. American Society for Microbiology (ASM); 1996 Sep [cited 2016 Dec 30];70(9):6459–62. Available from: <http://www.ncbi.nlm.nih.gov/pubmed/8709282>

199. Ciuffi A, Llano M, Poeschla E, Hoffmann C, Leipzig J, Shinn P, et al. A role for LEDGF/p75 in targeting HIV DNA integration. *Nat Med* [Internet]. Nature Publishing Group; 2005 Dec 27 [cited 2016 Dec 30];11(12):1287–9. Available from: <http://www.nature.com/doi/10.1038/nm1329>
200. Shun M-C, Raghavendra NK, Vandegraaff N, Daigle JE, Hughes S, Kellam P, et al. LEDGF/p75 functions downstream from preintegration complex formation to effect gene-specific HIV-1 integration. *Genes Dev* [Internet]. Cold Spring Harbor Laboratory Press; 2007 Jul 15 [cited 2016 Dec 30];21(14):1767–78. Available from: <http://www.ncbi.nlm.nih.gov/pubmed/17639082>
201. Ciuffi A, Diamond TL, Hwang Y, Marshall HM, Bushman FD. Modulating Target Site Selection During Human Immunodeficiency Virus DNA Integration *In Vitro* with an Engineered Tethering Factor. *Hum Gene Ther* [Internet]. Mary Ann Liebert, Inc. 2 Madison Avenue Larchmont, NY 10538 USA ; 2006 Sep [cited 2016 Dec 30];17(9):960–7. Available from: <http://www.ncbi.nlm.nih.gov/pubmed/16972764>
202. Carteau S, Hoffmann C, Bushman F. Chromosome structure and human immunodeficiency virus type 1 cDNA integration: centromeric alphoid repeats are a disfavored target. *J Virol* [Internet]. 1998 May [cited 2016 Dec 30];72(5):4005–14. Available from: <http://www.ncbi.nlm.nih.gov/pubmed/9557688>
203. Pruss D, Bushman FD, Wolffe AP. Human immunodeficiency virus integrase directs integration to sites of severe DNA distortion within the nucleosome core. *Proc Natl Acad Sci U S A* [Internet]. National Academy of Sciences; 1994 Jun 21 [cited 2016 Dec 30];91(13):5913–7. Available from: <http://www.ncbi.nlm.nih.gov/pubmed/8016088>
204. Ocwieja KE, Brady TL, Ronen K, Huegel A, Roth SL, Schaller T, et al. HIV integration targeting: a pathway involving Transportin-3 and the nuclear pore protein RanBP2. *PLoS Pathog* [Internet]. Public Library of Science; 2011 Mar [cited 2016 Dec 30];7(3):e1001313. Available from: <http://www.ncbi.nlm.nih.gov/pubmed/21423673>
205. Lewinski MK, Bisgrove D, Shinn P, Chen H, Hoffmann C, Hannenhalli S, et al. Genome-Wide Analysis of Chromosomal Features Repressing Human Immunodeficiency Virus Transcription. *J Virol*. 2005;79(11):6610–9.
206. Yin Q, Tian Y, Kabaleeswaran V, Jiang X, Tu D, Eck MJ, et al. Cyclic di-GMP sensing via the innate immune signaling protein STING. *Mol Cell* [Internet]. Elsevier; 2012 Jun 29 [cited 2016 Dec 27];46(6):735–45. Available from: <http://www.ncbi.nlm.nih.gov/pubmed/22705373>
207. Lee K, Ambrose Z, Martin TD, Oztop I, Mulky A, Julias JG, et al. Flexible Use of Nuclear Import Pathways by HIV-1. *Cell Host Microbe* [Internet]. 2010 Mar 18 [cited 2017 Feb 12];7(3):221–33. Available from: <http://www.ncbi.nlm.nih.gov/pubmed/20227665>
208. Ruelas DS, Greene WC. An integrated overview of HIV-1 latency. *Cell* [Internet]. NIH Public

Access; 2013 Oct 24 [cited 2016 Dec 30];155(3):519–29. Available from: <http://www.ncbi.nlm.nih.gov/pubmed/24243012>

209. Mitchell RS, Beitzel BF, Schroder ARW, Shinn P, Chen H, Berry CC, et al. Retroviral DNA Integration: ASLV, HIV, and MLV Show Distinct Target Site Preferences. Michael Emerman, editor. PLoS Biol [Internet]. Public Library of Science; 2004 Aug 17 [cited 2017 Feb 12];2(8):e234. Available from: <http://dx.plos.org/10.1371/journal.pbio.0020234>
210. Chun T-W, Carruth L, Finzi D, Shen X, DiGiuseppe JA, Taylor H, et al. Quantification of latent tissue reservoirs and total body viral load in HIV-1 infection. Nature [Internet]. 1997 May 8 [cited 2017 Feb 12];387(6629):183–8. Available from: <http://www.ncbi.nlm.nih.gov/pubmed/9144289>
211. Siliciano JD, Kajdas J, Finzi D, Quinn TC, Chadwick K, Margolick JB, et al. Long-term follow-up studies confirm the stability of the latent reservoir for HIV-1 in resting CD4+ T cells. Nat Med. 2003;9(6):727–8.
212. Von Stockenström S, Odevall L, Lee E, Sinclair E, Bacchetti P, Killian M, et al. Longitudinal Genetic Characterization Reveals That Cell Proliferation Maintains a Persistent HIV Type 1 DNA Pool During Effective HIV Therapy.
213. Besson GJ, Lalama CM, Bosch RJ, Gandhi RT, Bedison MA, Aga E, et al. HIV-1 DNA Decay Dynamics in Blood During More Than a Decade of Suppressive Antiretroviral Therapy.
214. Zack JA, Arrigo SJ, Weitsman SR, Go AS, Haislip A, Chen IS. HIV-1 entry into quiescent primary lymphocytes: molecular analysis reveals a labile, latent viral structure. Cell [Internet]. 1990 Apr 20 [cited 2017 Feb 12];61(2):213–22. Available from: <http://www.ncbi.nlm.nih.gov/pubmed/2331748>
215. Bukrinsky M, Stanwick T, Dempsey M, Stevenson M. Quiescent T lymphocytes as an inducible virus reservoir in HIV-1 infection. Science (80- ). 1991;254(5030).
216. Van Kerckhove C, Liu A. HIGH LEVELS OF HIV-1 IN PLASMA DURING ALL STAGES OF INFECTION DETERMINED BY COMPETITIVE PCR. Pediatrics. 1995;96(2).
217. Bailey J, Blankson JN, Wind-Rotolo M, Siliciano RF. Mechanisms of HIV-1 escape from immune responses and antiretroviral drugs. Curr Opin Immunol. 2004;16(4):470–6.
218. Verdin E, Paras P, Van Lint C. Chromatin disruption in the promoter of human immunodeficiency virus type 1 during transcriptional activation. EMBO J [Internet]. 1993 Aug [cited 2017 Feb 12];12(8):3249–59. Available from: <http://www.ncbi.nlm.nih.gov/pubmed/8344262>
219. Ho Y-C, Shan L, Hosmane NN, Wang J, Laskey SB, Rosenbloom DIS, et al. Replication-competent noninduced proviruses in the latent reservoir increase barrier to HIV-1 cure. Cell [Internet]. Elsevier; 2013 Oct 24 [cited 2016 Dec 11];155(3):540–51. Available from:

<http://www.ncbi.nlm.nih.gov/pubmed/24243014>

220. Lorenzo-Redondo R, Fryer HR, Bedford T, Kim E-Y, Archer J, Kosakovsky Pond SL, et al. Persistent HIV-1 replication maintains the tissue reservoir during therapy. *Nature* [Internet]. Nature Publishing Group; 2016;530(7588):51–6. Available from: <http://dx.doi.org/10.1038/nature16933><http://www.nature.com/nature/journal/v530/n7588/abs/nature16933.html#supplementary-information><http://www.nature.com/doi/10.1038/nature16933>
221. Chomont N, DaFonseca S, Vandergeeten C, Ancuta P, Sékaly R-P. Maintenance of CD4+ T-cell memory and HIV persistence: keeping memory, keeping HIV. *Curr Opin HIV AIDS* [Internet]. 2011 Jan [cited 2017 Feb 12];6(1):30–6. Available from: <http://content.wkhealth.com/linkback/openurl?sid=WKPTLP:landingpage&an=01222929-201101000-00007>
222. Brodin J, Zanini F, Thebo L, Lanz C, Bratt G, Neher RA, et al. Establishment and stability of the latent HIV-1 DNA reservoir. *Elife* [Internet]. eLife Sciences Publications, Ltd; 2016 Nov 15 [cited 2017 Feb 6];5. Available from: <http://www.ncbi.nlm.nih.gov/pubmed/27855060>
223. Richman DD, Margolis DM, Delaney M, Greene WC, Hazuda D, Pomerantz RJ. The Challenge of Finding a Cure for HIV Infection. 2009 [cited 2017 Feb 12]; Available from: <http://www.sciencemag.org/cgi/content/full/323/5919/1304>
224. Deeks SG. HIV: Shock and kill. *Nature* [Internet]. 2012 Jul 25 [cited 2017 Feb 12];487(7408):439–40. Available from: <http://www.ncbi.nlm.nih.gov/pubmed/22836995>
225. Van Lint C, Emiliani S, Verdin E. The expression of a small fraction of cellular genes is changed in response to histone hyperacetylation. *Gene Expr* [Internet]. 1996 [cited 2017 Feb 12];5(4–5):245–53. Available from: <http://www.ncbi.nlm.nih.gov/pubmed/8723390>
226. Archin NM, Liberty AL, Kashuba AD, Choudhary SK, Kuruc JD, Crooks AM, et al. Administration of vorinostat disrupts HIV-1 latency in patients on antiretroviral therapy. *Nature* [Internet]. Nature Research; 2012 Jul 25 [cited 2017 Feb 12];487(7408):482–5. Available from: <http://www.nature.com/doi/10.1038/nature11286>
227. Bullen CK, Laird GM, Durand CM, Siliciano JD, Siliciano RF. New ex vivo approaches distinguish effective and ineffective single agents for reversing HIV-1 latency in vivo. *Nat Med* [Internet]. Nature Research; 2014 Mar 23 [cited 2017 Feb 12];20(4):425–9. Available from: <http://www.nature.com/doi/10.1038/nm.3489>
228. Colin L, Van Lint C. Molecular control of HIV-1 postintegration latency: implications for the development of new therapeutic strategies. *Retrovirology* [Internet]. BioMed Central; 2009 [cited 2017 Feb 12];6(1):111. Available from:

<http://retrovirology.biomedcentral.com/articles/10.1186/1742-4690-6-111>

229. Chiang CM, Roeder RG. Cloning of an intrinsic human TFIID subunit that interacts with multiple transcriptional activators. *Science* [Internet]. 1995 Jan 27 [cited 2017 Feb 12];267(5197):531–6. Available from: <http://www.ncbi.nlm.nih.gov/pubmed/7824954>
230. Perkins ND, Edwards NL, Duckett CS, Agranoff AB, Schmid RM, Nabel GJ. A cooperative interaction between NF-kappa B and Sp1 is required for HIV-1 enhancer activation. *EMBO J* [Internet]. European Molecular Biology Organization; 1993 Sep [cited 2017 Feb 12];12(9):3551–8. Available from: <http://www.ncbi.nlm.nih.gov/pubmed/8253080>
231. Williams SA, Chen L-F, Kwon H, Ruiz-Jarabo CM, Verdin E, Greene WC. NF-kappaB p50 promotes HIV latency through HDAC recruitment and repression of transcriptional initiation. *EMBO J* [Internet]. EMBO Press; 2006 Jan 11 [cited 2017 Feb 12];25(1):139–49. Available from: <http://www.ncbi.nlm.nih.gov/pubmed/16319923>
232. Gerritsen ME, Williams AJ, Neish AS, Moore S, Shi Y, Collins T. CREB-binding protein/p300 are transcriptional coactivators of p65. *Proc Natl Acad Sci U S A* [Internet]. 1997 Apr 1 [cited 2017 Feb 12];94(7):2927–32. Available from: <http://www.ncbi.nlm.nih.gov/pubmed/9096323>
233. Barboric M, Nissen RM, Kanazawa S, Jabrane-Ferrat N, Peterlin BM. NF-kappaB binds P-TEFb to stimulate transcriptional elongation by RNA polymerase II. *Mol Cell* [Internet]. 2001 Aug [cited 2017 Feb 12];8(2):327–37. Available from: <http://www.ncbi.nlm.nih.gov/pubmed/11545735>
234. Karn J, Stoltzfus CM. Transcriptional and posttranscriptional regulation of HIV-1 gene expression. *Cold Spring Harb Perspect Med* [Internet]. Cold Spring Harbor Laboratory Press; 2012 Feb [cited 2017 Feb 6];2(2):a006916. Available from: <http://www.ncbi.nlm.nih.gov/pubmed/22355797>
235. Wei P, Garber ME, Fang S-M, Fischer WH, Jones KA. A Novel CDK9-Associated C-Type Cyclin Interacts Directly with HIV-1 Tat and Mediates Its High-Affinity, Loop-Specific Binding to TAR RNA. *Cell*. 1998;92(4):451–62.
236. Tahirov TH, Babayeva ND, Varzavand K, Cooper JJ, Sedore SC, Price DH. Crystal structure of HIV-1 Tat complexed with human P-TEFb.pdf. *Nature* [Internet]. NIH Public Access; 2010 Jun 10 [cited 2016 Dec 30];465(7299). Available from: <http://www.ncbi.nlm.nih.gov/pubmed/20535204>
237. Legrain P, Rosbash M. Some cis- and trans-acting mutants for splicing target pre-mRNA to the cytoplasm. *Cell* [Internet]. 1989 May 19 [cited 2017 Feb 12];57(4):573–83. Available from: <http://www.ncbi.nlm.nih.gov/pubmed/2655924>
238. Cullen BR. Regulation of HIV-1 gene expression. *FASEB J* [Internet]. 1991 Jul [cited 2017 Feb

- 12];5(10):2361–8. Available from: <http://www.ncbi.nlm.nih.gov/pubmed/1712325>
239. Bolinger C, Boris-Lawrie K. Mechanisms employed by retroviruses to exploit host factors for translational control of a complicated proteome. *Retrovirology* [Internet]. 2009 Jan 24 [cited 2017 Feb 12];6(1):8. Available from: <http://www.ncbi.nlm.nih.gov/pubmed/19166625>
240. Sundquist WI, Kräusslich H-GG. HIV-1 assembly, budding, and maturation [Internet]. Cold Spring Harbor Perspectives in Medicine Cold Spring Harbor Laboratory Press; Jul, 2012 p. a006924. Available from: <http://www.ncbi.nlm.nih.gov/pubmed/22762019>
241. Carlson L-A, de Marco A, Oberwinkler H, Habermann A, Briggs JAG, Kräusslich H-G, et al. Cryo Electron Tomography of Native HIV-1 Budding Sites. Hope TJ, editor. *PLoS Pathog* [Internet]. Public Library of Science; 2010 Nov 24 [cited 2016 Dec 19];6(11):e1001173. Available from: <http://dx.plos.org/10.1371/journal.ppat.1001173>
242. Frankel AD, Young JAT. HIV-1: Fifteen Proteins and an RNA. *Annu Rev Biochem*. 1998;67:1–25.
243. Ono A, Freed EO. Plasma membrane rafts play a critical role in HIV-1 assembly and release. *Proc Natl Acad Sci* [Internet]. 2001 Nov 20 [cited 2016 Dec 19];98(24):13925–30. Available from: <http://www.ncbi.nlm.nih.gov/pubmed/11717449>
244. Dale BM, McNerney GP, Thompson DL, Hubner W, de los Reyes K, Chuang FYS, et al. Cell-to-Cell Transfer of HIV-1 via Virological Synapses Leads to Endosomal Virion Maturation that Activates Viral Membrane Fusion. *Cell Host Microbe* [Internet]. 2011 Dec 15 [cited 2017 Jan 18];10(6):551–62. Available from: <http://www.ncbi.nlm.nih.gov/pubmed/22177560>
245. Jouvenet N, Simon SM, Bieniasz PD. Imaging the interaction of HIV-1 genomes and Gag during assembly of individual viral particles. *Proc Natl Acad Sci U S A* [Internet]. National Academy of Sciences; 2009 Nov 10 [cited 2017 Feb 12];106(45):19114–9. Available from: <http://www.ncbi.nlm.nih.gov/pubmed/19861549>
246. Ono A, Ablan SD, Lockett SJ, Nagashima K, Freed EO. Phosphatidylinositol (4,5) bisphosphate regulates HIV-1 Gag targeting to the plasma membrane. *Proc Natl Acad Sci* [Internet]. 2004 Oct 12 [cited 2016 Dec 19];101(41):14889–94. Available from: <http://www.ncbi.nlm.nih.gov/pubmed/15465916>
247. Balasubramaniam M, Freed EO. New Insights into HIV Assembly and Trafficking. *Physiology (Bethesda)*. 2011;26(5):236–51.
248. Sundquist WI, Kräusslich HG. HIV-1 assembly, budding, and maturation. Vol. 2, Cold Spring Harbor Perspectives in Medicine. 2012.
249. Murakami T, Freed EO. The long cytoplasmic tail of gp41 is required in a cell type-dependent

manner for HIV-1 envelope glycoprotein incorporation into virions.

250. Lever AML. HIV-1 RNA Packaging. Vol. 55, *Advances in Pharmacology*. 2007. p. 1–32.
251. Nikolaitchik OA, Dilley KA, Fu W, Gorelick RJ, Tai SHS, Soheilian F, et al. Dimeric RNA Recognition Regulates HIV-1 Genome Packaging. *PLoS Pathog*. 2013;9(3).
252. Accola MA, Strack B, Göttlinger HG. Efficient particle production by minimal Gag constructs which retain the carboxy-terminal domain of human immunodeficiency virus type 1 capsid-p2 and a late assembly domain. *J Virol* [Internet]. 2000 Jun [cited 2016 Dec 19];74(12):5395–402. Available from: <http://www.ncbi.nlm.nih.gov/pubmed/10823843>
253. Fuller SD, Wilk T, Gowen BE, Kräusslich H-G, Vogt VM. Cryo-electron microscopy reveals ordered domains in the immature HIV-1 particle. *Curr Biol* [Internet]. 1997;7(10):729–38. Available from: <http://www.cell.com/article/S0960982206003319/fulltext>
254. Wright ER, Schooler JB, Ding HJ, Kieffer C, Fillmore C, Sundquist WI, et al. Electron cryotomography of immature HIV-1 virions reveals the structure of the CA and SP1 Gag shells. *EMBO J* [Internet]. 2007;26(8):2218–26. Available from: <http://www.pubmedcentral.nih.gov/articlerender.fcgi?artid=1852790&tool=pmcentrez&rendertype=abstract>
255. Bieniasz PD. The Cell Biology of HIV-1 Virion Genesis. *Cell Host Microbe* [Internet]. 2009 Jun 18 [cited 2016 Dec 19];5(6):550–8. Available from: <http://www.ncbi.nlm.nih.gov/pubmed/19527882>
256. Hurley JH, Hanson PI. Membrane budding and scission by the ESCRT machinery: it's all in the neck. *Nat Rev Mol Cell Biol* [Internet]. Nature Publishing Group; 2010 Aug 30 [cited 2016 Dec 19];11(8):556–66. Available from: <http://www.nature.com/doifinder/10.1038/nrm2937>
257. Usami Y, Popov S, Popova E, Inoue M, Weissenhorn W, G. Göttlinger H. The ESCRT pathway and HIV-1 budding: Figure 1. *Biochem Soc Trans* [Internet]. 2009 Feb 1 [cited 2016 Dec 19];37(1):181–4. Available from: <http://www.ncbi.nlm.nih.gov/pubmed/19143627>
258. Davies BA, Azmi IF, Payne J, Shestakova A, Horazdovsky BF, Babst M, et al. Coordination of Substrate Binding and ATP Hydrolysis in Vps4-Mediated ESCRT-III Disassembly. *Mol Biol Cell* [Internet]. 2010 Oct 1 [cited 2016 Dec 19];21(19):3396–408. Available from: <http://www.ncbi.nlm.nih.gov/pubmed/20702581>
259. Ivanchenko S, Godinez WJ, Lampe M, Kräusslich HG, Eils R, Rohr K, et al. Dynamics of HIV-1 assembly and release. *PLoS Pathog*. 2009;5(11).
260. Malim MH, Bieniasz PD. HIV restriction factors and mechanisms of evasion. *Cold Spring Harb Perspect Med*. 2012;2(5).

261. Hill M, Tachedjian G, Mak J. The Packaging and Maturation of the HIV-1 Pol Proteins. *Curr HIV Res* [Internet]. 2005 Jan 1 [cited 2016 Dec 19];3(1):73–85. Available from: <http://openurl.ingenta.com/content/xref?genre=article&issn=1570-162X&volume=3&issue=1&spage=73>
262. Tang C, Louis JM, Aniana A, Suh J-Y, Clore GM. Visualizing transient events in amino-terminal autoprocessing of HIV-1 protease. *Nature* [Internet]. 2008 Oct 2 [cited 2017 Feb 12];455(7213):693–6. Available from: <http://www.ncbi.nlm.nih.gov/pubmed/18833280>
263. Janeway CA. Approaching the Asymptote? Evolution and Revolution in Immunology. *Cold Spring Harb Symp Quant Biol* [Internet]. 1989 Jan 1 [cited 2017 Feb 18];54(0):1–13. Available from: <http://symposium.cshlp.org/cgi/doi/10.1101/SQB.1989.054.01.003>
264. Platanias LC. Mechanisms of type-I- and type-II-interferon-mediated signalling. *Nat Rev Immunol* [Internet]. Nature Publishing Group; 2005 May [cited 2016 Dec 20];5(5):375–86. Available from: <http://www.nature.com/doi/10.1038/nri1604>
265. Rustagi A, Gale M. Innate antiviral immune signaling, viral evasion and modulation by HIV-1. Vol. 426, *Journal of Molecular Biology*. 2014. p. 1161–77.
266. Freed EO, Gale M. Antiviral innate immunity: editorial overview. *J Mol Biol* [Internet]. 2014 Mar 20 [cited 2017 Feb 17];426(6):1129–32. Available from: <http://linkinghub.elsevier.com/retrieve/pii/S0022283614000436>
267. Horowitz A, Strauss-Albee DM, Leipold M, Kubo J, Nemat-Gorgani N, Dogan OC, et al. Genetic and environmental determinants of human NK cell diversity revealed by mass cytometry. *Sci Transl Med* [Internet]. 2013;5(208):208ra145. Available from: <http://www.ncbi.nlm.nih.gov/pubmed/24154599%5Cnhttp://www.pubmedcentral.nih.gov/articlerender.fcgi?artid=PMC3918221>
268. Bashirova AA, Thomas R, Carrington M. HLA/KIR Restraint of HIV: Surviving the Fittest. *Annu Rev Immunol* [Internet]. 2011;29(1):295–317. Available from: <http://www.annualreviews.org/doi/abs/10.1146/annurev-immunol-031210-101332>
269. Cohen GB, Gandhi RT, Davis DM, Mandelboim O, Chen BK, Strominger JL, et al. The selective downregulation of class I major histocompatibility complex proteins by HIV-1 protects HIV-infected cells from NK cells. *Immunity*. 1999;10(6):661–71.
270. Norman JM, Mashiba M, McNamara LA, Onafuwa-Nuga A, Chiari-Fort E, Shen W, et al. The antiviral factor APOBEC3G enhances the recognition of HIV-infected primary T cells by natural killer cells. *Nat Immunol* [Internet]. 2011;12(10):975–83. Available from: <http://www.ncbi.nlm.nih.gov/pubmed/21874023%5Cnhttp://www.pubmedcentral.nih.gov/articlerender.fcgi?artid=PMC3530928>

271. Pedersen C, Lindhardt BO, Jensen BL, Lauritzen E, Gerstoft J, Dickmeiss E, et al. Clinical course of primary HIV infection: consequences for subsequent course of infection. *BMJ*. 1989;299(6692):154–7.
272. Altfeld M, Addo MM, Rosenberg ES, Hecht FM, Lee PK, Vogel M, et al. Influence of HLA-B57 on clinical presentation and viral control during acute HIV-1 infection. *AIDS*. 2003;17(April):2581–91.
273. Vaidya SA, Korner C, Sirignano MN, Amero M, Bazner S, Rychert J, et al. Tumor necrosis factor  $\alpha$  is associated with viral control and early disease progression in patients with HIV type 1 infection. *J Infect Dis* [Internet]. 2014;210(7):1042–6. Available from: <http://www.pubmedcentral.nih.gov/articlerender.fcgi?artid=4215080&tool=pmcentrez&rendertype=abstract>
274. Kawai T, Akira S. The role of pattern-recognition receptors in innate immunity: update on Toll-like receptors. *Nat Immunol* [Internet]. Nature Research; 2010 May 20 [cited 2016 Dec 20];11(5):373–84. Available from: <http://www.nature.com/doi/10.1038/ni.1863>
275. Wu J, Chen ZJ. Innate Immune Sensing and Signaling of Cytosolic Nucleic Acids. *Annu Rev Immunol* [Internet]. Annual Reviews ; 2014 Mar 21 [cited 2016 Dec 19];32(1):461–88. Available from: <http://www.annualreviews.org/doi/10.1146/annurev-immunol-032713-120156>
276. Rathinam VAK, Vanaja SK, Fitzgerald KA. Regulation of inflammasome signaling. *Nat Immunol* [Internet]. Nature Research; 2012 Mar 19 [cited 2016 Dec 27];13(4):333–332. Available from: <http://www.nature.com/doi/10.1038/ni.2237>
277. Lester SN, Li K. Toll-Like Receptors in Antiviral Innate Immunity. *J Mol Biol* [Internet]. 2014 Mar 20 [cited 2017 Feb 18];426(6):1246–64. Available from: <http://www.ncbi.nlm.nih.gov/pubmed/24316048>
278. Pandey S, Kawai T, Akira S. notes on Microbial sensing by Toll-like receptors and intracellular nucleic acid sensors. 2015;1(Table 1).
279. Hemmi H, Takeuchi O, Kawai T, Kaisho T, Sato S, Sanjo H, et al. A Toll-like receptor recognizes bacterial DNA. *Nature* [Internet]. 2000 Dec 7 [cited 2014 Dec 22];408(6813):740–5. Available from: <http://www.ncbi.nlm.nih.gov/pubmed/11130078>
280. Xagorari A, Chlichlia K. Toll-like receptors and viruses: induction of innate antiviral immune responses. *Open Microbiol J* [Internet]. Bentham Science Publishers; 2008 [cited 2016 Dec 19];2:49–59. Available from: <http://www.ncbi.nlm.nih.gov/pubmed/19088911>
281. Hou F, Sun L, Zheng H, Skaug B, Jiang Q-X, Chen ZJ, et al. MAVS forms functional prion-like aggregates to activate and propagate antiviral innate immune response. *Cell* [Internet]. Elsevier;

- 2011 Aug 5 [cited 2016 Dec 20];146(3):448–61. Available from: <http://www.ncbi.nlm.nih.gov/pubmed/21782231>
282. Liu S, Chen J, Cai X, Wu J, Chen X, Wu Y-T, et al. MAVS recruits multiple ubiquitin E3 ligases to activate antiviral signaling cascades. *Elife* [Internet]. eLife Sciences Publications Limited; 2013 Aug 14 [cited 2016 Dec 22];2:e00785. Available from: <http://www.ncbi.nlm.nih.gov/pubmed/23951545>
283. Clark K, Peggie M, Plater L, Sorcek RJ, Young ERR, Madwed JB, et al. Novel cross-talk within the IKK family controls innate immunity. *Biochem J* [Internet]. 2011 Feb 15 [cited 2017 Mar 6];434(1):93–104. Available from: <http://www.ncbi.nlm.nih.gov/pubmed/21138416>
284. Malathi K, Saito T, Crochet N, Barton DJ, Gale M, Silverman RH. RNase L releases a small RNA from HCV RNA that refolds into a potent PAMP. *RNA* [Internet]. 2010;16(11):2108–19. Available from: <http://www.pubmedcentral.nih.gov/articlerender.fcgi?artid=2957051&tool=pmcentrez&rendertype=abstract>
285. Malathi K, Dong B, Gale MJ, Silverman RH. Small self-RNA generated by RNase L amplifies antiviral innate immunity. *Nature*. 2007;448(7155):816–9.
286. Keating SE, Baran M, Bowie AG. Cytosolic DNA sensors regulating type I interferon induction. *Trends Immunol* [Internet]. 2011 Dec [cited 2015 Jan 27];32(12):574–81. Available from: <http://www.sciencedirect.com/science/article/pii/S1471490611001451>
287. Ishii KJ, Kawagoe T, Koyama S, Matsui K, Kumar H, Kawai T, et al. TANK-binding kinase-1 delineates innate and adaptive immune responses to DNA vaccines. *Nature* [Internet]. Nature Publishing Group; 2008 Feb 7 [cited 2016 Dec 28];451(7179):725–9. Available from: <http://www.nature.com/doifinder/10.1038/nature06537>
288. Gray EE, Winship D, Snyder JM, Child SJ, Geballe AP, Stetson Correspondence DB, et al. The AIM2-like Receptors Are Dispensable for the Interferon Response to Intracellular DNA. *Immunity* [Internet]. Elsevier Inc.; 2016;1–12. Available from: <http://dx.doi.org/10.1016/j.immuni.2016.06.015>
289. Yoh SM, Schneider M, Seifried J, Soonthornvacharin S, Akleh RE, Olivieri KC, et al. PQBP1 Is a Proximal Sensor of the cGAS-Dependent Innate Response to HIV-1. *Cell* [Internet]. 2015 Jun [cited 2016 Dec 28];161(6):1293–305. Available from: <http://linkinghub.elsevier.com/retrieve/pii/S0092867415005255>
290. Abe T, Barber GN. Cytosolic-DNA-Mediated, STING-Dependent Proinflammatory Gene Induction Necessitates Canonical NF- B Activation through TBK1. *J Virol* [Internet]. 2014 Mar 5 [cited 2015 Apr 12];88(10):5328–41. Available from:

<http://www.pubmedcentral.nih.gov/articlerender.fcgi?artid=4019140&tool=pmcentrez&rendertype=abstract>

291. Schoggins JW, MacDuff DA, Imanaka N, Gainey MD, Shrestha B, Eitson JL, et al. Pan-viral specificity of IFN-induced genes reveals new roles for cGAS in innate immunity. *Nature* [Internet]. 2013 Nov 27 [cited 2017 Feb 18];505(7485):691–5. Available from: <http://www.ncbi.nlm.nih.gov/pubmed/24284630>
292. Chen Q, Sun L, Chen ZJ. Regulation and function of the cGAS–STING pathway of cytosolic DNA sensing. *Nat Immunol* [Internet]. *Nature Research*; 2016 Sep 20 [cited 2016 Dec 24];17(10):1142–9. Available from: <http://www.nature.com/doi/10.1038/ni.3558>
293. Sun L, Wu J, Du F, Chen X, Chen ZJ. Cyclic GMP-AMP synthase is a cytosolic DNA sensor that activates the type I interferon pathway. *Science* [Internet]. 2013;339(6121):786–91. Available from: <http://www.pubmedcentral.nih.gov/articlerender.fcgi?artid=3863629&tool=pmcentrez&rendertype=abstract>
294. Zhang X, Wu J, Du F, Xu H, Sun L, Chen Z, et al. The Cytosolic DNA Sensor cGAS Forms an Oligomeric Complex with DNA and Undergoes Switch-like Conformational Changes in the Activation Loop. *Cell Rep* [Internet]. 2014 Feb [cited 2016 Dec 22];6(3):421–30. Available from: <http://linkinghub.elsevier.com/retrieve/pii/S2211124714000047>
295. Bridgeman A, Maelfait J, Davenne T, Partridge T, Peng Y, Mayer A, et al. Viruses transfer the antiviral second messenger cGAMP between cells. *Science* (80- ) [Internet]. 2015 Sep 11 [cited 2017 Feb 18];349(6253):1228–32. Available from: <http://www.ncbi.nlm.nih.gov/pubmed/26229117>
296. Gentili M, Kowal J, Tkach M, Satoh T, Lahaye X, Conrad C, et al. Transmission of innate immune signaling by packaging of cGAMP in viral particles. *Science* (80- ) [Internet]. 2015 Sep 11 [cited 2017 Feb 18];349(6253):1232–6. Available from: <http://www.ncbi.nlm.nih.gov/pubmed/26229115>
297. Zhong B, Yang Y, Li S, Wang Y-Y, Li Y, Diao F, et al. The adaptor protein MITA links virus-sensing receptors to IRF3 transcription factor activation. *Immunity* [Internet]. Elsevier; 2008 Oct 17 [cited 2016 Dec 22];29(4):538–50. Available from: <http://www.ncbi.nlm.nih.gov/pubmed/18818105>
298. Ishikawa H, Barber GN. STING is an endoplasmic reticulum adaptor that facilitates innate immune signalling. *Nature* [Internet]. *Nature Publishing Group*; 2008 Nov 13 [cited 2016 Dec 22];456(7219):274–274. Available from: <http://www.nature.com/doi/10.1038/nature07432>
299. Gao P, Ascano M, Zillinger T, Wang W, Dai P, Serganov AA, et al. Structure-Function Analysis

- of STING Activation by c[G(2',5')pA(3',5')p] and Targeting by Antiviral DMXAA. *Cell* [Internet]. 2013 Aug 15 [cited 2017 Feb 18];154(4):748–62. Available from: <http://www.ncbi.nlm.nih.gov/pubmed/23910378>
300. Yin Q, Tian Y, Kabaleeswaran V, Jiang X, Tu D, Eck MJ, et al. Cyclic di-GMP Sensing via the Innate Immune Signaling Protein STING. *Mol Cell* [Internet]. 2012 Jun 29 [cited 2017 Feb 18];46(6):735–45. Available from: <http://www.ncbi.nlm.nih.gov/pubmed/22705373>
  301. Ouyang S, Song X, Wang Y, Ru H, Shaw N, Jiang Y, et al. Structural Analysis of the STING Adaptor Protein Reveals a Hydrophobic Dimer Interface and Mode of Cyclic di-GMP Binding. *Immunity* [Internet]. 2012 Jun 29 [cited 2017 Feb 18];36(6):1073–86. Available from: <http://www.ncbi.nlm.nih.gov/pubmed/22579474>
  302. Wu J, Sun L, Chen X, Du F, Shi H, Chen C, et al. Cyclic GMP-AMP is an endogenous second messenger in innate immune signaling by cytosolic DNA. *Science* [Internet]. 2013;339(6121):826–30. Available from: <http://www.ncbi.nlm.nih.gov/pubmed/23258412> <http://www.pubmedcentral.nih.gov/articlerender.fcgi?artid=3855410&tool=pmcentrez&rendertype=abstract>
  303. Danilchanka O, Mekalanos JJ. Cyclic Dinucleotides and the Innate Immune Response. *Cell* [Internet]. 2013 Aug [cited 2016 Dec 26];154(5):962–70. Available from: <http://linkinghub.elsevier.com/retrieve/pii/S0092867413010088>
  304. Tsuchiya Y, Jounai N, Takeshita F, Ishii KJ, Mizuguchi K. Ligand-induced Ordering of the C-terminal Tail Primes STING for Phosphorylation by TBK1. *EBioMedicine* [Internet]. 2016 Jul [cited 2016 Dec 26];9:87–96. Available from: <http://linkinghub.elsevier.com/retrieve/pii/S2352396416302419>
  305. Ishikawa H, Ma Z, Barber GN. STING regulates intracellular DNA-mediated, type I interferon-dependent innate immunity. *Nature* [Internet]. Nature Publishing Group; 2009;461(7265):788–92. Available from: <http://dx.doi.org/10.1038/nature08476>
  306. Tanaka Y, Chen ZJ. STING Specifies IRF3 Phosphorylation by TBK1 in the Cytosolic DNA Signaling Pathway. *Sci Signal*. 2012;5(214).
  307. Abe T, Harashima A, Xia T, Konno H, Konno K, Morales A, et al. STING recognition of cytoplasmic DNA instigates cellular defense. *Mol Cell* [Internet]. 2013 Apr 11 [cited 2015 Mar 18];50(1):5–15. Available from: <http://www.pubmedcentral.nih.gov/articlerender.fcgi?artid=3881179&tool=pmcentrez&rendertype=abstract>
  308. Chen H, Sun H, You F, Sun W, Zhou X, Chen L, et al. Activation of STAT6 by STING is critical for antiviral innate immunity. *Cell* [Internet]. Elsevier; 2011 Oct 14 [cited 2016 Dec

- 27];147(2):436–46. Available from: <http://www.ncbi.nlm.nih.gov/pubmed/22000020>
309. Schoggins JW, Wilson SJ, Panis M, Murphy MY, Jones CT, Bieniasz P, et al. A diverse range of gene products are effectors of the type I interferon antiviral response. *Nature* [Internet]. *Nature Research*; 2011 Apr 28 [cited 2016 Dec 26];472(7344):481–5. Available from: <http://www.nature.com/doi/10.1038/nature09907>
310. Xia T, Konno H, Ahn J, Barber GN. Deregulation of STING Signaling in Colorectal Carcinoma Constrains DNA Damage Responses and Correlates With Tumorigenesis. *Cell Rep*. 2016;14(2):282–97.
311. Graham FL, Smiley J, Russell WC, Nairn R. Characteristics of a Human Cell Line Transformed by DNA from Human Adenovirus Type 5. *J gen Virol*. 1977;36:59–7.
312. Znidar K, Bosnjak M, Cemazar M, Heller LC. Cytosolic DNA Sensor Upregulation Accompanies DNA Electrotransfer in B16.F10 Melanoma Cells. *Mol Ther Nucleic Acids* [Internet]. Nature Publishing Group; 2016 Jun 7 [cited 2016 Dec 19];5(6):e322. Available from: <http://www.ncbi.nlm.nih.gov/pubmed/27271988>
313. Berg RK, Rahbek SH, Kofod-Olsen E, Holm CK, Melchjorsen J, Jensen DG, et al. T cells detect intracellular DNA but fail to induce type I IFN responses: implications for restriction of HIV replication. *PLoS One* [Internet]. 2014 Jan [cited 2015 Apr 5];9(1):e84513. Available from: <http://www.pubmedcentral.nih.gov/articlerender.fcgi?artid=3880311&tool=pmcentrez&rendertype=abstract>
314. Seo GJ, Yang A, Tan B, Kim S, Liang Q, Choi Y, et al. Akt Kinase-Mediated Checkpoint of cGAS DNA Sensing Pathway. *Cell Rep* [Internet]. 2015 Oct [cited 2016 Dec 26];13(2):440–9. Available from: <http://linkinghub.elsevier.com/retrieve/pii/S2211124715010189>
315. Abe T, Barber GN. Cytosolic-DNA-Mediated, STING-Dependent Proinflammatory Gene Induction Necessitates Canonical NF- $\kappa$ B Activation through TBK1. *J Virol* [Internet]. 2014;88(10):5328–41. Available from: <http://www.ncbi.nlm.nih.gov/pubmed/24600004>
316. Nazli A, Kafka JK, Ferreira VH, Anipindi V, Mueller K, Osborne BJ, et al. HIV-1 gp120 induces TLR2- and TLR4-mediated innate immune activation in human female genital epithelium. *J Immunol* [Internet]. 2013;191(8):4246–58. Available from: <http://www.ncbi.nlm.nih.gov/pubmed/24043886>
317. Schlaepfer E, Audigé A, Joller H, Speck RF. TLR7/8 triggering exerts opposing effects in acute versus latent HIV infection. *J Immunol* [Internet]. 2006;176(5):2888–95. Available from: <http://www.ncbi.nlm.nih.gov/pubmed/16493046>
318. Wang Y, Wang X, Li J, Zhou Y, Ho W. RIG-I activation inhibits HIV replication in macrophages.

- J Leukoc Biol [Internet]. 2013;94(2):337–41. Available from: <http://www.ncbi.nlm.nih.gov/pubmed/23744645>
319. Berg RK, Melchjorsen J, Rintahaka J, Diget E, Søbystad S, Horan KA, et al. Genomic HIV RNA induces innate immune responses through RIG-I-dependent sensing of secondary-structured RNA. *PLoS One* [Internet]. 2012 Jan [cited 2013 Feb 28];7(1):e29291. Available from: <http://www.pubmedcentral.nih.gov/articlerender.fcgi?artid=3250430&tool=pmcentrez&rendertype=abstract>
  320. Perez-Caballero D, Zang T, Ebrahimi A, McNatt MW, Gregory DA, Johnson MC, et al. Tetherin Inhibits HIV-1 Release by Directly Tethering Virions to Cells. *Cell*. 2009;139(3):499–511.
  321. Neil SJD, Zang T, Bieniasz PD. Tetherin inhibits retrovirus release and is antagonized by HIV-1 Vpu. *Nature*. 2008;451(7177):425–30.
  322. Hotter D, Sauter D, Kirchhoff F. Emerging role of the host restriction factor tetherin in viral immune sensing. Vol. 425, *Journal of Molecular Biology*. 2013. p. 4956–64.
  323. Price AJ, Fletcher AJ, Schaller T, Elliott T, Lee KE, KewalRamani VN, et al. CPSF6 Defines a Conserved Capsid Interface that Modulates HIV-1 Replication. *PLoS Pathog*. 2012;8(8).
  324. Hilditch L, Towers GJ. A model for cofactor use during HIV-1 reverse transcription and nuclear entry. *Curr Opin Virol* [Internet]. 2014 [cited 2017 Mar 21];4:32–6. Available from: <http://dx.doi.org/10.1016/j.coviro.2013.11.003>
  325. Lee K, Ambrose Z, Martin TD, Oztop I, Mulky A, Julias JG, et al. Flexible use of nuclear import pathways by HIV-1. *Cell Host Microbe* [Internet]. NIH Public Access; 2010 Mar 18 [cited 2017 Feb 12];7(3):221–33. Available from: <http://www.ncbi.nlm.nih.gov/pubmed/20227665>
  326. Gao D, Wu J, Wu Y-T, Du F, Aroh C, Yan N, et al. Cyclic GMP-AMP synthase is an innate immune sensor of HIV and other retroviruses. *Science* [Internet]. 2013 Aug 23 [cited 2015 Feb 8];341(6148):903–6. Available from: <http://www.pubmedcentral.nih.gov/articlerender.fcgi?artid=3860819&tool=pmcentrez&rendertype=abstract>
  327. Manel N, Hogstad B, Wang Y, Levy DE, Unutmaz D, Littman DR. A cryptic sensor for HIV-1 activates antiviral innate immunity in dendritic cells. *Nature* [Internet]. 2010;467(7312):214–7. Available from: <http://www.pubmedcentral.nih.gov/articlerender.fcgi?artid=3051279&tool=pmcentrez&rendertype=abstract>
  328. Wei W, Yu X. Previews HIV-1 / HIV-2 versus SAMHD1 Restriction : A Tale of Two Viruses. *Cell Host Microbe* [Internet]. Elsevier Inc.; 2015;17(1):8–9. Available from:

<http://dx.doi.org/10.1016/j.chom.2014.12.005>

329. Hrecka K, Hao C, Gierszewska M, Swanson SK, Kesik-Brodacka M, Srivastava S, et al. Vpx relieves inhibition of HIV-1 infection of macrophages mediated by the SAMHD1 protein. *Nature* [Internet]. 2011;474(7353):658–61. Available from: <http://www.nature.com/nature/journal/v474/n7353/pdf/nature10195.pdf><http://www.nature.com/doi/10.1038/nature10195>
330. Lahaye X, Satoh T, Gentili M, Cerboni S, Conrad C, Hurbain I, et al. The Capsids of HIV-1 and HIV-2 Determine Immune Detection of the Viral cDNA by the Innate Sensor cGAS in Dendritic Cells. *Immunity* [Internet]. 2013 Nov 20 [cited 2013 Dec 13];1–11. Available from: <http://www.ncbi.nlm.nih.gov/pubmed/24269171>
331. Wälde S, Thakar K, Hutten S, Spillner C, Nath A, Rothbauer U, et al. The nucleoporin Nup358/RanBP2 promotes nuclear import in a cargo- and transport receptor-specific manner. *Traffic* [Internet]. 2012 Feb [cited 2013 Apr 18];13(2):218–33. Available from: <http://www.ncbi.nlm.nih.gov/pubmed/21995724>
332. Meehan AM, Saenz DT, Guevera R, Morrison JH, Peretz M, Fadel HJ, et al. A cyclophilin homology domain-independent role for Nup358 in HIV-1 infection. *PLoS Pathog* [Internet]. 2014 Feb [cited 2015 Apr 16];10(2):e1003969. Available from: <http://www.pubmedcentral.nih.gov/articlerender.fcgi?artid=3930637&tool=pmcentrez&rendertype=abstract>
333. Brass AL, Dykxhoorn DM, Benita Y, Yan N, Engelman A, Xavier RJ, et al. Identification of host proteins required for HIV infection through a functional genomic screen. *Science* (80- ) [Internet]. 2008;319(5865):921–6. Available from: <http://www.ncbi.nlm.nih.gov/pubmed/18187620><http://www.sciencemag.org/content/319/5865/921.full.pdf>
334. Matreyek K a, Engelman A. The requirement for nucleoporin NUP153 during human immunodeficiency virus type 1 infection is determined by the viral capsid. *J Virol* [Internet]. 2011 Aug [cited 2013 Mar 29];85(15):7818–27. Available from: <http://www.pubmedcentral.nih.gov/articlerender.fcgi?artid=3147902&tool=pmcentrez&rendertype=abstract>
335. Yan N, Regalado-Magdos AD, Stiggelbout B, Lee-Kirsch MA, Lieberman J. The cytosolic exonuclease TREX1 inhibits the innate immune response to human immunodeficiency virus type 1. *Nat Immunol* [Internet]. 2010;11(11):1005–13. Available from: <http://www.pubmedcentral.nih.gov/articlerender.fcgi?artid=2958248&tool=pmcentrez&rendertype=abstract>
336. Yan N, Regalado-Magdos AD, Stiggelbout B, Lee-Kirsch MA, Lieberman J. The cytosolic

- exonuclease TREX1 inhibits the innate immune response to human immunodeficiency virus type 1. *Nat Immunol* [Internet]. Nature Publishing Group, a division of Macmillan Publishers Limited. All Rights Reserved.; 2010 Nov [cited 2015 Mar 1];11(11):1005–13. Available from: <http://dx.doi.org/10.1038/ni.1941>
337. Crow YJ, Chase DS, Lowenstein Schmidt J, Szykiewicz M, Forte GMA, Gornall HL, et al. Characterization of human disease phenotypes associated with mutations in *TREX1*, *RNASEH2A*, *RNASEH2B*, *RNASEH2C*, *SAMHD1*, *ADAR*, and *IFIH1*. *Am J Med Genet Part A* [Internet]. 2015 Feb [cited 2017 Mar 14];167(2):296–312. Available from: <http://www.ncbi.nlm.nih.gov/pubmed/25604658>
338. Hasan M, Koch J, Rakheja D, Pattnaik AK, Brugarolas J, Dozmorov I, et al. Trex1 regulates lysosomal biogenesis and interferon-independent activation of antiviral genes. *Nat Immunol* [Internet]. Nature Publishing Group; 2013;14(November):61–71. Available from: <http://www.ncbi.nlm.nih.gov/pubmed/23160154>  
<http://www.pubmedcentral.nih.gov/articlerender.fcgi?artid=3522772&tool=pmcentrez&rendertype=abstract>
339. Thompson MR, Sharma S, Atianand M, Jensen SB, Carpenter S, Knipe DM, et al. Interferon Gamma Inducible protein (IFI)16 transcriptionally regulates type I interferons and other interferon stimulated genes and controls the interferon response to both DNA and RNA viruses. *J Biol Chem* [Internet]. 2014;23568–82. Available from: <http://www.ncbi.nlm.nih.gov/pubmed/25002588>
340. Jakobsen MR, Bak RO, Andersen A, Berg RK, Jensen SB, Tengchuan J, et al. IFI16 senses DNA forms of the lentiviral replication cycle and controls HIV-1 replication. *Proc Natl Acad Sci U S A* [Internet]. 2013 Nov 26 [cited 2015 Apr 11];110(48):E4571-80. Available from: <http://www.pubmedcentral.nih.gov/articlerender.fcgi?artid=3845190&tool=pmcentrez&rendertype=abstract>
341. Kerur N, Veetil MV, Sharma-Walia N, Bottero V, Sadagopan S, Otageri P, et al. IFI16 acts as a nuclear pathogen sensor to induce the inflammasome in response to Kaposi Sarcoma-associated herpesvirus infection. *Cell Host Microbe* [Internet]. Elsevier Inc.; 2011;9(5):363–75. Available from: <http://dx.doi.org/10.1016/j.chom.2011.04.008>
342. Monroe KM, Yang Z, Johnson JR, Geng X, Doitsh G, Krogan NJ, et al. IFI16 DNA sensor is required for death of lymphoid CD4 T cells abortively infected with HIV. *Science* [Internet]. 2014;343(6169):428–32. Available from: <http://www.pubmedcentral.nih.gov/articlerender.fcgi?artid=3976200&tool=pmcentrez&rendertype=abstract>
343. Doitsh G, Galloway NLK, Geng X, Yang Z, Monroe KM, Zepeda O, et al. Cell death by pyroptosis drives CD4 T-cell depletion in HIV-1 infection. *Nature* [Internet]. 2013 Dec 19 [cited 2013 Dec

19]; Available from: <http://www.nature.com/doi/10.1038/nature12940>

344. Li M, Kao E, Gao X, Sandig H, Limmer K, Pavon-Eternod M, et al. Codon-usage-based inhibition of HIV protein synthesis by human schlafen 11. *Nature* [Internet]. 2012;491(7422):125–8. Available from: <http://www.ncbi.nlm.nih.gov/pubmed/23000900><http://www.pubmedcentral.nih.gov/articlerender.fcgi?artid=PMC3705913>
345. Goujon C, Moncorgé O, Bauby H, Doyle T, Ward CC, Schaller T, et al. Human MX2 is an interferon-induced post-entry inhibitor of HIV-1 infection. *Nature* [Internet]. 2013;502(7472):559–62. Available from: <http://www.nature.com/doi/10.1038/nature12542><http://www.ncbi.nlm.nih.gov/pubmed/24048477>
346. Lu J, Pan Q, Rong L, Liu S-L, Liang C. The IFITM Proteins Inhibit HIV-1 Infection. *J Virol* [Internet]. 2010;85(5):2126–37. Available from: <http://www.pubmedcentral.nih.gov/articlerender.fcgi?artid=3067758&tool=pmcentrez&rendertype=abstract>
347. Liu Z, Pan Q, Ding S, Qian J, Xu F, Zhou J, et al. The interferon-inducible MxB protein inhibits HIV-1 infection. *Cell Host Microbe*. 2013;14(4):398–410.
348. Kluge SF, Sauter D, Vogl M, Peeters M, Li Y, Bibollet-Ruche F, et al. The transmembrane domain of HIV-1 Vpu is sufficient to confer anti-tetherin activity to SIVcpz and SIVgor Vpu proteins: cytoplasmic determinants of Vpu function. *Retrovirology* [Internet]. BioMed Central; 2013 Mar 20 [cited 2017 Mar 14];10:32. Available from: <http://www.ncbi.nlm.nih.gov/pubmed/23514615>
349. Strebel K, Klimkait T, Maldarelli F, Martin MA. Molecular and biochemical analyses of human immunodeficiency virus type 1 vpu protein. *J Virol* [Internet]. American Society for Microbiology; 1989 Sep [cited 2017 Mar 15];63(9):3784–91. Available from: <http://www.ncbi.nlm.nih.gov/pubmed/2788224>
350. Klimkait T, Strebel K, Hoggan MD, Martin MA, Orenstein JM. The human immunodeficiency virus type 1-specific protein vpu is required for efficient virus maturation and release. *J Virol* [Internet]. 1990 Feb [cited 2017 Mar 15];64(2):621–9. Available from: <http://www.ncbi.nlm.nih.gov/pubmed/2404139>
351. Varthakavi V, Smith RM, Bour SP, Strebel K, Spearman P. Viral protein U counteracts a human host cell restriction that inhibits HIV-1 particle production. *Proc Natl Acad Sci* [Internet]. 2003 Dec 9 [cited 2017 Mar 14];100(25):15154–9. Available from: <http://www.ncbi.nlm.nih.gov/pubmed/14657387>

352. Galão RP, Le Tortorec A, Pickering S, Kueck T, Neil SJD. Innate sensing of HIV-1 assembly by tetherin induces NFκB-dependent proinflammatory responses. *Cell Host Microbe*. 2012;12(5):633–44.
353. Bieniasz PD. Restriction factors: a defense against retroviral infection. *Trends Microbiol* [Internet]. 2003 Jun [cited 2017 Mar 14];11(6):286–91. Available from: <http://www.ncbi.nlm.nih.gov/pubmed/12823946>
354. Wilson SJ, Webb BLJ, Ylinen LMJ, Verschoor E, Heeney JL, Towers GJ. Independent evolution of an antiviral TRIMCyp in rhesus macaques. *Proc Natl Acad Sci U S A*. 2008;105(9):3557–62.
355. Pertel T, Hausmann S, Morger D, Züger S, Guerra J, Lascano J, et al. TRIM5 is an innate immune sensor for the retrovirus capsid lattice. *Nature* [Internet]. *Nature Research*; 2011 Apr 21 [cited 2017 Feb 20];472(7343):361–5. Available from: <http://www.nature.com/doi/10.1038/nature09976>
356. Mangeat B, Turelli P, Caron G, Friedli M, Perrin L, Trono D. Broad antiretroviral defence by human APOBEC3G through lethal editing of nascent reverse transcripts. *Nature* [Internet]. *Nature Publishing Group*; 2003 Jul 3 [cited 2017 Mar 14];424(6944):99–103. Available from: <http://www.nature.com/doi/10.1038/nature01709>
357. Zennou V, Perez-Caballero D, Gottlinger H, Bieniasz PD. APOBEC3G Incorporation into Human Immunodeficiency Virus Type 1 Particles. *J Virol* [Internet]. 2004 Nov 1 [cited 2017 Mar 14];78(21):12058–61. Available from: <http://www.ncbi.nlm.nih.gov/pubmed/15479846>
358. Holmes RK, Malim MH, Bishop KN. APOBEC-mediated viral restriction: not simply editing? *Trends Biochem Sci* [Internet]. 2007 Mar [cited 2017 Mar 14];32(3):118–28. Available from: <http://www.ncbi.nlm.nih.gov/pubmed/17303427>
359. Yu X, Yu Y, Liu B, Luo K, Kong W, Mao P, et al. Induction of APOBEC3G ubiquitination and degradation by an HIV-1 Vif-Cul5-SCF complex. *Science* [Internet]. 2003 Nov 7 [cited 2017 Mar 14];302(5647):1056–60. Available from: <http://www.sciencemag.org/cgi/doi/10.1126/science.1089591>
360. Guo Y, Dong L, Qiu X, Wang Y, Zhang B, Liu H, et al. Structural basis for hijacking CBF-β and CUL5 E3 ligase complex by HIV-1 Vif. *Nature* [Internet]. 2014 Jan 8 [cited 2017 Mar 14];505(7482):229–33. Available from: <http://www.ncbi.nlm.nih.gov/pubmed/24402281>
361. Mulder LCF, Harari A, Simon V. Cytidine deamination induced HIV-1 drug resistance. *Proc Natl Acad Sci U S A* [Internet]. *National Academy of Sciences*; 2008 Apr 8 [cited 2017 Mar 14];105(14):5501–6. Available from: <http://www.ncbi.nlm.nih.gov/pubmed/18391217>
362. Sato K, Takeuchi JS, Misawa N, Izumi T, Kobayashi T, Kimura Y, et al. APOBEC3D and

APOBEC3F Potently Promote HIV-1 Diversification and Evolution in Humanized Mouse Model. Ross SR, editor. PLoS Pathog [Internet]. Public Library of Science; 2014 Oct 16 [cited 2017 Mar 14];10(10):e1004453. Available from: <http://dx.plos.org/10.1371/journal.ppat.1004453>

363. Baldauf H-M, Pan X, Erikson E, Schmidt S, Daddacha W, Burggraf M, et al. SAMHD1 restricts HIV-1 infection in resting CD4(+) T cells. *Nat Med* [Internet]. 2012;18(11):1682–7. Available from: <http://www.pubmedcentral.nih.gov/articlerender.fcgi?artid=3828732&tool=pmcentrez&rendertype=abstract%5Cnhttp://www.ncbi.nlm.nih.gov/pubmed/22972397%5Cnhttp://www.pubmedcentral.nih.gov/articlerender.fcgi?artid=PMC3828732>
364. Laguette N, Sobhian B, Casartelli N, Ringeard M, Chable-Bessia C, Ségéral E, et al. SAMHD1 is the dendritic- and myeloid-cell-specific HIV-1 restriction factor counteracted by Vpx. *Nature* [Internet]. 2011;474(7353):654–7. Available from: <http://www.ncbi.nlm.nih.gov/pubmed/21613998%5Cnhttp://www.pubmedcentral.nih.gov/articlerender.fcgi?artid=PMC3595993>
365. Lahouassa H, Daddacha W, Hofmann H, Ayinde D, Logue EC, Dragin L, et al. SAMHD1 restricts the replication of human immunodeficiency virus type 1 by depleting the intracellular pool of deoxynucleoside triphosphates. *Nat Immunol* [Internet]. 2012 Feb 12 [cited 2017 Mar 14];13(3):223–8. Available from: <http://www.ncbi.nlm.nih.gov/pubmed/22327569>
366. Beloglazova N, Flick R, Tchigvintsev A, Brown G, Popovic A, Nocek B, et al. Nuclease Activity of the Human SAMHD1 Protein Implicated in the Aicardi-Goutieres Syndrome and HIV-1 Restriction. *J Biol Chem* [Internet]. 2013 Mar 22 [cited 2017 Mar 14];288(12):8101–10. Available from: <http://www.ncbi.nlm.nih.gov/pubmed/23364794>
367. Goujon C, Jarrosson-Wuillème L, Bernaud J, Rigal D, Darlix J-L, Cimarelli A. With a little help from a friend: increasing HIV transduction of monocyte-derived dendritic cells with virion-like particles of SIVMAC. *Gene Ther* [Internet]. 2006 Jun 9 [cited 2017 Mar 14];13(12):991–4. Available from: <http://www.ncbi.nlm.nih.gov/pubmed/16525481>
368. Sunseri N, O'Brien M, Bhardwaj N, Landau NR. Human Immunodeficiency Virus Type 1 Modified To Package Simian Immunodeficiency Virus Vpx Efficiently Infects Macrophages and Dendritic Cells. *J Virol* [Internet]. 2011 Jul 1 [cited 2017 Mar 14];85(13):6263–74. Available from: <http://www.ncbi.nlm.nih.gov/pubmed/21507971>
369. Bobadilla S, Sunseri N, Landau NR. Efficient transduction of myeloid cells by an HIV-1-derived lentiviral vector that packages the Vpx accessory protein. *Gene Ther* [Internet]. NIH Public Access; 2013 May [cited 2017 Mar 14];20(5):514–20. Available from: <http://www.ncbi.nlm.nih.gov/pubmed/22895508>
370. Le Rouzic E, Belaïdouni N, Estrabaud E, Morel M, Rain J-C, Transy C, et al. HIV1 Vpr Arrests

the Cell Cycle by Recruiting DCAF1/VprBP, a Receptor of the Cul4-DDB1 Ubiquitin Ligase. *Cell Cycle* [Internet]. 2007 Jan 15 [cited 2017 Mar 14];6(2):182–8. Available from: <http://www.ncbi.nlm.nih.gov/pubmed/17314515>

371. Hofmann H, Logue EC, Bloch N, Daddacha W, Polsky SB, Schultz ML, et al. The Vpx lentiviral accessory protein targets SAMHD1 for degradation in the nucleus. *J Virol* [Internet]. American Society for Microbiology (ASM); 2012 Dec [cited 2017 Mar 14];86(23):12552–60. Available from: <http://www.ncbi.nlm.nih.gov/pubmed/22973040>
372. Kim B, Nguyen LA, Daddacha W, Hollenbaugh JA. Tight interplay among SAMHD1 protein level, cellular dNTP levels, and HIV-1 proviral DNA synthesis kinetics in human primary monocyte-derived macrophages. *J Biol Chem* [Internet]. American Society for Biochemistry and Molecular Biology; 2012 Jun 22 [cited 2017 Mar 14];287(26):21570–4. Available from: <http://www.ncbi.nlm.nih.gov/pubmed/22589553>
373. Lim ES, Fregoso OI, McCoy CO, Matsen FA, Malik HS, Emerman M. The Ability of Primate Lentiviruses to Degrade the Monocyte Restriction Factor SAMHD1 Preceded the Birth of the Viral Accessory Protein Vpx. *Cell Host Microbe* [Internet]. 2012 Feb 16 [cited 2015 Apr 11];11(2):194–204. Available from: <http://www.pubmedcentral.nih.gov/articlerender.fcgi?artid=3288607&tool=pmcentrez&rendertype=abstract>
374. Etienne L, Hahn BH, Sharp PM, Matsen FA, Emerman M. Gene Loss and Adaptation to Hominids Underlie the Ancient Origin of HIV-1. *Cell Host Microbe* [Internet]. 2013 Jul 17 [cited 2017 Mar 14];14(1):85–92. Available from: <http://www.ncbi.nlm.nih.gov/pubmed/23870316>
375. Usami Y, Wu Y, Göttlinger HG. SERINC3 and SERINC5 restrict HIV-1 infectivity and are counteracted by Nef. *Nature* [Internet]. Nature Research; 2015 Sep 30 [cited 2017 Feb 19];526(7572):218–23. Available from: <http://www.nature.com/doifinder/10.1038/nature15400>
376. Rosa A, Chande A, Ziglio S, De Sanctis V, Bertorelli R, Goh SL, et al. HIV-1 Nef promotes infection by excluding SERINC5 from virion incorporation. *Nature* [Internet]. Nature Research; 2015 Sep 30 [cited 2017 Feb 19];526(7572):212–7. Available from: <http://www.nature.com/doifinder/10.1038/nature15399>
377. Goujon C, Malim MH. Characterization of the alpha interferon-induced postentry block to HIV-1 infection in primary human macrophages and T cells. *J Virol*. 2010;84(18):9254–66.
378. Abdel-Mohsen M, Raposo RAS, Deng X, Li M, Liegler T, Sinclair E, et al. Expression profile of host restriction factors in HIV-1 elite controllers. *Retrovirology* [Internet]. 2013;10:106. Available from: <http://www.pubmedcentral.nih.gov/articlerender.fcgi?artid=3827935&tool=pmcentrez&rendertype=abstract>

379. Qian J, Duff Y Le, Wang Y, Pan Q, Ding S, Zheng YM, et al. Primate lentiviruses are differentially inhibited by interferon-induced transmembrane proteins. *Virology*. 2015;474:10–8.
380. Compton AA, Bruel T, Porrot F, Mallet A, Sachse M, Euvrard M, et al. IFITM proteins incorporated into HIV-1 virions impair viral fusion and spread. *Cell Host Microbe*. 2014;16(6):736–47.
381. Tartour K, Appourchaux R, Gaillard J, Nguyen X-N, Durand S, Turpin J, et al. IFITM proteins are incorporated onto HIV-1 virion particles and negatively imprint their infectivity. *Retrovirology* [Internet]. 2014;11:103. Available from: <http://www.pubmedcentral.nih.gov/articlerender.fcgi?artid=4251951&tool=pmcentrez&rendertype=abstract>
382. DeLano W. Pymol: An open-source molecular graphics tool. *CCP4 Newsl Protein Crystallogr*. 2002;700.
383. Morellet N, Bouaziz S, Petitjean P, Roques B. NMR Structure of the HIV-1 Regulatory Protein VPR. *J Mol Biol* [Internet]. 2003 Mar [cited 2015 Apr 11];327(1):215–27. Available from: <http://www.sciencedirect.com/science/article/pii/S0022283603000603>
384. Wu Y, Zhou X, Barnes CO, DeLucia M, Cohen AE, Gronenborn AM, et al. The DDB1–DCAF1–Vpr–UNG2 crystal structure reveals how HIV-1 Vpr steers human UNG2 toward destruction. *Nat Struct Mol Biol* [Internet]. *Nature Research*; 2016 Aug 29 [cited 2017 Mar 16];23(10):933–40. Available from: <http://www.nature.com/doi/10.1038/nsmb.3284>
385. Strebel K, Berkhout B, Jeang K-T. HIV accessory proteins versus host restriction factors This review comes from a themed issue on Virus replication in animals and plants. *Curr Opin Virol* [Internet]. 2013 [cited 2017 Feb 19];3:692–9. Available from: <http://dx.doi.org/10.1016/j.coviro.2013.08.004>
386. Bouhamdan M, Benichou S, Rey F, Navarro JM, Agostini I, Spire B, et al. Human immunodeficiency virus type 1 Vpr protein binds to the uracil DNA glycosylase DNA repair enzyme. *J Virol* [Internet]. *American Society for Microbiology (ASM)*; 1996 Feb [cited 2017 Feb 28];70(2):697–704. Available from: <http://www.ncbi.nlm.nih.gov/pubmed/8551605>
387. Ahn J, Vu T, Novince Z, Guerrero-Santoro J, Ropic-Otrin V, Gronenborn AM. HIV-1 Vpr loads uracil DNA glycosylase-2 onto DCAF1, a substrate recognition subunit of a cullin 4A-RING E3 ubiquitin ligase for proteasome-dependent degradation. *J Biol Chem*. 2010;285(48):37333–41.
388. Romani B, Baygloo NS, Hamidi-Fard M, Aghasadeghi MR, Allahbakhshi E. HIV-1 Vpr Protein Induces Proteasomal Degradation of Chromatin-associated Class I HDACs to Overcome Latent Infection of Macrophages. *J Biol Chem* [Internet]. *American Society for Biochemistry and Molecular Biology*; 2016 Feb 5 [cited 2017 Feb 27];291(6):2696–711. Available from:

<http://www.ncbi.nlm.nih.gov/pubmed/26679995>

389. Laguette N, Brégnard C, Hue P, Basbous J, Yatim A, Larroque M, et al. Premature activation of the slx4 complex by vpr promotes g2/m arrest and escape from innate immune sensing. *Cell*. 2014;156:134–45.
390. Schwefel D, Groom HCT, Boucherit VC, Christodoulou E, Walker P a., Stoye JP, et al. Structural basis of lentiviral subversion of a cellular protein degradation pathway. *Nature* [Internet]. Nature Publishing Group; 2014;505(7482):234–8. Available from: <http://www.nature.com/nature/journal/v505/n7482/full/nature12815.html%5Cnhttp://www.nature.com/nature/journal/v505/n7482/pdf/nature12815.pdf>
391. Schröfelbauer B, Yu Q, Zeitlin SG, Landau NR. Human immunodeficiency virus type 1 Vpr induces the degradation of the UNG and SMUG uracil-DNA glycosylases. *J Virol* [Internet]. 2005 Sep 1 [cited 2017 Feb 27];79(17):10978–87. Available from: <http://jvi.asm.org/cgi/doi/10.1128/JVI.79.17.10978-10987.2005>
392. Zhou X, DeLucia M, Ahn J. SLX4-SLX1 protein-independent down-regulation of MUS81-EME1 protein by HIV-1 viral protein R (Vpr). *J Biol Chem*. 2016;291(33):16936–47.
393. Casey Klockow L, Sharifi HJ, Wen X, Flagg M, Furuya AKM, Nekorchuk M, et al. The HIV-1 protein Vpr targets the endoribonuclease Dicer for proteasomal degradation to boost macrophage infection. *Virology* [Internet]. 2013 Sep [cited 2017 Feb 25];444(1–2):191–202. Available from: <http://www.ncbi.nlm.nih.gov/pubmed/23849790>
394. Tristem M, Marshall C, Karpas A, Hill F. Evolution of the primate lentiviruses: evidence from vpx and vpr. *EMBO J* [Internet]. European Molecular Biology Organization; 1992 Sep [cited 2017 Feb 24];11(9):3405–12. Available from: <http://www.ncbi.nlm.nih.gov/pubmed/1324171>
395. Cohen EA, Terwilliger EF, Jalinoos Y, Proulx J, Sodroski JG, Haseltine WA. Identification of HIV-1 vpr product and function. *J Acquir Immune Defic Syndr* [Internet]. 1990 [cited 2017 Feb 25];3(1):11–8. Available from: <http://www.ncbi.nlm.nih.gov/pubmed/2136707>
396. Yuan X, Matsuda Z, Matsuda M, Essex M, Lee TH. Human immunodeficiency virus vpr gene encodes a virion-associated protein. *AIDS Res Hum Retroviruses* [Internet]. 1990 Nov [cited 2017 Feb 25];6(11):1265–71. Available from: <http://www.ncbi.nlm.nih.gov/pubmed/2150318>
397. Lu YL, Bennett RP, Wills JW, Gorelick R, Ratner L. A leucine triplet repeat sequence (LXX)4 in p6gag is important for Vpr incorporation into human immunodeficiency virus type 1 particles. *J Virol* [Internet]. 1995;69(11):6873–9. Available from: <http://www.pubmedcentral.nih.gov/articlerender.fcgi?artid=189602&tool=pmcentrez&rendertype=abstract>

398. Kondo E, Mammano F, Cohen E a, Göttlinger HG. The p6gag domain of human immunodeficiency virus type 1 is sufficient for the incorporation of Vpr into heterologous viral particles. *J Virol* [Internet]. 1995;69(5):2759–64. Available from: <http://www.pubmedcentral.nih.gov/articlerender.fcgi?artid=188969&tool=pmcentrez&rendertype=abstract>
399. Bachand F, Yao XJ, Hrimech M, Rougeau N, Cohen EA. Incorporation of Vpr into human immunodeficiency virus type 1 requires a direct interaction with the p6 domain of the p55 gag precursor. *J Biol Chem* [Internet]. 1999 Mar 26 [cited 2017 Feb 24];274(13):9083–91. Available from: <http://www.ncbi.nlm.nih.gov/pubmed/10085158>
400. Paxton W, Connor RI, Landau NR. Incorporation of Vpr into human immunodeficiency virus type 1 virions: requirement for the p6 region of gag and mutational analysis. *J Virol* [Internet]. 1993;67(12):7229–37. Available from: <http://www.pubmedcentral.nih.gov/articlerender.fcgi?artid=238185&tool=pmcentrez&rendertype=abstract>
401. Accola M a, Ohagen a, Göttlinger HG. Isolation of human immunodeficiency virus type 1 cores: retention of Vpr in the absence of p6(gag). *J Virol*. 2000;74(13):6198–202.
402. Fritz J V, Dujardin D, Godet J, Didier P, De Mey J, Darlix J-L, et al. HIV-1 Vpr oligomerization but not that of Gag directs the interaction between Vpr and Gag. *J Virol*. 2010;84(3):1585–96.
403. Singh SP, Tomkowicz B, Lai D, Cartas M, Mahalingam S, Kalyanaraman VS, et al. Functional role of residues corresponding to helical domain II (amino acids 35 to 46) of human immunodeficiency virus type 1 Vpr. *J Virol* [Internet]. 2000 Nov [cited 2017 Feb 24];74(22):10650–7. Available from: <http://www.ncbi.nlm.nih.gov/pubmed/11044109>
404. Kondo E, Göttlinger HG. A conserved LXXLF sequence is the major determinant in p6gag required for the incorporation of human immunodeficiency virus type 1 Vpr. *J Virol* [Internet]. 1996 Jan [cited 2017 Feb 24];70(1):159–64. Available from: <http://www.ncbi.nlm.nih.gov/pubmed/8523520>
405. Jenkins Y, Sanchez P V, Meyer BE, Malim MH. Nuclear export of human immunodeficiency virus type 1 Vpr is not required for virion packaging. *J Virol* [Internet]. 2001 Sep [cited 2017 Feb 24];75(17):8348–52. Available from: <http://www.ncbi.nlm.nih.gov/pubmed/11483780>
406. Müller B, Tessmer U, Schubert U, Kräusslich HG. Human immunodeficiency virus type 1 Vpr protein is incorporated into the virion in significantly smaller amounts than gag and is phosphorylated in infected cells. *J Virol* [Internet]. 2000 Oct [cited 2017 Feb 24];74(20):9727–31. Available from: <http://www.ncbi.nlm.nih.gov/pubmed/11000245>
407. Singh SP, Tungaturthi P, Cartas M, Tomkowicz B, Rizvi TA, Khan SA, et al. Virion-Associated

HIV-1 Vpr: Variable Amount in Virus Particles Derived from Cells upon Virus Infection or Proviral DNA Transfection. *Virology* [Internet]. 2001 Apr 25 [cited 2017 Feb 24];283(1):78–83. Available from: <http://www.ncbi.nlm.nih.gov/pubmed/11312664>

408. Bruns K, Fossen T, Wray V, Henklein P, Tessmer U, Schubert U. Structural Characterization of the HIV-1 Vpr N Terminus: Evidence of cis/trans-proline isomerism. *J Biol Chem*. 2003;278(44):43188–201.
409. Zhang S, Pointer D, Singer G, Feng Y, Park K, Zhao LJ. Direct binding to nucleic acids by Vpr of human immunodeficiency virus type 1. *Gene*. 1998;212(2):157–66.
410. Kamiyama T, Miura T, Takeuchi H. His-Trp cation- $\pi$  interaction and its structural role in an  $\alpha$ -helical dimer of HIV-1 Vpr protein. *Biophys Chem*. 2013;173–174:8–14.
411. Zander K, Sherman MP, Tessmer U, Bruns K, Wray V, Prechtel AT, et al. Cyclophilin A Interacts with HIV-1 Vpr and Is Required for Its Functional Expression. *J Biol Chem*. 2003;278(44):43202–13.
412. Le Rouzic E, Benichou S. The Vpr protein from HIV-1: distinct roles along the viral life cycle. *Retrovirology* [Internet]. 2005;2:11. Available from: <http://www.pubmedcentral.nih.gov/articlerender.fcgi?artid=554975&tool=pmcentrez&rendertype=abstract>
413. Coeytaux E, Coulaud D, Le Cam E, Danos O, Kichler A. The Cationic Amphipathic  $\alpha$ -Helix of HIV-1 Viral Protein R (Vpr) Binds to Nucleic Acids, Permeabilizes Membranes, and Efficiently Transfects Cells. *J Biol Chem* [Internet]. 2003 May 16 [cited 2017 Feb 24];278(20):18110–6. Available from: <http://www.ncbi.nlm.nih.gov/pubmed/12639957>
414. Sherman MP, Schubert U, Williams SA, de Noronha CMC, Kreisberg JF, Henklein P, et al. HIV-1 Vpr Displays Natural Protein-Transducing Properties: Implications for Viral Pathogenesis. *Virology* [Internet]. 2002;302(1):95–105. Available from: <http://www.sciencedirect.com/science/article/pii/S004268220291576X>
415. Kichler a., Pages J-CC, Leborgne C, Druillennec S, Lenoir C, Coulaud D, et al. Efficient DNA Transfection Mediated by the C-Terminal Domain of Human Immunodeficiency Virus Type 1 Viral Protein R. *J Virol* [Internet]. 2000;74(24):12003–12003. Available from: <http://jvi.asm.org/cgi/doi/10.1128/JVI.74.24.12003-12003.2000>
416. Mahalingam S, Ayyavoo V, Patel M, Kieber-Emmons T, Weiner DB. Nuclear import, virion incorporation, and cell cycle arrest/differentiation are mediated by distinct functional domains of human immunodeficiency virus type 1 Vpr. *J Virol* [Internet]. American Society for Microbiology (ASM); 1997 Sep [cited 2017 Feb 24];71(9):6339–47. Available from: <http://www.ncbi.nlm.nih.gov/pubmed/9261351>

417. Kogan M, Rappaport J. HIV-1 accessory protein Vpr: relevance in the pathogenesis of HIV and potential for therapeutic intervention. *Retrovirology* [Internet]. 2011;8:25. Available from: <http://www.pubmedcentral.nih.gov/articlerender.fcgi?artid=3090340&tool=pmcentrez&rendertype=abstract>
418. Bourbigot S, Beltz H, Denis J, Morellet N, Roques BP, Mély Y, et al. The C-terminal domain of the HIV-1 regulatory protein Vpr adopts an antiparallel dimeric structure in solution via its leucine-zipper-like domain. *Biochem J* [Internet]. 2005;387(Pt 2):333–41. Available from: <http://www.pubmedcentral.nih.gov/articlerender.fcgi?artid=1134961&tool=pmcentrez&rendertype=abstract>
419. Fritz J V, Didier P, Clamme J-P, Schaub E, Muriaux D, Cabanne C, et al. Direct Vpr-Vpr interaction in cells monitored by two photon fluorescence correlation spectroscopy and fluorescence lifetime imaging. *Retrovirology* [Internet]. 2008;5(1):87. Available from: <http://www.retrovirology.com/content/5/1/87>
420. Zhao LJ, Wang L, Mukherjee S, Narayan O. Biochemical mechanism of HIV-1 Vpr function. Oligomerization mediated by the N-terminal domain. *J Biol Chem*. 1994;269(51):32131–7.
421. Bolton DL, Lenardo MJ. Vpr cytopathicity independent of G2/M cell cycle arrest in human immunodeficiency virus type 1-infected CD4+ T cells. *J Virol* [Internet]. American Society for Microbiology; 2007 Sep [cited 2017 Feb 26];81(17):8878–90. Available from: <http://www.ncbi.nlm.nih.gov/pubmed/17553871>
422. Poon B, Grovit-Ferbas K, Stewart SA, Chen IS. Cell cycle arrest by Vpr in HIV-1 virions and insensitivity to antiretroviral agents. *Science* [Internet]. 1998 Jul 10 [cited 2017 Feb 25];281(5374):266–9. Available from: <http://www.ncbi.nlm.nih.gov/pubmed/9657723>
423. He JL, Choe S, Walker R, Dimarzio P, Morgan DO, Landau NR. Human-Immunodeficiency-Virus Type-1 Viral-Protein-R (Vpr) Arrests Cells in the G(2) Phase of the Cell-Cycle by Inhibiting P34(Cdc2) Activity. *J Virol*. 1995;69(11):6705–11.
424. Jowett JB, Planelles V, Poon B, Shah NP, Chen ML, Chen IS. The human immunodeficiency virus type 1 vpr gene arrests infected T cells in the G2 + M phase of the cell cycle. *J Virol* [Internet]. 1995;69(10):6304–13. Available from: <http://www.pubmedcentral.nih.gov/articlerender.fcgi?artid=189529&tool=pmcentrez&rendertype=abstract>
425. Stivahtis GL, Soares M a, Vodicka M a, Hahn BH, Emerman M. Conservation and host specificity of Vpr-mediated cell cycle arrest suggest a fundamental role in primate lentivirus evolution and biology. *J Virol*. 1997;71(6):4331–8.
426. Balliet JW, Kolson DL, Eiger G, Kim FM, McGann KA, Srinivasan A, et al. Distinct Effects in

- Primary Macrophages and Lymphocytes of the Human Immunodeficiency Virus Type 1 Accessory Genes vpr, vpu, and nef: Mutational Analysis of a Primary HIV-1 Isolate. *Virology* [Internet]. 1994 May 1 [cited 2017 Feb 27];200(2):623–31. Available from: <http://www.ncbi.nlm.nih.gov/pubmed/8178448>
427. Connor RI, Chen BK, Choe S, Landau NR. Vpr Is Required for Efficient Replication of Human Immunodeficiency Virus Type-1 in Mononuclear Phagocytes. *Virology* [Internet]. 1995 Feb [cited 2015 Apr 13];206(2):935–44. Available from: <http://www.sciencedirect.com/science/article/pii/S0042682285710161>
428. Eckstein DA, Sherman MP, Penn ML, Chin PS, De Noronha CM, Greene WC, et al. HIV-1 Vpr enhances viral burden by facilitating infection of tissue macrophages but not nondividing CD4+ T cells. *J Exp Med* [Internet]. 2001 Nov 19 [cited 2017 Feb 27];194(10):1407–19. Available from: <http://www.ncbi.nlm.nih.gov/pubmed/11714748>
429. Jacquot G, Le Rouzic E, Maidou-Peindara P, Maizy M, Lefrère J-J, Daneluzzi V, et al. Characterization of the Molecular Determinants of Primary HIV-1 Vpr Proteins: Impact of the Q65R and R77Q Substitutions on Vpr Functions. Lindenbach B, editor. *PLoS One* [Internet]. Public Library of Science; 2009 Oct 19 [cited 2017 Feb 25];4(10):e7514. Available from: <http://dx.plos.org/10.1371/journal.pone.0007514>
430. Goh WC, Rogel ME, Kinsey CM, Michael SF, Fultz PN, Nowak MA, et al. HIV-1 Vpr increases viral expression by manipulation of the cell cycle: a mechanism for selection of Vpr in vivo. *Nat Med* [Internet]. 1998;4(1):65–71. Available from: <http://www.ncbi.nlm.nih.gov/pubmed/9585240>
431. Belzile J-P, Duisit G, Rougeau N, Mercier J, Finzi A, Cohen ÉA. HIV-1 Vpr-Mediated G2 Arrest Involves the DDB1-CUL4AVPRBP E3 Ubiquitin Ligase. *PLoS Pathog* [Internet]. 2007 Jul [cited 2017 Feb 25];3(7):e85. Available from: <http://www.ncbi.nlm.nih.gov/pubmed/17630831>
432. Thierry S, Marechal V, Rosenzweig M, Nicolas J. Cell Cycle Arrest in G 2 Induces Human Immunodeficiency Virus Type 1 Transcriptional Activation through Histone Acetylation and Recruitment of CBP , NF- B , and c-Jun to the Long Terminal Repeat Promoter. *Society*. 2004;78(22):12198–206.
433. Sato K, Misawa N, Iwami S, Satou Y, Matsuoka M, Ishizaka Y, et al. HIV-1 Vpr Accelerates Viral Replication during Acute Infection by Exploitation of Proliferating CD4+ T Cells In Vivo. *PLoS Pathog*. 2013;9(12):1–12.
434. de Noronha CMC, Sherman MP, Lin HW, Cavrois M V., Moir RD, Goldman RD, et al. Dynamic disruptions in nuclear envelope architecture and integrity induced by HIV-1 Vpr. *Science*. 2001;294(5544):1105–8.
435. Lai M, Zimmerman ES, Planelles V, Chen J. Activation of the ATR pathway by human

- immunodeficiency virus type 1 Vpr involves its direct binding to chromatin in vivo. *J Virol*. 2005;79(24):15443–51.
436. Zimmerman ES, Chen J, Andersen JL, Ardon O, Dehart JL, Blackett J, et al. Human immunodeficiency virus type 1 Vpr-mediated G2 arrest requires Rad17 and Hus1 and induces nuclear BRCA1 and gamma-H2AX focus formation. *Mol Cell Biol* [Internet]. American Society for Microbiology (ASM); 2004 Nov [cited 2017 Feb 27];24(21):9286–94. Available from: <http://www.ncbi.nlm.nih.gov/pubmed/15485898>
437. Roshal M, Kim B, Zhu Y, Nghiem P, Planelles V. Activation of the ATR-mediated DNA damage response by the HIV-1 viral protein R. *J Biol Chem*. 2003;278(28):25879–86.
438. Laguette N, Brégnard C, Hue P, Basbous J, Yatim A, Larroque M, et al. Premature activation of the SLX4 complex by Vpr promotes G2/M arrest and escape from innate immune sensing. *Cell* [Internet]. 2014 Jan 16 [cited 2014 Jul 17];156(1–2):134–45. Available from: <http://www.ncbi.nlm.nih.gov/pubmed/24412650>
439. Belzile J-P, Richard J, Rougeau N, Xiao Y, Cohen EA. HIV-1 Vpr induces the K48-linked polyubiquitination and proteasomal degradation of target cellular proteins to activate ATR and promote G2 arrest. *J Virol* [Internet]. 2010;84(7):3320–30. Available from: <http://www.pubmedcentral.nih.gov/articlerender.fcgi?artid=2838092&tool=pmcentrez&rendertype=abstract>
440. Shimura M, Toyoda Y, Iijima K, Kinomoto M, Tokunaga K, Yoda K, et al. Epigenetic displacement of HP1 from heterochromatin by HIV-1 Vpr causes premature sister chromatid separation. *J Cell Biol*. 2011;194(5):721–35.
441. Koundrioukoff S, Polo S, Almouzni G. Interplay between chromatin and cell cycle checkpoints in the context of ATR/ATM-dependent checkpoints. *DNA Repair (Amst)* [Internet]. 2004 Aug [cited 2017 Feb 27];3(8–9):969–78. Available from: <http://www.ncbi.nlm.nih.gov/pubmed/15279783>
442. Cliby WA, Lewis KA, Lilly KK, Kaufmann SH. S Phase and G2 Arrests Induced by Topoisomerase I Poisons Are Dependent on ATR Kinase Function. *J Biol Chem* [Internet]. 2002 Jan 11 [cited 2017 Feb 27];277(2):1599–606. Available from: <http://www.ncbi.nlm.nih.gov/pubmed/11700302>
443. Le Rouzic E, Morel M, Ayinde D, Belaidouni N, Letienne J, Transy C, et al. Assembly with the Cul4A-DDB1DCAF1 Ubiquitin Ligase Protects HIV-1 Vpr from Proteasomal Degradation. *J Biol Chem* [Internet]. 2008 Aug 1 [cited 2017 Mar 14];283(31):21686–92. Available from: <http://www.ncbi.nlm.nih.gov/pubmed/18524771>
444. Schröfelbauer B, Yu Q, Zeitlin SG, Landau NR. Human Immunodeficiency Virus Type 1 Vpr

Induces the Degradation of the UNG and SMUG Uracil-DNA Glycosylases Human Immunodeficiency Virus Type 1 Vpr Induces the Degradation of the UNG and SMUG Uracil-DNA Glycosylases. *J Virol.* 2005;79(17):10978–87.

445. Angers S, Li T, Yi X, MacCoss MJ, Moon RT, Zheng N. Molecular architecture and assembly of the DDB1–CUL4A ubiquitin ligase machinery. *Nature* [Internet]. 2006 Sep 10 [cited 2017 Feb 27];443(7111):590–3. Available from: <http://www.ncbi.nlm.nih.gov/pubmed/16964240>
446. He YJ, McCall CM, Hu J, Zeng Y, Xiong Y. DDB1 functions as a linker to recruit receptor WD40 proteins to CUL4-ROC1 ubiquitin ligases. *Genes Dev* [Internet]. Cold Spring Harbor Laboratory Press; 2006 Nov 1 [cited 2017 Feb 27];20(21):2949–54. Available from: <http://www.ncbi.nlm.nih.gov/pubmed/17079684>
447. Wang H, Zhai L, Xu J, Joo H, Jackson S, Erdjument-Bromage H, et al. Histone H3 and H4 ubiquitylation by the CUL4-DDB-ROC1 ubiquitin ligase facilitates cellular response to DNA damage. *Mol Cell* [Internet]. 2006;22(3):383–94. Available from: [http://www.ncbi.nlm.nih.gov/entrez/query.fcgi?cmd=Retrieve&db=PubMed&dopt=Citation&list\\_uids=16678110%5Cnpapers3://publication/uuid/205FE83D-1C65-4190-8707-117F8D3D6FA4](http://www.ncbi.nlm.nih.gov/entrez/query.fcgi?cmd=Retrieve&db=PubMed&dopt=Citation&list_uids=16678110%5Cnpapers3://publication/uuid/205FE83D-1C65-4190-8707-117F8D3D6FA4)
448. Wen X, Duus KM, Friedrich TD, de Noronha CMC. The HIV1 Protein Vpr Acts to Promote G2 Cell Cycle Arrest by Engaging a DDB1 and Cullin4A-containing Ubiquitin Ligase Complex Using VprBP/DCAF1 as an Adaptor. *J Biol Chem* [Internet]. 2007 Sep 14 [cited 2017 Mar 14];282(37):27046–57. Available from: <http://www.ncbi.nlm.nih.gov/pubmed/17620334>
449. Fekairi S, Scaglione S, Chahwan C, Taylor ER, Tissier A, Coulon S, et al. Human SLX4 Is a Holliday Junction Resolvase Subunit that Binds Multiple DNA Repair/Recombination Endonucleases. *Cell* [Internet]. 2009 Jul 10 [cited 2017 Feb 27];138(1):78–89. Available from: <http://www.ncbi.nlm.nih.gov/pubmed/19596236>
450. Muñoz IM, Hain K, Déclais A-C, Gardiner M, Toh GW, Sanchez-Pulido L, et al. Coordination of Structure-Specific Nucleases by Human SLX4/BTBD12 Is Required for DNA Repair. *Mol Cell* [Internet]. 2009 Jul 10 [cited 2017 Feb 27];35(1):116–27. Available from: <http://www.ncbi.nlm.nih.gov/pubmed/19595721>
451. Wyatt HDM, Sarbajna S, Matos J, West SC, Boulton SJ, Elledge SJ, et al. Coordinated Actions of SLX1-SLX4 and MUS81-EME1 for Holliday Junction Resolution in Human Cells. *Mol Cell* [Internet]. Elsevier; 2013 Oct 24 [cited 2017 Mar 14];52(2):234–47. Available from: <http://www.ncbi.nlm.nih.gov/pubmed/24076221>
452. Castor D, Nair N, Déclais A-C, Lachaud C, Toth R, Macartney TJ, et al. Cooperative control of holliday junction resolution and DNA repair by the SLX1 and MUS81-EME1 nucleases. *Mol Cell* [Internet]. Elsevier; 2013 Oct 24 [cited 2017 Mar 15];52(2):221–33. Available from: <http://www.ncbi.nlm.nih.gov/pubmed/24076219>

453. Berger G, Lawrence M, Hué S, Neil SJD. G2/M cell cycle arrest correlates with primate lentiviral Vpr interaction with the SLX4 complex. *J Virol* [Internet]. American Society for Microbiology; 2015 Jan [cited 2016 Dec 3];89(1):230–40. Available from: <http://www.ncbi.nlm.nih.gov/pubmed/25320300>
454. McIlwain DR, Berger T, Mak TW. Caspase functions in cell death and disease. *Cold Spring Harb Perspect Biol* [Internet]. Cold Spring Harbor Laboratory Press; 2013 Apr 1 [cited 2017 Feb 25];5(4):a008656. Available from: <http://www.ncbi.nlm.nih.gov/pubmed/23545416>
455. Stewart SA, Poon B, Jowett JB, Chen IS. Human immunodeficiency virus type 1 Vpr induces apoptosis following cell cycle arrest. *J Virol* [Internet]. 1997 Jul [cited 2017 Feb 25];71(7):5579–92. Available from: <http://www.ncbi.nlm.nih.gov/pubmed/9188632>
456. Jones GJ, Barsby NL, Cohen ÉA, Holden J, Harris K, Dickie P, et al. HIV-1 Vpr Causes Neuronal Apoptosis and In Vivo Neurodegeneration. *J Neurosci*. 2007;27(14).
457. Lum JJ, Cohen OJ, Nie Z, Weaver JG, Gomez TS, Yao X-J, et al. Vpr R77Q is associated with long-term nonprogressive HIV infection and impaired induction of apoptosis. *J Clin Invest* [Internet]. American Society for Clinical Investigation; 2003 May 15 [cited 2015 Apr 12];111(10):1547–54. Available from: <http://www.jci.org/articles/view/16233>
458. Jacotot E, Ferri KF, El Hamel C, Brenner C, Druillennec S, Hoebeke J, et al. Control of mitochondrial membrane permeabilization by adenine nucleotide translocator interacting with HIV-1 viral protein rR and Bcl-2. *J Exp Med* [Internet]. 2001 Feb 19 [cited 2017 Feb 25];193(4):509–19. Available from: <http://www.ncbi.nlm.nih.gov/pubmed/11181702>
459. Macreadie IG, Castelli LA, Hewish DR, Kirkpatrick A, Ward AC, Azad AA. A domain of human immunodeficiency virus type 1 Vpr containing repeated H(S/F)RIG amino acid motifs causes cell growth arrest and structural defects. *Proc Natl Acad Sci* [Internet]. 1995 Mar 28 [cited 2016 Dec 19];92(7):2770–4. Available from: <http://www.pnas.org/cgi/doi/10.1073/pnas.92.7.2770>
460. Andersen JL, Zimmerman ES, DeHart JL, Murala S, Ardon O, Blackett J, et al. ATR and GADD45alpha mediate HIV-1 Vpr-induced apoptosis. *Cell Death Differ* [Internet]. 2005;12(4):326–34. Available from: <http://www.ncbi.nlm.nih.gov/pubmed/15650754>
461. Nishizawa M, Kamata M, Katsumata R, Aida Y. A carboxy-terminally truncated form of the human immunodeficiency virus type 1 Vpr protein induces apoptosis via G(1) cell cycle arrest. *J Virol* [Internet]. 2000;74(13):6058–67. Available from: <http://www.pubmedcentral.nih.gov/articlerender.fcgi?artid=112104&tool=pmcentrez&rendertype=abstract>
462. Jones GJ, Barsby NL, Cohen EA, Holden J, Harris K, Dickie P, et al. HIV-1 Vpr causes neuronal apoptosis and in vivo neurodegeneration. *J Neurosci* [Internet]. 2007 Apr 4 [cited 2017 Feb

- 27];27(14):3703–11. Available from:  
<http://www.jneurosci.org/cgi/doi/10.1523/JNEUROSCI.5522-06.2007>
463. Krokan HE, Drabløs F, Slupphaug G. Uracil in DNA--occurrence, consequences and repair. *Oncogene*. 2002;21(58):8935–48.
464. Mansky LM, Temin HM. Lower in vivo mutation rate of human immunodeficiency virus type 1 than that predicted from the fidelity of purified reverse transcriptase. *J Virol* [Internet]. 1995 Aug [cited 2017 Feb 27];69(8):5087–94. Available from:  
<http://www.ncbi.nlm.nih.gov/pubmed/7541846>
465. Chen R, Le Rouzic E, Kearney JA, Mansky LM, Benichou S. Vpr-mediated incorporation of UNG2 into HIV-1 particles is required to modulate the virus mutation rate and for replication in macrophages. *J Biol Chem* [Internet]. 2004 Jul 2 [cited 2017 Feb 27];279(27):28419–25. Available from: <http://www.jbc.org/cgi/doi/10.1074/jbc.M403875200>
466. Eldin P, Chazal N, Fenard D, Bernard E, Guichou J-F, Briant L. Vpr expression abolishes the capacity of HIV-1 infected cells to repair uracilated DNA. *Nucleic Acids Res* [Internet]. Oxford University Press; 2014 Feb [cited 2017 Feb 27];42(3):1698–710. Available from:  
<http://www.ncbi.nlm.nih.gov/pubmed/24178031>
467. Langevin C, Maidou-Peindara P, Aas PA, Jacquot G, Otterlei M, Slupphaug G, et al. Human Immunodeficiency Virus Type 1 Vpr Modulates Cellular Expression of UNG2 via a Negative Transcriptional Effect. *J Virol* [Internet]. 2009 Oct 1 [cited 2017 Feb 27];83(19):10256–63. Available from: <http://www.ncbi.nlm.nih.gov/pubmed/19625402>
468. Nekorchuk MD, Sharifi HJ, Furuya AK, Jellinger R, de Noronha CM. HIV relies on neddylation for ubiquitin ligase-mediated functions. *Retrovirology* [Internet]. BioMed Central; 2013 [cited 2017 Feb 27];10(1):138. Available from:  
<http://retrovirology.biomedcentral.com/articles/10.1186/1742-4690-10-138>
469. Guenzel C a, Hérate C, Le Rouzic E, Maidou-Peindara P, Sadler H a, Rouyez M-C, et al. Recruitment of the nuclear form of uracil DNA glycosylase into virus particles participates in the full infectivity of HIV-1. *J Virol* [Internet]. 2012;86(5):2533–44. Available from:  
<http://www.pubmedcentral.nih.gov/articlerender.fcgi?artid=3302282&tool=pmcentrez&rendertype=abstract>
470. Chen R, Wang H, Mansky LM. Roles of uracil-DNA glycosylase and dUTPase in virus replication. Vol. 83, *Journal of General Virology*. 2002. p. 2339–45.
471. Chen R, Le Rouzic E, Kearney JA, Mansky LM, Benichou S. Vpr-mediated incorporation of UNG2 into HIV-1 particles is required to modulate the virus mutation rate and for replication in macrophages. *J Biol Chem* [Internet]. American Society for Biochemistry and Molecular Biology;

- 2004 Jul 2 [cited 2016 Dec 3];279(27):28419–25. Available from: <http://www.ncbi.nlm.nih.gov/pubmed/15096517>
472. Weil AF, Ghosh D, Zhou Y, Seiple L, McMahon MA, Spivak AM, et al. Uracil DNA glycosylase initiates degradation of HIV-1 cDNA containing misincorporated dUTP and prevents viral integration. *Proc Natl Acad Sci U S A* [Internet]. National Academy of Sciences; 2013 Feb 5 [cited 2017 Mar 16];110(6):E448-57. Available from: <http://www.ncbi.nlm.nih.gov/pubmed/23341616>
473. Bukrinsky MI, Haffar OK. HIV-1 nuclear import: in search of a leader. *Front Biosci* [Internet]. 1999 Oct 15 [cited 2017 Feb 25];4:D772-81. Available from: <http://www.ncbi.nlm.nih.gov/pubmed/10525473>
474. Iijima S, Nitahara-Kasahara Y, Kimata K, Zhong Zhuang W, Kamata M, Isogai M, et al. Nuclear localization of Vpr is crucial for the efficient replication of HIV-1 in primary CD4+ T cells. *Virology* [Internet]. 2004 Oct 1 [cited 2017 Feb 25];327(2):249–61. Available from: <http://www.ncbi.nlm.nih.gov/pubmed/15351213>
475. Gallay P, Stitt V, Mundy C, Oettinger M, Trono D. Role of the karyopherin pathway in human immunodeficiency virus type 1 nuclear import. *J Virol* [Internet]. American Society for Microbiology (ASM); 1996 Feb [cited 2017 Feb 27];70(2):1027–32. Available from: <http://www.ncbi.nlm.nih.gov/pubmed/8551560>
476. Jenkins Y, McEntee M, Weis K, Greene WC. Characterization of HIV-1 vpr nuclear import: analysis of signals and pathways. *J Cell Biol* [Internet]. 1998 Nov 16 [cited 2017 Feb 27];143(4):875–85. Available from: <http://www.ncbi.nlm.nih.gov/pubmed/9817747>
477. Depienne C, Roques P, Créminon C, Fritsch L, Casseron R, Dormont D, et al. Cellular Distribution and Karyophilic Properties of Matrix, Integrase, and Vpr Proteins from the Human and Simian Immunodeficiency Viruses. *Exp Cell Res* [Internet]. 2000 Nov 1 [cited 2017 Feb 27];260(2):387–95. Available from: <http://www.ncbi.nlm.nih.gov/pubmed/11035935>
478. Di Marzio P, Choe S, Ebright M, Knoblauch R, Landau NR. Mutational analysis of cell cycle arrest, nuclear localization and virion packaging of human immunodeficiency virus type 1 Vpr. *J Virol*. 1995;69(12):7909–16.
479. Nitahara-Kasahara Y, Kamata M, Yamamoto T, Zhang X, Miyamoto Y, Muneta K, et al. Novel nuclear import of Vpr promoted by importin alpha is crucial for human immunodeficiency virus type 1 replication in macrophages. *J Virol* [Internet]. American Society for Microbiology; 2007 May [cited 2017 Feb 24];81(10):5284–93. Available from: <http://www.ncbi.nlm.nih.gov/pubmed/17344301>
480. Jenkins Y, Pornillos O, Rich RL, Myszka DG, Sundquist WI, Malim MH. Biochemical analyses

of the interactions between human immunodeficiency virus type 1 Vpr and p6(Gag). *J Virol* [Internet]. American Society for Microbiology; 2001 Nov [cited 2017 Feb 27];75(21):10537–42. Available from: <http://www.ncbi.nlm.nih.gov/pubmed/11581428>

481. Sherman MP, Schubert U, Williams SA, de Noronha CMC, Kreisberg JF, Henklein P, et al. HIV-1 Vpr displays natural protein-transducing properties: implications for viral pathogenesis. *Virology* [Internet]. 2002 Oct 10 [cited 2017 Feb 24];302(1):95–105. Available from: <http://www.ncbi.nlm.nih.gov/pubmed/12429519>
482. Fouchier RA, Meyer BE, Simon JH, Fischer U, Albright A V, González-Scarano F, et al. Interaction of the human immunodeficiency virus type 1 Vpr protein with the nuclear pore complex. *J Virol* [Internet]. 1998 Jul [cited 2017 Feb 27];72(7):6004–13. Available from: <http://www.ncbi.nlm.nih.gov/pubmed/9621063>
483. Popov S, Rexach M, Zybarth G, Reiling N, Lee MA, Ratner L, et al. Viral protein R regulates nuclear import of the HIV-1 pre-integration complex. *EMBO J* [Internet]. European Molecular Biology Organization; 1998 Feb 16 [cited 2017 Feb 20];17(4):909–17. Available from: <http://www.ncbi.nlm.nih.gov/pubmed/9463369>
484. Kobe B. Autoinhibition by an internal nuclear localization signal revealed by the crystal structure of mammalian importin alpha. *Nat Struct Biol* [Internet]. 1999 Apr 1 [cited 2017 Mar 15];6(4):388–97. Available from: <http://www.ncbi.nlm.nih.gov/pubmed/10201409>
485. Moore MS, Blobel G. Purification of a Ran-interacting protein that is required for protein import into the nucleus. *Proc Natl Acad Sci U S A* [Internet]. National Academy of Sciences; 1994 Oct 11 [cited 2017 Mar 15];91(21):10212–6. Available from: <http://www.ncbi.nlm.nih.gov/pubmed/7937864>
486. Melchior F, Guan T, Yokoyama N, Nishimoto T, Gerace L. GTP hydrolysis by Ran occurs at the nuclear pore complex in an early step of protein import. *J Cell Biol* [Internet]. The Rockefeller University Press; 1995 Nov [cited 2017 Mar 15];131(3):571–81. Available from: <http://www.ncbi.nlm.nih.gov/pubmed/7593180>
487. Jans DA, Jans P, Jülich T, Briggs LJ, Xiao C-Y, Piller SC. Intranuclear Binding by the HIV-1 Regulatory Protein VPR Is Dependent on Cytosolic Factors. *Biochem Biophys Res Commun* [Internet]. 2000 Apr 21 [cited 2017 Mar 15];270(3):1055–62. Available from: <http://www.ncbi.nlm.nih.gov/pubmed/10772949>
488. Popov S, Rexach M, Zybarth G, Reiling N, Lee MA, Ratner L, et al. Viral protein R regulates nuclear import of the HIV-1 pre-integration complex. *EMBO J* [Internet]. European Molecular Biology Organization; 1998 Feb 16 [cited 2017 Feb 24];17(4):909–17. Available from: <http://www.ncbi.nlm.nih.gov/pubmed/9463369>

489. Agostini I, Navarro J-M, Rey F, Bouhamdan M, Spire B, Vigne R, et al. The Human Immunodeficiency Virus Type 1 Vpr Transactivator: Cooperation with Promoter-bound Activator Domains and Binding to TFIIIB. *J Mol Biol* [Internet]. 1996 Sep [cited 2017 Feb 25];261(5):599–606. Available from: <http://linkinghub.elsevier.com/retrieve/pii/S0022283696904854>
490. Janket ML, DeRicco JS, Borowski L, Ayyavoo V. Human immunodeficiency virus (HIV-1) Vpr induced downregulation of NHE1 induces alteration in intracellular pH and loss of ERM complex in target cells. *Virus Res* [Internet]. NIH Public Access; 2007 Jun [cited 2017 Feb 27];126(1–2):76–85. Available from: <http://www.ncbi.nlm.nih.gov/pubmed/17349711>
491. Wang L, Mukherjee S, Jia F, Narayan O, Zhao LJ. Interaction of virion protein Vpr of human immunodeficiency virus type 1 with cellular transcription factor Sp1 and trans-activation of viral long terminal repeat. *J Biol Chem* [Internet]. American Society for Biochemistry and Molecular Biology; 1995 Oct 27 [cited 2017 Feb 25];270(43):25564–9. Available from: <http://www.ncbi.nlm.nih.gov/pubmed/7592727>
492. Liu X, Guo H, Wang H, Markham R, Wei W, Yu XF. HIV-1 Vpr suppresses the cytomegalovirus promoter in a CRL4(DCAF1) E3 ligase independent manner. *Biochem Biophys Res Commun* [Internet]. Elsevier Ltd; 2015;459(2):214–9. Available from: <http://dx.doi.org/10.1016/j.bbrc.2015.02.060>
493. Agostini I, Navarro JM, Rey F, Bouhamdan M, Spire B, Vigne R, et al. The human immunodeficiency virus type 1 Vpr transactivator: cooperation with promoter-bound activator domains and binding to TFIIIB. *J Mol Biol*. 1996;261(5):599–606.
494. Levy DN, Refaeli Y, MacGregor RR, Weiner DB. Serum Vpr regulates productive infection and latency of human immunodeficiency virus type 1. *Proc Natl Acad Sci U S A* [Internet]. National Academy of Sciences; 1994 Nov 8 [cited 2017 Mar 17];91(23):10873–7. Available from: <http://www.ncbi.nlm.nih.gov/pubmed/7971975>
495. Coeytaux E, Coulaud D, Le Cam E, Danos O, Kichler A. The cationic amphipathic  $\alpha$ -helix of HIV-1 viral protein R (Vpr) binds to nucleic acids, permeabilizes membranes, and efficiently transfects cells. *J Biol Chem*. 2003;278(20):18110–6.
496. Visnegarwala F, Raghavan SS, Mullin CM, Bartsch G, Wang J, Kotler D, et al. Sex differences in the associations of HIV disease characteristics and body composition in antiretroviral-naive persons. *Am J Clin Nutr* [Internet]. American Society for Nutrition; 2005 Oct [cited 2017 Feb 27];82(4):850–6. Available from: <http://www.ncbi.nlm.nih.gov/pubmed/16210716>
497. Bacchetti P, Gripshover B, Grunfeld C, Heymsfield S, McCreath H, Osmond D, et al. Fat distribution in men with HIV infection. *J Acquir Immune Defic Syndr* [Internet]. NIH Public Access; 2005 Oct 1 [cited 2017 Feb 27];40(2):121–31. Available from: <http://www.ncbi.nlm.nih.gov/pubmed/16186728>

498. Dubé MP. Disorders of Glucose Metabolism in Patients Infected with Human Immunodeficiency Virus. *Clin Infect Dis* [Internet]. 2000 Dec [cited 2017 Feb 27];31(6):1467–75. Available from: <http://www.ncbi.nlm.nih.gov/pubmed/11096014>
499. Agarwal N, Iyer D, Patel SG, Sekhar R V, Phillips TM, Schubert U, et al. HIV-1 Vpr induces adipose dysfunction in vivo through reciprocal effects on PPAR/GR co-regulation. *Sci Transl Med* [Internet]. NIH Public Access; 2013 Nov 27 [cited 2017 Feb 27];5(213):213ra164. Available from: <http://www.ncbi.nlm.nih.gov/pubmed/24285483>
500. Hoch J, Lang SM, Weeger M, Stahl-Hennig C, Coulibaly C, Dittmer U, et al. vpr deletion mutant of simian immunodeficiency virus induces AIDS in rhesus monkeys. *J Virol* [Internet]. 1995;69(8):4807–13. Available from: <http://www.pubmedcentral.nih.gov/articlerender.fcgi?artid=189293&tool=pmcentrez&rendertype=abstract>
501. Goh WC, Rogel ME, Kinsey CM, Michael SF, Fultz PN, Nowak MA, et al. HIV-1 Vpr increases viral expression by manipulation of the cell cycle: a mechanism for selection of Vpr in vivo. *Nat Med* [Internet]. 1998 Jan [cited 2017 Feb 25];4(1):65–71. Available from: <http://www.ncbi.nlm.nih.gov/pubmed/9427608>
502. Ardon O, Zimmerman ES, Andersen JL, DeHart JL, Blackett J, Planelles V. Induction of G2 arrest and binding to cyclophilin A are independent phenotypes of human immunodeficiency virus type 1 Vpr. *J Virol* [Internet]. 2006;80(8):3694–700. Available from: <http://www.pubmedcentral.nih.gov/articlerender.fcgi?artid=1440437&tool=pmcentrez&rendertype=abstract>
503. Solbak SMØ, Wray V, Horvli O, Raae AJ, Flydal MI, Henklein P, et al. The host-pathogen interaction of human cyclophilin A and HIV-1 Vpr requires specific N-terminal and novel C-terminal domains. *BMC Struct Biol* [Internet]. 2011 Jan [cited 2015 Apr 16];11:49. Available from: <http://www.pubmedcentral.nih.gov/articlerender.fcgi?artid=3269379&tool=pmcentrez&rendertype=abstract>
504. Solbak SMO, Reksten TR, Röder R, Wray V, Horvli O, Raae AJ, et al. HIV-1 p6-Another viral interaction partner to the host cellular protein cyclophilin A. *Biochim Biophys Acta - Proteins Proteomics* [Internet]. Elsevier B.V.; 2012;1824(4):667–78. Available from: <http://dx.doi.org/10.1016/j.bbapap.2012.02.002>
505. Colgan J, Asmal M, Luban J. Isolation, characterization and targeted disruption of mouse ppia: cyclophilin A is not essential for mammalian cell viability. *Genomics*. 2000;68(2):167–78.
506. Braaten D, Luban J. Cyclophilin A regulates HIV-1 infectivity, as demonstrated by gene targeting in human T cells. *EMBO J*. 2001;20(6):1300–9.

507. Votteler J, Wray V, Schubert U. Role of cyclophilin A in HIV replication. *Futur Virol.* 2007;2:65–78.
508. Solbak SM, Reksten TR, Wray V, Bruns K, Horvli O, Raae AJ, et al. The intriguing cyclophilin A-HIV-1 Vpr interaction: prolyl cis/trans isomerisation catalysis and specific binding. *BMC Struct Biol* [Internet]. 2010;10:31. Available from: <http://www.pubmedcentral.nih.gov/articlerender.fcgi?artid=2959089&tool=pmcentrez&rendertype=abstract>
509. Mansky LM, Preveral S, Selig L, Benarous R, Benichou S. The interaction of vpr with uracil DNA glycosylase modulates the human immunodeficiency virus type 1 In vivo mutation rate. *J Virol* [Internet]. American Society for Microbiology (ASM); 2000 Aug [cited 2017 Feb 27];74(15):7039–47. Available from: <http://www.ncbi.nlm.nih.gov/pubmed/10888643>
510. Boyer HW, Roulland-Dussoix D. A complementation analysis of the restriction and modification of DNA in *Escherichia coli*. *J Mol Biol* [Internet]. 1969 May 14 [cited 2017 Apr 12];41(3):459–72. Available from: <http://www.ncbi.nlm.nih.gov/pubmed/4896022>
511. Naldini L, Blömer U, Gallay P, Ory D, Mulligan R, Gage FH, et al. In vivo gene delivery and stable transduction of nondividing cells by a lentiviral vector. *Science* [Internet]. 1996 Apr 12 [cited 2017 Apr 14];272(5259):263–7. Available from: <http://www.ncbi.nlm.nih.gov/pubmed/8602510>
512. Benny Chain. Agilent expression array processing package [Internet]. 2013 [cited 2017 Apr 14]. Available from: <https://rdrr.io/bioc/agilp/>
513. Chain B, Bowen H, Hammond J, Posch W, Rasaiyaah J, Tsang J, et al. Error, reproducibility and sensitivity: a pipeline for data processing of Agilent oligonucleotide expression arrays. *BMC Bioinformatics* [Internet]. 2010 [cited 2017 Apr 14];11. Available from: <http://www.biomedcentral.com/1471-2105/11/344>
514. Breuer K, Foroushani AK, Laird MR, Chen C, Sribnaia A, Lo R, et al. InnateDB: systems biology of innate immunity and beyond--recent updates and continuing curation. *Nucleic Acids Res* [Internet]. Oxford University Press; 2013 Jan [cited 2017 Mar 9];41(Database issue):D1228-33. Available from: <http://www.ncbi.nlm.nih.gov/pubmed/23180781>
515. Price MN, Dehal PS, Arkin AP, Rojas M, Brodie E. FastTree 2 – Approximately Maximum-Likelihood Trees for Large Alignments. Poon AFY, editor. *PLoS One* [Internet]. Public Library of Science; 2010 Mar 10 [cited 2017 Mar 5];5(3):e9490. Available from: <http://dx.plos.org/10.1371/journal.pone.0009490>
516. O’Sullivan O, Suhre K, Abergel C, Higgins DG, Notredame C. 3DCoffee: Combining Protein Sequences and Structures within Multiple Sequence Alignments. *J Mol Biol* [Internet]. 2004 Jul

2 [cited 2017 Mar 8];340(2):385–95. Available from:  
<http://www.ncbi.nlm.nih.gov/pubmed/15201059>

517. Notredame C, Higgins DG, Heringa J. T-coffee: a novel method for fast and accurate multiple sequence alignment. *J Mol Biol* [Internet]. 2000 Sep 8 [cited 2017 Mar 8];302(1):205–17. Available from: <http://www.ncbi.nlm.nih.gov/pubmed/10964570>
518. Robert X, Gouet P. Deciphering key features in protein structures with the new ENDScript server. *Nucleic Acids Res* [Internet]. Oxford University Press; 2014 Jul [cited 2017 Mar 8];42(Web Server issue):W320–4. Available from: <http://www.ncbi.nlm.nih.gov/pubmed/24753421>
519. Wang JK, Li TX, Bai YF, Lu ZH. Evaluating the binding affinities of NF- $\kappa$ B p50 homodimer to the wild-type and single-nucleotide mutant Ig- $\kappa$ B sites by the unimolecular dsDNA microarray. *Anal Biochem* [Internet]. 2003 May [cited 2017 Mar 18];316(2):192–201. Available from: <http://linkinghub.elsevier.com/retrieve/pii/S0003269703000496>
520. Feriotto G, Finotti A, Volpe P, Treves S, Ferrari S, Angelelli C, et al. Myocyte enhancer factor 2 activates promoter sequences of the human AbetaH-J-J locus, encoding aspartyl-beta-hydroxylase, junctin, and junctate. *Mol Cell Biol* [Internet]. American Society for Microbiology (ASM); 2005 Apr [cited 2017 Mar 18];25(8):3261–75. Available from: <http://www.ncbi.nlm.nih.gov/pubmed/15798210>
521. Sen R, Baltimore D. Multiple nuclear factors interact with the immunoglobulin enhancer sequences. *Cell* [Internet]. 1986 Aug [cited 2017 Mar 20];46(5):705–16. Available from: <http://linkinghub.elsevier.com/retrieve/pii/0092867486903466>
522. Bauer DE, Haroutunian V, McCullumsmith RE, Meador-Woodruff JH. Expression of four housekeeping proteins in elderly patients with schizophrenia. *J Neural Transm*. 2009;116(4):487–91.
523. Chebath J, Merlin G, Metz R, Benech P, Revel M. Interferon-induced 56,000 Mr protein and its mRNA in human cells: molecular cloning and partial sequence of the cDNA. *Nucleic Acids Res* [Internet]. 1983 Mar 11 [cited 2017 Mar 3];11(5):1213–26. Available from: <http://www.ncbi.nlm.nih.gov/pubmed/6186990>
524. Chattopadhyay S, Marques JT, Yamashita M, Peters KL, Smith K, Desai A, et al. Viral apoptosis is induced by IRF-3-mediated activation of Bax. *EMBO J* [Internet]. European Molecular Biology Organization; 2010 May 19 [cited 2017 Mar 3];29(10):1762–73. Available from: <http://www.ncbi.nlm.nih.gov/pubmed/20360684>
525. Brownell J, Bruckner J, Wagoner J, Thomas E, Loo Y-M, Gale M, et al. Direct, interferon-independent activation of the CXCL10 promoter by NF- $\kappa$ B and interferon regulatory factor 3 during hepatitis C virus infection. *J Virol* [Internet]. American Society for Microbiology; 2014 Feb

[cited 2016 Dec 20];88(3):1582–90. Available from:  
<http://www.ncbi.nlm.nih.gov/pubmed/24257594>

526. Fensterl V, Sen GC. The ISG56/IFIT1 gene family. *J Interferon Cytokine Res.* 2011;31(1):71–8.
527. Thanos D, Maniatis T. Virus induction of human IFN $\gamma$  gene expression requires the assembly of an enhanceosome. *Cell.* 1995;83(7):1091–100.
528. Visvanathan K V, Goodbourn S. Double-stranded RNA activates binding of NF-kappa B to an inducible element in the human beta-interferon promoter. *EMBO J.* 1989;8(4):1129–38.
529. Grandvaux N, Servant MJ, TenOever B, Sen GC, Balachandran S, Barber GN, et al. Transcriptional profiling of interferon regulatory factor 3 target genes: direct involvement in the regulation of interferon-stimulated genes. *J Virol [Internet].* 2002;76(11):5532–9. Available from: <http://www.ncbi.nlm.nih.gov/pubmed/11991981><http://www.pubmedcentral.nih.gov/articlerender.fcgi?artid=PMC137057>
530. Vermeire J, Roesch F, Sauter D, Rua R, Hotter D, Van Nuffel A, et al. HIV Triggers a cGAS-Dependent, Vpu- and Vpr-Regulated Type I Interferon Response in CD4+ T Cells. *Cell Rep [Internet].* 2016 Oct [cited 2017 Feb 20];17(2):413–24. Available from: <http://linkinghub.elsevier.com/retrieve/pii/S2211124716312451>
531. Snyder A, Alsauskas ZC, Leventhal JS, Rosenstiel PE, Gong P, Chan JJK, et al. HIV-1 viral protein r induces ERK and caspase-8-dependent apoptosis in renal tubular epithelial cells. *AIDS [Internet]. NIH Public Access;* 2010 May 15 [cited 2017 Feb 25];24(8):1107–19. Available from: <http://www.ncbi.nlm.nih.gov/pubmed/20404718>
532. Patel CA, Mukhtar M, Pomerantz RJ. Human immunodeficiency virus type 1 Vpr induces apoptosis in human neuronal cells. *J Virol [Internet]. American Society for Microbiology (ASM);* 2000 Oct [cited 2017 Mar 1];74(20):9717–26. Available from: <http://www.ncbi.nlm.nih.gov/pubmed/11000244>
533. Gupta RK, Towers GJ. A Tail of Tetherin: How Pandemic HIV-1 Conquered the World. *Cell Host Microbe.* 2009;6(5):393–5.
534. Sauter D, Schindler M, Specht A, Landford WN, Münch J, Kim KA, et al. Tetherin-Driven Adaptation of Vpu and Nef Function and the Evolution of Pandemic and Nonpandemic HIV-1 Strains. *Cell Host Microbe.* 2009;6(5):409–21.
535. Ochsenbauer C, Edmonds TG, Ding H, Keele BF, Decker J, Salazar MG, et al. Generation of transmitted/founder HIV-1 infectious molecular clones and characterization of their replication capacity in CD4 T lymphocytes and monocyte-derived macrophages. *J Virol [Internet]. American Society for Microbiology;* 2012 Mar [cited 2017 Mar 4];86(5):2715–28. Available from:

<http://www.ncbi.nlm.nih.gov/pubmed/22190722>

536. Li Y, Kappes JC, Conway JA, Price RW, Shaw GM, Hahn BH. Molecular characterization of human immunodeficiency virus type 1 cloned directly from uncultured human brain tissue: identification of replication-competent and -defective viral genomes. *J Virol* [Internet]. American Society for Microbiology (ASM); 1991 Aug [cited 2016 Dec 20];65(8):3973–85. Available from: <http://www.ncbi.nlm.nih.gov/pubmed/1830110>
537. Li Y, Hui H, Burgess CJ, Price RW, Sharp PM, Hahn BH, et al. Complete Nucleotide Sequence, Genome Organization, and Biological Properties of Human Immunodeficiency Virus Type 1 In Vivo: Evidence for Limited Defectiveness and Complementation. *J Virol* [Internet]. 1992 [cited 2017 Mar 4];66(11):6587–600. Available from: <https://www.ncbi.nlm.nih.gov/pmc/articles/PMC240154/pdf/jvirol00042-0357.pdf>
538. Keele BF, Giorgi EE, Salazar-Gonzalez JF, Decker JM, Pham KT, Salazar MG, et al. Identification and characterization of transmitted and early founder virus envelopes in primary HIV-1 infection. *Proc Natl Acad Sci* [Internet]. 2008 May 27 [cited 2017 Mar 4];105(21):7552–7. Available from: <http://www.ncbi.nlm.nih.gov/pubmed/18490657>
539. Salazar-Gonzalez JF, Bailes E, Pham KT, Salazar MG, Guffey MB, Keele BF, et al. Deciphering human immunodeficiency virus type 1 transmission and early envelope diversification by single-genome amplification and sequencing. *J Virol* [Internet]. American Society for Microbiology (ASM); 2008 Apr [cited 2017 Mar 4];82(8):3952–70. Available from: <http://www.ncbi.nlm.nih.gov/pubmed/18256145>
540. Perelman P, Johnson WE, Roos C, Seung H, Ho S-Y, et al. A molecular phylogeny of living primates. *PLoS Genet*. 2011;7(3):1–17.
541. Sharp PM, Robertson DL, Hahn BH. Cross-Species Transmission and Recombination of “AIDS” Viruses. *Philos Trans R Soc B Biol Sci* [Internet]. 1995 Jul 29 [cited 2017 Mar 28];349(1327):41–7. Available from: <http://www.ncbi.nlm.nih.gov/pubmed/8748018>
542. Sharp PM, Bailes E, Gao F, Beer BE, Hirsch VM, Hahn BH. Origins and evolution of AIDS viruses: estimating the time-scale. *Biochem Soc Trans* [Internet]. 2000 Feb [cited 2017 Mar 28];28(2):275–82. Available from: <http://www.ncbi.nlm.nih.gov/pubmed/10816142>
543. Leoz M, Feyertag F, Kfutwah A, Mauclère P, Lachenal G, Damond F, et al. The Two-Phase Emergence of Non Pandemic HIV-1 Group O in Cameroon. Murcia PR, editor. *PLOS Pathog* [Internet]. Public Library of Science; 2015 Aug 4 [cited 2016 Dec 3];11(8):e1005029. Available from: <http://dx.plos.org/10.1371/journal.ppat.1005029>
544. Gonder MK, Locatelli S, Ghobrial L, Mitchell MW, Kujawski JT, Lankester FJ, et al. Evidence from Cameroon reveals differences in the genetic structure and histories of chimpanzee

- populations. *Proc Natl Acad Sci U S A* [Internet]. 2011 Mar 22 [cited 2015 Mar 24];108(12):4766–71. Available from: <http://www.pubmedcentral.nih.gov/articlerender.fcgi?artid=3064329&tool=pmcentrez&rendertype=abstract>
545. Ferreira Z, Hurle B, Andrés AM, Kretzschmar WW, Mullikin JC, Cherukuri PF, et al. Sequence diversity of pan troglodytes subspecies and the impact of WFDC6 selective constraints in reproductive immunity. *Genome Biol Evol.* 2013;5(12):2512–23.
  546. Etienne L, Nerrienet E, LeBreton M, Bibila GT, Foupouapouognigni Y, Rousset D, et al. Characterization of a new simian immunodeficiency virus strain in a naturally infected Pan troglodytes chimpanzee with AIDS related symptoms. *Retrovirology* 2011 81. *BioMed Central*; 2011;8(1):529–34.
  547. Zandi E, Rothwarf DM, Delhase M, Hayakawa M, Karin M. The IkappaB kinase complex (IKK) contains two kinase subunits, IKKalpha and IKKbeta, necessary for IkappaB phosphorylation and NF-kappaB activation. *Cell* [Internet]. 1997 Oct 17 [cited 2017 Mar 6];91(2):243–52. Available from: <http://www.ncbi.nlm.nih.gov/pubmed/9346241>
  548. Karin M, Rothwarf DM, Zandi E, Natoli G. IKK-gamma is an essential regulatory subunit of the IkappaB kinase complex. *Nature* [Internet]. 1998 Sep 17 [cited 2017 Mar 6];395(6699):297–300. Available from: <http://www.ncbi.nlm.nih.gov/pubmed/9751060>
  549. Scherer DC, Brockman JA, Chen Z, Maniatis T, Ballard DW. Signal-induced degradation of I kappa B alpha requires site-specific ubiquitination. *Proc Natl Acad Sci U S A* [Internet]. National Academy of Sciences; 1995 Nov 21 [cited 2017 Mar 6];92(24):11259–63. Available from: <http://www.ncbi.nlm.nih.gov/pubmed/7479976>
  550. Deng L, Wang C, Spencer E, Yang L, Braun A, You J, et al. Activation of the IkappaB kinase complex by TRAF6 requires a dimeric ubiquitin-conjugating enzyme complex and a unique polyubiquitin chain. *Cell* [Internet]. 2000 Oct 13 [cited 2017 Mar 11];103(2):351–61. Available from: <http://www.ncbi.nlm.nih.gov/pubmed/11057907>
  551. Oganessian G, Saha SK, Guo B, He JQ, Shahangian A, Zarnegar B, et al. Critical role of TRAF3 in the Toll-like receptor-dependent and -independent antiviral response. *Nature* [Internet]. 2006 Jan 12 [cited 2017 Mar 11];439(7073):208–11. Available from: <http://www.ncbi.nlm.nih.gov/pubmed/16306936>
  552. Kanayama A, Seth RB, Sun L, Ea C-K, Hong M, Shaito A, et al. TAB2 and TAB3 Activate the NF-κB Pathway through Binding to Polyubiquitin Chains. *Mol Cell* [Internet]. 2004 Aug 27 [cited 2017 Mar 11];15(4):535–48. Available from: <http://www.ncbi.nlm.nih.gov/pubmed/15327770>
  553. Wade EJ, Klucher KM, Spector DH. An AP-1 binding site is the predominant cis-acting regulatory

- element in the 1.2-kilobase early RNA promoter of human cytomegalovirus. *J Virol* [Internet]. American Society for Microbiology; 1992 Apr [cited 2017 Mar 18];66(4):2407–17. Available from: <http://www.ncbi.nlm.nih.gov/pubmed/1312636>
554. Shifera AS, Hardin JA. Factors modulating expression of Renilla luciferase from control plasmids used in luciferase reporter gene assays. *Anal Biochem* [Internet]. NIH Public Access; 2010 Jan 15 [cited 2016 Dec 19];396(2):167–72. Available from: <http://www.ncbi.nlm.nih.gov/pubmed/19788887>
555. Imbalzano AN, Coen DM, Delucal NA. Herpes Simplex Virus Transactivator ICP4 Operationally Substitutes for the Cellular Transcription Factor Sp1 for Efficient Expression of the Viral Thymidine Kinase Gene. *J Virol* [Internet]. 1991 [cited 2017 Mar 8];65(2):565–74. Available from: <https://www.ncbi.nlm.nih.gov/pmc/articles/PMC239793/pdf/jvirol00045-0019.pdf>
556. Isomura H, Stinski MF, Kudoh A, Daikoku T, Shirata N, Tsurumi T. Two Sp1/Sp3 binding sites in the major immediate-early proximal enhancer of human cytomegalovirus have a significant role in viral replication. *J Virol* [Internet]. American Society for Microbiology (ASM); 2005 Aug [cited 2017 Mar 18];79(15):9597–607. Available from: <http://www.ncbi.nlm.nih.gov/pubmed/16014922>
557. Hacein-Bey-Abina S, Von Kalle C, Schmidt M, McCormack MP, Wulffraat N, Leboulch P, et al. LMO2-Associated Clonal T Cell Proliferation in Two Patients after Gene Therapy for SCID-X1. *Science* (80- ) [Internet]. 2003 Oct 17 [cited 2017 Mar 20];302(5644):415–9. Available from: <http://www.ncbi.nlm.nih.gov/pubmed/14564000>
558. Lewis AF, Stacy T, Green WR, Tadesse-Heath L, Hartley JW, Speck NA. Core-binding factor influences the disease specificity of Moloney murine leukemia virus. *J Virol* [Internet]. American Society for Microbiology (ASM); 1999 Jul [cited 2017 Mar 20];73(7):5535–47. Available from: <http://www.ncbi.nlm.nih.gov/pubmed/10364302>
559. Bruce JW, Hierl M, Young JAT, Ahlquist P. Cellular transcription factor ZASC1 regulates murine leukemia virus transcription. *J Virol* [Internet]. American Society for Microbiology (ASM); 2010 Aug [cited 2017 Mar 20];84(15):7473–83. Available from: <http://www.ncbi.nlm.nih.gov/pubmed/20484494>
560. Neno M, Mita K, Ichimura S, Cartwright IL, Takahashi E, Yamauchi M, et al. Heterogeneous structure of the polyubiquitin gene UbC of HeLa S3 cells. *Gene* [Internet]. 1996 Oct 10 [cited 2017 Mar 18];175(1–2):179–85. Available from: <http://www.ncbi.nlm.nih.gov/pubmed/8917096>
561. Crinelli R, Bianchi M, Radici L, Carloni E, Giacomini E, Magnani M. Molecular Dissection of the Human Ubiquitin C Promoter Reveals Heat Shock Element Architectures with Activating and Repressive Functions. Massoumi R, editor. *PLoS One* [Internet]. Public Library of Science; 2015 Aug 28 [cited 2017 Mar 18];10(8):e0136882. Available from:

<http://dx.plos.org/10.1371/journal.pone.0136882>

562. Sörge S, Fraedrich K, Votteler J, Thomas M, Stamminger T, Schubert U. Perinuclear localization of the HIV-1 regulatory protein Vpr is important for induction of G2-arrest. *Virology*. 2012;432(2):444–51.
563. Vodicka MA, Koepp DM, Silver PA, Emerman M. HIV-1 Vpr interacts with the nuclear transport pathway to promote macrophage infection. *Genes Dev* [Internet]. 1998 Jan 15 [cited 2017 Apr 30];12(2):175–85. Available from: <http://www.ncbi.nlm.nih.gov/pubmed/9436978>
564. Sawaya BE, Khalili K, Gordon J, Srinivasan A, Richardson M, Rappaport J, et al. Transdominant activity of human immunodeficiency virus type 1 Vpr with a mutation at residue R73. *J Virol* [Internet]. 2000 May [cited 2017 Apr 30];74(10):4877–81. Available from: <http://www.ncbi.nlm.nih.gov/pubmed/10775627>
565. Liu R, Lin Y, Jia R, Geng Y, Liang C, Tan J, et al. HIV-1 Vpr stimulates NF-kappaB and AP-1 signaling by activating TAK1. *Retrovirology* [Internet]. 2014;11(1):45. Available from: <http://www.ncbi.nlm.nih.gov/pubmed/24912525>
566. Tcherepanova I, Starr A, Lackford B, Adams MD, Routy J-P, Boulassel MR, et al. The Immunosuppressive Properties of the HIV Vpr Protein Are Linked to a Single Highly Conserved Residue, R90. Zhang L, editor. *PLoS One* [Internet]. Public Library of Science; 2009 Jun 10 [cited 2017 Apr 30];4(6):e5853. Available from: <http://dx.plos.org/10.1371/journal.pone.0005853>
567. Fletcher AJ, Mallery DL, Watkinson RE, Dickson CF, James LC. Sequential ubiquitination and deubiquitination enzymes synchronize the dual sensor and effector functions of TRIM21. *Proc Natl Acad Sci U S A* [Internet]. National Academy of Sciences; 2015 Aug 11 [cited 2016 Dec 9];112(32):10014–9. Available from: <http://www.ncbi.nlm.nih.gov/pubmed/26150489>
568. Fletcher AJ, Christensen DE, Nelson C, Tan CP, Schaller T, Lehner PJ, et al. TRIM5a requires Ube2W to anchor Lys63-linked ubiquitin chains and restrict reverse transcription. *EMBO J* [Internet]. 2015 [cited 2017 May 3];34:2078–95. Available from: <http://onlinelibrary.wiley.com/store/10.15252/embj.201490361/asset/embj201490361.pdf;jsessionid=3C06319F87474886089B1664EE58F4FE.f02t04?v=1&t=j290cabb&s=c88a3703d7c0ce670955481716b3b47d1e6479ba>
569. Andersen J, VanScoy S, Cheng T-F, Gomez D, Reich NC. IRF-3-dependent and augmented target genes during viral infection. *Genes Immun* [Internet]. Nature Publishing Group; 2008 Mar 20 [cited 2017 Mar 8];9(2):168–75. Available from: <http://www.nature.com/doifinder/10.1038/sj.gene.6364449>
570. Elco CP, Guenther JM, Williams BRG, Sen GC. Analysis of genes induced by Sendai virus infection of mutant cell lines reveals essential roles of interferon regulatory factor 3, NF-kappaB,

- and interferon but not toll-like receptor 3. *J Virol* [Internet]. American Society for Microbiology (ASM); 2005 Apr [cited 2017 Mar 8];79(7):3920–9. Available from: <http://www.ncbi.nlm.nih.gov/pubmed/15767394>
571. Wietek C, Miggin SM, Jefferies CA, O'Neill LAJ. Interferon Regulatory Factor-3-mediated Activation of the Interferon-sensitive Response Element by Toll-like receptor (TLR) 4 but Not TLR3 Requires the p65 Subunit of NF- $\kappa$ B. *J Biol Chem* [Internet]. 2003 Dec 19 [cited 2017 Mar 8];278(51):50923–31. Available from: <http://www.ncbi.nlm.nih.gov/pubmed/14557267>
572. Taniguchi T, Ogasawara K, Takaoka A, Tanaka N. IRF FAMILY OF TRANSCRIPTION FACTORS AS REGULATORS OF HOST DEFENSE. *Annu Rev Immunol* [Internet]. 2001 Apr [cited 2017 Mar 8];19(1):623–55. Available from: <http://www.ncbi.nlm.nih.gov/pubmed/11244049>
573. Ogawa S, Lozach J, Benner C, Pascual G, Tangirala RK, Westin S, et al. Molecular Determinants of Crosstalk between Nuclear Receptors and Toll-like Receptors. *Cell* [Internet]. 2005 Sep 9 [cited 2017 Mar 8];122(5):707–21. Available from: <http://www.ncbi.nlm.nih.gov/pubmed/16143103>
574. Apostolou E, Thanos D. Virus Infection Induces NF- $\kappa$ B-Dependent Interchromosomal Associations Mediating Monoallelic IFN- $\beta$  Gene Expression. *Cell* [Internet]. 2008 Jul 11 [cited 2017 Mar 8];134(1):85–96. Available from: <http://www.ncbi.nlm.nih.gov/pubmed/18614013>
575. Cheng CS, Feldman KE, Lee J, Verma S, Huang DB, Huynh K, et al. The specificity of innate immune responses is enforced by repression of interferon response elements by NF- $\kappa$ B p50. *Sci Signal*. 2011;4(161):ra11.
576. Guenzel CA, Hérate C, Benichou S. HIV-1 Vpr-a still “enigmatic multitasker.” Vol. 5, *Frontiers in Microbiology*. 2014.
577. Zander K, Sherman MP, Tessmer U, Bruns K, Wray V, Prechtel AT, et al. Cyclophilin A interacts with HIV-1 Vpr and is required for its functional expression. *J Biol Chem* [Internet]. American Society for Biochemistry and Molecular Biology; 2003 Oct 31 [cited 2017 Apr 30];278(44):43202–13. Available from: <http://www.ncbi.nlm.nih.gov/pubmed/12881522>
578. Lallemand-Breitenbach V, de Thé H. PML nuclear bodies. *Cold Spring Harb Perspect Biol* [Internet]. Cold Spring Harbor Laboratory Press; 2010 May [cited 2017 May 5];2(5):a000661. Available from: <http://www.ncbi.nlm.nih.gov/pubmed/20452955>
579. Stuurman N, Meijne AM, van der Pol AJ, de Jong L, van Driel R, van Renswoude J. The nuclear matrix from cells of different origin. Evidence for a common set of matrix proteins. *J Biol Chem* [Internet]. 1990 Apr 5 [cited 2017 May 5];265(10):5460–5. Available from: <http://www.ncbi.nlm.nih.gov/pubmed/2180926>

580. Renner F, Moreno R, Schmitz ML. SUMOylation-Dependent Localization of IKK $\epsilon$  in PML Nuclear Bodies Is Essential for Protection against DNA-Damage-Triggered Cell Death. *Mol Cell* [Internet]. 2010 [cited 2017 May 5];37(4):503–15. Available from: <http://www.sciencedirect.com/science/article/pii/S1097276510000699>
581. Brameier M, Krings A, MacCallum RM. NucPred Predicting nuclear localization of proteins. *Bioinformatics* [Internet]. 2007 May 1 [cited 2017 Mar 9];23(9):1159–60. Available from: <http://www.ncbi.nlm.nih.gov/pubmed/17332022>
582. Cokol M, Nair R, Rost B. Finding nuclear localization signals. *EMBO Rep* [Internet]. 2000;1(5):411–5. Available from: <http://www.pubmedcentral.nih.gov/articlerender.fcgi?artid=1083765&tool=pmcentrez&rendertype=abstract>
583. Trinkle-Mulcahy L. Resolving protein interactions and complexes by affinity purification followed by label-based quantitative mass spectrometry. *Proteomics* [Internet]. 2012 May [cited 2017 Mar 9];12(10):1623–38. Available from: <http://doi.wiley.com/10.1002/pmic.201100438>
584. Cox J, Mann M. Is Proteomics the New Genomics? *Cell* [Internet]. 2007 Aug 10 [cited 2017 Mar 9];130(3):395–8. Available from: <http://www.ncbi.nlm.nih.gov/pubmed/17693247>
585. Fregoso OI, Emerman M. Activation of the DNA Damage Response Is a Conserved Function of HIV-1 and HIV-2 Vpr That Is Independent of SLX4 Recruitment. *MBio* [Internet]. American Society for Microbiology; 2016 Sep 13 [cited 2017 Feb 27];7(5):e01433-16. Available from: <http://www.ncbi.nlm.nih.gov/pubmed/27624129>
586. Blondot M-L, Dragin L, Lahouassa H, Margottin-Goguet F. How SLX4 cuts through the mystery of HIV-1 Vpr-mediated cell cycle arrest. [cited 2017 Mar 14]; Available from: [http://download.springer.com/static/pdf/392/art%253A10.1186%252Fs12977-014-0117-5.pdf?originUrl=http%3A%2F%2Fretrovirology.biomedcentral.com%2Farticle%2F10.1186%2Fs12977-014-0117-5&token2=exp=1489510622~acl=%2Fstatic%2Fpdf%2F392%2Fart%25253A10.1186%25252Fs12977-014-0117-5.pdf\\*~hmac=e3da2941f5694e1e0b85fd025cec1d5456c00e9aa4b31bdab5fe7e4c6a302ccb](http://download.springer.com/static/pdf/392/art%253A10.1186%252Fs12977-014-0117-5.pdf?originUrl=http%3A%2F%2Fretrovirology.biomedcentral.com%2Farticle%2F10.1186%2Fs12977-014-0117-5&token2=exp=1489510622~acl=%2Fstatic%2Fpdf%2F392%2Fart%25253A10.1186%25252Fs12977-014-0117-5.pdf*~hmac=e3da2941f5694e1e0b85fd025cec1d5456c00e9aa4b31bdab5fe7e4c6a302ccb)
587. Brégnard C, Benkirane M, Laguette N. DNA damage repair machinery and HIV escape from innate immune sensing. *Front Microbiol* [Internet]. Frontiers; 2014 Jan 22 [cited 2015 Jan 30];5:176. Available from: <http://journal.frontiersin.org/article/10.3389/fmicb.2014.00176/abstract>
588. de Silva S, Planelles V, Wu L, Margottin-Goguet F, Jensen S, Tengchuan J, et al. Differential Effects of Vpr on Single-cycle and Spreading HIV-1 Infections in CD4+ T-cells and Dendritic Cells. Sawaya BE, editor. *PLoS One* [Internet]. BioMed Central; 2012 May 3 [cited 2017 Mar

14];7(5):e35385. Available from: <http://dx.plos.org/10.1371/journal.pone.0035385>

589. Connor RI, Chen BK, Choe S, Landau NR. Vpr is required for efficient replication of human immunodeficiency virus type-1 in mononuclear phagocytes. *Virology* [Internet]. 1995;206(2):935–44. Available from: <http://www.sciencedirect.com/science/article/pii/S0042682285710161>
590. Chen R, Le Rouzic E, Kearney JA, Mansky LM, Benichou S. Vpr-mediated incorporation of UNG2 into HIV-1 particles is required to modulate the virus mutation rate and for replication in macrophages. *J Biol Chem* [Internet]. American Society for Biochemistry and Molecular Biology; 2004 Jul 2 [cited 2017 Mar 17];279(27):28419–25. Available from: <http://www.ncbi.nlm.nih.gov/pubmed/15096517>
591. Jordan A, Defechereux P, Verdin E. The site of HIV-1 integration in the human genome determines basal transcriptional activity and response to Tat transactivation. *EMBO J* [Internet]. European Molecular Biology Organization; 2001 Apr 2 [cited 2017 Feb 12];20(7):1726–38. Available from: <http://www.ncbi.nlm.nih.gov/pubmed/11285236>
592. Vanitharani R, Mahalingam S, Rafaeli Y, Singh SP, Srinivasan a, Weiner DB, et al. HIV-1 Vpr transactivates LTR-directed expression through sequences present within -278 to -176 and increases virus replication in vitro. *Virology*. 2001;289(2):334–42.
593. McCutchan JH, Pagano JS. Enhancement of the infectivity of simian virus 40 deoxyribonucleic acid with diethylaminoethyl-dextran. *J Natl Cancer Inst* [Internet]. Oxford University Press; 1968 Aug [cited 2017 Mar 18];41(2):351–7. Available from: <http://www.ncbi.nlm.nih.gov/pubmed/4299537>
594. Vaheri A, Pagano JS. Infectious poliovirus RNA: a sensitive method of assay. *Virology* [Internet]. 1965 Nov [cited 2017 Mar 18];27(3):434–6. Available from: <http://www.ncbi.nlm.nih.gov/pubmed/4285107>
595. Kim TK, Eberwine JH. Mammalian cell transfection: the present and the future. *Anal Bioanal Chem* [Internet]. Springer; 2010 Aug [cited 2017 Mar 17];397(8):3173–8. Available from: <http://www.ncbi.nlm.nih.gov/pubmed/20549496>
596. Heinzinger NK, Bukrinskyt MI, Haggerty SA, Ragland AM, Kewalramani V, Leet M-A, et al. The Vpr protein of human immunodeficiency virus type 1 influences nuclear localization of viral nucleic acids in nondividing host cells (AIDS/preintegration complex transport). *Biochemistry*. 1994;91:7311–5.
597. Gao D, Wu J, Wu Y-T, Du F, Aroh C, Yan N, et al. Cyclic GMP-AMP Synthase Is an Innate Immune Sensor of HIV and Other Retroviruses. *Science* (80- ) [Internet]. 2013 Aug 23 [cited 2016 Dec 26];341(6148):903–6. Available from:

<http://www.sciencemag.org/cgi/doi/10.1126/science.1240933>

598. König R, Zhou Y, Elleder D, Diamond TL, Bonamy GMC, Irelan JT, et al. Global Analysis of Host-Pathogen Interactions that Regulate Early-Stage HIV-1 Replication. *Cell*. 2008;135(1):49–60.
599. Zhou H, Xu M, Huang Q, Gates AT, Zhang XD, Castle JC, et al. Genome-Scale RNAi Screen for Host Factors Required for HIV Replication. *Cell Host Microbe* [Internet]. 2008;4(5):495–504. Available from: <http://www.ncbi.nlm.nih.gov/pubmed/18976975><http://linkinghub.elsevier.com/retrieve/pii/S1931312808003302>
600. Bosco DA, Kern D. Catalysis and binding of cyclophilin A with different HIV-1 capsid constructs. *Biochemistry*. 2004;43(20):6110–9.
601. Thali M, Bukovsky A, Kondo E, Rosenwirth B, Walsh CT, Sodroski J, et al. Functional association of cyclophilin A with HIV-1 virions. Vol. 372, *Nature*. 1994. p. 363–5.
602. Schaller T, Ocwieja KE, Rasaiyaah J, Price AJ, Brady TL, Roth SL, et al. HIV-1 Capsid-Cyclophilin Interactions Determine Nuclear Import Pathway, Integration Targeting and Replication Efficiency. Aiken C, editor. *PLoS Pathog* [Internet]. Public Library of Science; 2011 Dec 8 [cited 2016 Dec 30];7(12):e1002439. Available from: <http://dx.plos.org/10.1371/journal.ppat.1002439>
603. Meehan AM, Saenz DT, Guevera R, Morrison JH, Peretz M, Fadel HJ, et al. A Cyclophilin Homology Domain-Independent Role for Nup358 in HIV-1 Infection. Aiken C, editor. *PLoS Pathog* [Internet]. Public Library of Science; 2014 Feb 20 [cited 2017 Mar 17];10(2):e1003969. Available from: <http://dx.plos.org/10.1371/journal.ppat.1003969>
604. Warren WC, Jasinska AJ, García-Pérez R, Svardal H, Tomlinson C, Rocchi M, et al. The genome of the vervet (*Chlorocebus aethiops sabaeus*). *Genome Res* [Internet]. Cold Spring Harbor Laboratory Press; 2015 Dec [cited 2017 Mar 20];25(12):1921–33. Available from: <http://www.ncbi.nlm.nih.gov/pubmed/26377836>
605. Bernardi R, Papa A, Pandolfi PP. Regulation of apoptosis by PML and the PML-NBs. *Oncogene* [Internet]. 2008 Oct 20 [cited 2017 May 7];27(48):6299–312. Available from: <http://www.ncbi.nlm.nih.gov/pubmed/18931695>
606. Bernardi R, Pandolfi PP. Structure, dynamics and functions of promyelocytic leukaemia nuclear bodies. *Nat Rev Mol Cell Biol* [Internet]. 2007 Dec [cited 2017 May 7];8(12):1006–16. Available from: <http://www.ncbi.nlm.nih.gov/pubmed/17928811>
607. Dellaire G, Ching RW, Ahmed K, Jalali F, Tse KCK, Bristow RG, et al. Promyelocytic leukemia

nuclear bodies behave as DNA damage sensors whose response to DNA double-strand breaks is regulated by NBS1 and the kinases ATM, Chk2, and ATR. *J Cell Biol* [Internet]. 2006 Oct 9 [cited 2017 May 7];175(1):55–66. Available from: <http://www.ncbi.nlm.nih.gov/pubmed/17030982>

608. Lavin MF. Ataxia-telangiectasia: from a rare disorder to a paradigm for cell signalling and cancer. *Nat Rev Mol Cell Biol* [Internet]. 2008 Oct [cited 2017 May 7];9(10):759–69. Available from: <http://www.ncbi.nlm.nih.gov/pubmed/18813293>
609. Wu Z-H, Shi Y, Tibbetts RS, Miyamoto S. Molecular Linkage Between the Kinase ATM and NF- $\kappa$ B Signaling in Response to Genotoxic Stimuli. *Science* (80- ) [Internet]. 2006 Feb 24 [cited 2017 May 7];311(5764):1141–6. Available from: <http://www.ncbi.nlm.nih.gov/pubmed/16497931>
610. Hayden MS, Ghosh S. Shared Principles in NF- $\kappa$ B Signaling. *Cell* [Internet]. 2008 Feb 8 [cited 2017 May 7];132(3):344–62. Available from: <http://www.ncbi.nlm.nih.gov/pubmed/18267068>
611. Mabb AM, Wuerzberger-Davis SM, Miyamoto S. PIASy mediates NEMO sumoylation and NF- $\kappa$ B activation in response to genotoxic stress. *Nat Cell Biol* [Internet]. 2006 Sep 13 [cited 2017 May 7];8(9):986–93. Available from: <http://www.ncbi.nlm.nih.gov/pubmed/16906147>
612. Janssens S, Tschopp J. Signals from within: the DNA-damage-induced NF- $\kappa$ B response. *Cell Death Differ* [Internet]. 2006 May 13 [cited 2017 May 7];13(5):773–84. Available from: <http://www.ncbi.nlm.nih.gov/pubmed/16410802>
613. Habraken Y, Piette J. NF- $\kappa$ B activation by double-strand breaks. *Biochem Pharmacol* [Internet]. 2006 Oct 30 [cited 2017 May 7];72(9):1132–41. Available from: <http://www.ncbi.nlm.nih.gov/pubmed/16965765>
614. Li M, Gao F, Mascola JR, Stamatatos L, Polonis VR, Koutsoukos M, et al. Human immunodeficiency virus type 1 env clones from acute and early subtype B infections for standardized assessments of vaccine-elicited neutralizing antibodies. *J Virol* [Internet]. American Society for Microbiology (ASM); 2005 Aug [cited 2017 Apr 16];79(16):10108–25. Available from: <http://www.ncbi.nlm.nih.gov/pubmed/16051804>
615. Stanojevic M, Papa A, Papadimitriou E, Zerjav S, Jevtovic D, Salemovic D, et al. HIV-1 Subtypes in Yugoslavia. *AIDS Res Hum Retroviruses* [Internet]. 2002 May 1 [cited 2017 Apr 16];18(7):519–22. Available from: <http://www.ncbi.nlm.nih.gov/pubmed/12015906>
616. Simon F, Maucière P, Roques P, Loussert-Ajaka I, Müller-Trutwin MC, Saragosti S, et al. Identification of a new human immunodeficiency virus type 1 distinct from group M and group O. *Nat Med* [Internet]. 1998 Sep [cited 2017 Apr 16];4(9):1032–7. Available from: <http://www.ncbi.nlm.nih.gov/pubmed/9734396>

617. Keele BF, Van Heuverswyn F, Li Y, Bailes E, Takehisa J, Santiago ML, et al. Chimpanzee reservoirs of pandemic and nonpandemic HIV-1. *Science*. 2006;313(5786):523–6.
618. Bibollet-Ruche F, Bailes E, Gao F, Pourrut X, Barlow KL, Clewley JP, et al. New simian immunodeficiency virus infecting De Brazza's monkeys (*Cercopithecus neglectus*): evidence for a cercopithecus monkey virus clade. *J Virol* [Internet]. American Society for Microbiology (ASM); 2004 Jul [cited 2017 Mar 5];78(14):7748–62. Available from: <http://www.ncbi.nlm.nih.gov/pubmed/15220449>
619. Dazza M, Ekwalinga M, Nende M, Shamamba K Bin, Bitshi P, Paraskevis D, et al. Characterization of a Novel vpu -Harboring Simian Immunodeficiency Virus from a Dent ' s Mona Monkey ( *Cercopithecus mona denti* ). 2005;79(13):8560–71.
620. Takehisa J, Kraus MH, Ayouba A, Bailes E, Van Heuverswyn F, Decker JM, et al. Origin and Biology of Simian Immunodeficiency Virus in Wild-Living Western Gorillas. *J Virol* [Internet]. 2009 Feb 15 [cited 2017 Apr 16];83(4):1635–48. Available from: <http://www.ncbi.nlm.nih.gov/pubmed/19073717>
621. Peeters M, Courgnaud V, Abela B, Auzel P, Pourrut X, Bibollet-Ruche F, et al. Risk to human health from a plethora of Simian immunodeficiency viruses in primate bushmeat. *Emerg Infect Dis*. 2002;8(5):451–7.
622. Bailey AL, Lauck M, Ghai RR, Nelson CW, Heimbruch K, Hughes AL, et al. Arteriviruses, Pegiviruses, and Lentiviruses Are Common among Wild African Monkeys.
623. Baumann B, Wagner M, Aleksic T, von Wichert G, Weber CK, Adler G, et al. Constitutive IKK2 activation in acinar cells is sufficient to induce pancreatitis in vivo. *J Clin Invest* [Internet]. American Society for Clinical Investigation; 2007 Jun [cited 2017 Apr 16];117(6):1502–13. Available from: <http://www.ncbi.nlm.nih.gov/pubmed/17525799>

